ALMA MATER STUDIORUM
UNIVERSITÀ DI BOLOGNA

DOTTORATO DI RICERCA IN

Scienze Chirurgiche e Tecnologie Innovative

Ciclo 38

Settore Concorsuale: 06/A3 – Microbiologia e Microbiologia Clinica

Settore Scientifico Disciplinare: MED/07 Microbiologia e Microbiologia Clinica

APPLICATION OF HIGH HYDROSTATIC PRESSURE (HHP) FOR THE PRODUCTION OF WHOLE VIRUS INACTIVATED VACCINES: DEVELOPMENT OF SARS-COV-2 AND WEST NILE VIRUS VACCINE CANDIDATES

Presentata da: Martina Brandolini

Coordinatore Dottorato
Prof.ssa Emanuela Marcelli

Supervisore
Prof. Vittorio Sambri

Co-supervisore
Prof.ssa Stefania Varani

Esame finale anno 2026

Abstract

Vaccination remains the most effective strategy to prevent infectious diseases and mitigate their global impact. The rapid development of SARS-CoV-2 vaccines demonstrated the transformative potential of novel biotechnologies but also exposed challenges in production scalability, cold-chain logistics, antigen preservation, and rapid adaptation to emerging variants. Meanwhile, arboviral infections, particularly West Nile virus (WNV), have become persistent threats in Europe and beyond, driven by ecological changes and climate warming, albeit no effective human vaccine exists. High Hydrostatic Pressure (HHP) processing, widely used in the food industry for microbial inactivation and product preservation, represents a promising, chemical-free viral inactivation method. Preliminary evidence indicates that pressure-induced structural alterations can suppress viral replication while preserving antigenic structures. However, systematic investigations into immunogenicity, antigen preservation, and thermostability of HHP-inactivated viral vaccines are still limited.

This study aimed to develop and validate an HHP-based methodology for producing inactivated vaccines against SARS-CoV-2 and WNV. The specific objectives were to: (i) assess HHP inactivation efficacy on structurally distinct viruses; (ii) characterize morphological and antigenic modifications induced by pressure; (iii) evaluate immunogenicity in a murine model; and (iv) examine thermostability under storage conditions relevant to low-resource environments. The overarching goal was to establish HHP as a versatile platform for pandemic preparedness and control of endemic arboviruses.

SARS-CoV-2 (B.1 and BQ.1.1 lineages) and WNV (lineages 1 and 2) were selected as representative models of pandemic and endemic threats. Viral stocks subjected to high hydrostatic pressure processing in an Avure system. Pressures between 400 and 600 MPa were tested for 5-10 minutes, while heat inactivation was used as a control. Residual infectivity was assessed by endpoint titration and replication assays in Vero E6 cells, while morphological and antigenic integrity were evaluated through negative-staining electron microscopy and Western blotting, focusing on the main structural proteins of each virus. The immunogenicity of the SARS-CoV-2 vaccine candidates was evaluated *in vivo* in Swiss CD-1 mice, which received HHP- or heat-inactivated preparations (10 μg of purified antigen) following a prime-boost regimen. Humoral responses were longitudinally evaluated over 53 days by ELISA, Western blot, and neutralization assays, while T-cell responses were evaluated at the final

timepoint through IFN-γ ELISpot. Parametric and non-parametric statistics were used to address significant differences within and among groups. Thermostability was studied by storing inactivated viral preparations at 4 °C and 25 °C for up to 30 days, with antigenicity assessed periodically by Western blot.

HHP demonstrated to inactivate SARS-CoV-2 and WNV while preserving critical antigenic determinants. For SARS-CoV-2, 400 MPa reduced infectivity but allowed residual replication; 500 MPa completely abolished infectivity while preserving virion morphology with moderate loss of spike definition. At 600 MPa, extensive collapse of virions was observed. Western blot confirmed retention of nucleocapsid and membrane protein reactivity across all HHP conditions, though spike antigenicity declined with increasing pressure. In vivo, HHP-inactivated SARS-CoV-2 vaccines induced robust humoral immunity. The 500 MPa group showed the highest and most sustained titers, accompanied by strong neutralizing activity. Epitope profiling revealed that HHP vaccines elicited a broader antibody repertoire targeting both S and N proteins, whereas heat inactivation induced mainly N-specific antibodies. T-cell activation was also robust in HHP immunization groups. Thermostability assays revealed that 500-MPa-inactivated SARS-CoV-2 preparation maintained antigenic integrity for at least 30 days at 4 °C and for up to 14 days at 25 °C, suggesting improved distribution potential without dependence on ultra-cold storage. For WNV, standard 5-minute HHP treatments were insufficient for full inactivation, but 10-minute exposures achieved complete loss of infectivity. Electron microscopy revealed collapsed, amorphous particles, while Western blot confirmed preserved immunoreactivity of envelope, capsid, and NS1 proteins.

This study demonstrates that high hydrostatic pressure is a versatile and effective approach for viral inactivation that preserves critical antigenic determinants while abolishing infectivity. Overall, HHP offers a promising technology for whole-virus vaccine development with applications extending from pandemic preparedness against rapidly evolving coronaviruses to endemic or imported arboviral threats. The approach offers advantages in scalability and distribution logistics, addressing global inequities in vaccine access. Future work should refine virus-specific protocols, expand testing to additional pathogens such as Dengue virus, whose expanding distribution underscores the urgent need for resilient vaccine technologies.

TABLE OF CONTENTS

1. INTRODUCTION 1

1.1 Historical perspective of vaccine use in infectious diseases control: from early roots to the evolution of the "Public Health" concept towards global equity 2

1.2 An overview of vaccine categories: live attenuated, inactivated, viral vectors, virus-like particles (VLP), recombinant protein, DNA and mRNA vaccines 5
1.2.1 Live attenuated vaccines 5
1.2.2 Viral vector vaccines 6
1.2.3 Recombinant protein vaccines 7
1.2.4 Virus-like Particles (VLPs) vaccines 8
1.2.5 DNA and mRNA vaccines 8
1.2.6 Inactivated vaccines: scientific bases of viral inactivation, definition and principle 9
1.2.6.1 Traditional inactivation method: advantages and limits 10
1.2.6.2 Inactivation impact on antigen preservation and immunogenicity 12
1.2.6.3 Dynamics of immune responses to inactivated vaccines 12
1.2.6.4 Inactivated vaccines relevance in the context of public health 15

1.3 SARS-CoV-2: A critical case study 18
1.3.1 General overview 19
1.3.1.1 Major antigenic sites and elicited responses 20
1.3.2 COVID-19 vaccines 24
1.3.3 SARS-CoV-2 evolution, emergence of new variants, reinfections and vaccine breakthrough 25
1.3.4 COVID-19 pandemic global vaccine effort: achievements and challenges 27

1.4 Beyond SARS-CoV-2: A look at other global health emergencies 33
1.4.1 West Nile virus: general overview 37
1.4.1.1 Major antigenic sites and elicited responses 39
1.4.2 WNV ecology 44
1.4.3 WNV epidemiology 46
1.4.4 WNV genetic diversity and evolution 49
1.4.5 WNV vaccines 52

1.5 Development of new viral inactivation strategies 54
1.5.1 High Hydrostatic Pressure: application in food science and beyond 54
1.5.2 HHP mode of action 57
1.5.3 Use of HHP in whole inactivated virus vaccine production: repurposing of and old method for a new application 59

2. SCOPE 63

3. MATERIALS AND METHODS 65

3.1 Cells and virus 65

3.2 Preparation of SARS-CoV-2 and WNV stock and HHP processing 67

3.3 Inactivation assessment 69

3.4 Antigen purification 71

3.5 Structural and antigenicity analysis **72**
3.5.1 Negative Staining Electron Microscopy (nsEM) 72
3.5.2 Western blot 72

3.6 *In vivo* safety and immunogenicity testing **77**
3.6.1 B cell response assessment 80
3.6.1.1 Enzyme-Linked Immunosorbent Assay (ELISA) 80
3.6.1.2 Humoral response specificity characterization 80
3.6.1.3 Virus neutralization test 82
3.6.2 T cell response assessment 82
3.6.2.1 ELISpot assay on PBMC and splenocytes 82

3.7 Data analysis and statistical evaluation of immunogenicity **84**

3.8 Thermostability assessment **85**

4. RESULTS **86**

4.1 SARS-CoV-2 **86**
4.1.1 Inactivation assessment 87
4.1.2 Structural and antigenicity analysis 89
4.1.2.1 Negative Staining Electron Microscopy (nsEM) 89
4.1.2.2 Western blot 93
4.1.3 *In vivo* safety and immunogenicity 96
4.1.3.1 Anti-SARS-CoV-2 IgG titers 96
4.1.3.2 Epitopal characterization 101
4.1.3.3 Virus neutralization 103
4.1.4 T cell responses 108
4.1.5 Comparative analysis of immune response profiles 110
4.1.6 Thermostability assessment 112

4.2 West Nile virus **114**
4.2.1 Short HHP protocol 114
4.2.2 Refined long HHP protocol 116
4.2.3 Structural and antigenicity analysis 118
4.2.3.1 Negative Staining Electron Microscopy (nsEM) 118
4.2.3.2 Western blot 121

5. DISCUSSION **124**

6. REFERENCES **156**

1. Introduction

Vaccines represent one of the most powerful tools in medicine and public health, transforming once devastating and life-threatening diseases into preventable, often eradicated illnesses. From the historic eradication of smallpox to the ongoing efforts to control polio, vaccine development is the results of decades, if not centuries, of research and scientific debate, and the overcoming of technological challenges.

In recent years, the COVID-19 pandemic brought the critical importance of vaccine development into sharp focus. In a matter of months, the urge to produce effective vaccine against COVID-19 has prompted laboratories around the world to engage in an unprecedentedly expeditious vaccine development effort in order to provide an effective prophylactic countermeasure to stem SARS-CoV-2 spread in the human population. All vaccines which have received authorization by international drug regulation agencies in the last year, have thus far proved to effectively reduce morbidity and mortality connected with the disease, with new technologies like mRNA vaccines rapidly moving from research benches to millions of arms across the globe, demonstrating both the power and potential of modern biotechnology.

This extraordinarily rapid response was a stark demonstration to how far vaccine science has moved from the rudimentary beginnings of immunization centuries ago, but it also raised new questions about the future of vaccine technology, ongoing scientific, logistical, and ethical challenges, igniting the complex and evolving world of vaccine development and giving new momentum to the exploration of the scientific principles that guide the progress of vaccine science, ultimately aiming at the

development of safe and effective solutions through cutting-edge innovations poised to shape the next generation of immunizations. In a tight intersection between science and society, vaccines are not only medical achievements but also pivotal tools in public health strategy and their development balances optimism with the realities of scientific and global health challenges acting as powerful agents of social change. In this perspective, vaccines are inherently social tools, whose importance extends beyond science boundaries, deeply influencing societies, public health, collective responsibility and even global cooperation.

The COVID-19 crisis exposed stark inequalities in healthcare infrastructures worldwide, with many low-income countries experiencing delayed or limited access to vaccines. This imbalance sparked urgent debates about vaccine nationalism versus global solidarity, raising ethical questions about equity, justice, and the right to health. Moreover, vaccine hesitancy during the pandemic, fueled by misinformation, political polarization, and historical mistrust in medical systems, demonstrated that scientific achievement alone is insufficient without effective public communication and engagement. The social contract implicit in vaccination relies on mutual responsibility: individuals protect not only themselves but also the wider community, especially the most vulnerable. Thus, vaccination becomes an expression of civic duty and social cohesion.

As we confront current and future infectious threats, from resurgences of known diseases to novel pathogens, understanding the history, present, and future of vaccine development is more important than ever because the next great breakthrough could save millions of lives.

1.1 Historical perspective of vaccine use in infectious diseases control: from early roots to the evolution of the "Public Health" concept towards global equity

From an historical perspective, the development and deployment of vaccines is not merely a scientific achievement, but it is the result of a shift in the consideration and understanding of health, diseases, and the role of public institutions and of the collaborative responsibility in protecting collective health. In this perspective, the success of vaccination is deeply interconnected with the concept of collectiveness and sense of community.

The use of vaccines has ancient origins, predating the advent of medical science, as modernly intended, with the earliest forms of inoculation being traced back up to the 10th century, when variolation practices were developed, laying the groundwork for future advancements in immunization.

For what regards Western world, Edward Jenner experiments at the end of the 1700s on the inoculation with material from a cowpox sore and exposure to smallpox, led to world revolutionary first vaccine[1], not only from a medical perspective, but also for the profound impact it had on the understanding of diseases prevention. Yet, while Jenner's work laid the foundation for immunization, his efforts still represented the infancy of vaccination under a public health perspective[2].

A key watershed in the advancements of vaccine practices was germ theory, pioneered by Pasteur and Koch in the 19th century, which transformed the way diseases were understood and, by extension, how they could be prevented[3,4]. At a time when infectious diseases as cholera, tuberculosis, and typhoid fever were raging in an increasingly urbanized setting, vaccines became a critically important tool in building an organized and structured public health apparatus. Despite this, the interdependence between vaccine practices and public health policies was still at a primordial stage: while governments recognized the utility of vaccines, widespread vaccination campaigns were sporadic and often resisted by segments of the population, particularly in societies where public mistrust of medical interventions remained strong[5].

The so-called golden moment for vaccine development was represented by the 20th century, which saw the implementation of vaccines for some of the deadliest and most pervasive infectious diseases in human history: diphtheria, tetanus, pertussis, polio, measles, and mumps, among others. These advances were made possible by progress in the fields of microbiology and immunology, as well as biotechnology, but also to improved production techniques that allowed vaccines to be provided on a larger scale and with greater safety[6].

The World Health Organization (WHO) foundation in 1948, marked the institutionalization of public health efforts formalizing a global approach to disease control, which emphasized the need for coordinated efforts in vaccination and disease prevention[7]. Mass vaccination campaigns gained more and more importance, leading to the introduction of routine immunizations, especially in young children[8]. From a perspective of comprehensive health and egalitarian access to prevention, the

Expanded Programme on Immunization (EPI), launched by the WHO in 1974, aimed at extending vaccination campaigns for basic immunization to children in low- and middle-income countries, addressing disparities in access that had previously been largely ignored[9].

At the end of the century, the WHO's smallpox eradication campaign, began in 1967, with the global goal to eradicate smallpox best demonstrated the interdependence of vaccine development and deployment in mass vaccination, surveillance and outbreaks containment, which led to the total eradication of life-threatening diseases[10]. Thereby, smallpox, from one of the greatest threats to human health, became a symbol of the potential and strength of vaccines[11], showcasing not only the potential of vaccines to eliminate diseases but also the essential role of organized, global public health efforts in ensuring their effectiveness[12].

As the 21st century began, the epidemiological and global public health context became more complex, posing new challenges to vaccination practices. On the one hand, while vaccines had now reduced the burden represented by communicable diseases in the most developed countries, the interconnectedness brought by globalization led to the spread of once-distant diseases across borders, making global cooperation in disease containment more essential than ever[13]: SARS, MERS, and Ebola highlighted the ongoing need for vaccine innovation and robust public health systems[14]. On the other hand, increased globalization has resurfaced the pressing issue of developing countries and vaccine equity, surely one of the greatest health challenges of the century. While vaccines have been developed for many diseases, access to these life-saving interventions has been uneven between wealthier countries and low-income countries, with profound implications for the latter, where the burden of these diseases is often the greatest[15]. Efforts such as the Global Alliance for Vaccines and Immunization (GAVI), established in 2000, have sought to address this imbalance by improving access to vaccines in the world's poorest countries, playing a critical role in expanding immunization coverage, particularly for children in order to make the benefits of vaccine developments universally shared[16].

The COVID-19 pandemic, which saw unprecedented efforts in vaccine development and distribution[17], has brought these issues into even sharper focus, with the "global" distribution of these vaccines marked by stark inequalities. While high-income countries secured early access to vaccines, many low-income countries have been only marginally touched by immunization campaigns and faced delays in

obtaining sufficient doses for good population coverage, in what appeared to the eyes of many as mere paternalism[18]. This inequity not only resulted in preventable deaths but also prolonged the pandemic, as unvaccinated populations in one part of the world allowed the virus to continue spreading and mutating. This inequity has highlighted not only the moral imperative of vaccine distribution but also the practical reality that no country is safe from a pandemic unless all countries are, underscoring the need for a more equitable global public health system, where vaccines and other health interventions are accessible to all, regardless of geography or income[19].

Vaccines are not only a result of scientific research and discovery, but their history is deeply and reciprocally connected with public health, sense of collective duty and public global policies. From the eradication of smallpox, marking the first and greatest milestone of vaccines success, to the ongoing fight against COVID-19, passing through new emerging-but-still-poorly-understood pathogens, vaccines have been a critical and decisive tool in the control of infectious diseases. At the same time, the deployment and wide distribution of vaccines have depended upon the recognition of the collective nature of health and the sense of collective duty, which far transcend the borders of scientific development[20]. As the world faces new and emerging health threats, the interdependence of vaccines and public health will remain central to safeguarding global health across borders, highlighting how vaccine development is not just a national priority but also a global imperative that requires international cooperation and coordination. The challenge for the future will be to ensure that the benefits of vaccines are shared equitably and that public health systems are equipped to respond to the ever-changing landscape of infectious diseases[7].

As we continue to innovate in the field of immunization, it is essential to recognize that the success of vaccines relies not only on science but also on the strength of the societies they aim to protect.

1.2 An overview of vaccine categories: live attenuated, inactivated, viral vectors, virus-like particles (VLP), recombinant protein, DNA and mRNA vaccines

1.2.1 Live attenuated vaccines

Live attenuated vaccines are produced from an avirulent strain of the viruses of interest, which as a result no longer cause disease in immunocompetent individuals but can nonetheless elicit an immune response akin to that elicited by its virulent

counterpart. Viral attenuation is achieved through several methods, including serial passage in non-human cells, by inducing temperature-sensitive mutations, or by genetic manipulation to delete or alter virulence factors. Live attenuated vaccines can elicit robust and long-lasting immunity and induce both humoral and cellular immune responses. Many preventable diseases are put under control through attenuated vaccines, such as measles, mumps, rubella, and varicella[21]. However, there are medical risks associated with live attenuated vaccines. Immunocompromised individuals may develop the disease from the attenuated pathogen, and there is also the rare possibility of reversion to a virulent form[22].

The production of live attenuated vaccines is relatively cost-effective once the attenuation process is optimized, as they use well-established cell culture techniques. However, the high initial costs of developing a safe attenuated strain, along with the requirement for rigorous safety testing, make initial development expensive. In addition, their sensitivity to temperature fluctuations and the requirement of strict cold chain storage, complicates large-scale distribution, especially in developing countries where refrigeration infrastructure may be lacking[23].

1.2.2 Viral vector vaccines

Viral vector vaccines rely on non-pathogenic or scarcely virulent virus, such as an adenovirus, engineered to encode genes for one or several antigens cloned into the vector backbone. Viral vectors can be engineered to be replication deficient (replication incompetent), while maintaining the ability to infect cells and express the encoded antigen. Replication-competent vectors are considered true infections akin to live-attenuated vaccines. The vesicular stomatitis virus (VSV)-derived Ebola vaccine, encoding the Ebola surface glycoprotein, is an example of replication-competent vaccine[24]. Examples of replication deficient vaccine include the AstraZeneca COVID-19 vaccine[25,26], which uses a replication deficient chimpanzee adenovirus (ChAd) vector encoding surface spike glycoprotein. Other viruses used for the development of viral-based replication deficient vaccines include human adenovirus, Adeno-associated virus (AAV), modified vesicular stomatitis virus, modified vaccinia virus Ankara (MVA), poxvirus, and Newcastle disease virus (NDV)[27,28].

Viral vector vaccines can induce both humoral and cellular immune responses, hence providing a broad immune protection. Moreover, because replication deficient vector viruses do not replicate in the body, they are considered safe for most individuals, although there is some concern about pre-existing immunity to the vector virus, which

may reduce the vaccine's efficacy. This is especially problematic for vaccines using common human adenovirus vectors, as pre-existing immunity can neutralize the vector before it has a chance to deliver antigens[29].

From a production standpoint, viral vector vaccines are more complex to manufacture than live attenuated or inactivated vaccines because they require the growth of live viral vectors in cell culture systems[30]. This increases the cost and time involved in scaling up production. However, the manufacturing can be streamlined in a multistep process comprising of modular plug-and-play steps. Due to the versatility of the manufacturing platform viral vector vaccines can be easily deployed in the event of an epidemic or pandemic. Moreover, once these vaccines are produced, their storage requirements are more flexible than for other vaccines, typically requiring only refrigeration[31].

1.2.3 Recombinant protein vaccines

Recombinant protein vaccines are created by producing viral proteins (antigens) using recombinant DNA technology. This involves inserting a gene encoding the antigen into a host cell (such as yeast, bacteria, or mammalian cells) and allowing the cells to produce large amounts of the antigen. The protein is then purified and used in the vaccine. Examples include the hepatitis B (HBV) vaccine and the human papillomavirus (HPV) vaccine. Recombinant protein vaccines are highly safe, as they do not contain live pathogens and cannot cause disease. They also elicit strong humoral immune responses, particularly when combined with adjuvants to enhance their immunogenicity. The main challenge with recombinant protein vaccines is that they typically elicit weaker cellular immune responses and may require multiple doses or boosters for long-lasting immunity. In addition, they often need to be combined with adjuvants to enhance the immune response, which can sometimes increase the risk of local or systemic reactions[32].

The production of recombinant protein vaccines is relatively cost-effective once the expression systems are optimized. Yeast and bacterial cells are inexpensive to grow and maintain, though the purification of the protein can be a costly and complex process. The scalability of recombinant protein vaccines is a major advantage, as they can be produced in large quantities without the need for biosafety containment, unlike live attenuated or inactivated vaccines[33].

1.2.4 Virus-like Particles (VLPs) vaccines

Virus-like particles (VLPs) are macromolecular assemblies designed to mimic the morphology of a native virus (e.g., size, shape, and surface epitopes). VLP-derived vaccines are typically manufactured in bioreactors following transfection of insect, yeast, bacterial, plant, or mammalian cells with one or multiple genetic constructs. It has been established that the constructs encode a minimum of two structural components of the original virus, thus enabling self-assembly into replication-incompetent particles[34–37]. The immunogenicity of VLPs can be tuned during the design and manufacturing phases by means of chemical modifications of the surface, the addition of immunogenic/dominant peptides and/or adjuvants, or the choice of the VLP system[38,39]. This technology has been used to develop several licensed vaccines such as the human papillomavirus vaccine but has also been explored against Chikungunya, ZIKV, and SARS-CoV-2[40–42].

1.2.5 DNA and mRNA vaccines

Nucleic acid vaccines use DNA or RNA molecules that encode for pathogen-specific antigenic proteins. The former use a plasmid as the vehicle for the genetic material, while the latter have mostly used encapsulation in lipid nanoparticles[43].

When a DNA vaccine is administered, it is believed to transfect myocytes, keratinocytes, and tissue-resident APCs. Internalized DNA is translocated to the nucleus, where it is transcribed into mRNA. The mRNA is transported out of the nucleus, to the ribosomes responsible for synthesizing the desired antigen. This antigen undergoes processing and presentation to immune cells, thus eliciting a specific immune response[44]. Compared with the conventional inactivated, attenuated, and recombinant subunit vaccine platforms, DNA vaccines are faster, cheaper, and easier to manufacture. Despite positive clinical data, no DNA-based vaccine is licensed for human use, likely because generation of robust B and T cell responses with this platform requires at least a prime, and two-three booster administration. However, several DNA vaccines have been licensed for veterinary applications, e.g. West Nile virus in horses[45,46]. Safe and effective application of these vaccines in animals will likely be instrumental in providing proof-of-concept assisting in eventual application for clinical use in humans.

Recent improvements in sequence engineering and codon optimization, as well as in capping strategies, in addition to the evolution of potent and relatively safe delivery systems such as lipid nanoparticles, have significantly advanced the development and

regulatory approval of mRNA-based vaccines. Their principle relies on introducing synthetic mRNA encoding a specific viral protein into human cells, where the mRNA is translated into the corresponding viral protein, which then elicits an immune response[47,48]. The production of mRNA vaccines involves synthesizing the mRNA molecule in vitro, followed by encapsulation in lipid nanoparticles to protect the mRNA and facilitate its entry into cells[49]. mRNA vaccines have demonstrated several advantages, particularly highlighted by the success of the Pfizer-BioNTech and Moderna COVID-19 vaccines[50,51]. They are highly effective, with a strong ability to induce both antibody and T-cell responses. Moreover, the mRNA platform allows for rapid design and production, making it highly adaptable for emerging infectious diseases. The long-term duration of immunity remains subject of ongoing research, although suggesting the necessity for periodic booster doses[52,53].

The mRNA platform does not require live pathogen culture, eliminating many biosafety concerns and reducing production times. Additionally, mRNA vaccine production can be rapidly scaled up to meet global demands. However, the requirement for ultra-cold storage increases distribution costs and presents logistical challenges for global distribution[54].

1.2.6 Inactivated vaccines: scientific bases of viral inactivation, definition and principle

Inactivated vaccines consist of viruses or bacteria that have been inactivated using heat, chemicals (such as formaldehyde), or radiation[55]. This process ensures that the pathogen can no longer replicate or cause disease. However, it maintains the structural characteristics of major antigenic proteins, which are recognized by the immune system, eliciting a specific immune response[56]. One of the primary advantages of inactivated vaccines is their safety; since the pathogen cannot replicate, there is no risk of disease even in immunocompromised individuals. This safety profile makes inactivated vaccines, suitable for a broad population base. Inactivated vaccines generally produce weaker immune responses compared to live attenuated vaccines, require adjuvants, and often require multiple doses and booster shots to achieve and maintain protective immunity[57].

Despite the initial biosafety risk posed by culturing large quantities of the pathogen in the production facility for inactivation, inactivated vaccines have less strict storage requirements, often tolerating refrigeration rather than freezing, which enhances their logistical viability[58]. However, inactivated vaccines tend to require adjuvants

(immune-boosting substances) and booster doses, which adds to their overall long-term cost[59]. Furthermore, maintaining large quantities of the pathogen in the production facility for inactivation poses biosafety risks.

1.2.6.1 Traditional inactivation method: advantages and limits

Chemical inactivation is one of the most commonly used methods in the production of inactivated vaccines and the two most widely used chemical agents for viral inactivation are formaldehyde and β-propiolactone (BPL)[60].

Formaldehyde is a well-established agent used to inactivate viruses by cross-linking proteins and nucleic acids, hampering adsorption and entrance into cells, notwithstanding maintaining the structure of viral surface proteins involved in the activation of the immune response. Formaldehyde has been used for decades in the production of vaccines such as the inactivated polio vaccine (IPV)[61,62] and the hepatitis A vaccine[60,63]. Formaldehyde is effective against a wide range of viruses, including both enveloped and non-enveloped viruses and is a relatively inexpensive chemical, making it suitable for large-scale production. One major limitation is that formaldehyde can induce modifications in viral proteins structure thereby reducing their immunogenicity; to mitigate this, precise control of concentration and exposure time is necessary during the inactivation process. Moreover, formaldehyde inactivation can be time-consuming, taking several days to ensure complete inactivation.

B-propiolactone is another chemical widely used for viral inactivation. It works by binding to nucleic acids and disrupting the viral genome while leaving proteins largely unaffected. BPL is commonly used in the production of rabies vaccines[64,65] and some influenza vaccines[57,66]. BPL has the advantage of being a rapid inactivating agent, often achieving complete viral inactivation in a matter of a few hours (the majority of inactivation protocols suggest an overnight incubation with BPL for complete inactivation). Unlike formaldehyde, it has minimal impact on the antigenic structures of the virus, helping preserve the vaccine's immunogenicity. As a downside, BPL is extremely unstable and needs to be carefully handled, as it degrades into potentially toxic byproducts like β-hydroxypropionic acid at neutral pH, making its storage and handling more complicated[60,64].

Physical methods of viral inactivation rely on the application of heat to disrupt viral structures and replication. The most common physical method used in vaccine

production is heat inactivation, though other methods such as ultraviolet (UV) irradiation are also employed.

Heat inactivation involves exposing the virus to high temperatures, typically between 56 °C and 65 °C, for a specified period. This process denatures viral proteins and nucleic acids, rendering the virus non-infectious. Heat inactivation has been historically used in the production of vaccines such as the early influenza and yellow fever vaccines[67]. Heat inactivation is a straightforward and inexpensive method that does not require toxic and often carcinogenic chemical reagents and is relatively fast, with viral inactivation occurring within minutes to hours, depending on the temperature and virus. On the other hand, heat can denature the virus's surface proteins, potentially compromising the vaccine's immunogenicity. This means that the immune response elicited by a heat-inactivated vaccine may not be as robust or long-lasting compared to chemically inactivated vaccines. Thus, precise control of temperature is critical to ensure complete inactivation without over-damaging the viral antigens[68].

UV irradiation is another physical method that inactivates viruses by causing damage to their nucleic acids, particularly through the formation of thymine dimers, which disrupt viral replication. This method has been explored in the development of experimental vaccines, although it is less commonly used in large-scale production. Like heat inactivation, UV irradiation is a non-chemical method, eliminating the need for potentially hazardous reagents and it can be performed quickly and can be scaled for industrial use with appropriate equipment[69]. As a disadvantage for the application of UV irradiation, UV light has limited penetration depth, meaning it may not be as effective at inactivating viruses in large volumes of liquid or in complex mixtures. Moreover, UV exposure can damage proteins, altering their structure and reducing the vaccine's immunogenicity[70].

Radiation inactivation involves the use of ionizing radiation, such as gamma rays, to disrupt viral structures and inactivate the virus. This method is less commonly used for commercial vaccine production but has been explored in research settings for its potential to inactivate highly pathogenic viruses. Gamma irradiation, for example, works by inducing breaks in the viral nucleic acids, preventing replication. Unlike chemical methods, radiation does not involve the introduction of external substances, making it a cleaner process in terms of residuals. Gamma irradiation can penetrate deeply into liquids and solid materials, making it effective for large-scale inactivation

processes and it has a minimal impact on the virus's surface proteins, helping to preserve immunogenicity[71]. On the other hand, gamma irradiation requires specialized equipment, which can be expensive to install and maintain, limiting its use to specific facilities with the necessary infrastructure. From the antigenicity standpoint, high doses of radiation can cause damage to viral proteins, which may reduce the vaccine's effectiveness. Finding the right balance between effective inactivation and protein preservation is a key challenge[72].

1.2.6.2 Inactivation impact on antigen preservation and immunogenicity

The choice of viral inactivation method directly impacts the safety and efficacy of inactivated vaccines. Chemical methods, such as formaldehyde and BPL, are well-established and have been used for decades in vaccines with proven safety profiles. However, they require strict control to avoid incomplete inactivation, which could lead to the presence of infectious virus in the final product. Physical and radiation methods, while effective, often face challenges in preserving the immunogenicity of the virus, as excessive damage to viral proteins can reduce the vaccine's ability to stimulate a strong immune response[73]. The success of an inactivated vaccine thus relies not only on its inactivation method but also on the meticulous balance between safety, production efficiency and immunogenicity.

Chemical inactivation methods, such as formaldehyde and β-propiolactone, are widely used due to their effectiveness and established safety profiles, though they require precise control to avoid compromising immunogenicity. Physical methods, including heat and UV irradiation, offer alternatives, but they can negatively affect viral proteins if not carefully managed. Radiation methods, though less common, provide another route for viral inactivation. Each method has its own advantages and limitations, and the choice of technique depends on the specific virus, production capabilities, and the desired characteristics of the final vaccine product[73] in order to balance the need for complete viral inactivation with the preservation of immunogenicity[74].

1.2.6.3 Dynamics of immune responses to inactivated vaccines

The immunogenicity of whole inactivated virus vaccines largely depends on their ability to induce both humoral and cellular immune responses[74].

The humoral immune response is primarily mediated by B lymphocytes, which are responsible for producing antibodies that neutralize pathogens and mark them for

destruction by other immune cells. Upon vaccination with whole inactivated virus vaccines, the antigens of the inactivated pathogen are presented to the immune system, particularly to antigen-presenting cells (APCs) such as dendritic cells. These APCs process the antigens and present them on their surface to helper T cells (CD4+ T cells), which in turn activate B cells. The activation of B cells following vaccination with whole inactivated virus vaccines requires two signals. The first is the recognition of the antigen through the B cell receptor (BCR), which binds to the pathogen or its components. The second signal is provided by helper T cells through the engagement of the CD40 ligand on the T cell with the CD40 receptor on the B cell. This interaction induces B cell proliferation and differentiation into plasma cells, which are specialized for the production of antibodies[75]. Following this process, plasma cells begin to secrete large quantities of antibodies specific to the pathogen. In the case of whole inactivated virus vaccines, antibodies target surface proteins of the inactivated pathogen, such as viral envelope glycoproteins or bacterial surface polysaccharides. These antibodies play a critical role in neutralizing the pathogen by binding to it and preventing it from infecting host cells. Furthermore, antibodies can facilitate opsonization, where the pathogen is coated with antibodies, leading to enhanced phagocytosis by macrophages and neutrophils[75]. In addition to the production of plasma cells, the humoral response to whole inactivated virus vaccines generates memory B cells, which persist in the body long after the initial exposure to the vaccine antigen. Memory B cells enable a rapid and robust response upon subsequent exposure to the pathogen. Unlike naïve B cells, which require a longer time to produce antibodies, memory B cells can quickly proliferate and differentiate into plasma cells upon antigen re-encounter, providing long-lasting immunity[76].

While the humoral response plays a pivotal role in neutralizing extracellular pathogens, the cellular immune response is essential for eliminating intracellular pathogens such as viruses that have entered host cells. The cellular immune response is mainly mediated by T cells, which are divided into two major subsets: helper T cells (CD4+ T cells) and cytotoxic T cells (CD8+ T cells)[75].

CD4+ T cells play a key role in orchestrating the immune response to whole inactivated virus vaccines. After antigen uptake and processing by APCs, fragments of the pathogen are presented on major histocompatibility complex (MHC) class II molecules, which are recognized by CD4+ T cells. Upon activation, CD4+ T cells differentiate into various effector subsets, including TH1 and TH2. Each subset

secretes different cytokines that modulate the immune response. TH1 cells are essential for activating macrophages and enhancing their microbicidal activity, thus aiding in the clearance of pathogens. TH2 cells, on the other hand, support the humoral immune response by promoting B cell proliferation, differentiation, and antibody class switching[77].

In contrast to CD4+ T cells, CD8+ T cells are primarily responsible for directly killing infected cells. After vaccination with whole inactivated virus vaccines, some viral proteins may be taken up by APCs and presented on MHC class I molecules, which are recognized by CD8+ T cells. Once activated, CD8+ T cells differentiate into cytotoxic T lymphocytes (CTLs) that are capable of recognizing and destroying cells infected with the pathogen. Similar to B cells, T cells can also differentiate into memory cells after vaccination. Memory CD4+ and CD8+ T cells persist in the body and provide long-term protection by responding rapidly to subsequent infections. Memory T cells are classified into two main types: central memory T cells (T-CM), which reside in lymphoid tissues and are responsible for rapid proliferation upon antigen re-exposure, and effector memory T cells (T-EM), which circulate in peripheral tissues and can mount an immediate effector response[78]. The generation of memory T cells following whole inactivated virus vaccines administration contributes to long-lasting immunity and enhances the efficacy of booster vaccinations[79].

Whole inactivated virus vaccines have been demonstrated to primarily induce a humoral response, i.e., total antibody and neutralizing antibody responses, which closely correlate with vaccine efficacy and for whom correlates of protection have extensively been investigated[80]. Regarding T cell responses, TH1 or TH2 cell are only weakly induced by the primary vaccination and later enhanced substantially after the booster vaccine dose[81–83]. To address this limitation, adjuvants are often incorporated into whole inactivated virus formulations to enhance antigen presentation and promote a more balanced immune response[84]. However, it is important to note that inactivated virus vaccines may not always induce strong cellular immune responses compared to other vaccine platforms, such as live attenuated vaccines or viral vectors. The inability of whole inactivated virus vaccines to replicate within host cells limits the activation of CD8+ T cells, as cross-presentation is often less efficient than direct presentation of endogenous antigens[85,86]. Although whole inactivated virus vaccines typically induce a weaker CD8+ T cell response compared to other vaccine platforms, they can still promote the activation of CTLs

under certain conditions. The addition of adjuvants, such as alum or Toll-like receptor (TLR) agonists, can enhance the immunogenicity of whole inactivated virus vaccines by promoting the activation of APCs and facilitating cross-presentation of antigens on MHC class I molecules. This can lead to the generation of a more robust cellular immune response, which is particularly important for protection against intracellular pathogens[77,87].

1.2.6.4 Inactivated vaccines relevance in the context of public health

The use of inactivated vaccines dates back to the early 20th century, with the first inactivated bacterial vaccine developed for cholera, followed by the first inactivated viral vaccine for polio[76]. Several inactivated pathogen-based vaccines are currently in use, targeting a variety of diseases. These include vaccines for poliovirus, hepatitis A, influenza, rabies, and Japanese encephalitis:

- The inactivated poliovirus vaccine (IPV) was first developed by Jonas Salk in the 1950s. It contains three inactivated serotypes of the poliovirus and has played a pivotal role in the near eradication of polio globally. Unlike the oral polio vaccine (OPV), which contains live attenuated virus, IPV is administered intramuscularly or subcutaneously and does not pose the risk of vaccine-derived poliovirus[88]. IPV remains an essential part of the global polio eradication initiative[89].
- The hepatitis A virus (HAV) causes liver disease, and inactivated hepatitis A vaccines, such as Havrix and Vaqta, are highly effective in preventing infection. These vaccines are produced by growing the virus in cell culture and inactivating it with formaldehyde. Administered intramuscularly, these vaccines generate strong immune responses, and a two-dose schedule offers long-term protection[63,90].
- Influenza vaccines are produced annually to protect against seasonal influenza viruses. The most common form, the inactivated influenza vaccine (IIV), is typically administered via intramuscular injection. IIV provides protection against multiple strains of influenza, with its formulation adjusted annually based on predictions about circulating strains. While the efficacy of IIV varies from season to season, it remains a cornerstone of influenza prevention, particularly among the elderly, young children, and individuals with underlying health conditions[23,66].

- Rabies is a viral disease that is almost universally fatal once symptoms appear. Inactivated rabies vaccines are essential for post-exposure prophylaxis (PEP) and are given to individuals at high risk of exposure, such as veterinarians and laboratory workers. The inactivated rabies virus is typically cultured in cell lines and then inactivated using β-propiolactone. The vaccine induces a strong immune response, especially when combined with rabies immunoglobulin in cases of potential exposure[64].
- Japanese encephalitis (JEV) is a mosquito-borne viral infection endemic to parts of Asia. The inactivated JEV vaccine, such as IXIARO, is widely used to prevent the disease in travelers and populations in endemic regions. It is derived from an inactivated strain of the virus, and like other inactivated vaccines, it requires a booster dose for long-term protection[91].

The COVID-19 pandemic has revitalized interest in inactivated virus vaccines. Several COVID-19 vaccines based on inactivated SARS-CoV-2 virus have been developed and used, particularly in countries such as China and India. Notable examples include the CoronaVac vaccine developed by Sinovac, BBIBP-CorV developed by Sinopharm, and BBV152 (Covaxin) developed by Bharat Biotech[50]. These vaccines have shown efficacy in preventing COVID-19 and have added to the global arsenal of tools to combat the pandemic.

Characteristics of the vaccine platforms discussed above are briefly summarized in Table 1.

Table 1. Comparative characteristics of different vaccine platforms. The table summarizes key attributes of vaccine types, including immunogenicity, booster requirements, antigen stability, and recommended storage conditions. Live attenuated vaccines generally elicit strong humoral and cellular responses with minimal booster needs but are sensitive to environmental conditions. Whole inactivated vaccines tend to elicit a moderate and mainly humoral response, often requiring adjuvants and multiple-doses regimens for long-lasting immunity; they are generally highly stable under refrigeration conditions. Subunit, virus-like particle (VLP), recombinant protein, DNA, mRNA, and viral vector vaccines vary in the balance of humoral and cellular immunity, the necessity for booster doses, stability of the antigen, and specific storage requirements, highlighting critical considerations for vaccine design, deployment, and long-term efficacy.

Vaccine type	Immunogenicity	Booster Requirement	Antigen Stability	Storage Conditions
Live attenuated vaccines 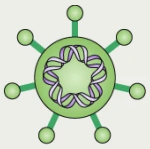	High; elicit both humoral and cellular immunity	Often not required	Sensitive to heat, light, and chemical agents	Refrigeration at 2–8 °C
Whole inactivated vaccines 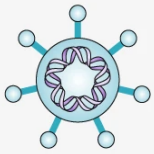	Moderate; primarily humoral response; adjuvants usually required	Required; multiple doses for long-lasting immunity	High stability; proteins may degrade if mishandled	Refrigeration at 2–8 °C
Virus-like particle (VLP) vaccines 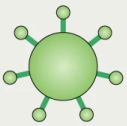	High; elicit both humoral and cellular immunity	Often required for sustained protective titers	Relatively stable	Refrigeration at 2–8 °C; lyophilized formulations
Recombinant protein vaccines 	Moderate; primarily humoral response; adjuvants often required	Required; multiple doses needed for durable protection	Good stability; susceptible to proteolytic degradation or denaturation if improperly formulated	Refrigeration at 2–8 °C; lyophilized formulations
DNA vaccines 	Variable; generally stronger cellular immunity; weaker humoral response	Often required for robust protective titers	Relatively stable; resistant to heat and enzymatic degradation	Refrigeration at 2–8 °C or frozen for long-term storage
mRNA vaccines 	High; elicit both humoral and cellular responses	Often required; dosing regimen influences protection	Unstable; sensitive to RNases and temperature	Typically frozen at -80 °C (-20 °C in some cases)
Viral vector vaccines 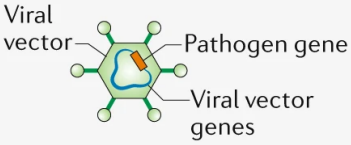	High; stimulate humoral and cellular responses; dependent on vector type	May be required, especially if pre-existing anti-vector immunity exists	Relatively stable; some vectors are sensitive to high temperatures	Refrigeration at 2–8 °C; some require freezing for long-term storage

1.3 SARS-CoV-2: A critical case study

At the end of December 2019, a series of cases of atypical pneumonia of probable infectious origin was notified in Wuhan (Hubei Province, China). The isolation of the pathogen confirmed the viral etiology of this febrile respiratory disease, identifying a new Coronavirus as the causative agent. Due to sequence homology with another *Betacoronavirus* of zoonotic origin, Severe Acute Respiratory Syndrome Coronavirus (SARS-CoV), the new virus has been renamed Severe Acute Respiratory Syndrome 2 (SARS-CoV-2). The disease caused by this is known as Coronavirus Disease (COVID-19 for short)[92–95].

To date, SARS-CoV-2 is the third Coronavirus of zoonotic origin that in less than two decades has been able to cross the species barrier and infect humans, causing severe lung infections, along with the Severe Acute Respiratory Syndrome Coronavirus (SARS-CoV) and the Middle East Respiratory Syndrome Coronavirus (MERS-CoV)[96,97]. Unlike other human coronaviruses, SARS-CoV, MERS-CoV and SARS-CoV-2 have been widely documented to be much more pathogenic and lethal due to their tendency to infect the lower respiratory tract. The resulting lung damage and acute respiratory distress syndrome (ARDS), in addition to septic shock due to systemic extension of infection and abnormal activation of the immune response, can rapidly lead to multi-organ failure, with almost inevitably fatal outcomes[98,99].

Despite some common characteristics shared by these three viruses, in particular with regard to the animal reservoir (all of them probably derive from bat coronaviruses[93,100–104]), the mechanism underlying their pathogenicity, the human-to-human transmission route and, at least to some extent, the range of partially overlapping clinical manifestations[105,106], the new Coronavirus has some unique characteristics (in particular remarkable transmissibility), which have allowed it to spread uncontrollably globally, regardless of the containment measures adopted. On March 11, 2020, the World Health Organization declared a state of pandemic. To date, more than 770 million confirmed cases and about 7.1 million deaths in more than 200 countries are attributable to SARS-CoV-2 infection[107]. From this point, the pandemic increased exponentially, with unprecedented and far-reaching consequences on the social and economic level. The implementation of testing facilities, hospital wards dedicated to COVID-19 patients, the fast development of vaccines to stem SARS-CoV-2 almost uncontrolled spread led to a slow but promising decrease in COVID-19 cases and deaths and led to the declaration of the end of the pandemic phase[108].

In the pandemic scenario, great concern was aroused by the continuous genetic evolution of SARS-CoV-2 which has been and still is responsible for the emergence of new variants bearing mutations that can contribute to the spread of the virus as well as the possible evasion of the immune response (both natural and vaccination-induced). In particular, it was the accumulation of mutations in the gene coding for the Spike that caused great apprehension not only because this glycoprotein mediates the initial attack and entry of the virus into the cell[109], but also because it is the main target of neutralizing antibodies produced as a result of infection or vaccination[110].

1.3.1 General overview

Coronaviruses are a very diverse family of viruses belonging to the order *Nidovirales*, suborder *Nidovirinae*, family *Coronaviridae*. This includes the subfamily *Orthocoronavirinae*, which is divided into four genera (*Alpha-*, *Beta-*, *Gamma-* and *Deltacoronavirus*) based on their phylogenetic relationships and the structure of their genome. *Alpha-* and *Betacoronaviruses* infect mammals, including humans, while *Delta-* and *Gammacoronaviruses* have a wider host spectrum and are able to infect, in addition to mammals, also avian species. In both animal hosts and humans, they cause a broad spectrum of respiratory and gastrointestinal manifestations. All known human coronaviruses belong to the *Alpha-* and *Betacoronavirus* genera. HCoV-NL63 and -229E belong to the genus *Alphacoronavirus*; HCoV-OC43 and -HKU1, SARS-CoV and MERS-CoV belong to the *Betacoronavirus* genus. Lineage A includes OC43 and HKU1; lineage B includes SARS-CoV and SARSr-CoV from bats. The C lineage includes MERS-CoV and several bat coronaviruses. Lineage D is represented solely by bat coronaviruses[111,112].

Coronaviruses are enveloped viruses and, when observed under an electron microscope, have a rounded structure with a diameter of approximately 80 to 150 nm. A peculiar feature of these viruses, from which they derive their name, is the presence, on the envelope, of protrusions consisting of glycoprotein S (~ 150 kDa) organized into homotrimers, which together form a crown surrounding the virion. S-glycoprotein trimers are class I fusion proteins and are responsible for the interaction with the cell receptor and the subsequent internalization of the virion and therefore determine the host and tissue tropism of the virus, as well as its pathogenicity. The membrane protein, or M protein (~ 25-30 kDa), is the most abundant structural protein and plays a central role in the late stages of the viral replication cycle, in particular in the assembly of viral progeny and in their egress from the cell, also contributing to the

extracellular morphology of the virion. The envelope protein, or protein E, is a highly variable protein among coronaviruses, present in small amounts in the virion. Like the M protein, it intervenes in the assembly and release of the virus from the infected cell, but unlike this it is not strictly necessary for viral replication, even if it promotes pathogenesis. The nucleocapsid protein, or N protein, binds and stabilizes genomic RNA strands to form a helical-shaped ribonucleoprotein complex. The N protein also binds nsp3, a key component of the viral replication complex, and the M protein, thus promoting, by contiguity, the transcription of the viral genome and its subsequent packaging within the mature viral particle[113,114] (Figure 1a).

The genome of SARS-CoV-2 (Figure 1b), like that of all coronaviruses, consists of a linear single strand RNA with positive polarity, ranging in size from 26 to 32 kb. Based on the characteristics of their genome, viruses belonging to the Coronaviridae family are attributable to class IV viruses, according to the Baltimore classification system. The genome has the structure and function of a messenger RNA so it has, at the 5' end, a cap of 7-methylguanosine, and, at the 3' end, a poly-A tail. At both ends there are untranslated sequences that contain cis-regulatory structures essential for genomic RNA translation and transcription[115,116]. The coronavirus genome comprises a total of 14 open reading frames (ORFs). At the 5' there is a large ORF, called ORF1ab, which overall occupies two thirds of the genome. ORF1ab encodes 16 non-structural proteins (nsp), which make up the RetroTranscription Complex (RTC) and are involved in the processes of transcription and modification of RNAs, including those responsible for proofreading and thus maintaining genome integrity. At the 3' of the genome there are the ORFs that code for the structural proteins mentioned above; these are produced by translation of a series of nested subgenomic mRNAs (sg mRNAs). Interspersed among the genes coding for structural proteins are a variable number of genes coding for accessory proteins, which are poorly conserved within the family and for which, in most cases, the function has not yet been well understood, although some are suspected to intervene as determinants of pathogenicity and modulators of the host's immune responses[116,117].

1.3.1.1 Major antigenic sites and elicited responses

For what regards humoral immune responses, the Spike glycoprotein is the major contributor in the activation of an effective antiviral response. Trimeric S glycoproteins (Figure 1c) are class I fusion proteins divided into two distinct functional domains, S1 and S2. The N-terminal S1 subunit, exposed on the surface of the virion, contains the

receptor binding domain (RBD) whose function is to bind the membrane receptor of the target cell, thus determining the tropism and pathogenicity of the virus[118]. In addition to the RBD, the S1 subunit also contains an additional domain, referred to as the N-terminal domain (NTD). The membrane receptor used by SARS-CoV-2 is ACE2, the same recognized by SARS-CoV. The C-terminal subunit S2 contains the fusion peptide, which, by bringing the cell membrane and the viral envelope into close proximity, mediates their fusion. Activation of the fusogenic activity of the S2 subunit requires proteolytic cleavage of two specific sites. The first cleavage occurs at the level of the S1/S2 interface, specifically at the level of the peptide bond Arg685-Ser686, resulting in separation of the two domains, which remain non-covalently associated, and exposure of the S2 domain in a pre-fusion conformation. The second cleavage occurs at the level of the S2' site (peptide bond affected Arg815-Ser816), with exposure of the fusion peptide Ser816-Phe833 and profound conformational change of the glycoprotein, which is now competent for the fusion between the viral envelope and the cell membrane, resulting in the release of genomic RNA inside the host cell[119–123]. Although the RBD domains of SARS-CoV and SARS-CoV-2 recognize the same membrane receptor, the study of the crystal structure of the SARS-CoV-2 RBD has highlighted small but important differences compared to the SARS-CoV counterpart, which determine the greatest binding affinity to the receptor (10 to 20 times greater)[124,125], but if we consider the spike as a whole, the affinity of SARS-CoV and SARS-CoV-2 for ACE2 is comparable[109,126]. These results might seem paradoxical and contradictory, but we must consider that the RBD is dynamic and can be in a so-called "standing-up state", which allows binding to the receptor, or in a "lying-down state", which is not able to bind the receptor[127,128]. Cryo-electron microscopy studies have shown that the RBD of SARS-CoV is predominantly in the "standing-up state", while the RBD of SARS-CoV-2 is in the "lying-down state"[121,124]. Thus, despite the fact that the RBD of SARS-CoV-2 has a higher affinity for ACE2, it is less accessible. The result is that the binding affinity between spike and ACE2 is comparable for SARS-CoV and SARS-CoV-2. The advantage of having a less accessible RBD is greater protection against immune responses (a conformational masking mechanism also adopted by other viruses, such as HIV[129] and picornaviruses[130]). However, it is also true that this could compromise the recognition of the receptor and consequently the entry into the host cell[126].

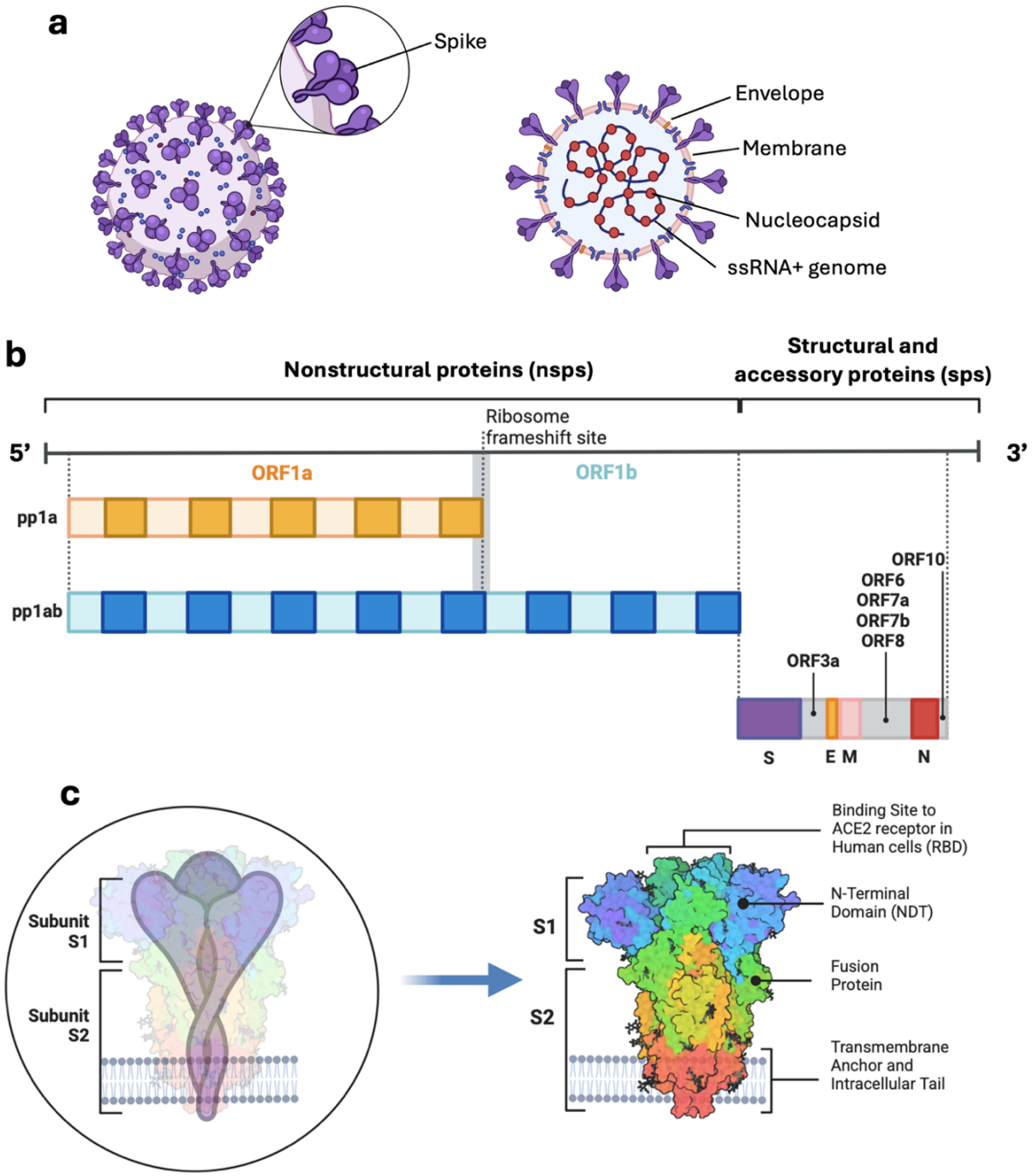

Figure 1. Structural and genomic organization of a coronavirus. A. Schematic representation of the coronavirus virion, highlighting the spike (S) protein protruding from the viral envelope. The right panel illustrates the internal structure, including the single-stranded positive-sense RNA (ssRNA+) genome encapsidated by the nucleocapsid (N) protein, along with the envelope (E) and membrane (M) proteins. B. Genomic organization of the coronavirus. The 5' end encodes nonstructural proteins (nsps) within ORF1a and ORF1b, which are translated as polyproteins pp1a and pp1ab following a ribosomal frameshift. The 3' end encodes structural proteins (S, E, M, and N) and accessory proteins (ORF3a, ORF6, ORF7a, ORF7b, ORF8, and ORF10). C. Structural representation of the spike (S) protein. The left panel shows the membrane-anchored S protein divided into subunits S1 and S2. The right panel provides a detailed view of the spike protein, highlighting key functional domains, including the receptor-binding

domain (RBD) for ACE2 interaction, the N-terminal domain (NTD), the fusion protein region, and the transmembrane anchor with its intracellular tail.

Given the importance of the interaction between the S glycoprotein and the ACE2 membrane receptor for the replication cycle, this process is an important target for immune responses, especially for humoral adaptive ones. Considering the crucial role played in particular by the S1 subunit of the Spike protein in the very early stages of the viral replication cycle, it is the main target of the humoral immune response. In fact, it has been shown that neutralizing antibodies from convalescent patients can inhibit viral replication by directly interfering with the binding between RBD and ACE2 or by destabilizing the pre-fusion complex by binding to different epitopes[131]. Specifically, evaluating the neutralizing activity of convalescent sera, it was estimated that antibodies directed against RBD represent about 80-90% of total antibodies, while those directed against NTD represent a smaller percentage, varying between 5 and 20%, but no less important in neutralizing the virus[110]. The reduced immunogenicity of NTD may be due to the N-terminal glycan coating[121,132,133]. The immune response represents a selective pressure to which the virus is subjected, which therefore favors the onset of mutations, both in RBD and NTD, which reduce or completely abrogate the ability of the specific antibodies produced during infection to recognize the epitopes against which they are directed. Most of the variants evolved during the pandemic have caused an important antigenic change and consequently have been responsible for a lower susceptibility to neutralization, as evidenced by the cases of reinfection that are increasingly being reported in literature[134].

On the other hand, T cells also play several critical roles during SARS-CoV-2 infection, beyond their direct cytotoxic functions. CD4+ T cells are important for orchestrating the immune response, particularly by helping B cells produce neutralizing antibodies against the spike protein[135]. Without this T cell help, the antibody response may be weak or poorly sustained, which could lead to reinfection or incomplete viral clearance. Moreover, CD4+ T cells secrete cytokines such as interferon-gamma (IFN-γ), which activate macrophages and enhance antiviral defenses[136]. CD8+ T cells, by recognizing and killing infected cells, limit the spread of the virus within the host. Studies have shown that individuals with robust CD8+ T cell responses tend to have faster viral clearance and less severe disease[137].

The Spike protein is the most studied and immunologically significant target for T cells. Both CD4+ and CD8+ T cell responses are generated against the spike protein.

CD4+ T cells specific to the spike protein assist in the activation of B cells to produce neutralizing antibodies, while CD8+ T cells recognizing spike-derived peptides kill infected cells. Several studies have identified a range of T cell epitopes within the spike protein, some of which are conserved across different SARS-CoV-2 variants, making them valuable targets for vaccine development[136,138]. In contrast to the humoral immune response, in the cell-mediated one, the other structural proteins of SARS-CoV-2 also contribute. The N protein, which is abundantly produced in infected cells and exposed on the plasma membrane, is another major target for CD8+ T cell responses, which have been shown to be crucial for viral clearance. Furthermore, T cell responses to the N protein tend to be broader and less affected by mutations in circulating variants compared to responses against the spike protein. Moreover, while not as immunodominant as the spike or nucleocapsid proteins, both M and E proteins can elicit T cell responses, suggesting that these proteins contribute to the overall T cell-mediated immune response[138,139].

The importance of T cell-mediated immunity in SARS-CoV-2 infection has significant implications for vaccine design. Most COVID-19 vaccines focus on generating neutralizing antibodies against the spike protein. However, the emergence of variants with mutations in the spike protein, such as Delta and Omicron, has raised concerns about vaccine efficacy, particularly in terms of antibody escape. T cell responses, by targeting multiple viral proteins beyond the spike, are less affected by these mutations[140,141]. Thus, incorporating additional viral proteins that elicit T cell responses may enhance vaccine efficacy, particularly in the face of emerging variants, making them a key component of long-lasting immunity[142]. In the context of whole inactivated virus vaccines, if, on the one hand they would be able to present to adaptive immunity the full array of viral proteins for B and T cell activation, all aforementioned limitations regarding the induction of a robust and effective T cell response must be taken into considerations.

1.3.2 COVID-19 vaccines

To date, 12 vaccines have received approval by the World Health Organization for global use. These are based on four different vaccine production platforms: inactivated virus vaccines (Sinopharm's Covilo, Sinovac's CoronaVac, and Bharat Biotech's Covaxin), messenger RNA (mRNA) vaccines (Moderna's Spikevax mRNA-1273 and Pfizer–BioNTech's Comirnaty BNT162b2), non-replicating adenovirus vector–based vaccines (AstraZeneca's Vaxzevria and Covishield ChAdOx1, Johnson & Johnson–

Janssen's Ad26.COV2.S and CanSino Convidecia), and protein subunit vaccines (Novavax's Nuvaxovid, Covovax NVX-CoV2373 and SKYCovione). Other vaccines have been approved by other regulatory bodies and have been used or are still currently in use in different countries.

Besides inactivated vaccines, which induce an immune response akin to natural infection, for other vaccine platforms the Spike has been target of great interest for the development of protective SARS-CoV-2 vaccines or for therapeutic mAbs[143]. The use of the spike protein for the development of the first monovalent vaccines based on the ancestral SARS-CoV-2 strain (Wuhan-Hu-1) represented a double-edged sword. While on the one hand the focus on the spike protein, or often only on particularly immunologically relevant domains, determined their initial success, guaranteeing the development of protective immunity against infection in a large portion of the population, on the other hand this approach succumbed to the incessant emergence of new variants[134], with antigenic characteristics that differed significantly from the ancestral strain used for vaccine development and therefore capable of immune escape. This has forced the initially authorized vaccines to be reformulated, making them bivalent vaccines, containing immunogenic epitopes of other variants (particular interest has been placed on the Delta and Omicron variants for their extraordinary escape capabilities)[144]. While the E, M, and N proteins are not primary targets for neutralizing antibodies, they have been demonstrated to immune modulation and may enhance the efficacy of multivalent vaccines, suggesting that future vaccine strategies should consider incorporating multiple structural proteins to elicit comprehensive and long-lasting immunity[83,145].

1.3.3 SARS-CoV-2 evolution, emergence of new variants, reinfections and vaccine breakthrough

The mutations that arise in the genetic material constitute a natural by-product of viral replication: the main cause of the introduction of these random mutations is in fact the intrinsic error rate of the viral polymerase, which is therefore called error-prone. RNA viruses typically exhibit higher mutation rates than DNA viruses as they do not possess proofreading mechanisms. The absence of exonuclease activity increases the rate of point mutation of the genome making it impossible to correct errors during the replication process of the viral genome, consequently enormously increasing the overall load of random mutations, so much so that the concept of viral quasispecies has been introduced to describe the genetic heterogeneity of the viral population that

is formed. consisting of the set of genetically distinct but closely related subpopulations generated around a consensus or master sequence. For RNA viruses, the error rate is at the limit of mutational tolerability (or “error threshold”) so that even small increases in the error rate cause what is called "mutational meltdown" or “error catastrophe”, in which due to the excessive number of mutations the viral fitness plummets, leading to the extinction of the viral species. While it may seem like a questionable evolutionary strategy, provided the viral population size is large enough, maintaining a high error rate allows RNA viruses to produce a myriad of potentially evolutionarily advantageous mutations in a very short time[146,147]. Focusing attention on the propensity to accumulate mutations as a driving force in viral evolution, however, tends to overlook the enormous cost of low replicative fidelity. Most of the mutations that arise have deleterious effects on viral fitness, and only a small minority will have a positive impact on the viral phenotype, conferring an advantage. These mutations can alter various aspects of the biology of the virus, including pathogenicity, infectivity, transmissibility and/or antigenicity. It is therefore tolerance to the mutational burden that determines the nature and extent of genetic diversity that can be maintained in the population. RNA viruses are therefore at an equilibrium point of replicative fidelity, and small changes in one direction or another can have detrimental effects on viral fitness[148].

In the last few years, successive variants have displaced their predecessors through relatively minor genetic mutations, particularly in the spike glycoprotein (S) and other genes, raising concern of the scientific community not only for their greater transmissibility and virulence, but also for their ability to escape the antibody response induced by infection or vaccination. Many of these genetic variants have been classified under the umbrella definition of Variants of Concern, defined as variants which, compared to a reference isolate, have mutations with ascertained or suspected phenotypic consequences associated with changes with relevance to public health, such as increased transmissibility, increased virulence or change in the clinical presentation of the disease, decreased effectiveness of social and public health measures or diagnosis, vaccines or available therapies[149].

The emergence of SARS-CoV-2 variants has posed significant challenges to global vaccination efforts[150]. Studies have shown that variants carrying E484K, L452R, and multiple Omicron-related mutations exhibit decreased susceptibility to neutralization by antibodies induced by mRNA (Pfizer-BioNTech, Moderna), viral vector

(AstraZeneca, Johnson & Johnson), and inactivated virus vaccines (Sinopharm, Sinovac)[151–153]. This reduction led to an increased risk of breakthrough infections, particularly in individuals who have received only the primary vaccine series without booster doses[154–156].

The combination of viral evolution and waning immunity over time necessitated adaptation of vaccines and vaccine schedules to enhance protection in the face of an evolving landscape of SARS-CoV-2 variants. Studies indicated that booster doses with updated formulations, particularly bivalent mRNA vaccines targeting Omicron subvariants, improved neutralizing antibody responses against immune-evasive variants. However, the durability of this protection remains a subject of ongoing research[157].

The continuous evolution of SARS-CoV-2 highlights the need for dynamic vaccine strategies to maintain effective protection. While current vaccines still provide substantial defense against severe disease, the emergence of highly mutated variants underscores the importance of booster vaccinations, updated formulations, multivalent or pan-coronavirus designs, and novel immunization approaches to combat viral immune escape[158].

1.3.4 COVID-19 pandemic global vaccine effort: achievements and challenges

A few months into the pandemic, it became clear that the only possible way to stem SARS-CoV-2 dissemination was to immunize as large a share of the population as possible and many research teams rose to the challenge to develop effective vaccine strategies in a collective global race against the virus. To date, 382 vaccines have been developed[159], but only 12 of these received approval for emergency use by World Health Organization[160]. A variety of platforms were used by the licensed vaccines (mRNA, viral vector, protein/peptide, and inactivated virus). Interestingly, new approaches, i.e. mRNA vaccines, which had been never tested against infectious disease before the pandemic, and much older technologies, such as whole inactivated vaccines, coexisted[161]. The efficacy of these different technologies was compared in terms of neutralizing and binding antibody titers and effectiveness in vitro; the findings indicate that compared to viral-vectors and inactivated virus vaccinations, there may be greater antibody responses to mRNA vaccines and the Novavax protein subunit vaccine[162]. Reported vaccine efficacies varied, ranging from 60% to 94%. However, due to variations in trial design, end point measurement, trial location, population studied, and prevalence of SARS-CoV-2 variants during the trial, it is not

feasible to conduct head-to-head comparisons between the various vaccine platforms[163,164]. Having multiple approaches to achieve the crucial end goal of an effective vaccine was pragmatically more important than delaying studies to enable direct comparisons to be made, which could have delayed vaccine rollout and thereby contribute to increased deaths, even though differences in the setup of the clinical trials make comparisons between vaccines more difficult.

However, despite the effort, achieving global vaccine coverage remains a major hurdle; this is not just a matter of equity but is also an important part of the process to control the virus. The global distribution of COVID-19 vaccines has starkly highlighted the inequalities between industrialized nations and developing countries, particularly in Africa[165]. While vaccines became available at unprecedented speed in 2020, access to these lifesaving tools has been highly uneven[166,167]. High-income countries quickly secured large quantities of vaccines and began widespread immunization campaigns, while many low- and middle-income countries, especially in Africa, faced significant challenges in accessing sufficient doses. This disparity not only raises ethical concerns but also poses a global health risk, as unvaccinated populations remain vulnerable to new variants of the virus[168].

The World Health Organization suggested in 2021 that by the end of June 2022, at least 70% of the world population should be completely vaccinated[169]. Since 70% was thought to be a reliable estimate of the herd immunity threshold, i.e. the bare minimum of COVID-19 vaccines that would permit disruption of the chain of transmissions, this goal was established to provide worldwide COVID-19 protection. Only high-income and upper-middle-income nations met that target. The comparison with the 70% vaccination coverage level is still instructive about the significant disparity in vaccination coverage across nations, despite the fact that COVID-19 herd immunity is now regarded as an elusive goal because of the ongoing emergence of new variants that evade infection-acquired and vaccination-acquired immunity[170].

As of mid-2024 (latest vaccination data update), vaccine coverage in most LMICs remains significantly lower than in industrialized countries (Figure 2). According to Our World in Data, only about 50% of the population in low-income countries had received at least one dose of a COVID-19 vaccine, compared to over 70% in high-income countries. This vast disparity is most pronounced where logistical, economic, and political challenges have exacerbated the vaccine distribution gap, with staggering

examples from Burundi, where the percentage of the vaccinated population (with at least one dose) is below 1%, Yemen (2.75%) and Papua New Guinea (3.74%)[171].

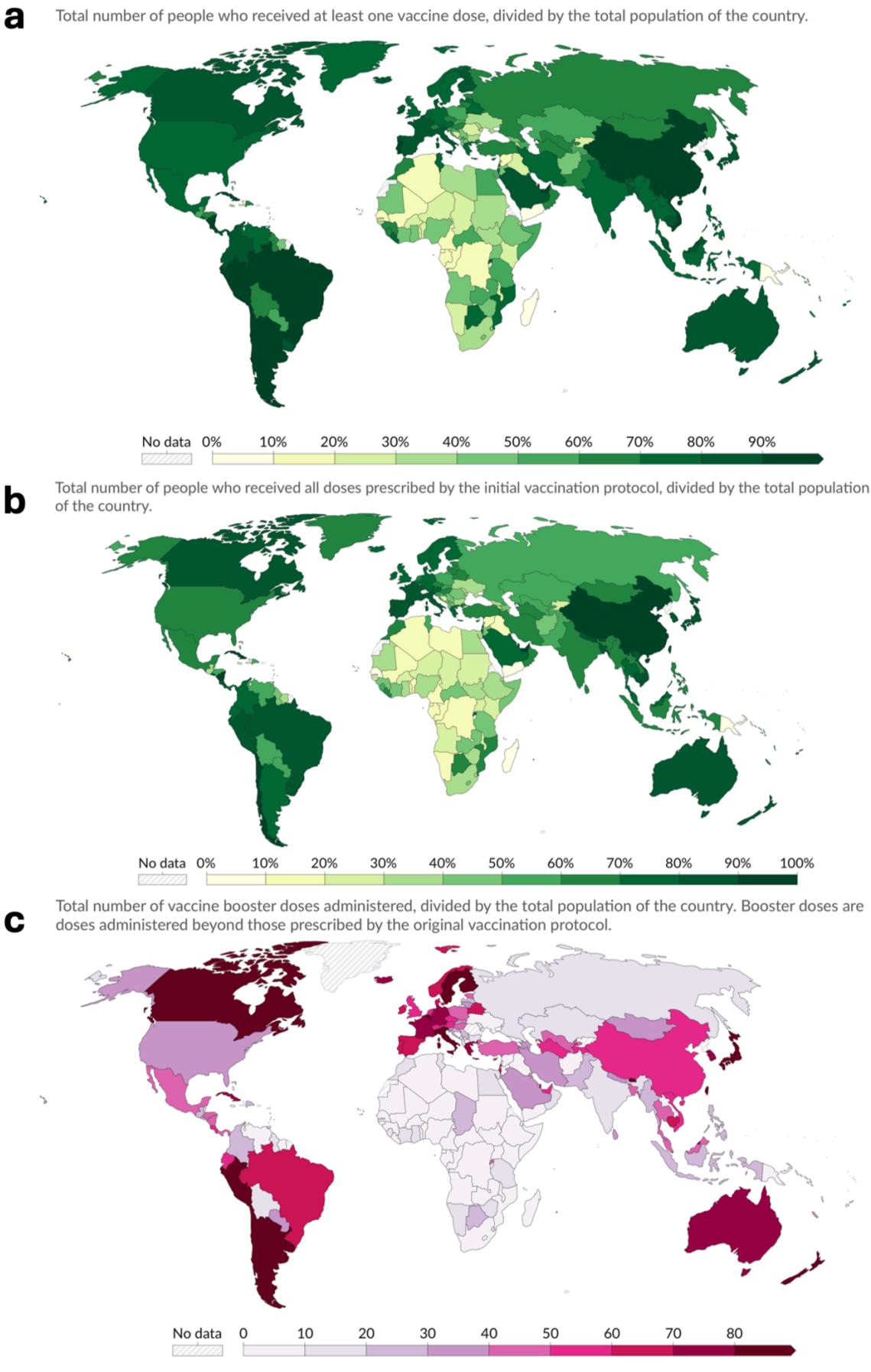

Figure 1. Global Distribution of COVID-19 Vaccine Coverage as of August 12, 2024 [171]. A. Proportion of the population in each country that has received at least one dose of a COVID-19 vaccine, completed the first immunization protocol, or received boosters. B. Proportion of the population in each country that has received all doses prescribed in the vaccination protocol. C. Number of boosted doses administered in each country following the completion of the initial vaccination protocol. Countries are shaded according to vaccination coverage, with darker colors indicating higher percentages. Some regions lack data, represented in gray. The map highlights disparities in vaccine distribution, with higher coverage in North America, Europe, and parts of Asia, while lower rates are observed in several African nations.

By jointly analyzing vaccine coverage (doses of vaccine doses received per % of population)[172], gross domestic product (GDP) per capita[173], and the total final supply of vaccines secured or expected through bilateral agreements, donations, international aid, and domestic procurement[174], strong positive correlation emerges between GDP per capita and vaccine coverage (Figure 3): countries with higher GDP levels are consistently positioned toward the upper-right of the chart, indicating both broader access to vaccines and higher administration rates. These nations, primarily in Europe, Oceania, and parts of the Americas and Asia, not only secured significantly larger vaccine stocks—as illustrated by the larger bubbles—but also succeeded in delivering them to a greater share of their populations. In contrast, countries with lower GDP per capita cluster in the lower-left quadrant, reflecting limited fiscal capacity, smaller secured supplies, and substantially lower vaccination rates. This pattern underscores how national income is a major determinant of both the ability to procure vaccines and the infrastructure necessary to distribute them effectively. Exceptions, such as certain Oceanic countries with moderate GDP but very high vaccine coverage, suggest the influence of targeted external support or efficient health governance, while isolated cases of high-income countries with moderate coverage may point to delays in rollout or public hesitancy. Overall, the data demonstrate a pronounced inequity in global vaccine distribution, tightly coupled to economic disparities, and underscore the critical need for mechanisms that ensure equitable access regardless of national income levels.

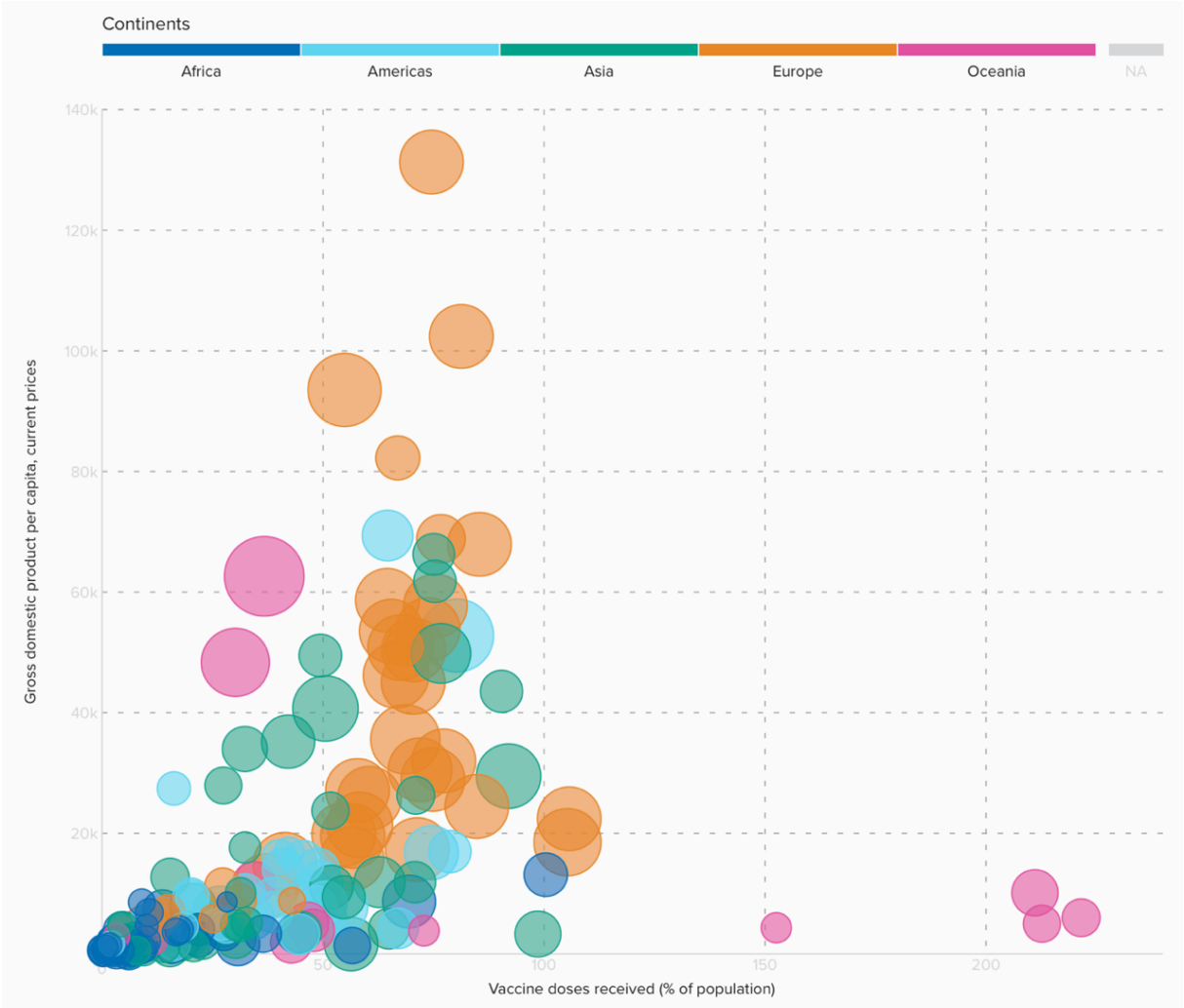

Figure 2. Relationship between COVID-19 vaccine coverage, GDP per capita, and total secured vaccine supply across countries. Each bubble represents a country, with its position indicating the percentage of the population vaccinated (x-axis) and GDP per capita (y-axis); bubble size reflects the total vaccine supply secured or expected as a percentage of the population, and colors denote continents. The chart reveals a clear positive correlation between GDP per capita and vaccine coverage: higher-income countries tend to secure larger vaccine supplies and achieve greater population coverage, while lower-income countries remain concentrated in the lower-left quadrant, with limited access and administration capacity. This distribution highlights persistent global inequalities in vaccine availability and uptake, closely linked to economic resources[175].

Much of Africa's access to vaccines has come through international aid, particularly through COVAX (Coordinated by Gavi, the Vaccine Alliance, the Coalition for Epidemic Preparedness Innovations (CEPI) and the WHO), which, moved by the motto "no one is safe, until everyone is safe" aimed to provide vaccines to low- and middle-income countries. However, COVAX has faced numerous challenges, including delays in vaccine deliveries and inadequate funding. The initiative initially set a goal to deliver 2 billion doses by the end of 2021, but it fell far short of that target,

primarily due to supply chain disruptions and wealthier countries prioritizing their own populations. Despite the missed target, the COVAX program has delivered nearly 2 billion doses to 146 participating economies by December 31, 2023, contributing to the prevention of approximately 2.7 million deaths in low-income countries enrolled in the initiative[18,176].

One of the primary factors contributing to low vaccination rates in Africa was the limited supply of vaccines[177]. Early in the pandemic, high-income countries dominated the global vaccine market, securing the majority of available doses through advance purchase agreements with manufacturers. As a result, many African countries were left without access to sufficient vaccine doses in the critical first year of vaccine rollouts[166]. COVAX, the global initiative aimed at ensuring equitable access to vaccines, struggled to deliver on its promises due to a combination of funding shortfalls and supply chain disruptions. Many African nations lacked the financial resources to compete with wealthier countries in purchasing vaccines. While industrialized nations could afford to buy vaccines in bulk at premium prices, many African governments relied heavily on donations from COVAX, the African Union, or bilateral partnerships[167]. Even when vaccines became available, the high cost of transporting, storing, and administering the vaccines presented additional financial barriers. For example, vaccines like Pfizer-BioNTech and Moderna require ultra-cold storage, which many African countries, often lacking basic refrigeration capabilities, struggled to provide consistently. Moreover, the logistical difficulties of distributing vaccines across vast, often rural, areas further hindered Africa's vaccination efforts. Many countries in the region lacked the infrastructure to support large-scale immunization campaigns. In rural and remote regions, reaching populations has been particularly challenging. Poor road networks, limited cold chain capacity, and shortages of healthcare workers have all contributed to delays in vaccine delivery and administration, ultimately leading to vast disparities in vaccination coverage within countries[166].

The cost of vaccines per se also represented a nonnegligible constrain for equal vaccine distribution, with a mean cost of a single dose of the vaccine ranging from $2 to $40 and delivery costs estimated at $3.70 per person vaccinated with two doses. This represents a significant financial burden for low-income countries, where the average annual per capita health expenditure amounts to $41. While the implementation of vaccination programmes was anticipated to result in an increase in healthcare

expenditures across all nations, this impact was particularly pronounced in low-income countries, expected to experience a staggering increase in their health expenditure of 30-60 percent to achieve a vaccination rate of 70 percent of the population. In contrast, high-income countries were projected to increase their expenditure by a mere 0.8 percent to achieve a similar vaccination rate within a year[175].

Addressing these disparities is not only a matter of equity but also a necessity for global health security. The uneven distribution of COVID-19 vaccines between industrialized and developing nations, particularly in Africa, poses significant global health risks. Unvaccinated populations serve as reservoirs for the virus, allowing it to continue spreading and evolving. This creates opportunities for the emergence of new variants, some of which may be more transmissible or capable of evading immunity provided by current vaccines. The Delta and Omicron variants, for example, first spread rapidly in populations with low vaccination rates, demonstrating the global consequences of vaccine inequity[165].

Moreover, the disparity in vaccine distribution perpetuates existing global inequalities. While industrialized nations have been able to resume much of their pre-pandemic economic and social activities due to widespread vaccination, many African countries continue to face significant disruptions. The slower pace of vaccination in these regions delays economic recovery and exacerbates poverty and social inequality.

1.4 Beyond SARS-CoV-2: A look at other global health emergencies

The COVID-19 pandemic has underscored the critical importance of vaccination strategies in safeguarding public health and mitigating the devastating impact of global infectious diseases. With the declaration of end of COVID-19 as a global health emergency made by WHO on 5 May 2023, the world entered a new phase, which nonetheless represents a call to action to use what learnt during the pandemic wisely, to not waste the progress or the lessons of the past three years, but to sustain and learn from them. Now that the pandemic has died out and the threat from the spread of SARS-CoV-2 is no longer so pressing, we need to go back to considering other health emergencies that were wrongly put on the back burner during the pandemic. The most striking example of this is represented by arboviruses, i.e. viruses transmitted to humans by arthropods (mosquitoes, sandflies and ticks). Despite some exceptions,

they are maintained in nature through a transmission cycle involving wild birds or mammals, acting as reservoirs[178], and vector-competent arthropods[179,180].

From a temporal standpoint, over the last two decades we have assisted to an expansion of arboviruses geographical distribution as a consequence of climate change, which created suitable weather condition for competent vectors to thrive, transmission cycles to establish and for human infection cases to skyrocket in once-non-indigenous countries. This led (for some arboviruses, like West Nile virus) and is currently leading (for other, i.e. Dengue virus) to the generation of local outbreaks independently from introduction of historically endemic countries, with an ongoing shift in the epidemiology of these viruses in many European countries[181,182].

Arboviruses pose significant threats to human and animal health globally, with their emergence and spread presenting ongoing challenges. In the face of rampant climate change (rising temperatures, altered rainfall patterns and increased humidity) and natural habitats exploitation, which, soon, could modify or even overturn the ecology of natural hosts and vectors responsible for transmission to humans, contributing to an overall expansion of their habitats, it is plausible that arboviruses will become increasingly prominent players in human pathology all around the European continent. It has in fact already been demonstrated that the degradation of ecosystems and the loss of natural habitats may have driven a change in bird migration routes, favoring arbovirus dispersal to new territories, while increasing uncontrolled urbanization is likely to favor the expansion of mosquito populations, combinedly increasing the risk of vector-borne diseases transmission[184,185]. Anthropogenic factors and therefore derived climate and natural habitats changes are likely to gain more and more relevance in shaping vector-borne pathogens dispersal, favoring the colonization of different territories and niches, and consequently giving them unprecedented chances to evolve and diversify.

Overall, arboviruses are estimated to be responsible for millions of infections annually, albeit the actual number of infections is of complex estimation, largely depending on the presence of effective surveillance programs and the availability of data across different countries. A striking example of a possible evolution of arbovirus epidemiology is represented by Dengue, which is being currently responsible for an unprecedented surge of cases in the Americas as well as in Europe[186], putting the health systems of non-endemic countries on alert for possible outbreaks of autochthonous cases[187–189]. Rising global interconnectedness through travel and

trade can in fact further increases the likelihood of arbovirus introduction into new areas. In such scenarios, the existence of pre-approved or readily adaptable vaccines would allow for rapid deployment during outbreak responses, minimizing both transmission and socio-economic impact. This is particularly relevant in the context of climate-driven increases in extreme weather events and natural disasters, which often create favorable conditions for arboviral outbreaks due to population displacement and compromised public health infrastructure. Current distribution of mosquito-, tick- and sandfly-transmitted Arboviruses are reported in Figure 4.

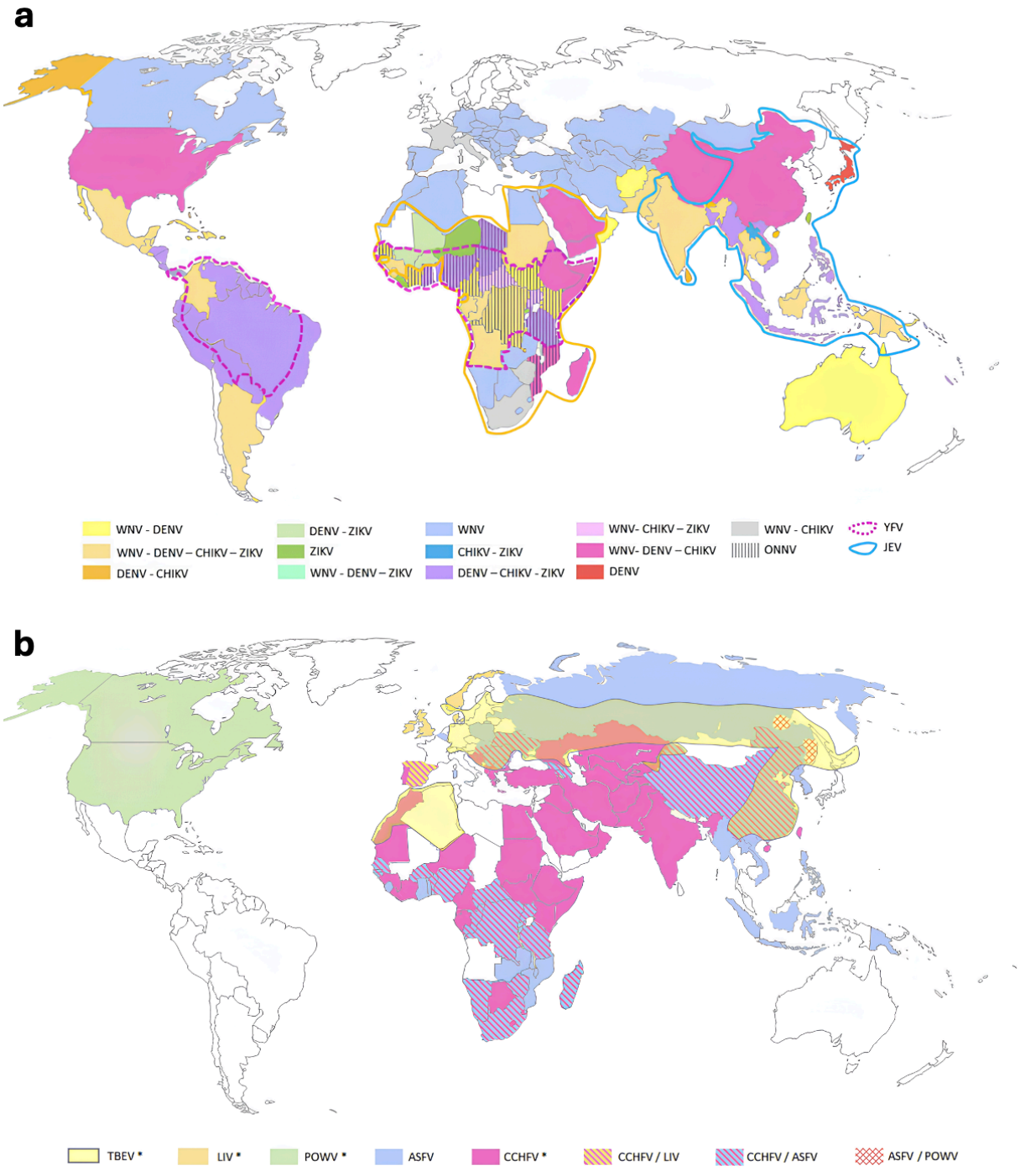

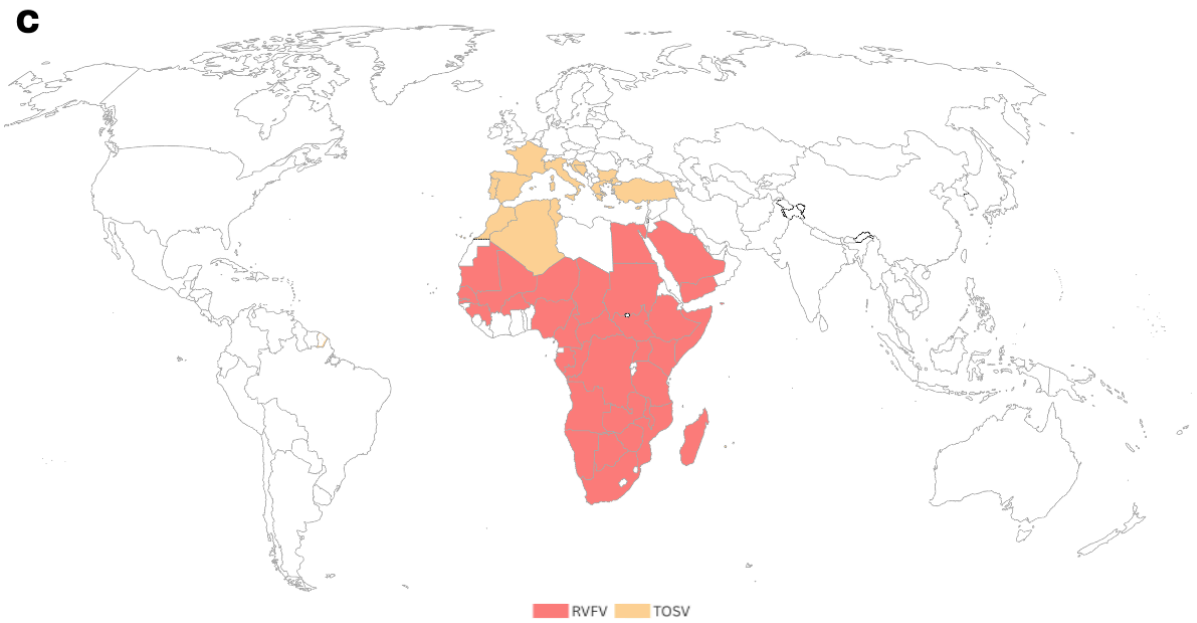

Figure 4. Distributions of arboviruses spread by mosquitos, ticks and phlebotomine vectors. A. Map showing the primary arboviruses spread by *Aedes*, *Culex*, and *Anopheles* species, including the *Alphaviridae* Chikungunya (CHIKV) and O'nyong'nyong virus (ONNV), and the *Flaviviridae* Yellow Fever virus (YFV), Japanese Encephalitis virus (JEV), Dengue virus (DENV), Zika virus (ZIKV), and West Nile virus (WNV); modified from [182]. B. Map of the main arboviruses transmitted by ticks, including the *Flaviviridae* Tick-Borne encephalitis virus (TBEV), Louping Ill virus (LIV), and Powasan virus (POWV), the *Asfiviridae* African swine fever virus (ASFV), and the *Nairoviridae* Crimean-Congo hemorrhagic fever virus (CCHFV); modified from [182]. C. Map of the main arboviruses transmitted by phlebotomine, including the *Phenuiviridae* Rift Valley Fever virus (RVFV) and Toscana virus (TOSV); based on the data presented in [183].

The increasing public health burden posed by arboviruses has highlighted the urgent need for effective preventive tools, particularly vaccines, to mitigate the risk of human infection. The expansion of the geographical range of arbovirus vectors, primarily *Aedes* and *Culex* species, fueled by global warming, urbanization, deforestation, and international mobility, has resulted in the emergence and re-emergence of these viruses in both endemic and non-endemic regions. Therefore, the likelihood of outbreaks is rising in previously unaffected areas, including parts of Europe and North America, underscoring the vulnerability of global populations to vector-borne disease threats[190].

Given the absence of specific antiviral treatments for most arboviruses, vaccination remains the most promising strategy to control their spread and reduce associated morbidity and mortality. However, traditional vaccine development pipelines are often too slow to respond effectively to rapidly evolving epidemiological contexts, as

seen during the Zika outbreak in the Americas or the periodic resurgence of Dengue epidemics with shifting serotype dominance. This calls for the establishment of flexible and responsive vaccine platforms capable of rapid adaptation to emerging threats.

In this evolving epidemiological landscape, the strategic development and deployment of vaccines targeting both endemic and potentially imported arboviruses have become increasingly urgent to prevent outbreaks and reduce morbidity and mortality. In this regard, the development of broadly protective, scalable, and rapid-to-produce vaccine platforms, such as those utilizing HHP inactivation, may offer a crucial advantage. These technologies could enable the creation of flexible, "plug-and-play" vaccine infrastructures capable of addressing multiple arboviruses with minimal adjustments in production protocols. By investing in vaccines against arboviruses as part of climate adaptation and resilience strategies, public health systems can be better positioned to prevent disease burden and contain outbreaks in a warming and increasingly unpredictable world.

For what entails endemic Arbovirus, one of the most relevant for human pathology in Italy is represented by West Nile virus (WNV), which, from being a virus causing sporadic and isolated cases of human infection, became an endemic virus responsible for seasonal outbreaks and among the main causes of aseptic meningitis[191,192].

1.4.1 West Nile virus: general overview

West Nile Virus is a mosquito-borne zoonotic flavivirus (*Flaviviridae* family, *Orthoflavivirus* genus). WNV is a small (approximately 50 nm in diameter), spherical, enveloped flavivirus whose genome consists of a single-stranded RNA molecule of positive polarity that encodes three structural and seven non-structural proteins. The genomic RNA is enclosed within a nucleocapsid formed by the capsid (C) protein, which constitutes the core of the virion and is enveloped by a lipid bilayer derived from the host cell. In this bilayer, the membrane (M) protein and the envelope (E) glycoprotein are organised in dimers (Figure 5a and 5b).

The genome of WNV is constituted of a single-stranded RNA molecule of positive polarity, with an approximate length of 11.000 nucleotides. This genome encodes a polyprotein in a single open reading frame (ORF), which is flanked by two untranslated regions (UTRs). The UTRs are located at the 5′ and 3′ ends of the genome, respectively, and extend for a length of approximately 100 and 400-700 nucleotides. The ORF is translated into a single polyprotein, which is then processed by viral and

cellular proteases, resulting in the production of ten major viral proteins: three structural (C, prM/M, and E) and seven non-structural (NS1, 2A, 2B, 3, 4A, 4B, and 5), as represented in Figure 5c[193].

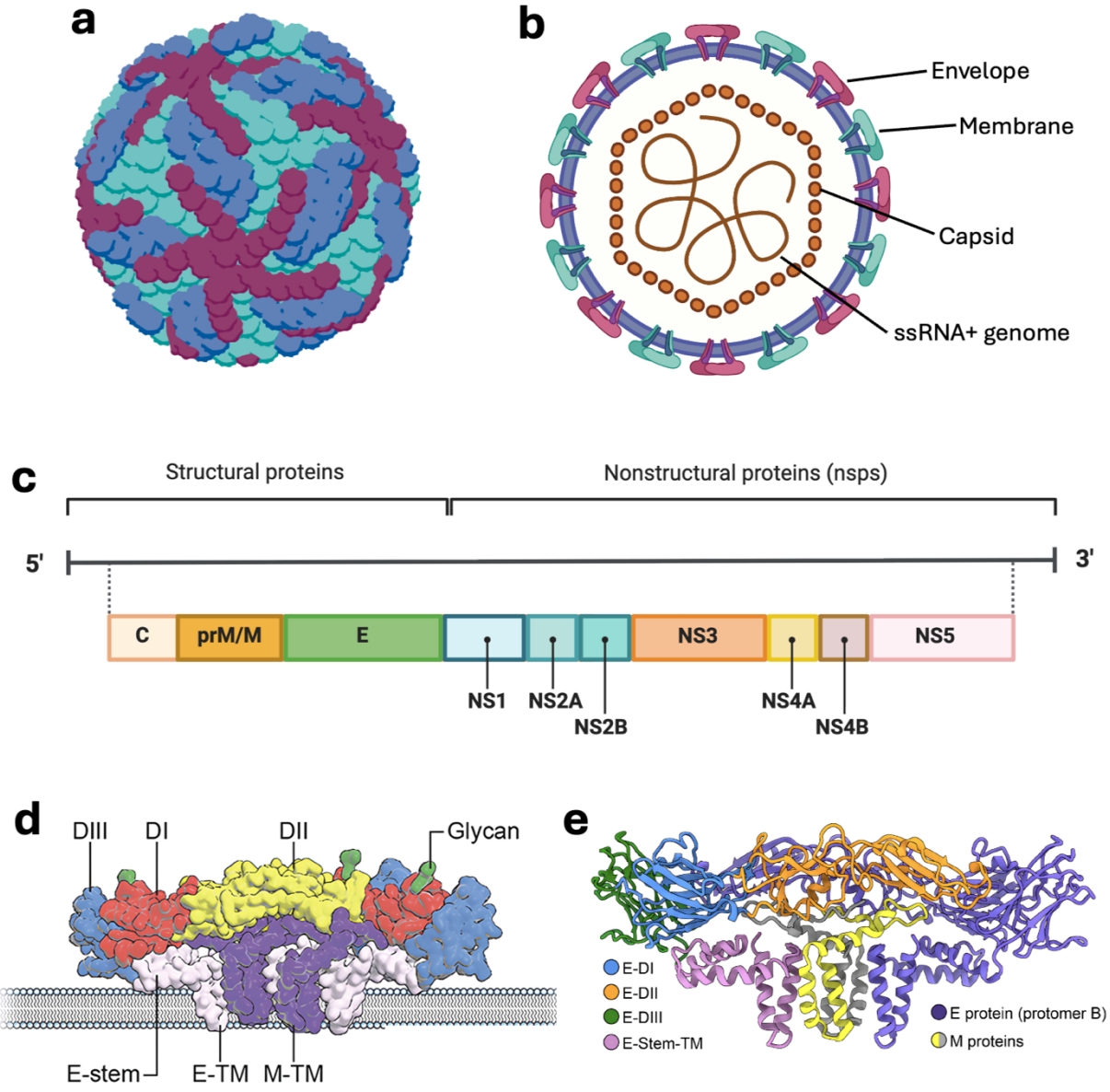

Figure 5. Structural and genomic organization of a flavivirus. A. Schematic representation of the WNV virion displaying the arrangement of E glycoprotein. B. Schematic view of WNV particle internal structure, including the single-stranded positive-sense RNA (ssRNA+) genome encapsidated by the capsid (C) protein, along with the envelope (E) and membrane (M) proteins. C. Genomic organization of WNV. The 5' end encodes structural proteins (C, prM/M and E); the 3' end encodes non-structural proteins (NS1-5). D. Structural representation of the membrane-anchored envelope (E) protein (modified from [194]). E. Crystal structure of an envelope (E) glycoprotein dimer, highlighting key functional domains (modified from [195]).

The structural proteins facilitate viral encapsulation and entry. The E protein has been demonstrated to mediate receptor binding and membrane fusion, while the prM protein has been shown to stabilise immature virions, which are subsequently cleaved into the membrane (M) protein for the purpose of infectivity. Non-structural proteins are vital for replication and immune modulation. It has been established that the NS1 assists in the formation of replication complexes and interferes with Toll-like receptor 3 (TLR3) signalling. In addition, the NS2A/NS4A have been shown to reshape host membranes for the purpose of RNA replication and to suppress interferon responses. The multifunctional NS3 protease and helicase process viral polyprotein and unwinds RNA, while NS5, the RNA-dependent RNA polymerase (RdRp), ensures genome replication and RNA capping. NS5 is the most conserved protein among flaviviruses, thus rendering it a key therapeutic target[196].

1.4.1.1 Major antigenic sites and elicited responses

The envelope (E) glycoprotein of the West Nile virus constitutes the primary surface component of the virion and performs a dual role in receptor binding and membrane fusion. Beyond these essential functions, the E protein plays a critical role in eliciting virus-neutralizing antibodies[197] and mediates key steps in viral attachment, penetration, and membrane fusion[198]. It also contributes to hemagglutination, virion assembly, and maturation, as well as determining host range, cell tropism, and virulence[199,200]. Structure of the envelope protein od Flaviviruses is reported in Figure 5d and 5e.

Structurally, the E protein forms a raft of 90 antiparallel homodimers arrayed on the viral membrane[201]. With a molecular weight ranging between 53 and 60 kDa depending on glycosylation, the E protein belongs to the class II fusion protein family characterized by a unique C-terminal double membrane-spanning anchor. Each monomer is organized into three distinct domains (EDI, EDII, and EDIII) linked by flexible hinges that undergo irreversible conformational rearrangements during viral entry and fusion[202–206]. The homodimeric arrangement of the E protein shields exposure of the DII fusion loop at neutral pH. Within the acidic environment of the endosome, these conformational shifts lead to the dissociation of the E homodimers and expose the conserved fusion peptide (FP) located at the distal end of EDII, facilitating viral–host membrane fusion[198].

EDI, positioned at the N-terminus but centrally located within the three-dimensional structure, forms an eight-stranded β-barrel serving as a hinge between EDII and EDIII.

Composed of approximately 120 amino acids, EDI largely contains type-specific, non-neutralizing epitopes[207,208]. This domain stabilizes the overall conformation of the E dimer and participates in pH-dependent conformational transitions during viral fusion. A conserved N-linked glycosylation site at Asn154, typical of flaviviruses, has been shown to influence viral attachment, neurovirulence, and pH sensitivity[209]. Mutations or deletions at this site reduce neuroinvasiveness and replication efficiency, underscoring its importance in viral pathogenesis. Furthermore, residues within the EDI–EDII hinge region modulate virion stability and neutralization sensitivity, potentially through interactions with cell-surface glycosaminoglycans (GAGs), which act as attachment receptors[206]. EDII forms an elongated finger-like structure composed of two discontinuous peptide regions linked to EDI by flexible loops, collectively forming the EDI-EDII hinge. This hinge region undergoes extensive rearrangement under acidic endosomal conditions, enabling exposure of the fusion loop (FL), involved in fusion and viral entry[210–212]. In immature virions, the prM protein interacts with EDII to shield the fusion loop, preventing premature fusion during viral maturation. Moreover, EDII contributes to antiparallel dimerization of E monomers, and mutations within this domain impair viral replication and attenuate virulence[212]. EDIII, located at the C-terminal end of the E protein, comprises approximately 100 residues organized into a compact immunoglobulin-like β-barrel of six antiparallel β-strands (β1–β6) stabilized by disulfide bridges[213]. This globular domain extends outward from the virion surface, forming protrusions that bear type- and subtype-specific epitopes. EDIII is believed to mediate interactions with host cellular receptors, contributing to viral attachment and entry. Structural and mutational analyses have revealed that alterations within EDIII can result in escape from neutralizing antibody responses.

A stem region comprising transmembrane domains (TM1 and TM2) anchors the E protein to the viral envelope[214]. TM1 functions as a stop-transfer signal, while TM2 serves as an internal signal sequence critical for the proper folding and localization of the NS1 protein[210]. Structural rearrangements involving these transmembrane segments form a hairpin-like configuration, which trimerizes under acidic conditions to promote membrane fusion and increase infectivity[211,215,216]. The carboxy-terminal ectodomain contains two α-helical stem elements (α1 and α2) that connect to the transmembrane region, contributing to the stability and fusion capacity of the protein. Conserved histidine residues at positions 144, 246, 284, and 319, located at

interdomain interfaces, are implicated in pH sensing, uncoating, and trimerization of the E protein under endosomal conditions[217].

The envelope glycoprotein represents the principal antigenic determinant of WNV and constitutes the major target of both humoral and cellular immune responses[218,219]. As the most abundant structural component of the virion surface, the E protein is responsible for eliciting neutralizing antibodies that provide protection against infection and disease progression[220,221]. These antibodies predominantly recognize conformational epitopes distributed across the three structural domains of the E protein (EDI–EDIII)[222,223]. Among these, the lateral ridge of domain III (DIII-LR) has been identified as a dominant epitope for potent neutralizing antibody binding[220,221,223].

Neutralizing antibodies against WNV exert their protective functions mainly through two mechanisms: inhibition of viral attachment by blocking receptor engagement, and interference with the low pH–induced conformational rearrangements required for membrane fusion within endosomes[220,224]. High-affinity antibodies directed toward epitopes on the DIII-LR region prevent the conformational transitions necessary for the exposure of the fusion loop, thereby neutralizing viral entry. In contrast, antibodies targeting epitopes on EDI and EDII are often less potent, recognizing more conserved or partially buried regions that can mediate cross-reactivity but not necessarily sterilizing immunity[221,225].

Studies in murine and human models have demonstrated that antibodies directed against DIII-specific epitopes confer strong and durable protective immunity[221,226]. DIII-targeted antibodies are generally virus type–specific and can differentiate WNV from other flaviviruses such as dengue virus (DENV) and Japanese encephalitis virus (JEV), underscoring their diagnostic and vaccine relevance[226,227]. Conversely, cross-reactive antibodies recognizing conserved epitopes in the fusion loop of EDII, although often weakly neutralizing, may contribute to antibody-dependent enhancement (ADE) of infection, a phenomenon observed across several flaviviruses[225,228,229].

Beyond humoral immunity, the E protein also contributes to the activation of cellular immune responses. $CD4^+$ T helper cells are stimulated by E protein-derived peptides presented on MHC class II molecules, promoting B-cell activation, isotype switching, and germinal center maturation to generate high-affinity neutralizing antibodies and long-lived plasma cells[230,231]. $CD8^+$ cytotoxic T lymphocytes (CTLs) recognize E

protein-derived peptides presented on MHC class I molecules and are crucial for the clearance of infected cells, particularly during acute infection. E-specific $CD8^+$ T cells secrete antiviral cytokines such as interferon-γ (IFN-γ) and tumor necrosis factor-α (TNF-α), which restrict viral replication and contribute to viral clearance[231,232].

While neutralizing antibodies are essential for preventing peripheral infection and controlling viremia, T-cell responses play a decisive role once the virus disseminates to the central nervous system (CNS)[232,233]. In murine models, depletion of $CD8^+$ T cells leads to uncontrolled viral replication within neuronal tissues, demonstrating their essential role in viral clearance from the CNS[231,232]. $CD4^+$ T cells also contribute to protection by secreting IFN-γ and supporting the recruitment and activation of macrophages and microglia[233]. Together, these adaptive immune mechanisms orchestrate effective viral control and limit neuroinvasion.

The immunogenic architecture of the E protein, combining conserved structural motifs with variable surface-exposed epitopes, makes it an attractive candidate for vaccine design. Recombinant subunit vaccines based on soluble E ectodomains or domain III fragments have successfully induced robust neutralizing antibody responses in experimental animal models, correlating with full protection against viral challenge[227]. Furthermore, the incorporation of conserved T-cell epitopes from the E protein into multivalent vaccine platforms may provide a promising strategy to elicit broad cellular immunity while minimizing the risk of ADE[234].

Overall, the WNV E protein functions as a multifunctional immunogen that bridges humoral and cellular immune responses through its dual roles in receptor interaction and immune activation. Elucidating the fine structural determinants that govern antibody binding, T-cell recognition, and immune modulation is critical for the rational design of next-generation vaccines and therapeutic antibodies capable of conferring cross-protective and durable immunity against WNV and related flaviviruses[219,223,234].

Antibodies against WNV proteins other than E have been identified. As introduced above, a subset of infectious WNV virions retain varying levels of uncleaved prM. Antibodies that bind to prM have been identified in WNV immune sera, and prM antibodies have been isolated from both mice and humans[235]. As reported for other flaviviruses, WNV antibodies specific for prM generally display weak neutralizing activity and limited protection in vivo. This likely stems from the limited number of prM molecules present on the surface of partially mature virions, the effects of which

will be discussed in detail below. Antibodies specific for the non-structural protein NS1 that demonstrate protective activity from WNV infection in vivo have been described[236]. Prophylactic treatment with some NS1 mAbs protected mice against lethal WNV infection, despite the fact that NS1 is not associated with the virion itself. NS1 antibodies are hypothesized to bind cell-surface expressed NS1 on infected cells and result in phagocytosis of infected cells through interactions with Fc-γ receptors (FcγR) expressed on macrophages. Finally, antibody responses directed at NS3 and NS5[237], as well as capsid have been observed, but little is known regarding their importance in protecting against WNV infection.

The clinical variability observed in human WNV infections has been attributed, among other factors, to immune-mediated mechanisms and to functional impairments of key immune components, both of which are influenced by host genetic background and age-related factors. Experimental models have provided compelling evidence for age-associated immune dysfunction. For instance, aged mice exhibit significantly reduced populations of total T helper (Th) and B lymphocytes[238]. Moreover, in murine models of age-dependent susceptibility to WNV, T-cell responses are markedly compromised, characterized by diminished cytolytic activity, impaired cytokine secretion, and reduced multifunctionality. Supporting these findings, adoptive transfer of T cells from adult, but not aged, donors effectively conferred protection against WNV infection in immunodeficient recipient mice. Conversely, $CD8^+$ T cells derived from aged mice demonstrated lower infiltration into brain tissues, indicating impaired neuroprotective capacity[239].

In human studies, the phenotypic characterization of WNV-specific T-cell subsets has revealed correlations between immune profiles and clinical outcomes. Patients experiencing neuroinvasive disease or belonging to older age groups tend to display increased frequencies of WNV-specific $CD8^+$ T cells. Furthermore, the $CD4^+$ T-cell repertoire in symptomatic individuals is often skewed toward restricted phenotypes, accompanied by a notable reduction in regulatory T-cell (Treg) frequency compared to asymptomatic individuals[240]. This observation aligns with experimental data showing that Treg-deficient mice exhibit significantly higher mortality rates following WNV infection than their wild-type counterparts, underscoring the protective role of Tregs in modulating immunopathology and limiting host tissue damage[241].

1.4.2 WNV ecology

WNV is maintained in nature through a transmission cycle involving wild birds, acting as reservoirs, in which the infection generally has a mild course but, in some cases, may cause severe neurological complications, potentially leading to death[178], and vector-competent mosquitos. WNV has been detected in over 150 species of mosquitoes belonging to, at least, 11 genera. However, its main vectors are those belonging to the *Culex pipiens* L. complex[179,180], which comprises many different members, such as *Cx. pipiens*, *Cx. quinquefasciatus*, *Cx. australicus*, and *Cx. globocoxitus*, the first two being the most relevant vectors of WNV. Both species are distributed in Africa, Asia and the Americas[242], and *Cx. pipiens* and *Cx. quinquefasciatus* are also present in Europe and Australia[243,244], respectively. *Cx. pipiens* is distributed in temperate regions, while *Cx. quinquefasciatus* habits in both tropical and subtropical areas. *Cx. quinquefasciatus* is regarded as an opportunistic feeder, exhibiting flexible host-feeding preferences that include both avian and mammalian hosts. In contrast, *Cx. pipiens* comprises two recognized biotypes, namely *Cx. p. pipiens* and *Cx. p. molestus*, which differ markedly in their physiological traits and behavioral patterns[245]. Although both forms are synanthropic, *Cx. p. molestus* is more commonly associated with human environments due to its mammophilic feeding behavior, positioning it as a key vector in the zoonotic transmission of WNV from avian reservoirs to humans. Conversely, *Cx. p. pipiens* exhibits a predominantly ornithophilic feeding preference, implicating it as a primary vector in the natural enzootic maintenance of WNV among bird populations[245]. Environmental factors such as temperature, precipitation, and humidity profoundly influence vector population dynamics and viral replication rates. Warmer temperatures shorten the extrinsic incubation period of WNV within mosquitoes, thereby enhancing transmission efficiency. Consequently, climate change and urbanization are expected to expand both the temporal and geographic range of WNV circulation[246].

Among avian hosts, *Passeriformes*, particularly members of the *Corvidae* family, serve as the principal natural reservoirs of WNV. These birds are highly efficient virus amplifiers, capable of developing high-titer viremias sufficient to sustain active viral transmission cycles in nature. Importantly, migratory birds contribute to the long-distance dispersal of WNV, linking enzootic foci across continents along major flyways such as the East Atlantic, Mediterranean-Black Sea, and East African routes. In contrast, resident bird populations are responsible for local amplification and overwintering, supporting virus persistence between transmission seasons. Moreover,

different dispersal scenarios were observed for lineage 1 and 2. Lineage 1 shows a complex evolutionary history due to constant connections and genetic flows among countries and continents around the world. In contrast, lineage 2 has a simpler history, with limited introductions from South Africa to Europe, where it became endemic due to favorable eco-climatic conditions[247].

Environmental and climatic factors exert a profound influence on the ecology and epidemiology of WNV. Temperature directly affects viral replication rates and shortens the extrinsic incubation period within mosquitoes, enhancing vector competence. Likewise, precipitation, humidity, and water availability shape mosquito breeding habitats and seasonal abundance. Urbanization and agricultural irrigation systems create favorable microhabitats for *Culex* mosquitoes, particularly synanthropic biotypes, thereby increasing the interface between vectors, avian hosts, and humans. As a consequence, climate change and land-use alterations are anticipated to extend both the temporal window and geographic range of WNV transmission in temperate zones.

Although species of the *Culex pipiens* complex represent the main vectors, secondary mosquito species, including *Aedes albopictus*, *Aedes vexans*, *Anopheles maculipennis*, and *Ochlerotatus caspius*, may contribute to local or sporadic transmission, particularly under favorable environmental or ecological conditions. The relevance of these alternative vectors often depends on their feeding behavior, vectorial competence, and ecological overlap with both avian reservoirs and human populations.

Transmission is markedly seasonal, typically peaking during late summer and early autumn, when mosquito densities and viral replication reach their maxima. In temperate regions, WNV is thought to overwinter in diapausing *Culex* females or, less commonly, through persistent infection in avian hosts, enabling re-emergence in subsequent transmission seasons. The relative contribution of each overwintering mechanism may vary across latitudes and environmental conditions.

From an epidemiological perspective, horses and humans are regarded as incidental "dead-end" hosts, since the predominantly ornithophilic feeding behavior of *Culex* vectors and the low viremia levels achieved in these species prevent further transmission. Nonetheless, both hosts are highly susceptible to neuroinvasive disease, and infections in these species have significant veterinary, public health, and economic implications[248]. Beyond humans and equines, other mammals such as bats, rodents,

and lagomorphs may act as sentinel or accidental hosts, contributing to local monitoring and ecological understanding of WNV circulation.

In summary, the ecology of WNV is shaped by the intricate interplay among vector species diversity, avian reservoir competence, environmental drivers, and human-induced ecological change. This dynamic system underlies the spatiotemporal patterns of viral emergence and highlights the importance of an integrated One Health approach to surveillance and control (Figure 6a).

1.4.3 WNV epidemiology

Over the past two decades, Europe has witnessed a marked north-ward expansion of WNV's geographic distribution, a shift largely driven by climate change, which has created increasingly favourable weather and environmental conditions for the establishment of transmission cycles and a concomitant rise in human infection cases. A key consequence of climate warming is the proliferation of milder winter temperatures, enabling WNV vectors and infected mosquitoes, particularly species of the genus *Culex*, to overwinter locally, thereby establishing autochthonous viral reservoirs that can generate outbreaks independently of seasonal reintroduction from southern Europe or Africa[181]. For instance, a recent modelling study quantified the isolated contribution of anthropogenic climate change to WNV's spatial expansion across Europe, identifying that current hotspot regions are very likely attributable to warming rather than other anthropogenic changes alone[249]. Concurrently, these shifts in viral ecology, namely prolonged vector activity seasons and enhanced virus transmission to resident bird species, have precipitated a fundamental change in WNV epidemiology across many European countries. Where once WNV infections appeared as sporadic and isolated events, the virus is now an endemic, seasonal zoonotic pathogen responsible for recurrent outbreaks, including cases of aseptic meningitis and encephalitis, often ranking among the principal causes of viral neuroinvasive disease in summer and early autumn[191,192]. An overview of the European epidemiological landscape is presented in Figure 6b.

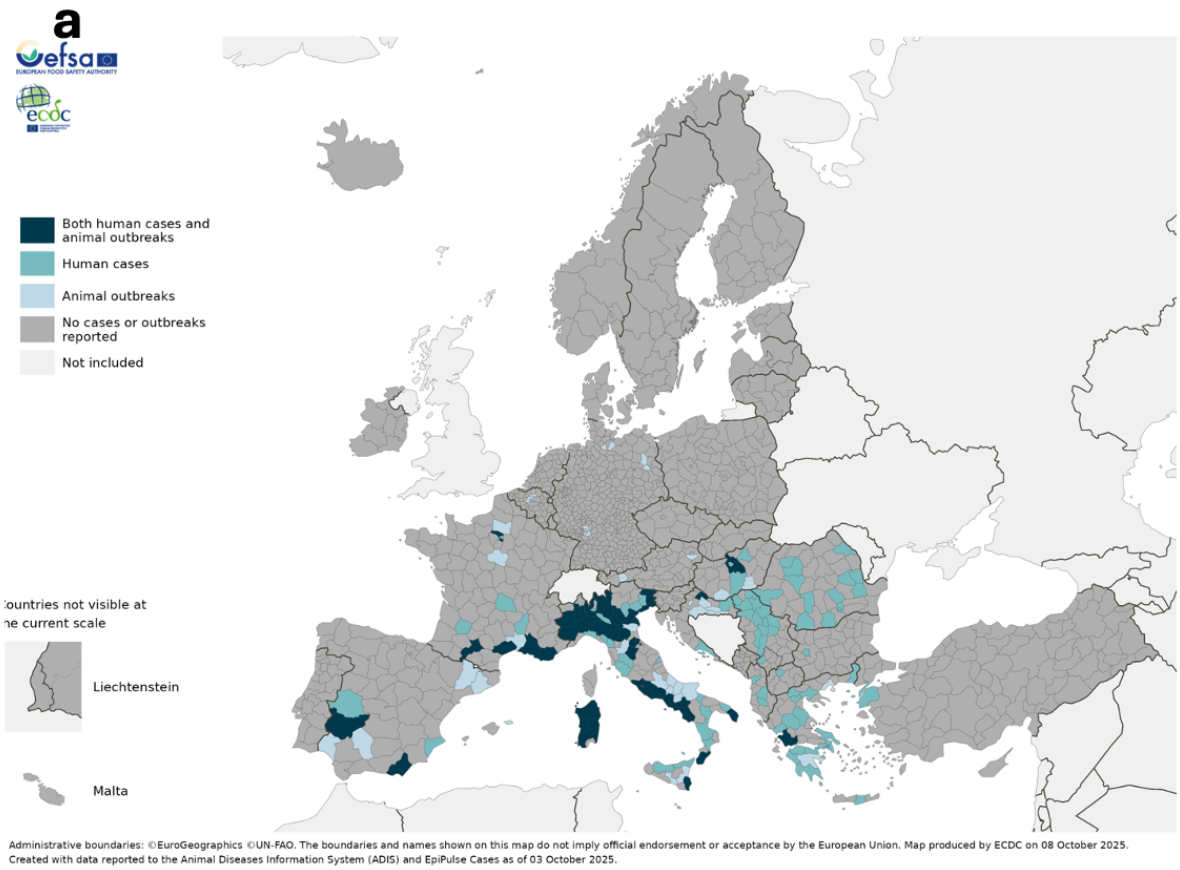
a
Both human cases and animal outbreaks
Human cases
Animal outbreaks
No cases or outbreaks reported
Not included
countries not visible at the current scale
Liechtenstein
Malta
Administrative boundaries: ©EuroGeographics ©UN-FAO. The boundaries and names shown on this map do not imply official endorsement or acceptance by the European Union. Map produced by ECDC on 08 October 2025.
Created with data reported to the Animal Diseases Information System (ADIS) and EpiPulse Cases as of 03 October 2025.

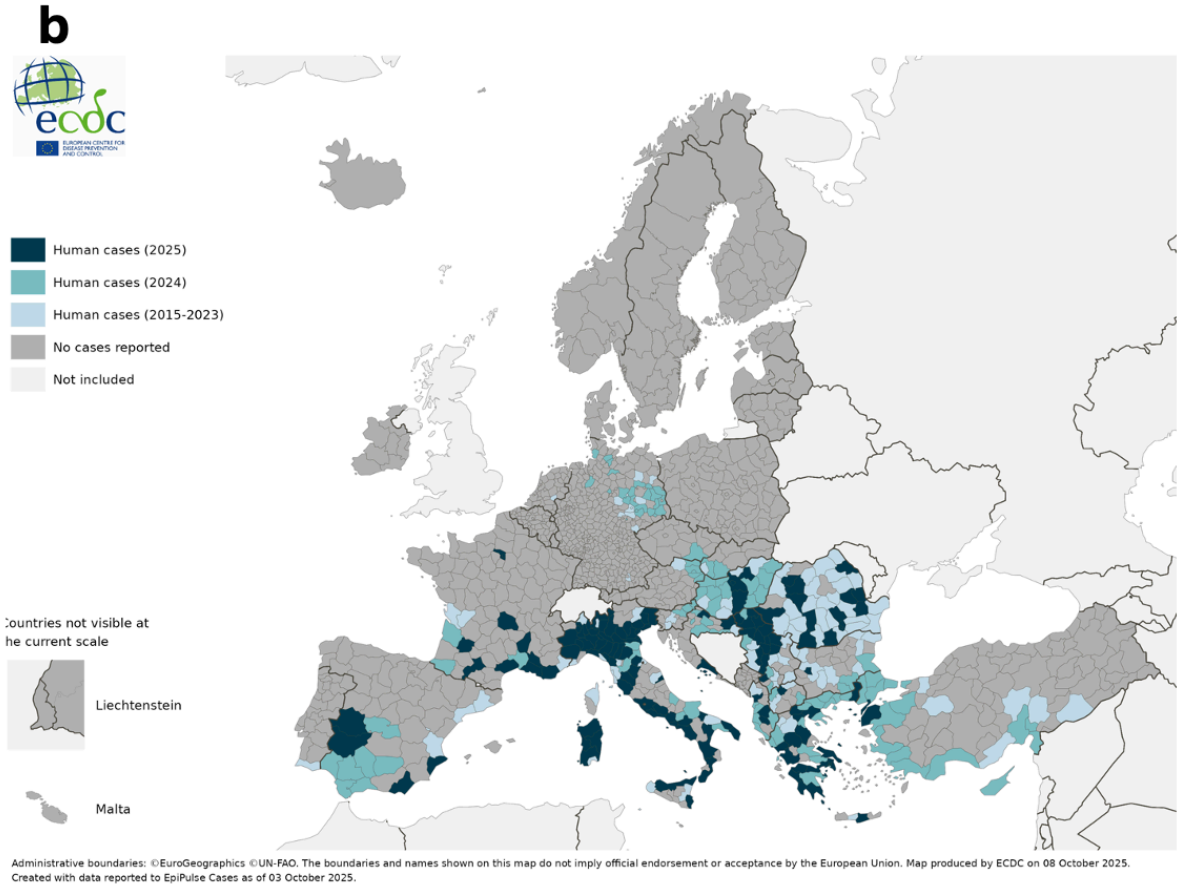
b
Human cases (2025)
Human cases (2024)
Human cases (2015-2023)
No cases reported
Not included
countries not visible at the current scale
Liechtenstein
Malta
Administrative boundaries: ©EuroGeographics ©UN-FAO. The boundaries and names shown on this map do not imply official endorsement or acceptance by the European Union. Map produced by ECDC on 08 October 2025.
Created with data reported to EpiPulse Cases as of 03 October 2025.

Figure 6. Geographic distribution of West Nile virus (WNV) cases and outbreaks in Europe between 2015 and 2025. A. Spatial distribution of WNV human cases and animal outbreaks (birds and equines) reported across Europe as of October 2025. Dark blue areas represent regions where both human cases and animal outbreaks have been detected, while lighter shades indicate regions with either human cases or animal outbreaks alone. Data were compiled from the Animal Diseases Information System (ADIS) and EpiPulse, illustrating the broad ecological overlap between human and animal WNV transmission cycles across the continent. B. Temporal overlay of human WNV cases reported between 2015 and 2025, showing the progressive northward and westward expansion of the virus. Darker tones correspond to more recent transmission seasons (2024–2025), emphasizing the ongoing geographical spread and the establishment of endemic foci in Central and Southern Europe. Administrative boundaries: ©EuroGeographics, CUN–FAO. Maps produced by ECDC (08 October 2025) using data reported to ADIS and EpiPulse as of 03 October 2025.

Despite efforts to control its spread, WNV continues to circulate, with periodic outbreaks reported in various regions worldwide, thus posing a significant public and animal health threat globally being recognized as one of the most relevant mosquito-borne pathogens and one of the most relevant causes of viral encephalitis and meningitis[250–252].

To date, based on the results published annually by the ECDC, autochthonous West Nile cases account for a mean of 95% of total recorded cases in Europe (calculated based on the data of the last seven transmission seasons, 2018-2024), to which Italy constitutes the major contributor, with a mean of 36% of autochthonous infections recorded over the Italian regions[253–258]. Although WNV infections are asymptomatic in the majority of cases (about 80%), a proportion of infected individuals (1%), particularly the elderly and immunocompromised, can develop severe neuroinvasive disease, including meningitis, encephalitis, and acute flaccid paralysis. WNV also has a considerable impact on equine health, with horses often serving as sentinel species for virus circulation. Equine WNV infection frequently presents with neurological symptoms and carries a substantial morbidity and mortality rate, especially in unvaccinated animals[259].

Looking ahead, the convergence of climate warming, land-use change, and increased vector surveillance suggests that the spatial footprint of WNV transmission in Europe may continue to expand, potentially affecting previously unaffected northern and western regions. This underscores the urgency of integrated One Health surveillance strategies, vector-control initiatives tailored to extended transmission seasons, and the development of preventive interventions, including vaccines for humans and equines, to mitigate the evolving threat posed by WNV.

1.4.4 WNV genetic diversity and evolution

West Nile virus (WNV) is characterized by a high degree of genetic diversity, with at least nine distinct phylogenetic lineages identified globally, four of which circulate primarily in Africa. These include lineage 1 (L1), lineage 2 (L2), lineage 7 (L7, later reclassified as Koutango virus), and the putative lineage 8 (L8). In Europe, lineages 1 and 2 are the most prevalent. Regarding WNV L1, the initial introduction of the virus into Europe is believed to have occurred more than 25 years ago from northwestern African countries to Italy or France, where it was first detected in 1998 and 2000, respectively. In contrast, lineage 2 (L2) was first identified in Hungary in 2004 and has since become the predominant strain, exhibiting sustained spread and stable establishment within avian and mosquito populations[247,260].

Similarly to other RNA viruses, WNV displays a quasispecies dynamic, characterized by a heterogeneous population structure and rapid intra-host evolution[261]. This genetic diversity serves as both a driver and a consequence of the virus's ability to adapt to distinct vertebrate hosts and arthropod vectors. Because WNV replicates across a broad phylogenetic spectrum of species, viral populations display variable replicative fitness that is highly sensitive to even minor genetic modifications. Consequently, the accumulation of genetic variation can promote the emergence of novel viral strains with differences in vector competence[262], transmission efficiency[263], viral replication kinetics[264], or ability to induce high-titer viremia in avian hosts[265].

At the molecular level, adaptive evolution has been frequently observed in genes encoding the envelope (E), NS3, and NS5 proteins, which are key determinants of viral infectivity and host adaptation. Mutations within the E protein, which mediates host-cell receptor binding and membrane fusion, have been linked to enhanced neuroinvasiveness and altered antigenicity. Similarly, substitutions in NS3 and NS5, involved in RNA replication and immune evasion, can increase viral replication efficiency and modulate interferon antagonism. Evidence of episodic positive selection in these loci suggests that WNV undergoes recurrent host-driven molecular adaptations, particularly during cross-species transmission events. Compensatory mutations within functionally constrained regions likely buffer deleterious effects, maintaining viral fitness across heterogeneous host environments[266].

The phylogeographic reconstruction of WNV evolution supports a pattern of multiple introductions and local diversification across Europe. Both L1 and L2 strains have

independently established regional subclades following their introduction, reflecting adaptation to local ecological conditions. Molecular clock analyses estimate an average substitution rate of 4-6 × 10^{-4} substitutions per site per year, comparable to other flaviviruses, consistent with a relatively stable evolutionary trajectory under dominant purifying selection. Nevertheless, sporadic bursts of diversification coincide with major epizootic events, suggesting that ecological and climatic factors can transiently accelerate viral evolution. Migratory bird flyways play a central role in facilitating the long-distance dispersal and genetic mixing of divergent WNV lineages between Africa and Eurasia, thereby contributing to the periodic reintroduction of novel genetic variants[246].

The role of both vertebrate and invertebrate hosts in shaping viral diversification and replication fitness has also been extensively examined. Elevated intra-host viral diversity within mosquito vectors has been demonstrated to increase viral fitness in mosquitoes[267]. Mosquitoes exhibit a particularly high degree of intra-host genetic diversification, which appears to be concentrated in genomic regions targeted by the mosquito innate immune response, particularly the RNA interference (RNAi) pathway[268], which exerts strong purifying selection. Therefore, highly diverse yet distinct viral subpopulations are detectable in mosquito saliva. Some studies suggested that intra-vector population expansion and selection vary among mosquito species[269–271]. Notably, WNV populations generated in mosquito hosts often lose replicative fitness in vertebrate hosts, underscoring the antagonistic fitness trade-offs between invertebrate and vertebrate replication cycles[272]. As a consequence, the genetic diversity generate within the vector markedly decreases after transmission to vertebrate hosts, reflecting a more stringent purifying selection in birds. The complex interplay of vertebrate innate immune mechanisms, including interferon-mediated pathways and cellular restriction factors, likely contributes to this constrained diversification.

Beyond host-driven diversification, WNV evolution is further influenced by interactions among co-circulating lineages. The ecological overlap of L1 and L2 in several European regions has raised concerns regarding competitive displacement and potential recombination events. Although recombination is relatively rare in WNV, mosaic genomes have occasionally been detected, suggesting limited genetic exchange that may generate novel phenotypic traits, including altered virulence or vector

competence. These processes highlight the potential for lineage interaction to shape the evolutionary trajectory of the virus.

Collectively, these inter- and intra-host evolutionary dynamics contribute to the relatively slow evolutionary rate observed in WNV, but more broadly in all mosquito-borne flaviviruses, compared with other RNA viruses, highlighting the evolutionary equilibrium maintained between replication fidelity, adaptability, and host specialization. As a consequence, while point mutations and lineage diversification do occur, the antigenic landscape of WNV remains relatively conserved across time and geography, and major antigenic shifts capable of compromising immune recognition are uncommon.

The epidemiological challenge posed by WNV is not driven by antigenic evolution but by ecological and climatic factors that favor viral persistence and expansion. Climate change, by extending the seasonal activity of vector populations, allowing overwintering of infected mosquitoes, and facilitating the northward spread of competent Culex species, has reshaped WNV transmission dynamics in Europe and beyond. These environmental modifications have transformed WNV from a virus responsible for sporadic outbreaks into one that exhibits endemic transmission patterns with recurrent seasonal peaks.

By contrast, the SARS-CoV-2 pandemic demonstrated how high genetic variability can directly drive global health responses. The virus exhibited an exceptional capacity for rapid evolution through the accumulation of spike protein mutations that enhanced receptor binding, transmissibility, and immune evasion. This ongoing diversification led to the successive emergence of variants of concern, such as Alpha, Delta, and Omicron, that significantly altered the epidemiological trajectory of the pandemic and necessitated the iterative reformulation of vaccine antigens to restore and sustain protective immunity. In this context, the adaptive capacity of SARS-CoV-2 exemplified the challenges posed by highly mutable RNA viruses, for which vaccine design must remain dynamic and responsive to antigenic drift and shift.

Therefore, while WNV genetic stability suggests that a single, broadly protective vaccine formulation could provide long-term efficacy without frequent updates, the urgency to develop such a vaccine stems primarily from the shifting ecological and climatic landscape rather than from viral antigenic variability. This contrasts sharply with the SARS-CoV-2 paradigm, where rapid genetic evolution continuously redefined both vaccine design and deployment strategies. In essence, WNV represents

a case in which epidemiological drivers, rather than molecular evolution, dictate vaccine necessity, a reminder that virological stability does not equate to diminished public health relevance in a changing climate.

These considerations highlight that the development of a West Nile virus vaccine should prioritize ecological predictability and sustained immunogenicity rather than antigenic adaptation, representing a distinct paradigm from the continually evolving vaccine landscape seen with SARS-CoV-2.

1.4.5 WNV vaccines

Despite this dual threat for human and veterinary pathology, vaccine availability and implementation remain uneven across sectors. Currently, several WNV vaccines are licensed for veterinary use, particularly in horses, where immunization has proven effective in reducing disease incidence and severity. These vaccines, typically based on inactivated or recombinant technologies, have become a cornerstone of equine preventive medicine in endemic areas[273].

As reported in literature, four vaccines have been approved for horses, including inactivated virus and canarypox-vectored platforms, which have been successful in veterinary medicine (West Nile-Innovator® by Zoetis, US; RECOMBITEK® by MERIAL Ltd., US)[274,275]. West Nile-Innovator® demonstrated 94% protection against viremia, while RECOMBITEK® induced cell-mediated immunity and neutralizing antibodies[274–280].

However, no WNV vaccine has yet progressed beyond phase I or II clinical trials for humans or received regulatory approval for human use[46]. This regulatory gap highlights a key vulnerability in public health preparedness, especially as WNV continues to expand its geographic range due to climate change, vector proliferation, and global mobility.

For example, ChimeriVax-WN02 (Sanofi Pasteur; NCT00442169, NCT00746798), a live attenuated chimeric vaccine, demonstrated seroconversion rates above 90% after a single dose in Phase II clinical trials[45,46,281]. A number of phase I clinical trials have evaluated alternative vaccine approaches, each of which has a distinct immunogenic profile. WN/DEN4-3'Δ30, a live attenuated chimeric vaccine, demonstrated seroconversion rates ranging from 55% to 95%, depending on the dosing schedule, in different clinical trials (NCT00094718, NCT00537147, NCT02186626)[45,46,282]. The efficacy of DNA-based candidates, exemplified by VRC-WNVDNA017-00-VP

(NCT00106769) and VRC-WNVDNA020-00-VP (NCT00300417), has been demonstrated through the observation of robust neutralizing antibody responses, accompanied by seroconversion rates that have surpassed 96% following a three-dose regimen[45,46]. Notable advancements in the field include the development of recombinant subunit vaccines, such as one employing the truncated E protein (rWNV-80E) in combination with adjuvants, which has been shown to elicit robust humoral and cellular immunity in murine models[45,46,283]. Inactivated whole-virus formulations, including HydroVax-001 (NCT02337868), have demonstrated moderate seroconversion rates (31–50%) following two doses, while a formalin-inactivated vaccine has induced peak antibody responses after a booster dose[45,46]. Despite the initial optimism, no candidate has progressed beyond the preliminary trials, underscoring significant challenges concerning immunogenicity, dosing, and scalability for human application.

The development of a WNV vaccine suitable for both human and veterinary applications would offer several strategic advantages. First, it would enable a comprehensive One Health approach to disease prevention, addressing zoonotic risks at the animal-human-environment interface. Second, it would provide a critical tool for outbreak containment in high-risk regions, reducing reliance on reactive vector control and post-exposure clinical care. Third, in the context of pandemic preparedness and emerging infectious diseases, a dual-use WNV vaccine platform could serve as a model for other arboviruses, streamlining production and regulatory pathways through shared technologies such as inactivated virus, recombinant proteins, or HHP-based platforms.

Furthermore, targeted immunization programs, whether seasonal or region-specific, could significantly reduce morbidity and mortality in vulnerable populations, particularly in areas where WNV is endemic or has shown episodic emergence. Vaccination could also protect frontline workers, such as veterinarians, farmers, and public health personnel, who may be at increased risk of exposure.

In conclusion, the development and deployment of a safe, effective, and scalable WNV vaccine for both humans and animals would represent a significant advance in the control of this arbovirus. As climatic and ecological changes continue to favor the spread of mosquito-borne diseases, investing in such cross-sectoral vaccine strategies is not only medically prudent but also economically and ethically justified.

1.5 Development of new viral inactivation strategies

High vaccine production costs and limited distribution in many regions have contributed and still contribute to unequal vaccine access. Vaccine production is complex, resource-intensive, and often centralized in high-income countries (HICs), where advanced biotechnological infrastructure and funding are more readily available. The majority of LMICs rely on imports or donations from HICs for vaccines, which often leads to delays in receiving vaccines and sometimes to restrictions on the volume of vaccines available[284].

The need for affordable vaccine production has been highlighted by the global response to the COVID-19 pandemic. Countries with limited access to vaccines faced devastating waves of infections and significant economic and social disruptions. The inequitable vaccine distribution fueled debates on intellectual property rights, vaccine nationalism, and the ethics of health resource allocation[285]. In response, the World Health Organization and other global health organizations have advocated for innovative, low-cost vaccine production solutions to ensure that LMICs are better equipped to handle future health crises.

Developing low-cost vaccine production strategies is essential to meet growing global demand, especially in LMICs, and to work toward achieving health equity. Developing low-cost vaccine production is not only a moral imperative but also an economic and strategic necessity. Affordable and accessible vaccines can help mitigate the economic impacts of disease outbreaks by reducing healthcare costs and maintaining workforce productivity[286]. Moreover, increased vaccine accessibility promotes health security and stability by reducing the risk of disease spread, which benefits both LMICs and HICs by preventing outbreaks from escalating into global pandemics[287,288].

1.5.1 High Hydrostatic Pressure: application in food science and beyond

High hydrostatic pressure (HHP) processing has emerged in the food industry as a valuable non-thermal food preservation technique, used for microbial inactivation in food products while preserving quality attributes like taste, texture, and nutritional value[289–291]. HPP involves applying pressures typically ranging from 100 to 800 MPa at refrigeration or mild process temperatures (< 45 °C) to food products, often for seconds or minutes, leading to microbial cell damage and death[292–294]. Unlike thermal pasteurization, HHP minimizes heat-induced changes, offering a promising solution for preserving heat-sensitive foods such as juices, seafood and meat products,

or ready-to-eat food[295–298]. Although HHP process does not require active heating, passive heating by adiabatic compression and passive cooling by adiabatic decompression are inevitable.

The effectiveness of HHP in microbial inactivation is due to its ability to disrupt cell membrane integrity, denature proteins, and interfere with cellular processes critical to microbial viability. The applied pressure affects the weakest cellular components first, specifically targeting the cell membrane[299]. Under high pressure, microbial membranes experience compression, leading to structural changes, which increases permeability and ultimately results in cell lysis[300]. In vegetative cells, the effects of high-pressure processing (HPP) extend beyond alterations in cell structure to encompass modifications in metabolic processes. HHP higher than 300 MPa can result in the unfolding and denaturation of proteins, which may also lead to enzyme inactivation[301–304].

Microorganisms exhibit varying degrees of resistance to HHP based on their structural and physiological characteristics. Research shows that gram-positive bacteria generally exhibit higher resistance to HHP than gram-negative bacteria. This resistance is attributed to the thicker peptidoglycan layer in gram-positive bacteria, which provides structural integrity under high-pressure conditions. For instance, *Listeria monocytogenes*, a gram-positive bacterium, demonstrates greater resilience compared to *Escherichia coli*, a gram-negative species[305,306]. Studies have shown that gram-negative bacteria can often be inactivated at pressures around 300 MPa, while gram-positive bacteria require pressures closer to 600 MPa for similar levels of inactivation[299].

Bacterial spores, such as those produced by *Bacillus* and *Clostridium* species, present a significant challenge in HHP processing due to their inherent resistance. These spores can survive extremely harsh conditions by entering a dormant state that protects cellular structures from damage. HHP alone is often insufficient to inactivate spores completely (spores from such species can tolerate pressure treatments above 1000 MPa at room temperature); however, a combination of HHP with moderate heat (referred to as thermos-pressurization) has shown promise in overcoming this challenge[307,308]. While many yeasts and molds are susceptible to HHP, the effectiveness can vary depending on the species and the food matrix. Yeasts like *Saccharomyces cerevisiae* generally exhibit moderate resistance but can be inactivated at pressures below 400 MPa. Recent research indicates that combining HHP with

antifungal agents can improve the effectiveness of HHP in mold inactivation, making it applicable for products prone to fungal spoilage, such as fruits and juices[309].

The primary viral pathogens responsible for food-borne illness transmission include Norovirus and Rotavirus, which cause gastroenteritis, as well as Hepatitis A and E viruses, which cause infectious hepatitis. All of these viruses are non-enveloped RNA viruses, which typically demonstrate high stability against a range of environmental conditions. Norovirus, Rotavirus, and Hepatitis A virus are excreted in the feces of infected individuals and contaminate food surfaces during the handling of food. Furthermore, shellfish and berries have frequently been identified as vehicles for virus transmission, with contamination occurring through contact with sewage or wastewater during their growth. In contrast, the Hepatitis E virus is zoonotic and widely distributed in subclinically infected pigs and wild boars. It has been demonstrated that meat and meat products produced from infected animals may serve as a source for human infection with this virus[310,311].

The use of HHP for the inactivation of viruses has been the subject of published studies for a range of foodborne virus species. This includes hepatitis A virus[312], human norovirus[313], avian influenza virus[314], rotavirus[315], human adenovirus[316], as well as different human pathogenic picornaviruses[317], including poliovirus[318]. The majority of studies have demonstrated that a treatment at 400 MPa for 5 minutes at 4 °C is an effective method for virus inactivation, resulting in a greater than 4 log10 decrease of the contaminating viral load. Nevertheless, the efficacy of HHP was contingent upon a number of variables, particularly the specific virus species under investigation. Consequently, in many instances, the requisite pressure/time combinations for substantial inactivation were considerably higher.

HHP processing has traditionally been applied for microbial inactivation in the food industry, but recent research points to several other promising applications beyond this field. HHP is increasingly being explored in the pharmaceutical and biomedical fields. Its ability to inactivate pathogens without residual chemicals makes it appealing for sterilizing sensitive materials and devices, including medical implants, lab equipment, and pharmaceutical compounds. In this context, HHP presents an alternative to chemical-based sterilization methods like ethylene oxide, which has known health risks and environmental implications[319,320].

1.5.2 HHP mode of action

The typical equipment used for HHP processing comprises a cylindrical pressure vessel and a HHP generation system. In the context of HHP processing, food products are initially placed within flexible packaging (typically a pouch or plastic bottle), subsequently sealed, and then positioned directly within the pressure chamber filled with a pressure-transmitting hydraulic fluid. The removal of air from the vessel is facilitated by an automatic deaeration valve in conjunction with a low-pressure fast fill-and-drain pump. The hydraulic fluid (typically water) within the chamber is pressurized by a pump, generating isostatic pressure, which is transmitted through the package into the foodstuff itself. Once the product has been loaded into the pressure vessel, isostatic pressure is generated either indirectly or directly. Once the desired pressure has been reached, the pressure is maintained for a predetermined period. The pressure is transmitted instantaneously and uniformly, irrespective of the dimensions and configuration of the foodstuff. Consequently, the shape of the foodstuff is maintained even when subjected to extreme pressures. Furthermore, the absence of heat during processing ensures the retention of the food's sensory and nutritional characteristics without compromising microbial safety. In the final stage of the process, the HHP vessel is decompressed to atmospheric pressure. The pressure vessels are discharged by either transferring the pressure-transmitting medium to the reservoir tank or moving a piston out of the vessel[321] (Figure 7).

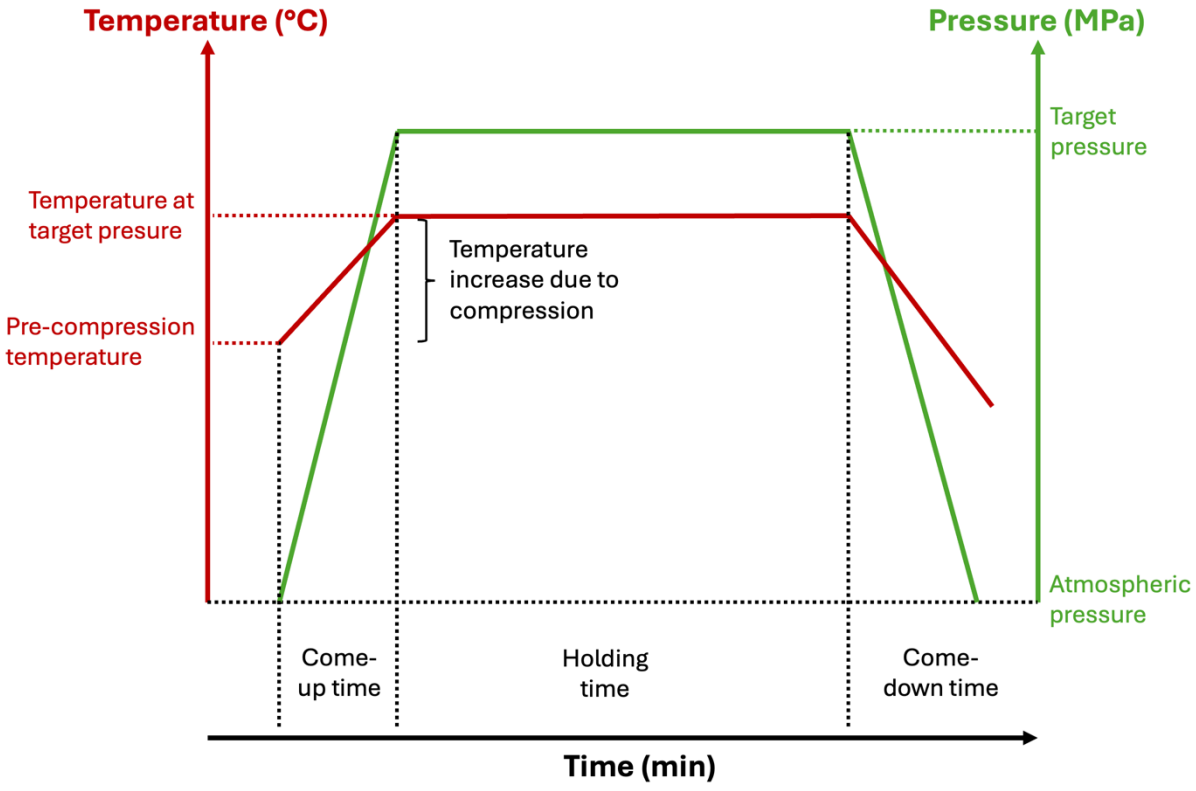

Figure 7. Graphical representation of the relationship between temperature (°C) and pressure (MPa) over time (minutes) during HHP process. The diagram illustrates the phases of the process, including come-up time, holding time, and come-down time. The red line denotes temperature variations, showing an initial pre-compression temperature, a temperature increase due to compression, and stabilization at the target pressure. The green line represents pressure changes, indicating the rise to target pressure, the maintenance phase, and the return to atmospheric pressure.

Two principal techniques may be employed to establish the requisite pressure within the system: direct and indirect pressure generation. HHP can be achieved through direct generation of pressure using a moving piston, which alters the specific volume within the pressure vessel. Accordingly, the pressure can be increased or decreased in accordance with the position of the piston. In contrast, indirect compression entails varying the quantity of pressure fluid in order to adjust the pressure within the vessel. Accordingly, a reservoir tank containing pressure fluid is connected to the vessel via pressure tubes. A system comprising a pump and valves is employed to regulate the volume of pressure fluid within the pressure vessel. In order to generate HHP, fluid is pumped from the reservoir tank into the vessel, thereby increasing the pressure applied. Conversely, after treatment, fluid is pumped from the pressure vessel into the reservoir tank, resulting in a decrease in pressure. Indirect compression method is the most widely used, as it offers more possibilities of fine pressure and temperature control[297].

In the pressure vessel, the products are typically surrounded by a fluid, which is often represented by water, and which acts as the pressurizing medium. Alternatively, fluids other than water can be employed; however, factors such as corrosion prevention properties, fluid viscosity changes under pressure, heat of compression, and effects on foods would have to be taken into consideration. Given the minimal adiabatic heating to which water is subjected during pressurization (approximately 3°C per 100 MPa), it is frequently regarded as the optimal choice for use as a pressurizing medium. The medium transmits pressure to food products in a uniform manner from all sides, thereby preventing the compression of food items during high-pressure processing. In order to facilitate the uniform distribution of pressure, it is necessary to pack the food items prior to processing. Conversely, a liquid food item may act as a pressure-transmitting medium itself if it is subjected to pressure[322]. HHP treatments through direct pressure generation in represented in Figure 8.

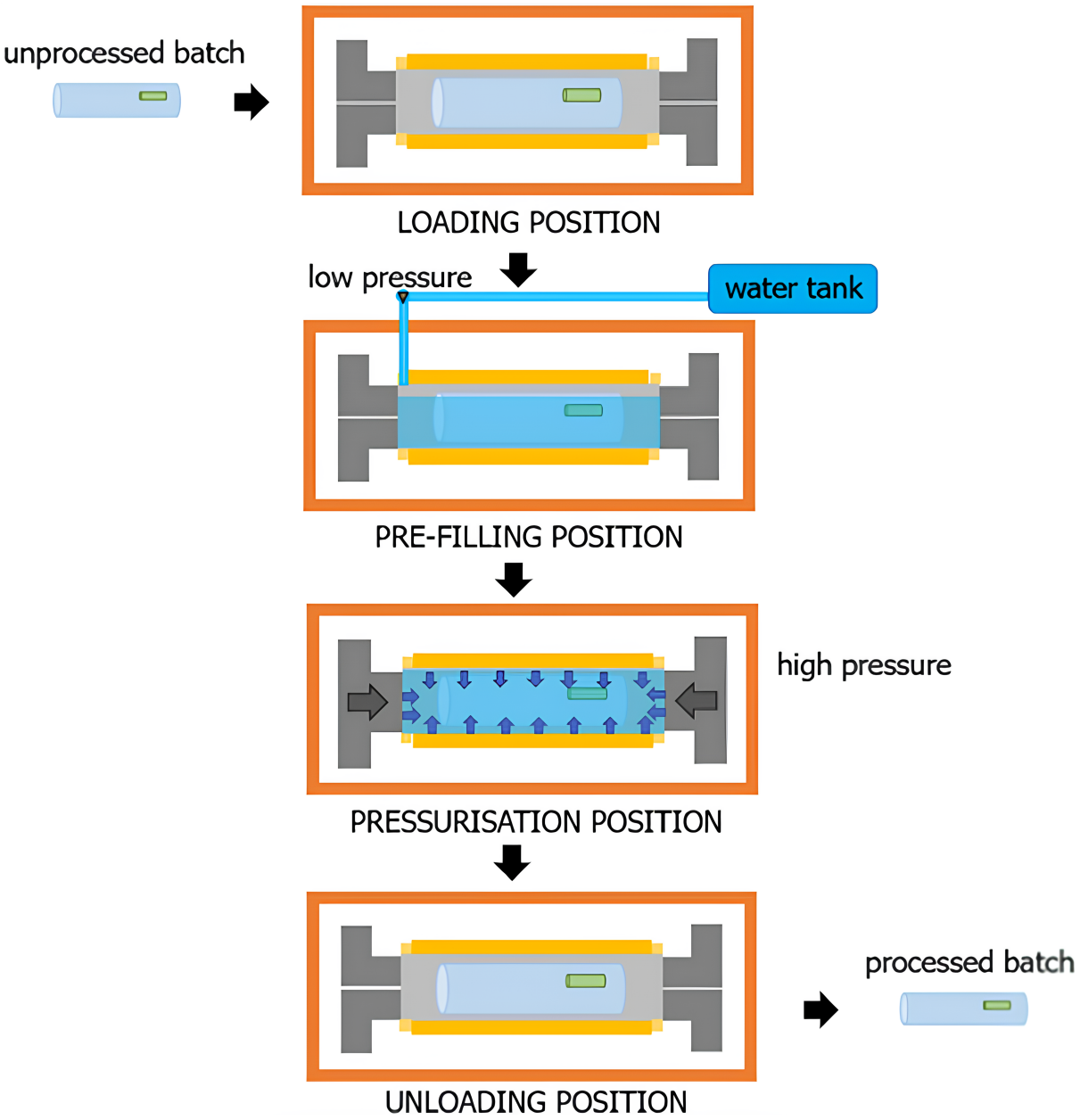

Figure 8. Diagram representing a commercial HPP treatment equipment and mode of action[321]. The process begins with the loading position, where an unprocessed batch is placed into the chamber. In the pre-filling position, water from a tank is introduced at low pressure. The pressurization position follows, where high pressure is applied uniformly to the product. Finally, in the unloading position, pressure is released, and the processed batch is removed.

1.5.3 Use of HHP in whole inactivated virus vaccine production: repurposing of and old method for a new application

The development of inactivated virus vaccines remains one of the most reliable and widely used strategies for immunization against viral pathogens. While traditional chemical and thermal methods effectively inactivate viruses for vaccine production, they often alter viral epitopes, potentially reducing immunogenicity. In contrast, HHP

offers an innovative approach by inactivating viruses while preserving their structural integrity and antigenicity. HHP technology involves applying pressures of 100-800 MPa to biological materials, a non-thermal process that maintains the native structure of viral proteins more effectively than heat or chemical treatments[323].

HHP achieves viral inactivation by irreversible structural changes of viral envelope and capsid proteins that prevent viral replication while preserving protein epitopes[317]. Unlike chemical agents like formaldehyde, which can alter protein conformation and mask antigenic sites, HHP does not involve chemical modification, reducing the risk of denaturation of essential epitopes that the immune system recognizes. For instance, studies on non-enveloped viruses such as Coxsackievirus and Enterovirus have shown that HHP can effectively inactivate viral infectivity without compromising structural antigens[317]. This preservation of antigenic sites is essential, as it may enhance the immune response by presenting a structure similar to the live virus, thus potentially increasing vaccine efficacy.

The application of HHP for vaccine production could provide several advantages, especially regarding safety, preservation of immunogenicity, and production efficiency.

The primary advantage of HHP over thermal and chemical methods is its ability to inactivate viruses while preserving structural proteins in their native conformations. For example, heat treatments can lead to protein denaturation and loss of structural integrity, particularly for complex viral proteins that play essential roles in immune recognition, requiring additional adjuvants or boosting doses to achieve adequate immunity. On the contrary, HHP applies non-thermal, isostatic pressure, which avoids the risk of heat-induced protein degradation. HHP-treated vaccines could potentially elicit a stronger immune response due to the presence of intact antigenic structures, which the immune system recognizes more readily[295]. For example, influenza and poliovirus studies have demonstrated that HHP can retain the integrity of critical antigenic regions, making HHP-inactivated viruses promising candidates for immunization[324], [325].

Safety is a paramount concern in vaccine production, especially regarding inactivation protocols. Chemical methods often require careful monitoring and removal of residual inactivating agents to ensure vaccine safety, as they can introduce potentially harmful byproducts. HHP inactivation reduces these risks by eliminating the need for chemicals, leading to a safer process and potentially faster production timelines. This

advantage translates into greater production efficiency and lower production costs, which are especially beneficial when rapid vaccine scaling is required, as demonstrated during global health emergencies like the COVID-19 pandemic. Inactivated whole-virus vaccines have been among the first types approved for emergency use, thanks to their relatively straightforward production process. For SARS-CoV-2, HHP could offer a novel approach to maintain spike protein structures crucial for immunogenicity, especially since chemical inactivation as well as other physical methods, i.e. heat, often compromises these proteins. HHP has shown efficacy in structurally similar viruses, such as SARS-CoV and MERS-CoV, making it a promising candidate for ongoing SARS-CoV-2 vaccine development[325]. Moreover, given the continuous emergence of new viral variants, HHP offers a rapid and efficient alternative to chemical inactivation, supporting quicker adaptation to circulating strains without compromising antigen integrity.

Whilst the majority of studies on HHP focused on the inactivation of foodborne viruses, HHP has also been explored as an innovative approach for vaccine production, demonstrating its ability to inactivate viruses whilst preserving antigenic structures crucial for immune recognition[326,327]. This has been investigated in several studies targeting a range of pathogenic viruses. For instance, Barroso et al.[326] successfully inactivated avian influenza viruses using HHP, paving the way for vaccine development against zoonotic threats. Similarly, de Souza et al.[327] explored the effects of HHP on the immune recognition of antigens from porcine parvovirus, highlighting its potential for veterinary vaccines. The seminal work of Shearer and Kniel[328] and the subsequent studies by Silva et al.[329] laid the foundation for the understanding of HHP inactivation across a wide spectrum of human and animal viruses. These findings collectively underscore the potential of HHP not only for food safety but also as a platform for developing effective vaccines against emerging and re-emerging viral threats, hence suggesting that this technology has promising potential to drive the next generation of vaccines. Moreover, drawing from its application in the food industry, where HHP enables effective long-term preservation of product quality at refrigeration temperatures, HHP technology offers the potential to produce vaccines that remain stable at refrigeration or ambient temperatures, reducing or eliminating the reliance on cold chain logistics for distribution[323].

Although the use of high hydrostatic pressure for the production of vaccines is still a largely unexplored area of research, as none of the aforementioned vaccine candidates

was ever deployed for use, the advantages of HHP in preserving antigenicity and offering a non-chemical inactivation method, mean this technology has promising potential to drive the next generation of vaccines. The potential of HHP technology in whole-virus inactivated vaccine production is promising due to its ability to inactivate viruses while preserving antigenic structures critical for a robust immune response. As an alternative to traditional thermal and chemical inactivation, HHP may offer a safer and more efficient approach to vaccine development. However, to bring HHP into mainstream vaccine production, challenges related to viral resistance, equipment costs, and regulatory hurdles must be addressed. With continued research and technological advancements, HHP may play a significant role in producing next-generation vaccines that are both effective and scalable, contributing to global health security and pandemic preparedness.

2. Scope

This doctoral thesis focuses on developing and validating a novel vaccine production methodology based on the viral inactivation achieved through high hydrostatic pressure (HHP) processing. This study aimed to develop and validate an HHP-based methodology for producing inactivated vaccines against SARS-CoV-2 and WNV. SARS-CoV-2 (B.1 and BQ.1.1 lineages) and WNV (lineages 1 and 2) were selected as representative models of pandemic and endemic threats. This research aims to establish HHP as a versatile and cost-effective platform for producing inactivated vaccines that combine affordability with high immunogenic potential. To achieve this goal, the study integrates comprehensive analyses of viral morphology and antigenicity with *in vivo* immunogenicity assessments, providing a multifaceted evaluation of the efficacy and safety of this approach. Moreover, thermostability of the vaccine candidates is systematically analyzed to determine their resistance to temperature variations and suitability for deployment in low-resource environments with scarce cold chain storage infrastructures, hence facilitating broader vaccine accessibility.

A primary focus of the research was to investigate the structural and morphological integrity of virions following HHP inactivation. Advanced imaging techniques, including negative staining electron microscopy (nsEM), were employed to visualize the ultrastructure and surface topology of virions post-HHP treatment and assess HHP effects on virion integrity. The subsequent phase of the study concentrated on evaluating the antigenicity of HHP-inactivated virions through Western blot. This

preliminary analysis provided critical insights into any potential alterations in morphology and antigenicity potentially impairing antigenic presentation and reduce immunogenic potential *in vivo*, thus influencing recognition by the immune system.

The most critical component of this research involved *in vivo* testing of the HHP-inactivated virus to evaluate its immunogenicity and efficacy. The aim was to develop a monitoring strategy that interrogated all aspects of immune response elicited by vaccines in order to comprehensively evaluate vaccine-induced immunity that can inform about vaccine efficacy. Using a murine model (Swiss CD1 mice), the study assessed the capacity of the HHP-inactivated vaccine to elicit both humoral and cellular immune responses, which are integral to effective and durable protection against viral infections. Humoral immunity was assessed by measuring the production of virus-specific antibodies, and assess their neutralizing capacity, using ELISA, Western blot and micro-neutralization tests. Cellular immunity was evaluated through ELISpot to quantify the activation of interferon-gamma (IFN-γ) producing cells.

The final objective of this study was to assess the thermostability of the HHP-inactivated vaccine candidate to determine its potential for distribution in low-resource settings. Vaccine stability under standard refrigeration conditions (2-8°C) is a critical factor influencing global accessibility, particularly in LMICs, where maintaining ultra-cold storage infrastructure is often infeasible, hence hampering distribution of those vaccines strictly requiring deep freezing temperatures for storage, like mRNA vaccines, largely employed during the COVID-19 pandemic. Thermostability studies were conducted to evaluate the antigenic properties of the vaccine over prolonged storage periods at room and mild refrigeration temperature, thereby assessing its suitability for widespread distribution. The ability of HHP-inactivated vaccines to remain stable at refrigeration temperatures for extended durations would significantly reduce cold-chain dependency, lowering logistical costs and facilitating deployment in remote and underserved regions.

Overall, the overarching goal of this research is to contribute to the broader goal of global health equity by developing a vaccine production platform that is both effective as well as economically and logistically accessible to populations with limited resources and healthcare infrastructures.

3. Materials and Methods

3.1 Cells and virus

Vero E6 (ATCC CRL 1585) cell cultures were maintained in Minimum Essential Medium (MEM) supplemented with 10% heat inactivated fetal bovine serum (FBS), 2 mM L-glutamine, 100 U/ml penicillin, 100 μg/ml streptomycin (EuroClone, Milan, Italy) and incubated at 37 °C in a humidified, 5% CO_2 atmosphere-enriched chamber[330]. Cultures were passaged every 2-5 days, when they reach 80-90% confluency, in ratios ranging from 1:2 to 1:10.

SARS-CoV-2 B.1 (hCoV-19/Italy/EMR-UOM-PVS_01O/2021, GISAID accession no. EPI_ISL_1908157) and BQ.1.1 (hCoV-19/Italy/EMR_AUSLRomagna_C107-22-01/2022, GISAID accession no. EPI_ISL_15630397) strains were isolated from SARS-CoV-2 positive nasopharyngeal swabs residual from routine activities and submitted to the Microbiology Unit, Greater Romagna Area Hub Laboratory, Cesena, Italy, for diagnostic purposes, as described previously[331]. Samples were sequenced as part of the project to monitor the prevalence and distribution of SARS-CoV-2 variants in Italy, sponsored by the Italian Institute of Public Health. Samples were sequenced using CleanPlex SARS-CoV-2 Flex (Paragon Genomics, Inc., Hayward, CA, USA) on an Illumina MiSeq (Illumina Inc., San Diego, CA, USA). Sequences were analyzed with SOPHiA DDM platform software (SOPHiA Genetics, Lausanne, Switzerland) for lineage assignment. The B.1 and BQ.1.1 variants of SARS-CoV-2 were selected for this study due to their different mutations profile, especially in the Spike protein: B.1 is an early lineage that was widely circulating at the beginning of the pandemic and serves

as a representative of the ancestral virus, while, in contrast, BQ.1.1 is a more recent subvariant of Omicron[332–334]. By including both variants, the study aimed to assess the effectiveness of the HHP inactivation against diverse viral strains.

West Nile virus lineage 1 strain (204913/2009, NCBI accession no. KU573078) was isolated from a positive *Culex pipiens* mosquito pool sampled in Ravenna during routine vector surveillance activities in 2009 and lineage 2 strain (LU_130823, NCBI BioProject accession no. PRJNA1096139) was isolated from a meningitis case detected in Conselice (Ravenna) in 2023. Lineage 1 strain was kindly provided by the Unit of Virology of the Istituto Zooprofilattico della Lombardia e dell'Emilia Romagna (IZSLER) in Brescia. Lineage 2 strain was isolated from positive cerebrospinal fluid from a patient with meningitis enrolled in the C.ARBO.SEQ project ("*Caratterizzazione genetica di Arbovirus mediante sequenziamento e implementazione di nuovi approcci diagnostici in biologia molecolare*") promoted and carried out by the Unit of Microbiology of the Greater Romagna Area Hub Laboratory in Cesena. Viral isolates were sequenced using Illumina RNA Prep with Enrichment Tagmentation (Illumina, San Diego, California, USA) and hybrid-capture-mediated target enrichment with Viral Surveillance Panel oligos (Illumina). After pre-processing, the trimmed reads were aligned to the reference genome (GenBank accession nos. NC_009942.1 for lineage 1 and NC_001563.2 for lineage 2) by using Bowtie2 v.2.4.1 and the consensus genome sequences were called using BCFtools v.1.13. In short, a Bowtie2 index was created to facilitate the incorporation of viral segment sequences via the bowtie2-build program. Subsequent short-read analysis was conducted using Bowtie2 in paired-end mode with the –S option, resulting in SAM format output. The resulting SAM format alignment files underwent sequential processing using SAMtools v.1.13 commands, including view and sort. A consensus sequence was generated through the "bcftools consensus" command[335].

Before being used in this study, all human samples underwent an anonymization procedure to comply with the regulations of the local ethics committee (AVR-PPC P09, rev.2; based on Burnett et al.[336]). The collection of human samples was approved by the Romagna Local Ethical Board (Comitato Etico della Romagna, CEROM) under protocol code COVdPCR of 7 February 2020 (SARS-CoV-2-positive samples) and C.ARBO.SEQ of 13 May 2023 (WNV-positive sample). Prior to the enrolment in the present study all participants gave their written informed consent for the collection and use of biological samples.

All activities involving the manipulation of infectious virus (virus isolation, viral stock preparation and inactivation assessment) were performed in a Biological Safety Level 3 (BSL-3) facility at the Unit of Microbiology, Greater Romagna Area Hub Laboratory, Cesena, Italy, in compliance with appropriate containment rules.

3.2 Preparation of SARS-CoV-2 and WNV stock and HHP processing

Passage three viral stocks were used to infect Vero E6 monolayers at 80-90% confluency at a multiplicity of infection of 0.1 MOI, optimized for maximal virus yield. The supernatant was harvested at 72 hours post-infection, when cytopathic effect involved approximately 80% of the cell monolayer, corresponding to the peak of viral yield. Virus-containing supernatant was centrifugation-clarified at 3.500 g for 20 minutes at 4 °C to remove cell debris and retain the virus in its native state. The purified viral stock was subsequently subjected to quality control assays to quantify the viral load and assess its infectivity (tissue culture infectious dose [$TCID_{50}$] assays) to ensure that the stock met the desired concentration standards and standardize the input material for downstream applications, including inactivation protocols. Once characterized, 10 ml of the viral stock was aliquoted in 5 cm x 5 cm clear food-safe polyethylene plastic pouches, air war removed, and pouches were hermetically sealed. Multiple pouches of each viral stock were prepared and stored at -80 °C to maintain stability until further use. Pouches were gently thawed in cold water immediately before HHP processing.

High-hydrostatic-pressure mediated inactivation was carried out with a high-pressure system (Avure Technologies Inc., Erlanger, Kentucky, USA). Pouches were then positioned directly within the pressure chamber; air was removed from the vessel by an automatic pump and water was pressurized to generate isostatic pressure transmitted through the virus-stock-containing pouches. As mentioned in the introduction, given the minimal adiabatic heating to which water is subjected during pressurization (approximately 3 °C per 100 MPa), it is frequently regarded as the optimal choice for use as a pressurizing medium. The pressure inside the chamber was increased at a rate of 200 MPa/minute. During the inactivation process, temperature increase inside the chamber was closely monitored in order not to exceed 2-3 °C / 100 MPa; at 600 MPa (the maximum pressure used for the study) the temperature reached a maximum of 20 °C. The pressure was maintained for 5 minutes (for WNV processing

time was extended to 10 minutes). Three different pressures were tested: 400, 500 and 600 MPa.

The operating pressure conditions were chosen to minimize the total processing time, aiming to develop a potentially high-throughput inactivation system. This approach required operating at relatively high pressures to achieve complete viral inactivation, in contrast to other inactivation protocols described in the literature[326,327], which employ lower pressures but require significantly longer treatment durations, on the order of hours rather than minutes. Each pressure condition was applied as an independent treatment cycle. After each pressurization cycle, the viral suspension subjected to that specific pressure was removed, and a fresh, untreated viral stock was introduced for the next cycle. This ensured that each viral stock was exposed to only one pressure condition, preserving the integrity of independent treatments. Pressure inside the chamber was continuously recorded throughout the entire series of treatments, including during decompression phases when the pressure returned to ambient levels, hence producing a sequential pressure-time profile. This methodological choice streamlined the workflow while maintaining precise control over pressure conditions.

For all experimental conditions, the inactivation process was monitored indirectly by recording the pressure and temperature parameters in real-time, ensuring consistency and reproducibility across batches. Once the treatment cycle was completed, fluid was pumped from the pressure vessel into the reservoir tank, resulting in a decrease in pressure. Pouches were removed from the vessel and then maintained at -80 °C until further analysis.

Following HHP treatment, the inactivated viral stock was subjected to rigorous quality control assays to confirm the success of inactivation. Infectivity assays, such as $TCID_{50}$ tests, were performed to ensure that no residual infectivity remained in the treated material, providing confidence that the virus has been rendered biologically inactive. Simultaneously, the structural integrity of the viral particles was assessed using by electron microscopy, which verified that the viral morphology has been preserved. Additionally, immunological assays, such as Western blotting, were employed to confirm the retention of antigenic epitopes, a critical requirement for downstream immunogenicity studies.

3.3 Inactivation assessment

Virus infectivity reduction was assessed by endpoint titration and complete inactivation was tested by culturing the putatively inactivated viral stock on Vero E6 cell culture; viral replication was evaluated by qRT-PCR. As a control, non HHP-treated counterpart was titrated and cultured together with HHP-treated viral stocks.

Viral titration was carried out by the endpoint dilution method, which allows the calculation of the average infectious dose of a tissue culture per ml (Tissue Culture Infecting Dose, $TCID_{50}$/mL), defined as the load of viral infectious particles per unit volume capable of causing an appreciable productive viral infection in the form of a cytopathic effect in half of the infected cell cultures. The day before infection, approximately 20.000 cells per well were seeded into 96-well cell culture plates (approximately 2.000.000 cells per plate) using MEM at 5% FBS, and then incubated overnight at 37 °C in a humidified atmosphere at 5% CO_2. On the day of infection, serial 10-fold dilutions were prepared in MEM at 2% FBS and used to infect a confluent monolayer of cells (100 µL of viral suspension for each well); each dilution was tested in eight replicates. In each plate, eight wells were used as cell control (in which only MEM at 2% FBS is present) and another eight wells were used as virus control (in which pure viral stock is present). Viral stocks were titrated in duplicate. The plates were incubated for 72 hours and observed daily to monitor the development of the cytopathic effect. On the third day, the cell culture supernatant was removed, and the cells were fixed and stained using a 4% formaldehyde solution (Fisher Chemical, Milan, Italy) in crystal violet (Delcon, Bergamo, Italy) incubated for 30 minutes at room temperature. The cytopathic effect (CPE) was assessed by eye. Positive wells for cytopathic effect appear completely unstained or will show larger or smaller areas where staining will not be present. CPE-negative wells, on the other hand, appear uniformly colored. Viral titers, expressed as $TCID_{50}$/ml, were calculated according to the Reed and Muench method[337,338] based on eight replicates by dilution.

For each dilution, the ratio between the cumulative number of positive wells and the sum of the cumulative number of positive wells and the cumulative number of negative wells was then calculated. The calculated ratio was then converted into a percentage.

The end-point dilution for which the mortality is exactly 50%, which corresponds to the $TCID_{50}$/ml, was hence calculated. To do this, a correction factor is first calculated that must be applied to the dilution that has produced a percentage of wells positive

for the cytopathic effect just above 50%, called proportionate distance, calculated as follows:

$$proportionate\ distance\ (PD) = \frac{(\%\ mortality\ just\ over\ 50\%) - 50\%}{(\%\ mortality\ just\ over\ 50\%) - (\%\ mortality\ just\ under\ 50\%)}$$

The value of $TCID_{50}/100\mu L$ results from the following calculation, corrected for the logarithm of the dilution factor:

$$TCID_{50}/ml = 10^{log_{10}\ of\ the\ dilution\ with\ mortality\ just\ over\ 50\% + (PD \cdot log_{10}\ of\ the\ dilution\ base)}$$

This value represents the concentration of infectious virus present in the volume of viral inoculum used for infection (100 µl). Multiplying this value by 10 gives the concentration of infectious virus present per ml, i.e. $TCID_{50}/ml$.

HHP-treated stocks viral titer was compared to non-HHP-treated counterpart titer and fold change was calculated.

Complete inactivation was further tested by culturing every HHP-treated viral stock on a confluent monolayer of Vero E6 cells for 72 hours. Cell culture supernatant was assayed by a commercial RT-PCR test for SARS-CoV-2 or an in-house assay for WNV at time 0 and every 12 hours after infection to assess viral replication.

For SARS-CoV-2, the Allplex SARS-CoV-2 Extraction-Free system (Seegene Inc., Seoul, Korea) was used. It allowed the simultaneous detection of four target genes, namely E gene, RdRP/S gene and N gene. Sample preparation, reaction setup and analysis were performed accordingly to the manufacturer instructions[339]. Briefly, 15 µl of cell culture supernatant were diluted 1:4 in 45 µl of RNase-free water in a 96-well PCR plate and hence 5 µl of the dilution were transferred to another plate with 16 µl of PCR master mix, containing 5 µl of MOM (MuDT Oligo Mixture, with dNTPs, oligos, primers and TaqMan 5' fluorophore/3' Black Hole Quencher probes), 5 µl of enzymes, 5 µl of RNase-free water and 1 µl of internal control for every reaction. Thermal cycling protocol was as follows: 50 °C for 20 minutes, 95 °C for 5 minutes, and 45 cycles of 95 °C for 10 seconds, 60 °C for 10 seconds and 72 °C for 10 seconds. Results analysis and targets quantification were performed with 2019-nCoV viewer from Seegene Inc.

For WNV, cell culture supernatant aliquots were extracted using CSC Pathogen Total Nucleic Acid Kit on CSC Maxwell Promega automated extractor. Primer pair and probe targeting the 3' UTR region (UnTranslated Region) designed by Tang et al.[340] were used:

- Forward primer: 5′ – AAGTTGAGTAGACGGTGCTG – 3′,
- Reverse primer: 5′ – AGACGGTTCTGAGGGCTTAC – 3′,
- Probe: 5′-FAM – CTCAACCCCAGGAGGACTGG – 3′-BHQ.

Reactions were setup with SuperScript™ IV One-Step RT-PCR Kit (ThermoFisher): 5 µl of Taqman enzyme (4x), 1 µl of Forward primer (final concentration 500 nM), 1 µl of Reverse primer (final concentration 500 nM), 0.4 µl of Probe (final concentration 200 nM), 2 µl of dNTPs (5 mM), 5.6 µl of RNase-free water. Thermal cycling protocol was as follows: 50 °C for 20 minutes, 95 °C for 5 minutes, and 45 cycles of 95 °C for 10 seconds, 58 °C for 20 seconds and 72 °C for 10 seconds.

Viral replication was quantified by comparing putatively HHP-inactivated virus stock and non-HHP-inactivated control ΔCt values.

3.4 Antigen purification

HHP-treated viral stocks and non-HHP treated counterparts were purified by ultracentrifugation over a sucrose cushion to isolate and concentrate intact viral particles. This method ensures the preservation of antigenic integrity and structural features critical for immunogenicity testing. The sucrose solution is formulated to create a density gradient that enables the separation of viral particles based on their buoyant density.

SARS-CoV-2 viral stocks were first concentrated by ultracentrifugation at 150.000 g for 1.5 hours at 4 °C, while WNV viral stocks were concentrated at 200.000 g for 4 hours at 4 °C (Sorvall™ WX+ Ultracentrifuge with rotor fixed-angle F50L-8x39, ThermoFisher, Waltham, Massachusetts, United States). Pellet was resuspended in 2 ml PBS and subsequently purified by ultracentrifugation on sucrose cushion. For each tube, 20 ml of sucrose solution at 25% (w/v in PBS, 20 mM HEPES, 155 mM NaCl, pH 7) were loaded, and 30 ml of viral suspension was gently pipetted onto the top of the cushion to avoid mixing and to maintain a sharp interface between the sample and the cushion. Tubes were centrifuged at 150.000 g for 2 hours at 4 °C. Final pellet was resuspended in PBS at a 100x concentration compared to the initial volume.

3.5 Structural and antigenicity analysis

3.5.1 Negative Staining Electron Microscopy (nsEM)

HHP-treated viral stocks were subjected to microscopy examination. This method provides detailed visualization of viral ultrastructure, allowing the assessment of the preservation of critical morphological features. This provides critical insights into the relationship between pressure treatment and virion morphology, informing the optimization of inactivation protocols for vaccine development.

The HHP-treated virus stocks and non-HHP-treated counterparts were subjected to negative staining electron microscopy using the Airfuge method[341,342] at the Unit of Virology of the Istituto Zooprofilattico della Lombardia e dell'Emilia Romagna. Samples were subjected to ultracentrifugation (Airfuge, Beckman Coulter Inc. Life Sciences, Indianapolis, Indiana, USA) for a period of 15 minutes at a speed of 82.000 g, using a rotor that could accommodate six 175-µl test tubes, into which specific adapters for 3 mm carbon-coated Formvar copper grids had been placed. Subsequently, the grids were stained with 2% w/v sodium phosphotungstate (pH 6.8) for 1.5 minutes and observed under a Tecnai G2 Spirit Biotwin transmission electron microscope (FEI, Hillsboro, Oregon, USA) at an accelerating voltage of 80 kV to provide optimal resolution for visualizing viral particles while minimizing radiation damage. Images were acquired at various magnifications (20.000-43.000 x) to assess the overall morphology and detailed structural features of the viral particles.

Identification of the observed viral particles was based on their morphological characteristics. Images were analyzed. Morphological differences in viral particles subjected to varying levels of high hydrostatic pressure were evaluated, enabling detailed visualization of structural changes and integrity preservation.

3.5.2 Western blot

HHP-treated viral stocks, non-HHP-treated counterparts and heat-inactivated stocks (subsequently used as controls for immunization) were probed with monoclonal and polyclonal commercially available or in-house-produced rabbit and mouse antibodies to analyze protein-antibody interactions, thereby elucidating the impact of HHP on viral antigenicity, thereby assessing the effects of HHP on viral epitopes, which may undergo conformational changes affecting immunogenicity.

Total proteins of sucrose-purified viral stocks were extracted in 20% (v/v) RIPA buffer (80 µl of sample, 20 µl of RIPA buffer) for 5 minutes on ice and quantified by Bradford method to ensure equal loading across lanes during electrophoresis.

For each sample, total proteins were diluted to 10 µg and denatured at 70 °C for 10 minutes with NuPAGE LDS Sample Buffer (6.25 µl per sample) and NuPAGE Reducing Agent (2.5 µl per sample). The viral proteins were separated by sodium dodecyl sulfate-polyacrylamide gel electrophoresis (SDS-PAGE). For each sample, 25 µl of denatured and reduced samples were loaded into gradient NuPAGE 4-12% Bis-Tris Gels (ThermoFisher) to achieve optimal resolution of viral proteins across a range of molecular weights. Electrophoretic separation was carried out with NuPAGE MES SDS Running Buffer (ThermoFisher) in reducing conditions at 150 V constant voltage for 30, 45 or 60 minutes, depending on the desired target protein molecular weight.

After gel wash in 200 ml of ultrapure water in agitation for 15 minutes, the semi-dry transfer of separated proteins was carried out on a Power Blotter XL (ThermoFisher) using nitrocellulose Power Blotter Select Transfer Stacks (ThermoFisher). Transfer stacks were separated into top and bottom halves, the latter was placed on the blotting surface (anode), the gel was placed on the bottom stack transfer membrane and the top stack was placed on top; cathode was placed to close the transfer apparatus. Blotting was performed at 1.3 A constant current for 5 or 7 minutes depending on the molecular weight of the target protein. Gel was checked for complete protein transfer by staining with Imperial™ Protein Stain (ThermoFisher) heated in the microwave for 90 seconds (or until boiling). Blotted membranes were washed with PBS three times for 5 minutes with shaking and blocked with StartingBlock™ Blocking Buffer, 0.05% Tween-20 for 1 hour at room temperature to minimize non-specific antibody binding and enhance the specificity of the subsequent detection steps.

Blocked membranes were probed with primary anti-SARS-CoV-2 and anti-WNV antibodies in PBS, 10% StartingBlock™ Blocking Buffer, 0.05% Tween-20.

The following primary antibodies were used for SARS-CoV-2 proteins probing:

- Rabbit Spike Protein S1/S2 Polyclonal Antibody (ThermoFisher, PA5-112048), at a final concentration of 0.5 µg/ml;
- Rabbit Nucleocapsid Monoclonal Antibody (ThermoFisher, MA5-36271), at a final concentration of 0.5 µg/ml;

- Rabbit Membrane Polyclonal Antibody (ThermoFisher, SARS-COV2-M-101AP) at a final concentration of 0.5 μg/ml;
- Mouse Spike Protein S1 (RBD) Monoclonal Antibody (IZSLER in-house produced, 3C12) at a concentration of 5 μg/ml.

The following primary antibodies were used for WNV proteins probing:

- Rabbit West Nile virus NS1 Protein Polyclonal Antibody (ThermoFisher, PA-111988) at a final concentration of 1 μg/ml;
- Mouse Envelope (Domain 3) Monoclonal Antibody (ISZLER in-house produced, 3D6) at a concentration of 5 μg/ml;
- Rabbit West Nile virus Capsid Protein Polyclonal Antibody (ThermoFisher, PA5-111982) at a final concentration of 1 μg/ml.

After overnight incubation protein-side up and in agitation with the primary antibody at 4 °C, membranes were washed 3 times with PBS in agitation for 10 minutes to remove unbound primary antibody. HRP (HorseRadish Peroxidase)-conjugated secondary antibody incubation was performed for 1 hour at room temperature in shaking. HRP-conjugated secondary antibodies targeting the Fc region of the primary antibody were diluted to the desired concentration in in PBS, 10% StartingBlock™ Blocking Buffer, 0.05% Tween-20. The following secondary antibodies were used:

- Goat anti-Rabbit IgG (H+L) Poly-HRP Secondary Antibody (ThermoFisher, 32260), at a final concentration of 25 ng/ml,
- Goat anti-Mouse IgG HRP (IZSLER in-house produced, 72689) at 50 ng/ml.

After secondary antibody incubation, membranes were washed 3 times for 20 minutes with PBS. Chemiluminescent signal was detected using SuperSignal™ West Pico PLUS Chemiluminescent Substrate (ThermoFisher) mixing equal parts of Substrate and Stable Peroxide solutions incubated for 5 minutes at room temperature with shaking. Membranes were imaged using the iBright 1500FL (ThermoFisher) imaging system with the SmartRange setting, adjusting exposure time if needed. The intensity and size of the protein bands observed on the blots provided critical information about the stability and antigenicity of the viral proteins. Detailed information on electrophoresis, blotting parameters, and antibody concentrations is summarized in Table 2 (SARS-CoV-2) and Table 2 (WNV).

Table 2. Summary of electrophoresis and blotting parameters, along with antibody probing conditions, commercial or in-house produced primary and secondary antibody and their respective working solution concentrations for the detection of SARS-CoV-2 Spike, Nucleocapsid, and Membrane proteins.

Target		Electrophoresis parameters		Blotting parameters		Primary antibody probing conditions			Secondary antibody probing conditions		
Protein	**Molecular weight**	**Voltage (V)**	**Time (minutes)**	**Current (A)**	**Time (minutes)**	**Primary antibody**	**Catalog number**	**Working solution concentration**	**Secondary antibody**	**Catalog number**	**Working solution concentration**
Spike	140-180 kDa (monomer) 540 kDa (trimer)	150	90	1.3	7	SARS-CoV-2 Spike Protein S1/S2 Polyclonal Antibody (rabbit) – ThermoFisher	PA5-112048	0.5 μg/ml	Goat anti-Rabbit IgG (H+L) Poly-HRP Secondary Antibody – ThermoFisher	32260	25 ng/ml
						SARS-CoV-2 2C12 Spike Protein S1-RBD (mouse) – IZSLER in-house produced	3C12	5 μg/ml	Goat anti-Mouse IgG HRP – IZSLER in-house produced	72689	50 ng/ml
Nucleocapsid	~ 46 kDa (monomer) ~ 90 kDa (dimer)	150	45	1.3	7	SARS-CoV-2 Nucleocapsid Monoclonal Antibody (HL448) (rabbit) – ThermoFisher	MA5-36271	0.5 μg/ml	Goat anti-Rabbit IgG (H+L) Poly-HRP Secondary Antibody – ThermoFisher	32260	25 ng/ml
Membrane	25 kDa (monomer) 50 kDa (dimer)	150	30	1.3	7	SARS-CoV-2 Membrane Glycoprotein Polyclonal Antibody (rabbit) – ThermoFisher	SARS-COV2-M-101AP	0.5 μg/ml	Goat anti-Rabbit IgG (H+L) Poly-HRP Secondary Antibody – ThermoFisher	32260	25 ng/ml

Table 3. Summary of electrophoresis and blotting parameters, along with antibody probing conditions, commercial or in-house produced primary and secondary antibody and their respective working solution concentrations for the detection of WNV NS1, Envelope and Capsid proteins.

Target		Electrophoresis parameters		Blotting parameters		Primary antibody probing conditions			Secondary antibody probing conditions		
Protein	**Molecular weight**	**Voltage (V)**	**Time (minutes)**	**Current (A)**	**Time (minutes)**	**Primary antibody**	**Catalog number**	**Working solution concentration**	**Secondary antibody**	**Catalog number**	**Working solution concentration**
NS1	~ 45 kDa (monomer) ~ 90 kDa (dimer)	150	45	1.3	7	West Nile virus NS1 Protein Polyclonal Antibody (rabbit) – ThermoFisher	PA-111988	1 µg/ml	Goat anti-Rabbit IgG (H+L) Poly-HRP Secondary Antibody – ThermoFisher	32260	25 ng/ml
Envelope	42 kDa	150	45	1.3	7	Envelope (Domain 3) Monoclonal Antibody (mouse) – ISZLER in-house produced	3D6	5 µg/ml	Goat anti-Mouse IgG HRP – IZSLER in-house produced	72689	50 ng/ml
Capsid	20 kDa	150	30	1.3	7	West Nile virus Capsid Protein Polyclonal Antibody (rabbit) – ThermoFisher	PA5-111982	1 µg/ml	Goat anti-Rabbit IgG (H+L) Poly-HRP Secondary Antibody – ThermoFisher	32260	25 ng/ml

The evaluation of Western blot results obtained from HHP-inactivated viruses was performed through both qualitative and quantitative approaches to provide a comprehensive assessment of the residual antigenicity of the viral proteins. The presence, absence, or alteration of protein bands corresponding to specific viral antigens was analyzed by visually inspecting the banding patterns on the blot. Particular attention was given to identifying key structural proteins of SARS-CoV-2, such as the spike (S), nucleocapsid (N) and membrane (M) proteins, and of WNV, such as non-structural protein 1 (NS1), envelope (E), and capsid (C) based on their expected molecular weights. These observations were compared to a molecular weight marker (PageRuler™ Plus Prestained Protein Ladder, 10 to 250 kDa, ThermoFisher) to ensure accurate identification of protein bands. By comparing banding pattern and intensity across experimental conditions (different HHP treatments and heat-inactivation), the analysis provided insight into the degree of preservation of antigenic integrity and putative antigenicity in the inactivated viral preparations. This dual qualitative and quantitative approach ensured a robust evaluation of the immunogenic properties of the HHP-inactivated viruses.

3.6 *In vivo* safety and immunogenicity testing

In vivo safety and immunogenicity testing was employed to assess whether the SARS-CoV-2 HHP-inactivated viruses could elicit a robust and protective immune response without adverse side effects. By administering the inactivated viruses to animal models and monitoring antibody production and T-cell responses, the assay provides crucial insights into the preservation of key antigenic epitopes post-HHP treatment, unequivocally validating HHP for producing immunogenic and non-replicative vaccine candidates.

The study was conducted on Swiss CD-1 mice, a widely used model in immunological studies due to their genetic uniformity, robust immune responses, and ease of handling. The experiment was conducted under controlled laboratory conditions, adhering to ethical guidelines for animal research. Animal care and all procedures were performed in accordance with guidelines and regulations of the Italian animal protection laws (e.g. DLSG 4/3 2014, n. 26 - National implementation of Directive 2010/63/EU). Ethical review was requested and authorization n° 258/2020-PR for animal testing was obtained. Animal testing was carried out at the animal facility of

the Istituto Zooprofilattico Sperimentale della Lombardia e dell'Emilia-Romagna in Brescia.

The mice were housed in pathogen-free facilities under controlled environmental conditions, including a 12-hour light/dark cycle, a constant temperature of 22-24 °C, and humidity levels of 40-60%. They were provided ad libitum access to a standard rodent diet and water, and their health status was monitored daily.

For the study, 28 female adult (6-month-old, weighing approximately 30-35 grams) were randomly assigned to 7 immunization groups (n = 4 per group) to minimize bias. Group allocations included:

- Mice in group 1 were injected with SARS-CoV-2 B.1 HHP-inactivated at 500 MPa;
- Mice in group 2 were injected with SARS-CoV-2 B.1 HHP-inactivated at 600 MPa;
- Mice in group 3 were injected with SARS-CoV-2 B.1 heat-inactivated;
- Mice in group 4, 5 and 6 were injected with SARS-CoV-2 BQ.1.1 HHP-inactivated at 500 MPa, at 600 MPa and heat-inactivated, respectively;
- Mice in group 7 were injected with PBS.

For *in vivo* testing, the purified antigen was quantified by NanoDrop spectrophotometer at 280 nm and diluted in PBS. For priming, antigen was combined in equal volumes with Freund's complete adjuvant (water-in-oil emulsion, 85% Drakeol 6VR mineral oil, 15% Mannide Monooleate Arlacel A, 1 mg/ml heat-inactivated *Mycobacterium tuberculosis* [H37Ra, ATCC 25177], Merck KGaA, Darmstadt, Germany). The mixture was vigorously vortexed to create a stable water-in-oil emulsion. The antigen, combined with the adjuvant, was diluted to a final concentration of 20 μg/ml (10 μg / 500 μl inoculation volume).

Mice were primed subcutaneously (on the scruff) with 10 μg / 500 μl of HHP- or heat-inactivated SARS-CoV-2 (or PBS in the control group) with complete Freund's adjuvant at day 0. Intraperitoneal boost at day 28 was carried out with the same final antigen concentration in PBS (without Freund's complete adjuvant).

To evaluate the safety of the vaccine, mice were closely monitored for signs of local and systemic adverse reactions. Local reactions, such as erythema or swelling at the injection site, were assessed visually. Systemic effects, including changes in body

weight, activity levels, or signs of distress, were monitored daily to ensure animal welfare.

Immunogenicity was assessed by measuring the production of antigen-specific antibodies and evaluating cellular immune responses.

For B-cell responses evaluation, blood samples were collected by submandibular puncture at day 0 (baseline serum), and at regular intervals post-immunization, i.e. on day 14, day 28 (before boost), day 35 and day 53. Serum was separated from whole blood by centrifugation at 3000 g for 10 minutes and stored at -20 °C until analysis. To quantify and characterize SARS-CoV-2-specific antibodies, enzyme-linked immunosorbent assay (ELISA), Western blot and virus neutralization were performed.

For assessing cellular immunity, splenocytes were isolated from mice sacrificed at the study's endpoint. At day 53 mice were euthanized by a competent person by exsanguination through transcardiac terminal bleeding. The procedure was carried out under general anesthesia (Ketamine 100 mg/kg and Xylazine 10 mg/kg by intraperitoneal administration). All the procedures and activities were performed in compliance with National Legislation (Legislative Decree n. 26/2014) and under Ministry of Health authorization. Blood collected through cardiac puncture was used for the characterization of circulating T-cell responses (ELISpot). Mice were hence necropsied, and spleen was removed for splenic T-cell responses assessment. Circulating peripheral blood mononucleate cells (PBMC) and splenocytes were processed immediately after sacrifice. Immunization and biological samples collection schedule is summarized in Figure 9.

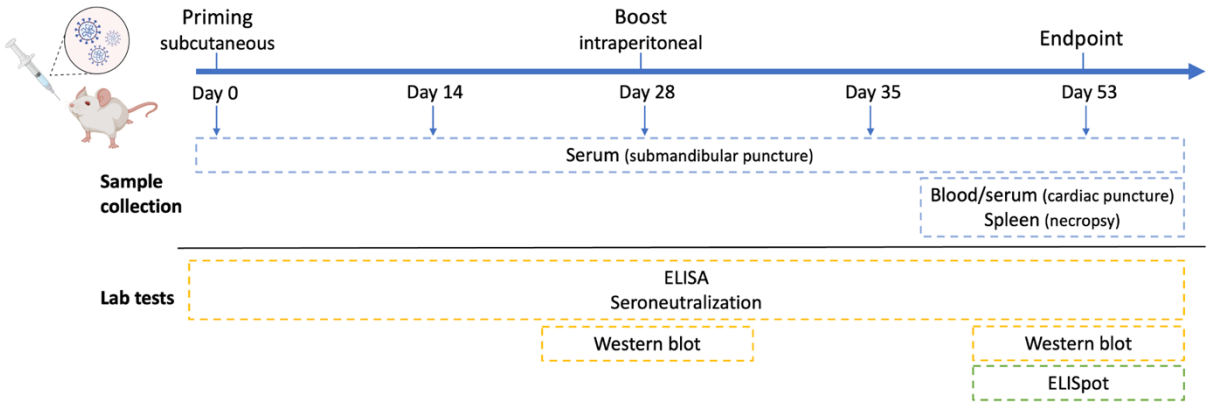

Figure 9. HHP-inactivated SARS-CoV-2 *in vivo* safety and immunogenicity testing. Experimental timeline and protocol for mouse immunization, including priming (day 0), boosting (day 28), biological samples collection, and endpoint (day 53).

3.6.1 B cell response assessment

3.6.1.1 Enzyme-Linked Immunosorbent Assay (ELISA)

Total anti-SARS-CoV-2 IgG antibodies developed following immunization were measured by indirect ELISA to provide a quantification of the total humoral immune response, capturing antibodies targeting various viral epitopes, including spike, nucleocapsid, and other structural proteins. ELISA was conducted at day 0, 14, 28, 35 and 53.

ELISA Medisorp plates (ThermoFisher) were coated with 50 µl per well of purified SARS-CoV-2 antigen (whole virion, beta-propiolactone-inactivated and sucrose-purified; IZSLER, 31902/46) at a saturating concentration by incubation overnight at 4 °C in ELISA coating buffer (0.05 M carbonate/bicarbonate buffer, pH 9.6, ThermoFisher). The plates were then washed three times with 250 µl of wash buffer (PBS, 0.05% Tween 20). Subsequently, 50 µl of 1:100 diluted mouse sera were added to each well and incubated for one hour at 37 °C. Following three washes, an HRP-conjugated Goat anti-Mouse IgG (IZSLER in-house produced, 72689) was added at 50 ng/ml in dilution buffer (PBS, 0.05% Tween 20 and 1% yeast extract) to each well and incubated for one hour at 37 °C. After a final wash cycle, 50 µl of substrate solution (orthophenylenediamine 0.5 mg/ml and 0.02% H_2O_2 in 50 mM phosphate citrate buffer, pH 5, ThermoFisher) was added. After 10 minutes, the colorimetric reaction was stopped by the addition of 2 N sulfuric acid; absorbance values were read at 492 nm using an ELISA reader. The endpoint antibody titer was determined via a 4-parameter-logistic (4PL) curve fit analysis of optical density (OD) values for serially diluted sera, with a cut-off value set to three times the background signal. IgG titers were compared within and across groups to monitor immune response maturation at different time-points after immunization and highlight differences among different immunization groups.

3.6.1.2 Humoral response specificity characterization

In order to ascertain which viral proteins elicited the antibody response identified by ELISA for total anti-SARS-CoV-2 IgG, mouse sera were assayed with total viral proteins extracted by chemical methods from whole inactivated SARS-CoV-2 virions. Such data were essential for understanding the immunological profile elicited by HHP-inactivated vaccines, aiding in their optimization and validating their potential as safe and effective vaccine candidates. Western blot was performed at day 28 and 53.

Total proteins of beta-propiolactone-inactivated and sucrose-purified SARS-CoV-2 (IZSLER, 31902/46) were extracted in 20% (v/v) RIPA buffer incubated for 5 minutes on ice, quantified, normalized to 10 μg and loaded into NuPAGE 4-12% Bis-Tris Gels, as previously described. SDS-PAGE electrophoretic separation was carried out with NuPAGE MES SDS Running Buffer (ThermoFisher) in reducing conditions at 150 V constant voltage for 60 minutes.

After gel wash in 200 ml of ultrapure water in agitation for 15 minutes, the semi-dry transfer of separated proteins was carried out on a Power Blotter XL (ThermoFisher) using nitrocellulose Power Blotter Select Transfer Stacks (ThermoFisher). Transfer stacks were separated into top and bottom halves, the latter was placed in the middle of the blotting surface (anode), the gel was placed on the bottom stack transfer membrane and the top stack was placed on top; cathode was placed to close the transfer apparatus. Blotting was performed at 1.3 A constant current for 7 minutes. Gel was checked for complete protein transfer by staining with Imperial™ Protein Stain (ThermoFisher) heated in the microwave for 90 seconds (or until boiling). Blotted membranes were washed with PBS three times for 5 minutes with shaking and blocked with StartingBlock™ Blocking Buffer, 0.05% Tween-20 for 1 hour at room temperature.

Membranes were hence cut vertically into strips, which were assayed with mouse sera diluted 1:50 in PBS, 10% StartingBlock™ Blocking Buffer, 0.05% Tween-20. Strips were incubated overnight at 4 °C with shaking to allow primary antibodies in the serum to bind specifically to their target viral protein targets immobilized on the membrane. Specific mouse anti-SARS-CoV-2 antibodies were detected using HRP-conjugated Goat anti-Mouse IgG (IZSLER in-house produced, 72689) at 50 ng/mL. After secondary antibody incubation, membranes were washed 3 times for 20 minutes with PBS. Chemiluminescent signal was detected using SuperSignal™ West Pico PLUS Chemiluminescent Substrate on an iBright FL1500 instrument.

The evaluation of humoral immune response specificity was carried out through qualitative analyses to assess the immune response elicited against specific viral proteins. The presence or absence of protein bands corresponding to key viral antigens, such as the spike (S) and nucleocapsid (N) proteins, was carefully examined. This analysis focused on identifying the banding patterns unique to each experimental group and assessing potential differences in the antigen recognition profiles of antibodies elicited by HHP-inactivated versus heat-inactivated viruses. Molecular weight markers (PageRuler™ Plus Prestained Protein Ladder, 10 to 250 kDa,

ThermoFisher) were used for accurate protein size estimation to validate the accuracy of protein identification. The data were compared across groups to evaluate variations in immune responses, with particular attention to any differences in antigenicity retention between the two inactivation methods.

3.6.1.3 Virus neutralization test

The neutralizing activity of immunized mice sera was assessed using a Vero E6 cell culture virus neutralization assay in which the cell culture is infected in the presence of serial serum concentrations. Virus neutralization was carried out at day 0, 14, 28, 35 and 53.

Serum samples were preincubated at 56 °C for 5 minutes for complement components inactivation. Sera samples were tested at a starting dilution of 1:100 and then further diluted 1:2 in 2% FBS MEM, reaching a dilution of 1:12.800. Each dilution was then mixed with an equal volume of viral solution (final volume: 100 µl per well) at the concentration of 2000 $TCID_{50}$/ml (corresponding to 100 $TCID_{50}$/well). After a one-hour incubation at 37 °C, the mixture was transferred in a 96-well plate containing a sub-confluent Vero E6 cell monolayer.

Plates were incubated at 37 °C, 5% CO_2 for 72 hours and then cells were fixed and stained using a 4% formaldehyde solution (Fisher Chemical, Milan, Italy) in crystal violet (Delcon, Bergamo, Italy) incubated for 30 minutes at room temperature. Every sample was tested in duplicate. Absence or presence of cytopathic effect at each dilution was assessed by comparison of each well with virus control and no-virus control wells. The neutralization titer was defined as the reciprocal of the highest serum dilution capable of inhibiting the appearance of a visible cytopathic effect. Neutralization titers were compared within and across groups to monitor maturation of the immune response at different time-points after immunization and highlight differences among different immunization groups.

3.6.2 T cell response assessment

3.6.2.1 ELISpot assay on PBMC and splenocytes

ELISpot assay was performed at 53 days after immunization for the *ex vivo* quantification of IFNγ-secreting cells (CD4+ and CD8+ T-cell lymphocytes) after stimulation with an appropriate stimulus *in vitro*. T-cell response was evaluated both on PBMC and on splenocytes.

Whole blood samples were collected from cardiac puncture in lithium-heparin and kept at room temperature until processing (within 8 hour). Blood was subsequently diluted 1:2 in RPMI 1640 supplemented with 10% heat inactivated FBS, 2 mM L-glutamine, 100 U/ml penicillin, 100 μg/ml streptomycin, and transferred into vials containing 1 ml of Ficoll®-Paque Premium (Merck KGaA, Darmstadt, Germany) separation medium (ratio of 1:3 between medium and diluted blood). Vials were centrifuged at 1000 g for 20 minutes and PBMC ring was collected, transferred into a clean vial and washed twice with supplemented RPMI 1640 by sequentially centrifuging at 600 g for 7 minutes and discarding the supernatant. Pellet was finally resuspended in 1 ml of supplemented RPMI 1640.

Speen were aseptically removed during necropsy and stored at room temperature in supplemented RPMI 1640 until processing (within 8 hours). Spleens were then transferred into sterile petri dishes, gently dissociated with a syringe piston and filtered through a 70 μm cell stainer. Splenocytes were washed twice in supplemented RPMI 1640 by centrifuging at 600 g for 7 minutes and discarding the supernatant. Final pellet was resuspended in 1 ml of supplemented RPMI 1640.

PBMC and splenocytes were counted in a hemocytometer following staining with Trypan Blue (50% v/v) and diluted to 2.5 x 10^6 cells/ml. ELISpot assay was carried out with Murine IFNγ ELISpot Kit (Diaclone SAS, Besancon Cedex, France). Cells were seeded (2.5 x 10^5 cells/well) in a skimmed-milk-blocked and anti-IFNγ-capture-antibody coated PVDF (polyvinylidene difluoride) bottomed-well plates. SARS-CoV-2 specific stimulus (beta-propiolactone-inactivated and sucrose-purified SARS-CoV-2 [IZSLER, 31902/46] was added at a concentration of 10 μg/ml. PHA (Phytohaemagglutinin) mitogen was used as a positive control at 5 μg/ml; PBS was used as a negative control. Plates were incubated at 37 °C with 5% of CO_2 for 24 hours.

Following incubation, plates were washed once with 100 μl of PBS, 0.05% Tween-20 added to each well and incubated at 4°C for 10 minutes. After incubation, the plate was then washed three times with PBS, 0.05% Tween-20. Following this, 100 μl of biotinylated anti-IFNγ Detection Antibody solution was added to each well, and the plate was covered and incubated at room temperature for 1.5 hours. The plates were washed three times with 100 μl of PBS, 0.05% Tween-20 per well and incubated with Streptavidin-AP (Alkaline Phosphatase) conjugate for 1 hour at room temperature. After incubation, the wells were emptied and washed three times with 100 μl of PBS, 0.05% Tween-20. The plastic covering the plate bottom was then removed, and both

sides of the plate were washed three times with distilled water, removing excess water by tapping onto absorbent paper. Next, 100 μl of ready-to-use BCIP/NBT (5-bromo-4-chloro-3-indolyl-1-phosphate/ nitroblue tetrazolium) substrate were added and incubated for 15 minutes in the dark, until spot development. Plates were washed three times with distilled water. The number of distinct dark-colored spots on the membrane of each well was counted through a stereomicroscope. Results were interpreted as follows:

- The number of spots for the negative control should be < 10;
- The number of spots for the positive control should be ≥ 20 or show saturation (if the positive control shows < 20 spots, the result should be considered invalid unless there is reactivity against the tested antigen);
- The sample is reactive towards the tested antigen if ≥ 8 spots have developed, while the sample is non-reactive to the tested antigen if < 4 spots have developed.

For the quantification of the reactogenicity of the sample against the specific SARS-CoV-2 stimulus, the number of spots recorded in the negative control well were subtracted from the number of spots recorded in the antigen-specific stimulus well. A "Reactive" result indicates that the sample contains effector T cells producing IFNγ when exposed to SARS-CoV-2 stimulus. A "Non-reactive" result indicates that no SARS-CoV-2-sensitised effector T cells were detected. IFNγ production was compared among immunization groups.

3.7 Data analysis and statistical evaluation of immunogenicity

The data collected in the *in vivo* safety and immunogenicity testing, encompassing antibody titers, neutralizing antibody titers, and levels of interferon production, were subjected to comprehensive statistical analysis to compare and evaluate immunogenicity outcomes across the different experimental groups. Descriptive statistics, including mean, median, standard deviation, and interquartile ranges, were calculated to provide a clear understanding of central tendencies and variability. The choice of statistical tests was carefully tailored to the nature of the data, taking into consideration factors such as the distribution (normal or non-normal), sample size, and variability within and between groups. One-way ANOVA followed by Tukey's HSD test for pairwise comparisons was used, provided the normality of data distribution

was confirmed via the Shapiro-Wilk test. In cases where the data did not meet normality assumptions, the Kruskal-Wallis test was employed, followed by Dunn's post-hoc test with Bonferroni correction to account for multiple comparisons. For every statistical test, two levels of statistical significance were considered ($p < 0.05$ **, $p < 0.01$ ***) to assess the results significance. The results were interpreted in the context of the vaccine's potential efficacy evaluation. Group differences were analyzed to identify significant trends and variations in both humoral and cellular immune responses. For humoral immunity, the focus was on total antibody titers and their neutralizing capabilities against the target pathogen. These measures were compared to evaluate the ability of each vaccine candidate to stimulate an effective antibody-mediated response. For cellular immunity, levels of interferon production, a critical marker of T-cell activation and immune modulation, were analyzed to determine the breadth and robustness of the cell-mediated response. This statistical approach was instrumental in interpreting the data in the broader context of the vaccine's potential to elicit targeted and protective immune responses while maintaining an acceptable safety profile.

3.8 Thermostability assessment

To evaluate the thermostability of HHP-inactivated viral vaccine, we implemented an experimental design that involved storing the preparation under two distinct temperature conditions: ambient temperature (25 °C) and refrigerated temperature (4 °C). These conditions were chosen to simulate real-world scenarios where cold-chain logistics and refrigeration infrastructure may be limited. The vaccine preparation was divided into aliquots, with samples retrieved for analysis at predefined intervals: 7, 14 and 30 days. After retrieval from storage, the samples were immediately processed to assess any changes that might have occurred during the storage period. The evaluation of immunogenicity through Western blot (as described in paragraph 3.5.2) focused on the Spike protein, which is key components in eliciting an immune response. Positive controls consisted of vaccine samples stored under ideal conditions (-80 °C). The data obtained from the Western blot analysis were analyzed to identify trends and differences across storage conditions and time points. The presence of strong, well-defined protein bands indicated that the vaccine preparation maintained its structural integrity and immunogenic potential, while weakened or smeared bands suggested degradation or loss of antigenicity.

4. Results

4.1 SARS-CoV-2

Hermetically sealed polyethylene pouches containing viral suspensions were subjected to HHP treatment at 400, 500 and 600 MPa for 5 minutes. The operating pressure conditions were chosen to minimize the total processing time, aiming to develop a potentially high-throughput inactivation system. This approach required operating at relatively high pressures to achieve complete viral inactivation, in contrast to other inactivation protocols described in the literature[326,327], which employ lower pressures but require significantly longer treatment durations, on the order of hours rather than minutes. Each pressure condition was applied as an independent treatment cycle. After each pressurization cycle, the viral suspension subjected to that specific pressure was removed, and a fresh, untreated viral stock was introduced for the next cycle. This ensured that each viral stock was exposed to only one pressure condition, preserving the integrity of independent treatments. Pressure inside the chamber was continuously recorded throughout the entire series of treatments, including during decompression phases when the pressure returned to ambient levels, hence producing a sequential pressure-time profile (Figure 10). This methodological choice streamlined the workflow while maintaining precise control over pressure conditions.

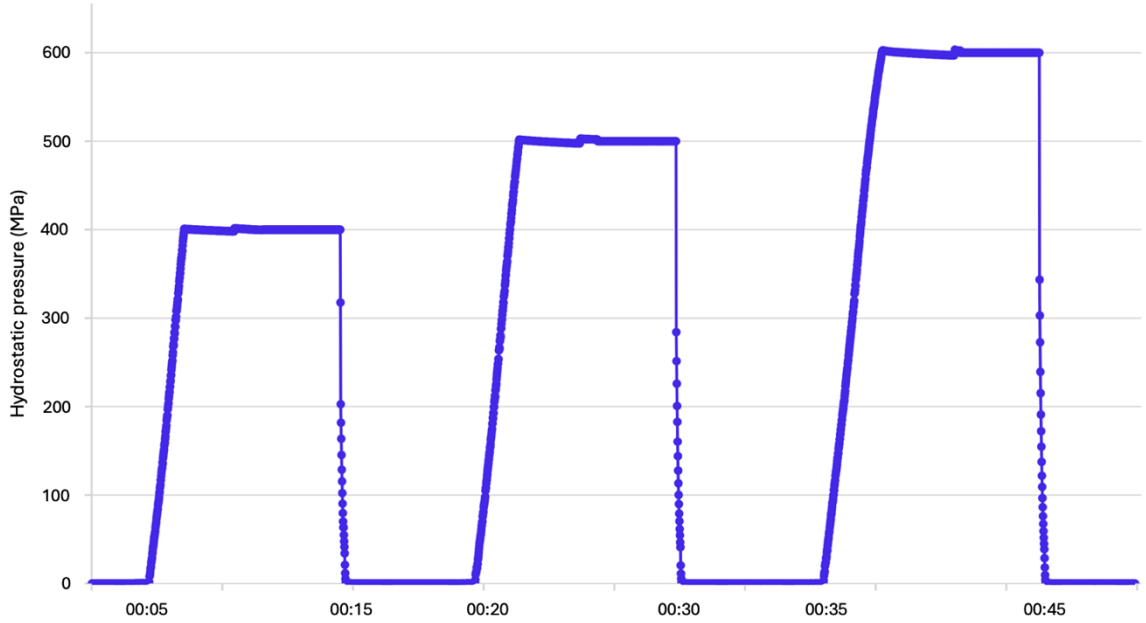

Figure 10. Pressure profile of high hydrostatic pressure (HHP) treatment applied over time. Each pressure was maintained for a fixed duration, followed by a rapid decompression phase to atmospheric pressure. After each pressurization cycle, the viral suspension subjected to the treatment was removed and replaced with a fresh suspension for the following cycle. The machine was maintained active throughout the entire series of treatments, continuously recording pressure, including during decompression phases when the pressure returned to ambient levels, resulting in the appearance of a sequential pressure profile in the figure, although each cycle was conducted separately.

4.1.1 Inactivation assessment

The reduction of viral infectivity under HHP treatments was assessed by endpoint titration. Treatment at 400 MPa resulted in substantial reductions in infectious titer, with log10 reductions of 2.9 and 3.9 for B.1 and BQ.1.1, respectively, compared to the non-HHP-treated control. This level of pressure, while significantly reducing infectivity, did not achieve complete inactivation of the virus. Conversely, treatments at 500 MPa and 600 MPa demonstrated no detectable infectious virus for either lineage, suggesting complete viral inactivation at these higher pressure levels.

To confirm the inactivation achieved at 500 MPa and 600 MPa, treated viral stocks were cultured on Vero E6 cells. Viral replication was monitored using qRT-PCR. Change in viral load during incubation was calculated using the delta Ct method. 400 MPa treatment temporarily suppressed viral replication, but was insufficient to maintain long-term inhibition, allowing a significant rebound in viral replication for both lineages at 48 hours post-infection. At 500 and 600 MPa, viral replication was consistently suppressed, and viral load declined progressively from 0 to 72 hours post-

infection, indicating that both pressures exerted a stronger inhibitory effect on viral replication, leading to complete abrogation (Figure 11).

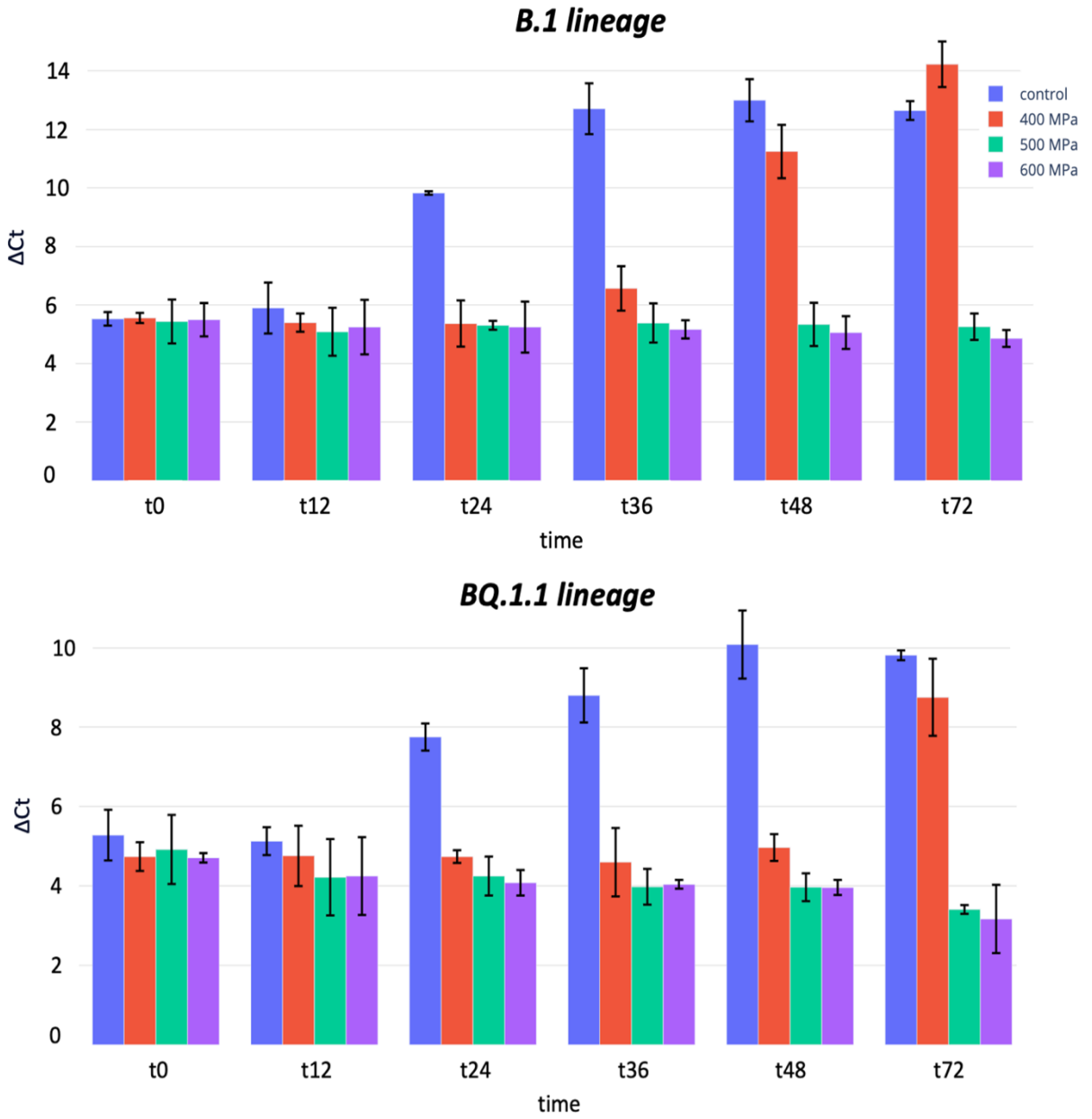

Figure 11. Viral replication dynamics, measured as ΔCt values of Real-Time PCR, for HHP-treated and non-HHP treated B.1 and BQ.1.1 lineages over time. Bar graph showing ΔCt values measured at six time points (t0, t12, t24, t36, t48, and t72 hours after infection) in samples treated with different HHP conditions (400 MPa, 500 MPa, 600 MPa) compared to an untreated control group. Error bars represent standard deviations.

The observed differences in viral replication dynamics across the three pressure levels highlighted the pressure-dependent effects of HHP on viral inactivation. At 400 MPa, the suppression of replication was transient, and the rebound observed at later stages suggests that the treatment was insufficient to permanently disrupt the virus's ability

to replicate. This partial inactivation may reflect minimal structural or functional damage to viral particles, allowing a subset of the virus to retain infectivity. In contrast, 500 MPa exerted a more potent inhibitory effect, with sustained suppression of viral replication and no evidence of recovery. This suggested that virion structural and functional integrity was more significantly compromised at this pressure level, preventing the initiation of replication. Similarly, at 600 MPa viral replication was effectively abrogated across all time points, likely due to extensive structural disruption or loss of critical functional components required for cell receptor engagement, cell entry and replication.

4.1.2 Structural and antigenicity analysis

4.1.2.1 Negative Staining Electron Microscopy (nsEM)

Negative staining electron microscopy (nsEM) imaging allowed for detailed observations of viral particles treated under different pressure conditions. The analysis revealed distinct morphological effects, providing important insights into how HHP impacted viral ultrastructure and helped explain the mechanisms through which HHP leads to viral inactivation.

At 400 MPa, the results from nsEM images showed that the overall morphology of the viral particles was fully preserved. The virions retained a typical coronavirus structure, characterized by spherical particles with clear surface projections (S proteins), which are essential for the virus's ability to bind and enter host cells. The surface spikes were still discernible, protruding from the viral envelope in a well-defined pattern, typical of coronaviruses. This structural integrity indicates that treatment at 400 MPa was effective in reducing viral infectivity but did not cause significant or irreversible structural damage to the virus. The fact that the virions retained their general form and spike structure suggested that this pressure level may have been sufficient to interfere with some viral functions or processes, but it was not potent enough to entirely abrogate infectivity. The preservation of the virus's surface spikes suggests that treatment at 400 MPa likely disrupted some aspect of the viral lifecycle, such as receptor binding or internalization, without causing major structural collapse. This finding was supported by the infectivity titration results, where a notable reduction in virus infectivity was observed, yet some residual infectivity remained. It is likely that the viral particles at this pressure level, while altered to some degree, still maintain enough structural integrity to infect host cells, albeit at a diminished capacity.

In contrast, viruses treated at 500 MPa exhibited a more significant morphological alteration. While viral particles remained visible in the electron micrographs and could still be identified as coronaviruses, a noticeable distortion in their appearance was observed. The general spherical shape of the virions remained intact; however, the surface spikes, which are crucial for viral attachment, were less defined and appeared partially distorted, and the overall arrangement of the spike proteins was irregular compared to untreated controls. This subtle alteration in the morphology of the virus suggested that 500 MPa induced structural damage to the surface proteins, specifically the spike proteins, which are essential for the virus's ability to bind to host cell receptors. The altered spikes may have led to a diminished ability to interact with the host cell receptor, a crucial step in the viral entry process. Although the virions maintained their general shape, the functional disruption of the surface spikes could have significantly reduced viral infectivity, possibly explaining the observed decrease in infectivity in endpoint titration assays and the inability of 500 MPa-treated virions to replicate in Vero E6 cell culture.

At 600 MPa, the morphological effects were much more pronounced, with significant structural disruption observed in the viral particles. nsEM images showed a dramatic reduction in the number of identifiable viral particles. This decrease in visible virions suggested that the high-pressure treatment at 600 MPa likely caused a substantial amount of viral particles to lose their structural integrity to the point where they were no longer discernible under electron microscopy. The viral particles that remained visible appeared drastically altered in shape and exhibited a variety of irregular, collapsed, or deformed structures, further confirming the destabilizing effects of this pressure level.

More notably, the surface spikes, which are crucial for viral attachment and entry into host cells, were entirely absent in the viral particles observed at 600 MPa. The surface of the virions appeared smooth, with no visible projections or protrusions where the spike proteins would normally be located. The complete loss of spike proteins, which are essential for the virus’s ability to recognize and bind to host cells, likely explains the observed complete inactivation of the virus at this pressure level. The absence of the spike proteins rendered the virions incapable of interacting with cellular receptors, effectively preventing viral entry into host cells.

In addition to the loss of the surface spikes, the overall structural integrity of the remaining virions was highly compromised. Many of the viral particles displayed

abnormal, collapsed, or fragmented shapes, indicative of severe destabilization of the viral envelope. This suggested that the 600 MPa pressure treatment led to extensive damage not only to the surface proteins but also to the other structures of the virus, including potential damage to the viral envelope, which could interfere with the virus's ability to maintain its stability and infectiousness. The substantial morphological alterations observed at 600 MPa supported the conclusion that this pressure level caused a profound and irreversible destabilization of the virus, effectively leading to complete viral inactivation. Findings of nsEM are summarized in Figure 12.

Overall, the findings from the analysis of the morphological effects at the different pressure levels highlighted a clear pressure-dependent effect on viral structure. Treatment at 400 MPa resulted in minimal structural damage, with the virus retaining its typical spherical shape and intact surface spikes, although infectivity was reduced. At 500 MPa, the pressure-induced alterations became more pronounced, with a partial loss of spike protein clarity and a less defined structure. These changes likely impact the virus's ability to bind to host cells, leading to inhibited infectivity. The most dramatic and irreversible effects were observed at 600 MPa, where the viral particles displayed severe morphological disruptions, including the complete loss of spike proteins and the collapse of the viral envelope. This treatment level caused significant structural damage that rendered the virus incapable of binding to host cells or maintaining its structural integrity, resulting in complete inactivation.

In conclusion, the morphological analysis of viruses treated with varying levels of HHP provides valuable insights into the mechanisms through which HHP exerts its antiviral effects. At 400 MPa, viral morphology remains largely intact, suggesting that this pressure level reduces infectivity without inducing substantial structural damage. At 500 MPa, more pronounced alterations in the spike proteins and surface structures were observed, while at 600 MPa, nsEM analysis highlighted the complete loss of spike proteins and structural collapse. Both treatment conditions led to complete viral inactivation. These findings underscore the pressure-dependent nature of HHP-induced viral inactivation and provide a deeper understanding of how high hydrostatic pressures can disrupt viral ultrastructure, thereby preventing viral infection.

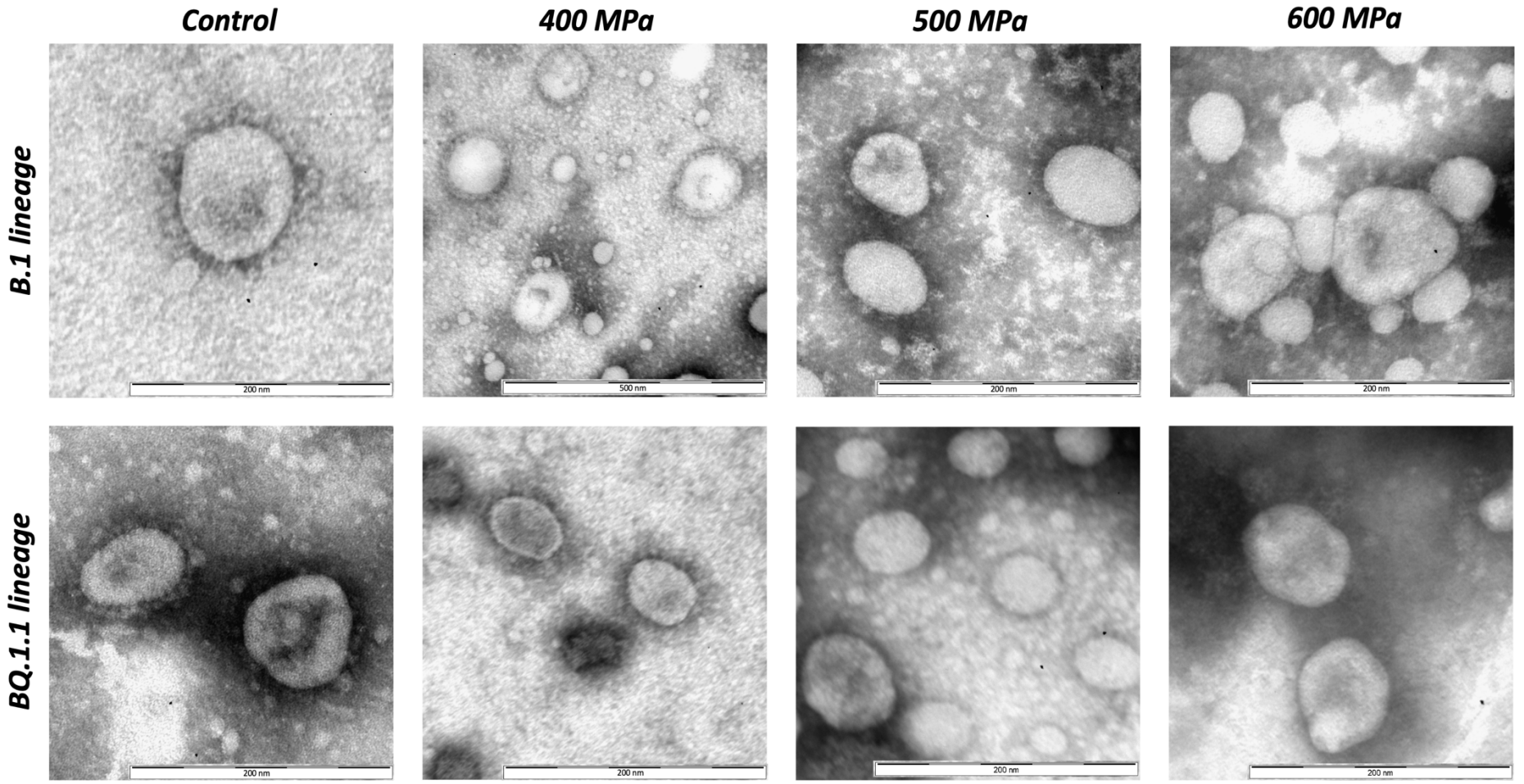

Figure 12. nsEM images of SARS-CoV-2 viral particles from B.1 and BQ.1.1 lineages subjected to different levels of high hydrostatic pressure: untreated control, 400 MPa, 500 MPa, and 600 MPa. Increasing pressure levels induce progressive morphological alterations in viral structure, with a marked loss of envelope integrity and progressive loss of surface spike proteins observed at higher pressures. Scale bar: 200 nm.

4.1.2.2 Western blot

Western blot analysis of the spike protein from viruses subjected to HHP treatments at 400 MPa, 500 MPa, and 600 MPa provided insights into the impact of HHP on the structural integrity of the viral protein and its potential effect on the virus's functionality. This analysis specifically focused on the monomeric and trimeric forms of the spike protein, which are critical for viral entry into host cells. The results demonstrated distinct patterns of change in the spike protein's structure across the different pressures, offering important implications for viral inactivation.

One of the key findings from the Western blot analysis was a noticeable reduction in the signals corresponding to both monomeric (~ 140 kDa) and trimeric (~ 450 kDa) forms of the spike protein across all pressure treatments, suggesting that high-pressure treatment may have led to some level of structural destabilization or dissociation of the spike. Interestingly, only slight and non-significant differences were observed between the three pressure levels in terms of the extent of reduction in the monomeric and trimeric spike signals.

In addition to the reduction in the monomeric and trimeric forms of the spike protein, the Western blot analysis revealed the appearance of higher molecular weight bands (> 450 kDa) that were less represented in untreated viral samples. These additional bands likely represent macromolecular aggregates, which may have been induced by the HHP treatment. The intensity of these higher molecular weight bands increased progressively from 400 MPa to 600 MPa. These high molecular weight bands were particularly prominent at higher pressures, with the 600 MPa treatment leading to the most intense signals, suggesting that the extent of macromolecular aggregation is pressure dependent. This observation suggested that higher pressures led to more extensive macromolecular aggregation, which could play a significant role in viral inactivation.

HHP is known to apply physical stress to proteins, potentially causing them to misfold, undergo conformational changes, or aggregate. In the case of the spike protein, the application of pressure may have led to protein-protein interactions, either among spike proteins themselves or with other viral components. These interactions could have resulted in the formation of larger complexes that migrate more slowly on the Western blot, appearing as higher molecular weight bands. This aggregation phenomenon was observed to be more pronounced at higher pressures, with 600 MPa showing the most intense higher molecular weight bands. The increase in intensity of

the higher molecular weight bands with increasing pressure suggests that higher pressures lead to more extensive protein aggregation. This pressure-dependent effect is important because it provides further insight into the mechanisms by which HHP may inactivate the virus. While the reduction in the monomeric and trimeric forms of the spike protein is significant, the appearance of higher molecular weight aggregates suggests that the aggregation of viral proteins is a major factor contributing to viral inactivation. At the highest pressure (600 MPa), the most intense higher molecular weight bands were observed, indicating that this pressure induced the most severe structural disruption in the spike protein.

In addition to the spike protein, Western blot analysis was also conducted on other structural proteins of the virus, specifically the membrane and the nucleocapsid proteins. The results revealed no substantial differences between the treated samples and the untreated control, nor were there any discernible changes between the different pressure treatments in terms of signal intensity and band pattern, indicating that the integrity of the membrane and nucleocapsid proteins was largely preserved under high pressure conditions. The minimal reduction in M and N protein signals in HHP-treated samples suggests that the inactivation process caused by pressure may primarily target the spike protein while leaving other structural proteins more intact.

Western blot analyses were also performed on heat-inactivated viral propagates, which were later used as controls for mouse immunizations, and the results were compared with 500 MPa and 600 MPa HHP-treated viral stocks. The comparison of these different viral inactivation methods revealed significant differences in the preservation of key structural proteins.

The heat-inactivated virus showed a profound alteration in its protein profile. Notably, the signal corresponding to the spike protein was completely absent in the heat-inactivated virus, indicating a complete loss of this critical viral protein upon heat treatment. This loss suggests that heat inactivation induces more severe structural damage to the spike protein compared to HHP treatment. In contrast, the M and N proteins in the heat-inactivated virus showed only a partial reduction in their respective signals, suggesting that while heat treatment affected these proteins to some extent, it did not lead to their complete degradation.

When comparing these heat-inactivated samples to the virus treated with high hydrostatic pressure at 500 MPa and 600 MPa, several key differences were observed. Both HHP treatments resulted in a notable reduction in the spike protein signal,

although, unlike the heat-inactivated virus, the spike protein was not completely absent. The reduction in the spike protein signal after HHP treatment suggests that while the pressure treatment compromises the protein's structure, it does not entirely eliminate it. This finding contrasts with heat inactivation, which resulted in a complete loss of the spike protein and implies that HHP treatment may be a less aggressive method of inactivation, preserving some functional or structural components of the virus. In contrast to the complete loss of the spike protein, the membrane and nucleocapsid proteins in the heat-inactivated virus showed a partial reduction in their signals, but these proteins were not entirely absent. This partial reduction suggests that, although heat inactivation did affect the M and N proteins, it was not as detrimental to these proteins as it was to the spike protein. Results of Western blot analysis performed on HHP- and heat-inactivated propagates are reported in Figure 13.

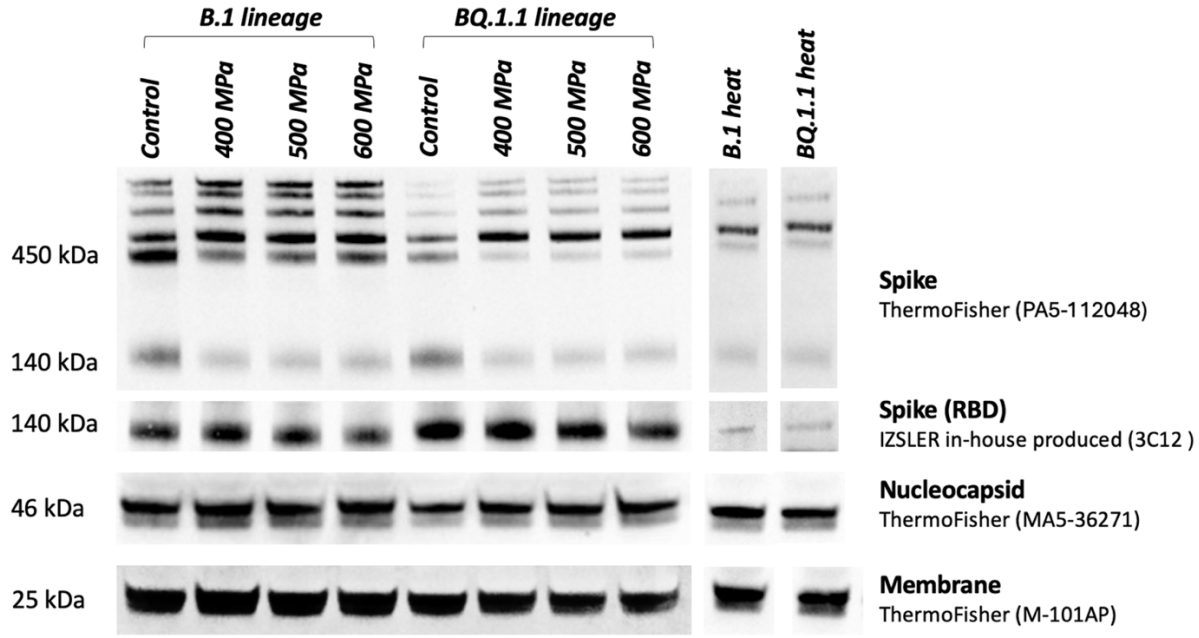

Figure 13. Western blot analysis of SARS-CoV-2 structural proteins (Spike, Spike RBD [Receptors Binding Domain], Nucleocapsid, and Membrane) in viral particles from B.1 and BQ.1.1 lineages subjected to HHP treatments at 400, 500, and 600 MPa, as well as heat inactivation. Untreated controls for both lineages are included for comparison. Protein detection was performed using specific primary monoclonal and polyclonal antibodies: Spike (ThermoFisher PA5-112048), Spike RBD (IZSLER in-house produced, 3C12), Nucleocapsid (ThermoFisher MA5-36271), and Membrane (ThermoFisher M-101AP). Protein band intensities indicate progressive loss or modification of Spike protein structure under increasing HHP, with relative preservation of Nucleocapsid and Membrane proteins.

4.1.3 *In vivo* safety and immunogenicity

In vivo experiments were conducted on 28 6-month-old Swiss CD-1 mice subcutaneously vaccinated and intraperitoneally boosted at day 28 with 10 μg of inactivated virus. All animal procedures were conducted in accordance with institutional and national ethical guidelines for animal experimentation. Following immunization, mice were monitored daily to assess their general health status and detect any potential adverse effects. Monitoring included evaluation of clinical signs such as behavior, posture, coat condition, and body weight. In some animals, a localized swelling was observed on the scruff at the site of the first injection, likely due to adjuvant accumulation. This reaction did not appear to cause any signs of discomfort or distress. Overall, no adverse effects were recorded, and the immunization protocols were well tolerated.

4.1.3.1 Anti-SARS-CoV-2 IgG titers

The levels of anti-SARS-CoV-2 IgG responses against whole virus were evaluated at days 14, 28, 35 and 53 after first immunization. The seroconversion rate was 100% at 14 days after immunization in HHP-immunized groups as well as in heat-immunized groups and antibody responses steadily but consistently increased until day 28. After the booster dose, antibody titers in both HHP-inactivated immunization groups increased consistently and peaked at day 35 (7 days after second immunization). In contrast, for heat-inactivated immunization group peak titer was reached on day 53.

The 500 MPa group exhibited the most dramatic increase in antibody titers over time. At t14, titers ranged from 110 to 170 (mean = 140, standard deviation [SD] = 29) for B.1 lineage and from 130 to 230 (mean = 183, SD = 50) for BQ.1.1 lineage, comparable to the heat group at this early stage. By t28, the titers surged to 2796-4643 (mean = 3474, SD = 843) for B.1 lineage and 2154-3213 (mean = 2555, SD = 469) for BQ.1.1 lineage, reflecting a significantly heightened immune activation. At t35, titers reached their highest values, with two mice for B.1 lineage and two mice for BQ.1.1 lineage achieving the assay's upper detection limit of 12800 and the remaining two of each group showing values of 6167 and 6233 (B.1 lineage) and 5213 and 8952 (BQ.1.1 lineage), with an overall mean of 9500 (SD = 3811) for B.1 and 9941 (SD = 3637) for BQ.1.1. At t53, antibody titers remained overall stable, with only slight increases in some individuals: for both lineages two mice achieved the assay upper detection limits (12800), while for the other two an increased antibody titer was observed (7562 and 7432 for B.1 lineage and 7988 and 9017 for BQ.1.1 lineage), with means attesting at 10149 (SD = 3062) and

10651 (SD = 2516), respectively. This rapid and substantial increase highlighted the strong immunogenic potential of virus inactivated at 500 MPa, with sustained antibody production observed across all mice.

The 600 MPa group showed a more modest increase in titers compared to the 500 MPa group. At t14, titers ranged from 80 to 150 (mean = 110, SD = 32) for B.1 lineage and from 120 to 180 (mean = 158, SD = 26) for BQ.1.1 lineage, slightly lower than the other groups. By t28, titers increased to 997–1456 (mean = 1207, SD = 197) for B.1 lineage and to 938-1397 (mean = 1217, SD = 232) for BQ.1.1 lineage, indicating a moderate response. At t35, titers ranged from 4214 to 7195 (mean = 4981, SD = 1252) for B.1 lineage and from 3146 to 6978 (mean = 4576, SD = 1730) for BQ.1.1 lineage, reflecting continued antibody production but with less consistency among individuals. At t53, titers remained overall stable ranging from 4278 to 7195 (mean = 5955, SD = 1294) for B.1 lineage and from 3614 to 7021 (mean = 4962, SD = 1451) for BQ.1.1 lineage. Although the immune response improved over time, it did not match the magnitude observed in the 500 MPa group, suggesting that higher pressure may have some impact on antigen presentation or immunogenicity.

The heat-inactivated group showed a steady increase in IgG titers over time. At t14, titers ranged from 110 to 220 (mean = 179, SD = 47), for B.1 lineage and from 120 to 350 for BQ.1.1 lineage (mean = 183, SD = 112), reflecting the initiation of the antibody response. By t28, titers increased substantially to a range of 1284-1895 (mean = 1513, SD = 288) for B.1 lineage and 1268-2193 (mean = 1707, SD = 506) for BQ.1.1 lineage, indicating a robust antibody production in response to immunization. At t35, the titers reached values in the range of 3722-4782 (mean = 4454, SD = 494) for B.1 lineage and 3569-4770 (mean = 4066, SD = 508) for BQ.1.1 lineage. Overall, peak titers were reached at the latest time point, t53, with values ranging from 3963 to 5276 (mean = 4505, SD = 552) for B.1 lineage and from 4236 to 6803 (mean = 5275, SD = 1095) for BQ.1.1 lineage. Overall, heat inactivation elicited a consistent response, albeit with less pronounced increases compared to HHP treatments.

The One Way ANOVA test indicated a significant difference in the antibody titer among the different time points for both tested viral lineages and for all immunization groups (B.1 lineage: F = 15.2, p = 2.19E-4 for 500 MPa-inactivated; F = 39.4, p = 1.74E-6 for 600 MPa-inactivated; F = 118.8, p = 3.45E-09 for heat-inactivated; BQ.1.1 lineage: F = 48.8, p = 5.37E-07 for heat-inactivated; F = 22.31, p = 3.37E-5 for 500 MPa-inactivated; F = 17.90, p = 9.99E-5 for 600 MPa-inactivated). The post-hoc Tukey's HSD test for

pairwise comparisons highlighted a consistent and statistically significant increase from day 0 to 14, 14 to 28 and 28 to 35 in all groups. Afterward, antibody titers plateaued in all experimental groups, with only slight and non-significant increases or decreases at day 53 (Figure 14a and 14b for B.1 lineage and BQ.1.1 lineage, respectively). No SARS-CoV-2 specific antibody response was detected in the control group.

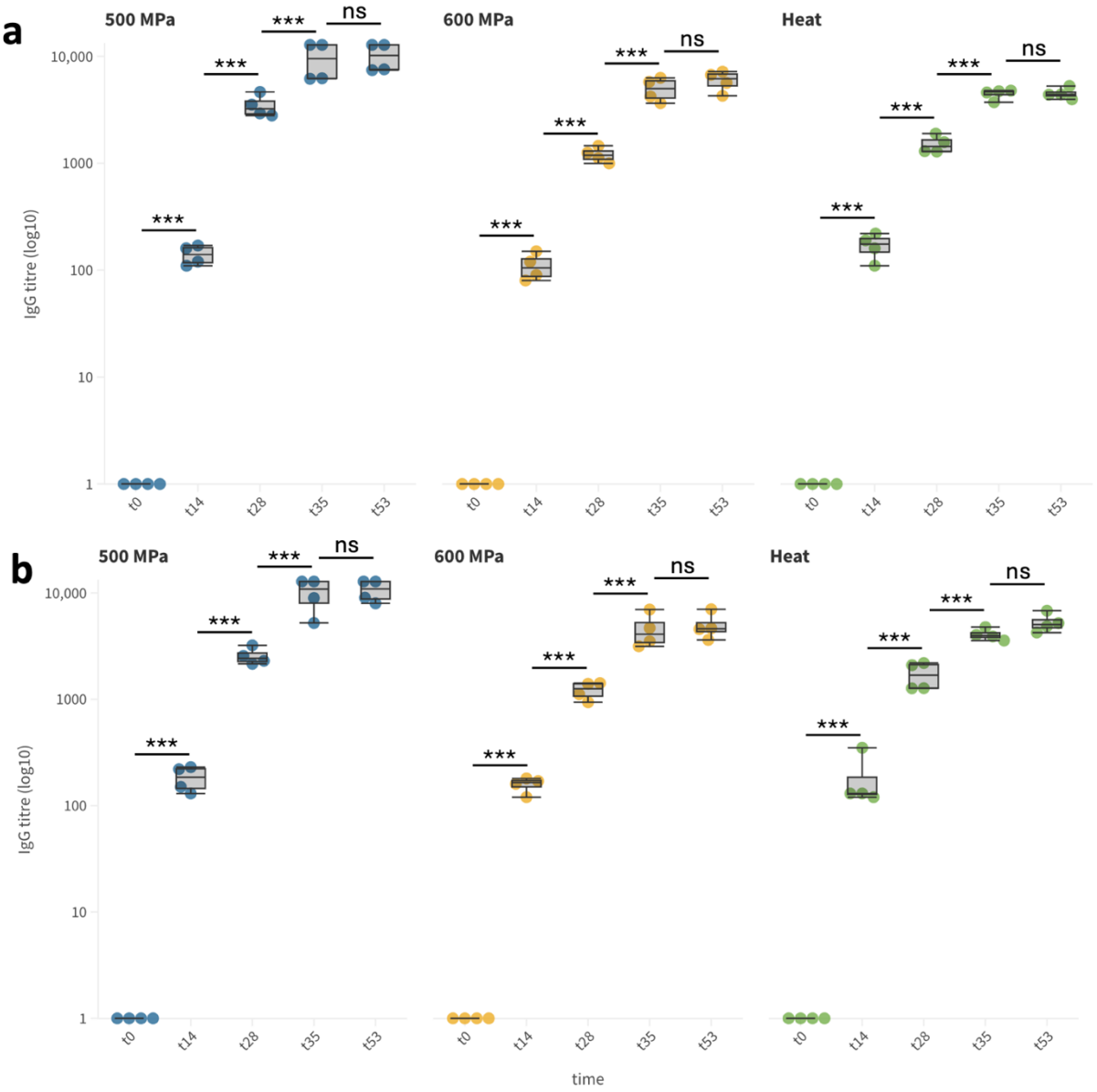

Figure 14. Intragroup comparison of IgG titers (log10) measured via ELISA in mice immunized with SARS-CoV-2 B.1 (A) and BQ.1.1. (B) lineages inactivated by high hydrostatic pressure (500 MPa and 600 MPa) or heat treatment, measured at different time points (t0, t14, t28, t35, and t53) post-immunization. Data show a significant increase in IgG titers starting from day 14 (t14), with peak levels maintained through day 53 (t53). Statistical significance was determined using ANOVA followed by multiple

comparison tests. Statistically significant differences are indicated: ***$p < 0.001$, **$p < 0.05$, ns = not significant.

For what concerns intergroup evaluation, at the earliest timepoint, t14, all groups exhibited relatively low titers, with no significant differences between groups. This suggests that all three inactivation methods preserved basic immunogenicity to initiate an antibody response, though the differences may reflect variability in individual immune activation.

By the t28 intermediate time point, clear distinctions emerged. The 500 MPa group showed the highest titers, averaging 3474 for B.1 lineage and 2555 for BQ.1.1 lineage), significantly exceeding the heat-inactivated group (mean of 1513 for B.1 lineage and 1707 for BQ.1.1 lineage) and the 600 MPa group (mean of 1207 for B.1 lineage and 1217 for BQ.1.1 lineage). This suggests that virus inactivated at 500 MPa elicited a stronger immune response during the early phases of immunization. The heat group performed better than the 600 MPa group, indicating that heat inactivation was more effective than 600 MPa at this stage in maintaining immunogenicity.

Differences between immunization groups became even more pronounced at t35 point. The 500 MPa group maintained the highest titers, with half the mice reaching 12800 and the other half showing titers above 5000 for both lineages (overall mean of 9500 for B.1 lineage and 9941 for BQ.1.1 lineage). The 600 MPa group exhibited moderate titers, averaging 4981for B.1 lineage and 4576 for BQ.1.1 lineage), which were consistently higher than those of the heat group (4454 for B.1 lineage and 4066 for BQ.1.1 lineage). This pattern underscores the higher immunogenic potential of the 500 MPa treatment compared to both 600 MPa and heat inactivation, particularly in sustaining high IgG production over time.

At t53, the 500 MPa group exhibits markedly higher antibody titers, averaging 10149 for B.1 lineage and 10651 for BQ.1.1 lineage, including two peak values at the upper limit of 12800. The 600 MPa group yields intermediate titers, with means of 5955 for B.1 lineage and 4962 for BQ.1.1 lineage. While higher than those in the heat group, the antibody levels remain consistently lower than those in the 500 MPa group. The heat group displays the lowest antibody titers, with means of 4505 for B.1 lineage and 5275 for BQ.1.1 lineage.

When comparing the three groups at each time point, the 500 MPa HHP-treated group consistently showed the highest antibody titers at t28 (B.1: $F = 21.81$, $p = 3.54E\text{-}4$;

BQ.1.1: F = 10.38, p = 4.60E-3), t35 (B.1: F = 4.83, p = 3.76E-2, BQ.1.1: F = 7.72, p = 1.11E-2), and t53 (B.1: F = 9.08, p = 6.95E-3; BQ.1.1: F =12.74, p = 2.37E-3). At all three time points, the 500 MPa treatment elicited the most robust and consistent IgG response, with titers peaking significantly higher than those of the other groups. Furthermore, the antibody titers in the 500 MPa group remained high and sustained throughout the time course, indicating a robust immune response. In contrast, the heat-inactivated group showed a slower increase and lower overall antibody titers and lower titers compared to the 500 MPa group. The 600 MPa HHP-treated group showed a general increase in antibody titers over time, consistently exhibiting lower titers compared to the 500 MPa group. No statistically significant differences were detected between the 600 MPa group and the heat-inactivated group (Figure 15a for B.1 lineage and Figure 15b for BQ.1.1 lineage).

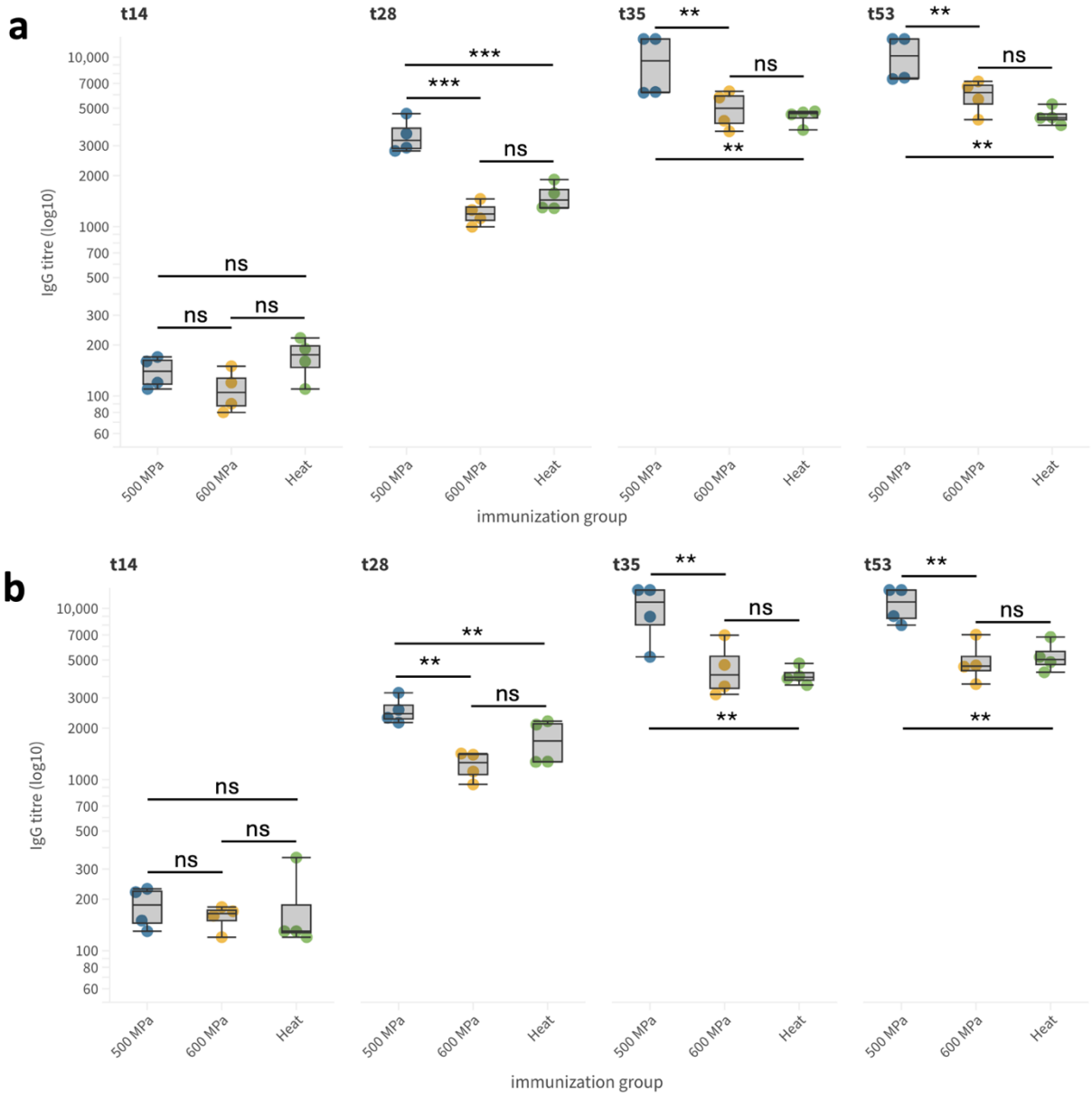

Figure 15. Intergroup comparison of IgG titers (log10) measured via ELISA at different time points (t0, t14, t28, t35, and t53) post-immunization in mice immunized with SARS-CoV-2 B.1 (A) and BQ.1.1 (B) lineages inactivated by high hydrostatic pressure (500 MPa and 600 MPa) or heat treatment. Statistically significant differences among group are evident from t28, with 500 MPa-inactivated vaccine candidate inducing the highest antibody response. Statistical significance was determined using ANOVA followed by multiple comparison tests. Statistically significant differences are indicated: ***$p < 0.001$, **$p < 0.05$, ns = not significant.

4.1.3.2 Epitopal characterization

The immune response elicited by HHP-inactivated or heat-inactivated viruses was comprehensively evaluated through Western blot analysis to identify the proteins targeted by the antibody immune response and to assess the specific antibody profiles induced by immunization. The Western blot analysis was carried out at two distinct time points, t35 and t53, to evaluate the progression and maturation of the immune response over time. These time points were chosen to provide insight into both the early and more advanced stages of the antibody response, allowing for a thorough examination of potential changes in the immune repertoire as the response matured. The analysis aimed to highlight whether there were any significant differences in the protein targets of the immune response, particularly in terms of the evolution of the antibody response to different viral proteins as the immune system adapted.

At time points t35 and t53, the Western blot analysis revealed clear and consistent differences in the humoral immune responses elicited by the different inactivation methods used for vaccine preparation (Figure 16). Notably, mice immunized with viral preparations inactivated by HHP at 500 MPa and 600 MPa developed a broader and more complex antibody response compared to those immunized with heat-inactivated virus.

Specifically, mice that were immunized with HHP-inactivated vaccine candidates at 500 MPa and 600 MPa exhibited a broader antibody response. These mice produced antibodies not only against the spike protein but also against the nucleocapsid protein. This was evident from the detection of two distinct immunoreactive bands in the Western blot corresponding to the expected molecular weights of the spike and nucleocapsid proteins. The antibodies against both of these viral proteins suggest that HHP treatment preserved key viral epitopes, allowing for the induction of a robust immune response against both the surface protein (spike) and the internal protein (nucleocapsid). These findings indicate that the immune response elicited by HHP-inactivated vaccine candidates was both broad, in terms of antigenic target, and

sustained, as the antibody response persisted over an extended period (up to t53). The preservation of spike protein immunogenicity is particularly relevant, given its role as the primary target of neutralizing antibodies involved in preventing viral entry into host cells. The concurrent antibody response against the nucleocapsid protein further suggests that HHP treatment maintains the antigenic presentation of internal viral components, likely due to the non-denaturing nature of the inactivation process at the molecular level.

In contrast, mice immunized with the heat-inactivated virus presented a markedly different and restricted antibody profile. At both time points these animals developed antibodies that specifically targeted the nucleocapsid protein. However, no significant antibody response against the spike protein was observed, as evidenced by the absence of a band corresponding to the spike protein at its expected molecular weight (Figure 13). This suggests that the heat inactivation process might have compromised or destroyed the structural integrity of the spike protein, making it unrecognizable to the immune system. In contrast to the HHP-treated virus, which generated a response against both the surface (spike) and internal (nucleocapsid) proteins, heat inactivation proved to be less effective in preserving the antigenic integrity of the spike protein, which is crucial for the induction of broad immunity, including the production of neutralizing antibodies that target viral entry into host cells. Neither anti-S nor anti-N antibodies were detected in the control group.

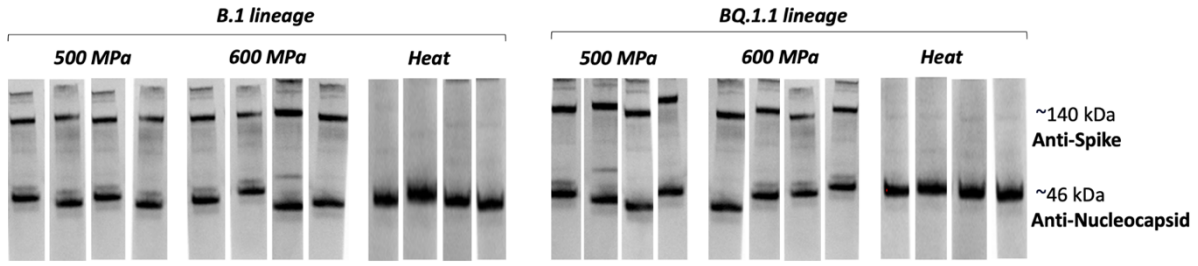

Figure 16. Western blot analysis of sera from mice immunized with B.1 and BQ.1.1 lineage viruses inactivated by 500 MPa, 600 MPa HHP, or heat. The sera from mice immunized with HHP-inactivated vaccines show the presence of both anti-Spike and anti-Nucleocapsid antibodies, whereas sera from mice immunized with heat-inactivated vaccines display reactivity only against the Nucleocapsid protein. These results indicate that HHP treatment better preserves Spike antigenicity compared to heat inactivation, potentially enhancing the breadth of the humoral immune response

4.1.3.3 Virus neutralization

Neutralizing activity of humoral response was assessed at days 14, 28, 35, and 53 post immunization, allowing for both intragroup (within the same group at different time points) and intergroup (comparison across groups at the same time point) evaluations.

In the 500 MPa group, a clear trend of increasing response was observed over time. At t14, values ranged from 8 to 32 (mean = 22, SD = 12) for B.1 lineage and from 8 to 64 (mean = 34, SD = 23) for BQ.1.1 lineage. At t28 values rose to 64-128 (mean = 112, SD = 32) for B.1 lineage and128-256 (mean = 160, SD = 64) for BQ.1.1 lineage. A marked amplification was evident at t35, where all individuals exhibited values of 256 or 512, with mean values of 448 (SD = 128) for B.1 and 384 (SD = 148) for BQ.1.1. By t53, three subjects for B.1 lineage and two subjects for BQ.1.1 lineage reached the maximum observed value of 1024 and means averaged 896 (SD = 256) and 768 (SD = 296) for the two lineages. This consistent increase across all individuals suggests a robust and sustained immunological activation under the 500 MPa treatment.

The 600 MPa group also demonstrated a general upward trend in response, though with greater inter-individual variability. At t14, values were generally low for both tested lineages (8-32, mean 16 and SD = 11 for B.1 lineage, 16-32, mean = 28 and SD = 8 for BQ.1.1 lineage), and at t28, responses remained moderate, ranging between 32 and 128 (mean = 72, SD = 40) for B.1 lineage and from 64 to 256 (mean = 128, SD = 91) for BQ.1.1 lineage. By t35, a steady increase was observed for both lineages, with values ranging from 64 to 256 (mean =144, SD = 81) for B.1 and from 128 to 256 (mean = 160, SD = 64) for BQ.1.1. At t53, three subjects achieved values between 512 and 1024, while one subject remained at 256 in the group immunized with B.1 lineage and two subjects remained at 128 and 256 in the group immunized with BQ.1.1 lineage, with overall means of 704 (SD = 384) and 480 (SD = 396) for B.1 and BQ.1.1, respectively. This pattern suggests that while 600 MPa immunization elicited a progressive increase, the response was less synchronized compared to the 500 MPa group, indicating possible differences in immune response kinetics and efficacy.

In contrast, the heat-treated group exhibited a markedly different profile. Across all time points, the immune response remained relatively low and stable. At t14, values ranged from 0 to 16 (mean = 8, SD = 7) for B.1 and from 8 to 16 (mean = 12, SD = 5) for BQ.1.1. At t28, there was a slight increase to a uniform response of 32 to 64 across all subjects, with mean values averaging 40 (SD = 16) and 48 (SD = 18) for the two lineages. However, no further significant amplification was observed at later time points (t35

and t53), with most values remaining at or below 32. This plateau indicates a minimal immunogenic effect induced by the heat treatment compared to pressure-based treatments.

Overall, intragroup comparisons reveal that the 500 MPa treatment yielded the most effective and consistent immune activation over time, followed by the 600 MPa treatment, which showed moderate but heterogeneous responses. The heat treatment, by contrast, resulted in minimal immune stimulation with no substantial progression beyond t28.

The intragroup analysis revealed clear temporal trends within each group. The 500 MPa group exhibited a steady and significant increase in neutralizing antibody titers across all time points, reflecting a strong priming of the immune system and subsequent maturation of the humoral response. The Kruskal-Wallis test with Dunn's post-hoc test with Bonferroni correction confirmed the statistical significance of this increase over time (B.1 lineage: $\chi 2(3) = 14.03$, $p = 0.003$; BQ.1.1 lineage: $\chi 2(3) = 13.52$, $p = 0.004$). The 600 MPa group followed a similar pattern, although the response was slightly less consistent, with more variability observed at intermediate time points. Statistical testing also supported a significant temporal increase in this group (B.1 lineage: $\chi 2(3) = 13.08$, $p = 0.004$; BQ.1.1 lineage: $\chi 2(3) = 11.22$, $p = 0.011$). In contrast, the heat-inactivated group displayed a much weaker temporal progression compared to HHP-treatments. This lack of significant improvement suggests that heat inactivation may compromise the immunogenicity of the viral antigens. (Figure 17a for B.1 lineage and Figure 17b for BQ.1.1 lineage). No effective neutralizing response was detected in the control group.

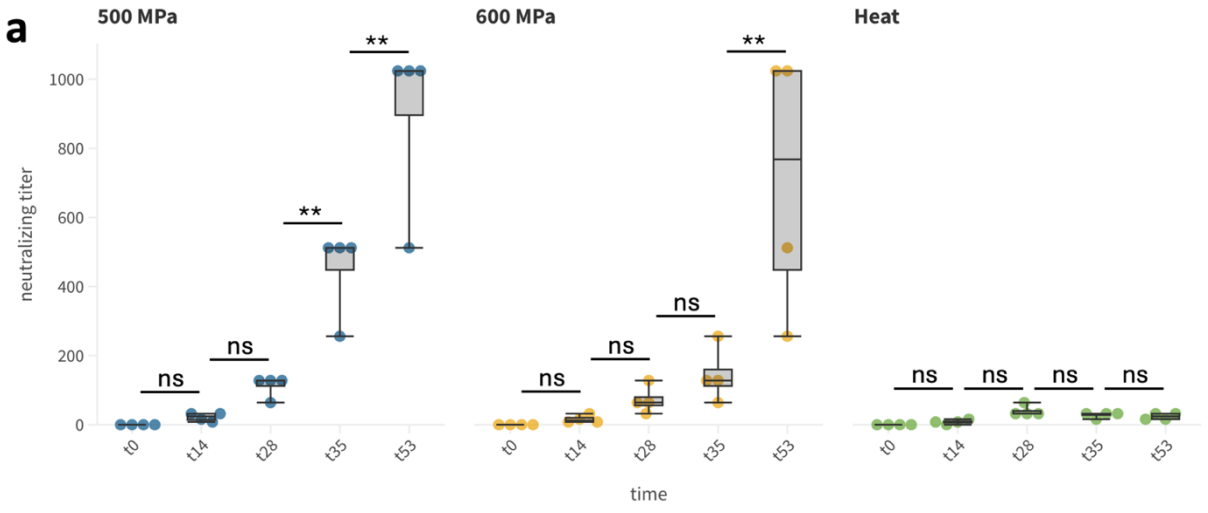

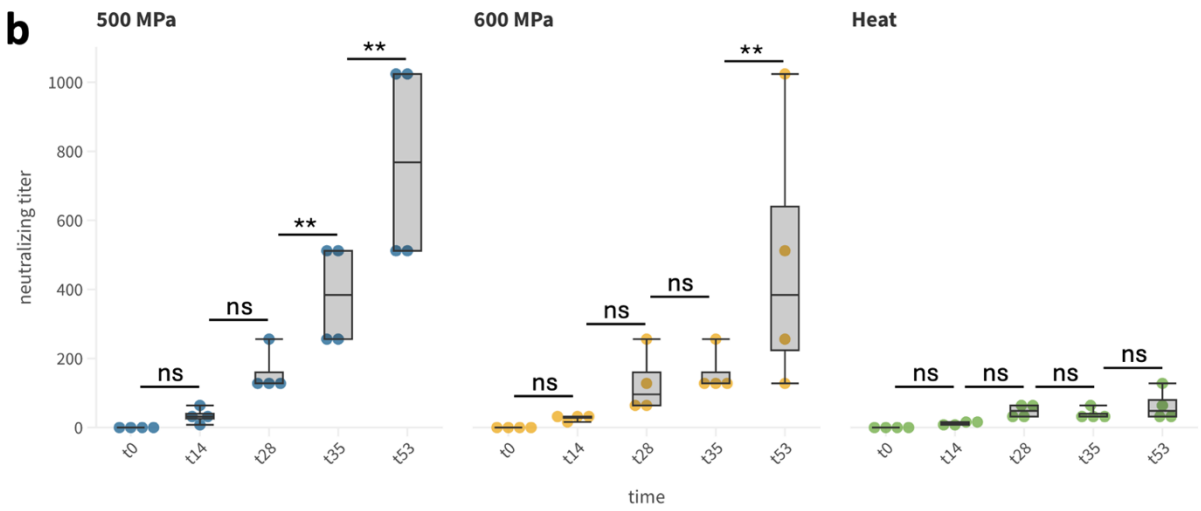

Figure 17. Intragroup comparison of neutralizing titers measured via cell culture virus neutralization in mice immunized with SARS-CoV-2 B.1 (A) and BQ.1.1 (B) lineages inactivated by high hydrostatic pressure (500 MPa and 600 MPa) or heat treatment, measured at different time points (t0, t14, t28, t35, and t53) post-immunization. Data show a significant increase in neutralizing titers starting from t35 for 500 MPa-immunized mice and at t53 for 600 MPa-immunized mice. No increased was observed in the heat-immunized group. Statistical significance was determined using ANOVA followed by multiple comparison tests. Statistically significant differences are indicated: ***$p < 0.001$, **$p < 0.05$, ns = not significant.

For what regards inter-group comparison, at day 14, a detectable neutralizing antibody response was observed in all immunization groups, indicating that each inactivation method was capable of priming the immune system. However, neutralizing titers were low across all groups at this early stage. These differences between groups, though minor, were not statistically significant, reflecting variability in individual immune responses.

By day 28, significant differences between groups began to emerge. The 500 MPa group showed a marked increase in neutralizing titers, averaging 112 for B.1 lineage and 160 for BQ.1.1 lineage, indicating a strong and consistent enhancement of the humoral response. In contrast, the 600 MPa group exhibited moderate titers (mean of 72 for B.1 and 128 for BQ.1.1), while the heat-inactivated group lagged behind with relatively low titers (means of 40 and 48 for the two lineages).

At day 35, the differences between groups became more pronounced. The 500 MPa group displayed the highest titers, averaging 448 for bìB.1 and 384 for BQ.1.1, reflecting a robust and sustained immune response. The 600 MPa group also showed increased titers (144 for B.1 and 160 for BQ.1.1), though these were consistently lower than those observed in the 500 MPa group. The heat-inactivated group remained

significantly weaker, with mean titers stagnating at 28 and 40 for the two lineages, showing little improvement from earlier time points. The data at t35 highlighted the superior capacity of HHP-inactivated vaccine candidates to elicit strong neutralizing antibody responses, with the 500 MPa treatment yielding the most robust results, followed by the 600 MPa treatment.

By the final time point at day 53, the divergence in neutralizing antibody responses between groups was even more evident. In the 500 MPa group, titers reached their peak, with some mice achieving values of 1024 and other individuals maintaining a titer of 512 for both lineages and overall means of 896 for B.1 and 768 for BQ.1.1. This indicated not only a strong response but also its durability over time. The 600 MPa group followed closely, with titers averaging 704 for B.1 and 480 for BQ.1.1. However, this group displayed slightly greater variability compared to the 500 MPa group, suggesting a less consistent response across individuals. In stark contrast, the heat-inactivated group showed no significant improvement, with titers plateauing at 24 for B.1 lineage and 64 for BQ.1.1 lineage, with only one individual achieving a titer of 128. The data from t53 further emphasized the limitations of heat inactivation in eliciting a sustained and effective neutralizing antibody response, particularly when compared to the enhanced and durable responses achieved with HHP treatments.

Intergroup comparisons at each time point further highlighted the superior efficacy of HHP treatments. At t14, differences between groups were minimal, reflecting the early stages of immune activation. By t28, however, the 500 MPa group began to outpace the other groups, achieving significantly higher titers compared to both the 600 MPa and heat-inactivated groups. These differences became more pronounced at t35 and t53, with the 500 MPa group consistently demonstrating the strongest and most sustained responses. The 600 MPa group, while slightly less effective, still outperformed the heat-inactivated group at every time point. The heat-inactivated group lagged significantly behind, with poor and plateaued responses that failed to match the robust and durable neutralizing antibody responses elicited by HHP treatments. These results indicate that both HHP treatments outperformed heat inactivation in driving a strong neutralizing antibody response, with the 500 MPa group demonstrating the most robust response ($\chi2 = 9.89$, $p = 0.007$ for B.1 and $\chi2 = 9.71$, $p = 0.008$ for BQ.1.1). By the final time point (t53), the 500 MPa group maintained the highest titers. The 600 MPa group followed closely. In the heat-inactivated group titers plateaued with a statistically evident difference from both HHP-inactivated

groups: $\chi 2 = 8.29$, $p = 0.016$ for B.1 and $\chi 2 = 7.9$, $p = 0.019$ for BQ.1.1 (Figure 18a for B.1 lineage and Figure 18b for BQ.1.1 lineage).

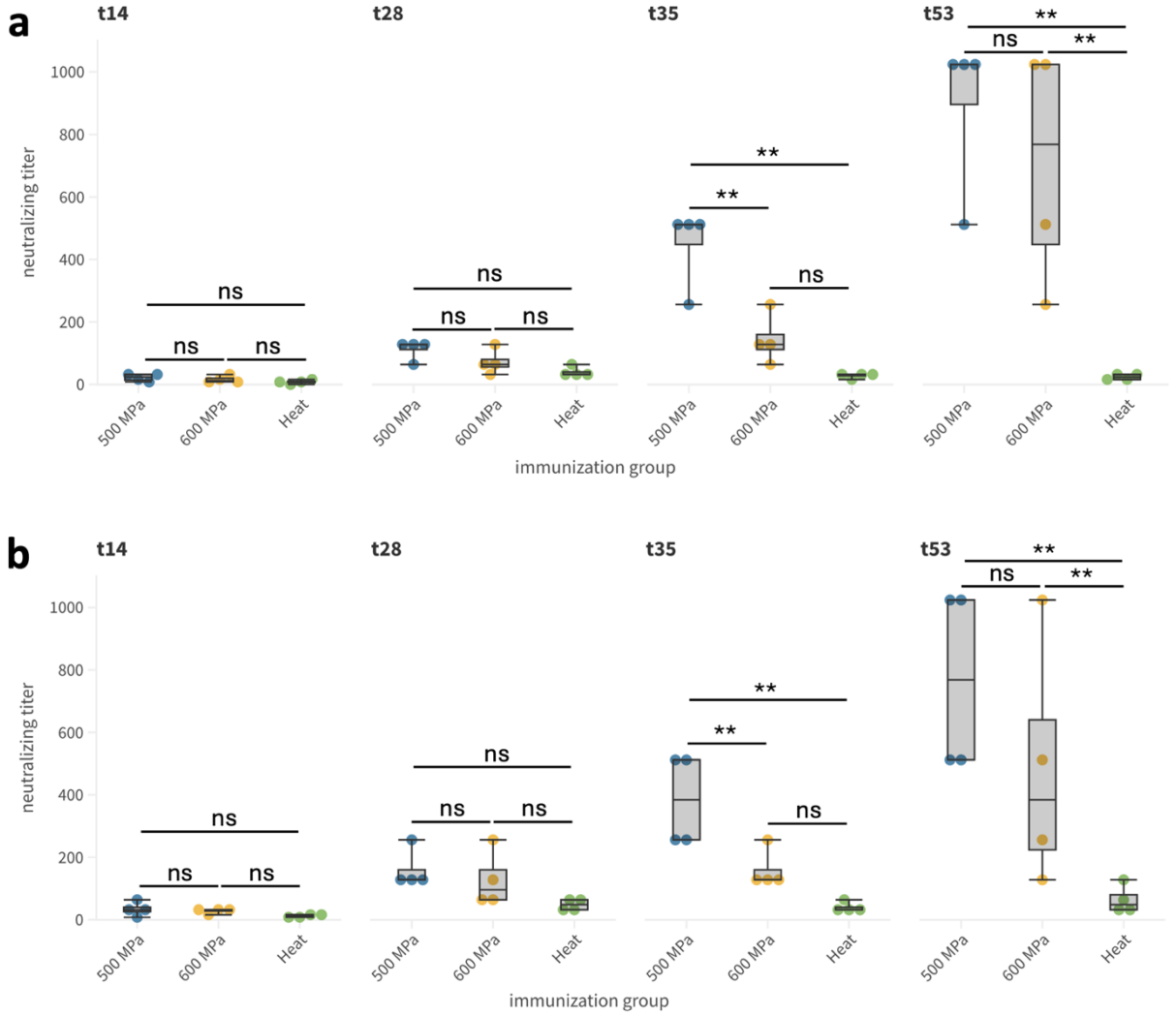

Figure 18. Intergroup comparison of neutralizing titers measured via cell culture virus neutralization at different time points (t0, t14, t28, t35, and t53) post-immunization in mice immunized with SARS-CoV-2 B.1 (A) and BQ.1.1 (B) lineages inactivated by high hydrostatic pressure (500 MPa and 600 MPa) or heat treatment. Statistically significant differences among group are evident from t35, with 500 MPa-inactivated vaccine candidate inducing the highest neutralizing antibody response. Statistical significance was determined using ANOVA followed by multiple comparison tests. Statistically significant differences are indicated: ***$p < 0.001$, **$p < 0.05$, ns = not significant.

These findings underscore the advantages of HHP as a method for viral inactivation in vaccine development. Both 500 MPa and 600 MPa treatments preserved the immunogenicity of viral antigens, leading to strong and sustained neutralizing antibody responses. The 500 MPa treatment was particularly effective, producing the highest titers and the most consistent responses across all time points. In contrast, heat inactivation resulted in a significantly weaker immune response, suggesting that this

method may lead to denaturation or degradation of key viral antigens, thereby limiting its effectiveness.

4.1.4 T cell responses

T-cell responses were evaluated on day 53 from PBMC and splenocytes. Intergroup differences were evaluated in order to assess the ability of the different immunization protocol to induce the activation of IFN-producing T cells at the peripherical and central level.

Mice immunized with virus inactivated at 500 MPa demonstrated strong T-cell-mediated immune responses. In whole blood samples, IFN-secreting cells ranged from 150 to 260/10^6 cells (mean = 218, SD = 45) for B.1 lineage and from 160 to 260 (mean = 215, SD = 87) for BQ.1.1 lineage. This consistent response indicates a moderate but stable level of T-cell activation across the group. Importantly, the spleen samples from this group showed a significantly higher number of IFN-secreting cells compared to whole blood, with counts ranging from 170 to 630 (mean = 410, SD = 199) for B.1 lineage and from 170 to 480 (mean = 353, SD = 146) for BQ.1.1 lineage. These findings highlight the potential of the 500 MPa inactivation method to preserve viral antigens in a manner that effectively stimulates robust cellular immune responses, particularly in lymphoid organs such as the spleen. The disparity between whole blood and spleen responses is consistent with the expected role of the spleen as a central lymphoid organ, where antigen presentation and subsequent T-cell activation occur at higher rates compared to peripheral blood.

The groups treated with virus inactivated at 600 MPa also exhibited notable T-cell responses, though with slightly greater variability compared to the 500 MPa group. In whole blood, IFN-secreting cells ranged from 150 to 260 (mean = 208, SD = 48) for B.1 and from 170 to 420 (mean = 215, SD = 42) for BQ.1.1, similar to the range observed in the 500 MPa group. This suggests that the 600 MPa inactivation protocol was equally capable of inducing the activation of antigen-specific T cells.

The heat-inactivated group demonstrated the weakest T-cell-mediated immune responses among the three experimental groups. In whole blood, IFN-secreting cells ranged from 0 to 120 for both lineages (mean = 68, SD = 51 for B.1 lineage and SD = 62 for BQ.1.1 lineage), indicating a poor overall response. Notably, some individuals in this group exhibited no detectable T-cell activation in whole blood, suggesting a complete lack of antigen-specific response in these cases. The spleen responses were

similarly weak, with spot counts ranging from 0 to 80 (mean = 50, SD = 36) for B.1 and from 0 to 90 (mean = 78, SD = 36) for BQ.1.1 lineage. These findings indicate that heat inactivation significantly impaired the immunogenicity of the virus, likely due to denaturation of viral proteins and loss of key epitopes required for effective antigen recognition and T-cell activation. The poor responses observed in this group align with previous findings that heat inactivation can lead to structural alterations in viral proteins, rendering them less capable of stimulating robust immune responses. The lack of significant T-cell activation in both whole blood and spleen samples further underscores the limitations of heat inactivation as a method for preparing immunogens capable of eliciting strong cellular immune responses. These results suggest that heat-inactivated viruses may not be suitable for use in vaccine formulations where robust cellular immunity is required.

When comparing the three groups, clear differences emerge in the strength and consistency of T-cell-mediated immune responses. The 500 MPa group consistently exhibited the strongest responses, particularly in spleen samples, where the highest spot counts were recorded. The 600 MPa group also elicited strong responses, though with slightly greater variability. The heat-inactivated group, in stark contrast, displayed minimal T-cell activation in both whole blood and spleen, with responses that were substantially weaker than those observed in the HHP-treated groups. Statistical analysis carried out with One Way ANOVA test highlighted a significant difference between 500-MPa inactivated and heat-inactivated groups and between 600-MPa inactivated and heat-inactivated groups on both PBMC, reported in Figure 19a and 19c for B.1 and BQ.1.1 lineage, respectively, and splenocytes, reported in Figure 19b and 19d for B.1 and BQ.1.1 lineage, respectively, (B.1 lineage: $F = 12.1585$, $p= 0.0027$ for PBMC and $F = 6.6474$, $p = 0.01687$ on splenocytes; BQ.1.1 lineage: $F = 6.7526$, $p = 0.01617$ for PBMC and $F = 7.3906$, $p = 0.01262$ for splenocytes). No significant difference was highlighted between the two HHP treatments. No SARS-CoV-2 specific T-cell response was detected in the control group.

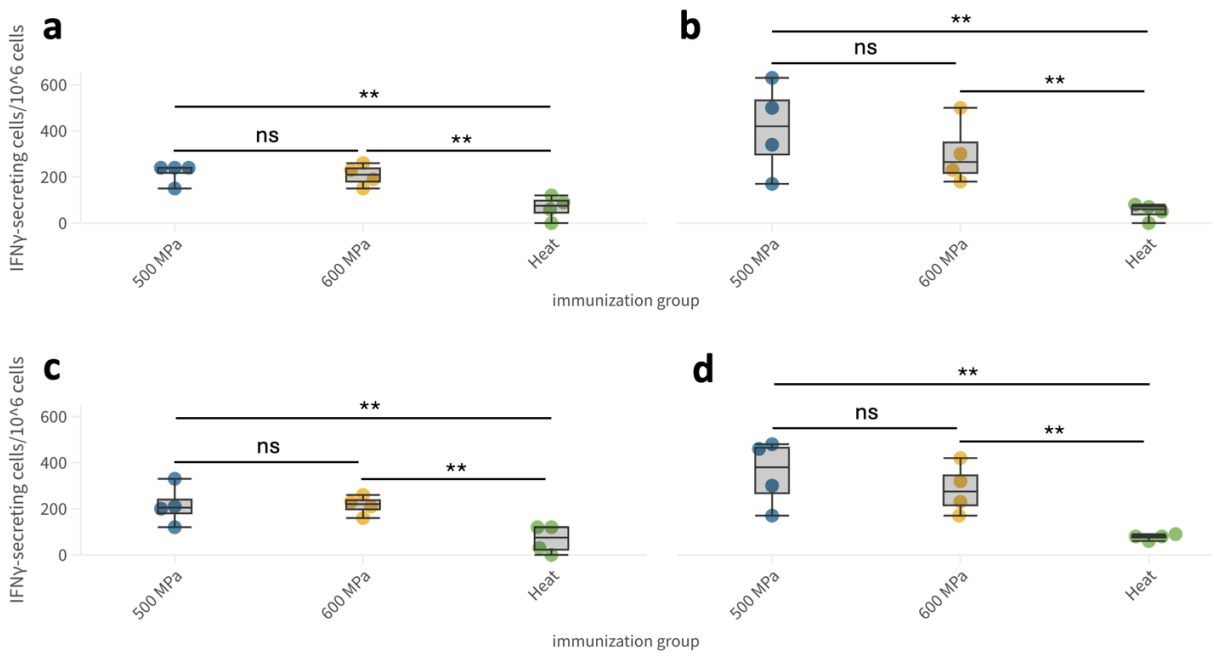

Figure 19. Induction of T-cell response in HHP-inactivated SARS-CoV-2 vaccinee. A and C. IFN-γ ELISpot results for PBMCs from mice immunized with B.1 (A) and BQ.1.1 (C) lineage viruses inactivated by 500 MPa, 600 MPa HHP, or heat. B and D. IFN-γ ELISpot results for splenocytes from mice immunized with B.1 (B) and BQ.1.1 (D) lineage viruses. Both vaccine candidate produced by HHP inactivation induces a significantly higher peripheral and central response compared to the HHP-inactivated vaccine candidate. Statistical significance: **$p < 0.05$, ns = not significant.

4.1.5 Comparative analysis of immune response profiles

The comparative analysis of the three immunization treatments revealed distinct and treatment-dependent patterns of humoral and cellular immune activation, reflecting the influence of processing conditions on antigen stability and immunogenic potential. The data collectively indicate that pressure-based inactivation approaches were generally more effective in preserving the conformational and functional features of viral antigens, thereby sustaining their capacity to elicit a coordinated immune response. In contrast, conventional thermal inactivation tended to compromise epitope integrity and, consequently, both antigen recognition and the overall quality of the elicited immune response.

Among the pressure-based treatments, the application of 500 MPa emerged as the most immunogenically favorable condition. This treatment supported a well-coordinated activation of both branches of the adaptive immune system. Immune determinants of surface proteins were largely maintained, as showed by microscopy and Western blot analysis, allowing efficient B-cell receptor engagement and subsequent maturation of antibody responses. Consequently, immunized subjects

developed strong total and neutralizing IgG responses, reflecting preserved antigenicity and functional competence of the viral components. Parallel assessment of cellular immunity revealed a consistent and elevated production of IFNγ by both peripheral and splenic lymphocytes, indicative of robust T-cell activation. This finding suggests that moderate high-pressure exposure not only promotes B-cell activation but also sustains T-helper and cytotoxic T-cell responses, thereby ensuring an integrated and durable form of immune protection. The balanced interplay between these humoral and cellular components represents a hallmark of an effective immunization strategy, capable of providing both immediate neutralizing defense and long-term immune memory.

Conversely, exposure to higher pressure levels (600 MPa) resulted in a measurable decline in immunogenicity. Although antigenic structures remained partially preserved, subtle conformational rearrangements likely altered critical epitopes, diminishing their recognition by immune receptors. As a result, both antibody production and T-cell activation were still detectable but appeared quantitatively reduced and functionally less efficient than those observed following moderate-pressure treatment. These findings highlight the existence of a threshold effect, whereby excessive mechanical stress may inadvertently compromise the antigenic fidelity essential for optimal immune priming.

Thermal inactivation, in contrast, generated the weakest immunogenic profile among the tested conditions. Denaturation of viral proteins led to the loss of conformational epitopes, impairing B-cell receptor binding and drastically reducing the generation of neutralizing antibodies. In parallel, the diminished frequency of IFNγ-secreting lymphocytes pointed to limited cellular activation, suggesting that heat treatment severely restricts both arms of the adaptive immune response. Overall, immunization with heat-inactivated preparations resulted in a markedly contracted and functionally inferior immune profile.

Overall, the comparative immune signatures illustrated in Figure 20 indicate that moderate HHP processing is the most favorable approach among those tested, representing the most advantageous compromise between antigen preservation and pathogen inactivation. By maintaining the structural integrity of key antigenic determinants while ensuring complete loss of infectivity, this approach promotes a balanced and potent activation of both humoral and cellular pathways. Such equilibrium is critical for the establishment of durable and protective immune

memory, as it enables synergistic interactions between antibody-mediated neutralization and T-cell–driven clearance mechanisms. Collectively, these findings support the conclusion that carefully controlled HHP treatment constitutes a promising platform for the development of next-generation vaccine formulations, offering a rational means to enhance immunogenicity without compromising antigenic structure or safety.

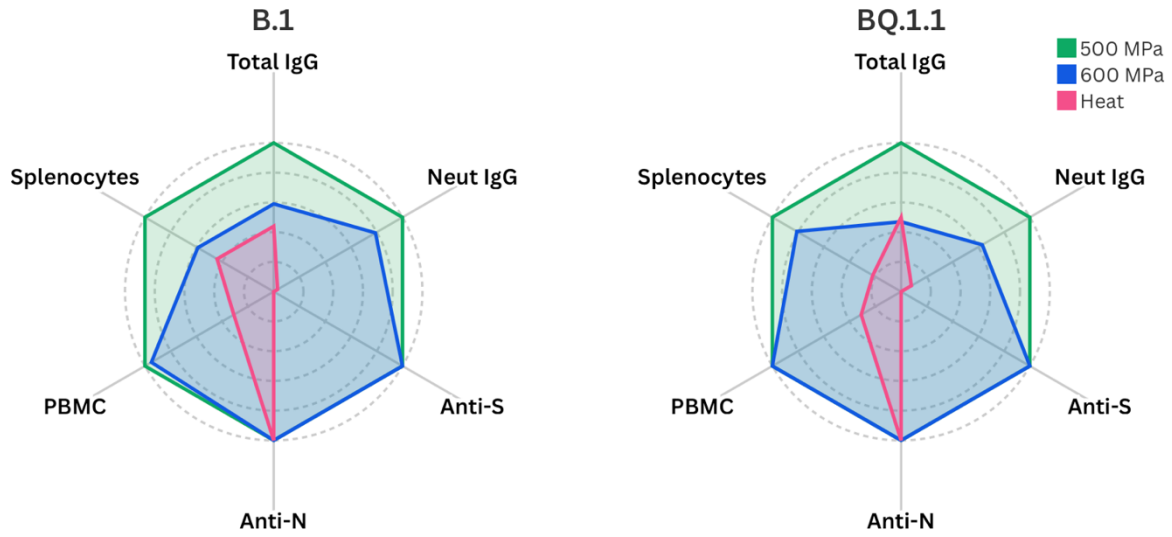

Figure 20. Radar plots of immune responses induced by different immunization treatments against SARS-CoV-2 B.1 and BQ.1.1 variants. The radar plots illustrate the overall humoral and cellular immune profiles elicited by the three experimental treatments (500 MPa [green], 6000 MPa [blue], and heat inactivation [red]) against the B.1 and BQ.1.1 variants. The following continuous variables were plotted: total and neutralizing IgG responses, and IFNγ-secreting cell frequencies in peripheral blood mononuclear cells (PBMCs) and splenocytes. The presence of anti-S and anti-N antibodies (categorical variables) was converted into binary numerical values, with 0 indicating absence and 1 indicating presence. Each polygon represents a normalized, multidimensional summary of key immune parameters. To allow a coherent visual comparison among immune parameters with markedly different absolute magnitudes and measurement units, the data were normalized prior to plotting: for each immunological variable, the values corresponding to all experimental groups were divided by the highest observed value for that specific parameter. This procedure resulted in a set of values ranging from 0 to 1, representing the relative magnitude of each response within its own variable scale. Such normalization preserved the proportional differences among treatments while preventing parameters with large numerical ranges (e.g., antibody titers) from dominating the graphical representation. As a result, all variables contribute equally to the overall shape of the radar chart, enabling an intuitive comparison of the immunological profiles elicited by the different treatments.

4.1.6 Thermostability assessment

To evaluate the preservation of antigenic integrity over time, the thermostability of viral preparations inactivated by HHP at 500 MPa and subsequently purified was

systematically assessed under different storage conditions for different periods of time. This analysis aimed to determine the optimal storage parameters that ensure the long-term stability of antigenic epitopes, which is critical for downstream immunological applications and vaccine development. Aliquots of the inactivated and purified virus were stored at two temperature conditions: 4 °C (refrigeration) and ambient room temperature. The antigenic stability of these samples was evaluated at multiple time points to monitor potential degradation or conformational alterations affecting the antigenic profile of the viral particles.

The results demonstrated that samples stored at 4 °C retained antigenic stability throughout the entire duration of the analysis (30 days). Across all evaluated time points, the loss of antigenic integrity was negligible, with no appreciable decrease in detectable antigen levels. This indicates that the conformational structures essential for antigen recognition remained preserved, thus maintaining the immunological relevance of the preparation under refrigerated conditions.In contrast, samples stored at room temperature exhibited a more limited stability profile. Antigenic integrity was maintained only up to 14 days post-storage, beyond which a progressive decline was observed. By day 30, a marked reduction in antigenic detectability was evident, suggesting structural degradation or partial denaturation of critical viral epitopes. This loss of antigenic quality underlines the temperature sensitivity of the preparation in the absence of refrigeration (Figure 21).

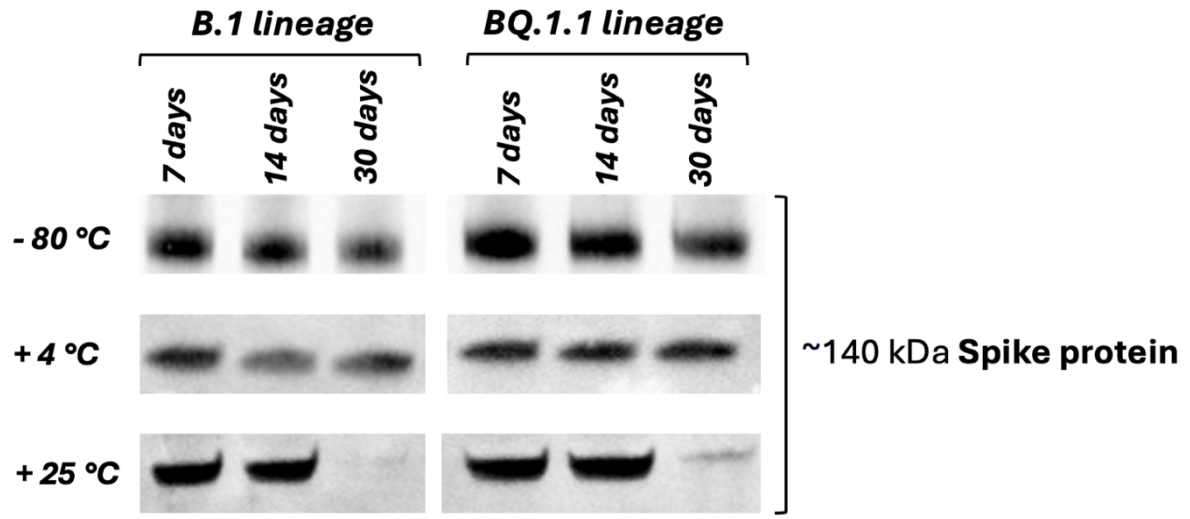

Figure 21. Western blot analysis of the Spike protein signal from SARS-CoV-2 B.1 and BQ.1.1 variants inactivated at 500 MPa, stored at different temperatures (-80 °C, 4 °C, 25 °C) and analyzed over various time points (7, 14, and 30 days). 500 MPa-inactivated vaccine candidate retained antigenicity up to 30 days if stored at refrigeration temperatures and up to 14 days if stored at room temperature.

These findings emphasize the robustness of HHP inactivation in preserving the native antigenic configuration of viral particles, provided that appropriate storage conditions are implemented. Notably, the capacity to maintain antigenic stability at 4 °C supports the use of refrigeration as a feasible and cost-effective alternative to freezing for the storage and distribution of HHP-inactivated viral preparations. This is particularly advantageous in scenarios where ultra-low temperature infrastructure is limited or unavailable.

4.2 West Nile virus

4.2.1 Short HHP protocol

For the initial HHP inactivation trials on West Nile virus, the procedure previously established for SARS-CoV-2 was employed without modification. Viral suspensions were subjected to each of the selected pressure levels for a duration of 5 minutes, as described in Figure 10.

The reduction of viral infectivity was assessed by endpoint titration. Treatment at 400 MPa resulted in substantial reductions in infectious titer, with log10 reductions of 4.3 and 4.5 for lineage 1 and lineage 2, respectively, compared to the non-HHP-treated control. Treatments at 500 MPa and 600 MPa also led to a reduction of infectious titer, albeit complete inactivation was not achieved at any tested pressure (log10 reduction of 5.3 and 6.2 for treatment at 500 MPa and of 7 and 7.7 for treatment at 600 MPa). Treated viral stocks were cultured on Vero E6 cells. Viral replication was monitored using qRT-PCR. Change in viral load during incubation was calculated using the delta Ct method. The 5-minute treatment protocol did not achieve complete inactivation of WNV at any of the tested pressures (Figure 22).

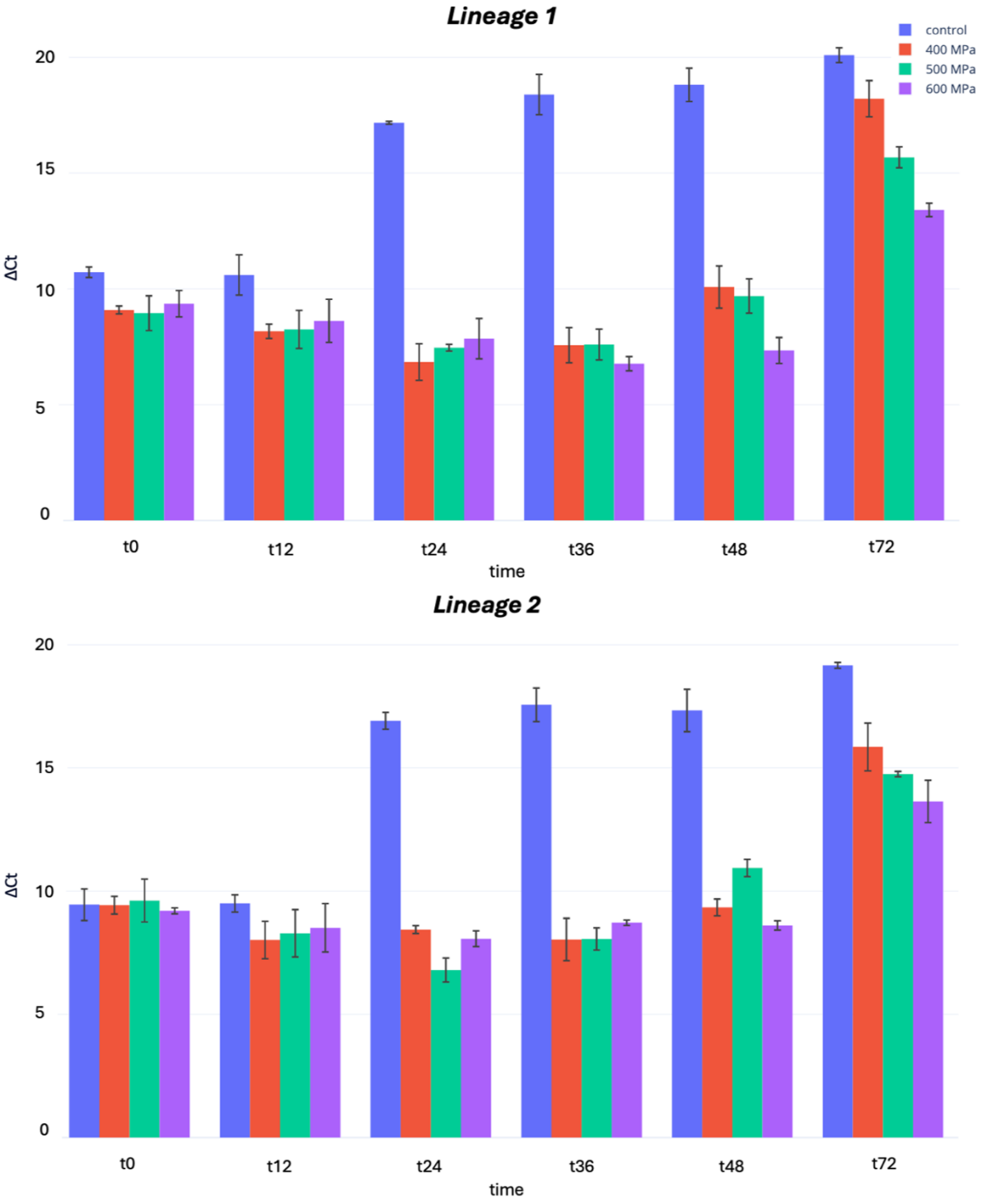

Figure 22. Viral replication dynamics, measured as ΔCt values of Real-Time PCR, for 5-minute-HHP-treated and non-HHP treated WNV lineage 1 and lineage 2 over time. Bar graph showing ΔCt values measured at six time points (t0, t12, t24, t36, t48, and t72 hours after infection) in samples treated with different HHP conditions (400 MPa, 500 MPa, 600 MPa) compared to an untreated control group. Error bars represent standard deviations.

4.2.2 Refined long HHP protocol

Modifications to the treatment protocol were implemented to enhance the likelihood of achieving complete viral inactivation. The main parameter adjusted was the exposure time to the applied pressure. Specifically, the duration of the HHP treatment was extended from 5 minutes to 10 minutes, while maintaining all other conditions identical to those used in the initial trials (Figure 23).

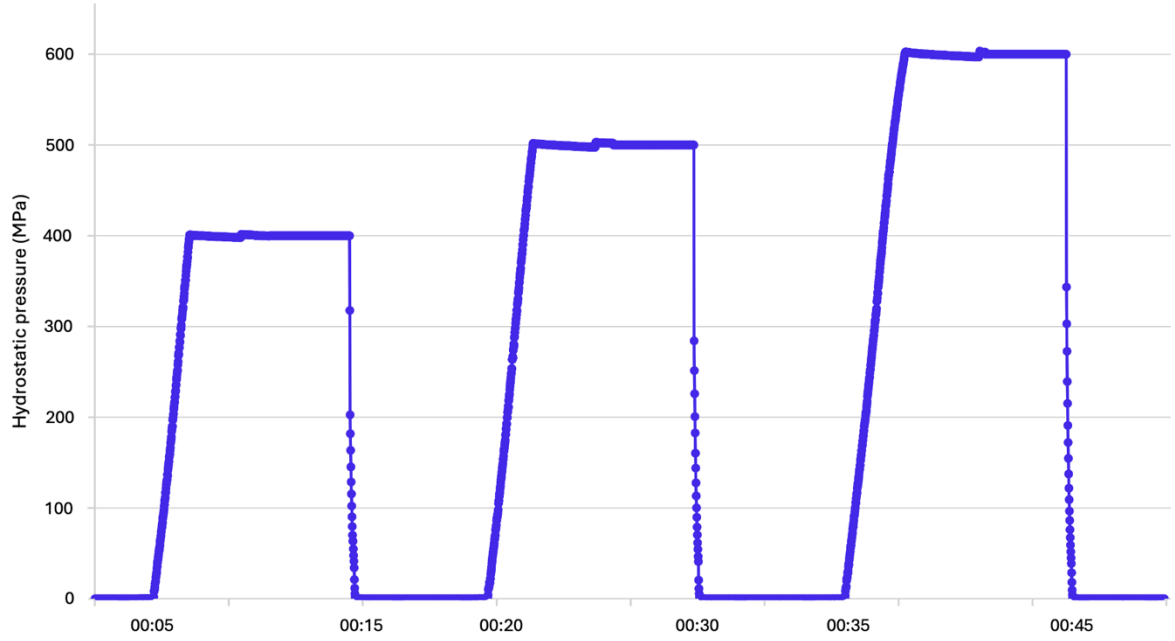

Figure 23. Pressure profile of high hydrostatic pressure (HHP) treatment applied over time. Each pressure was maintained for a fixed duration, followed by a rapid decompression phase to atmospheric pressure. After each pressurization cycle, the viral suspension subjected to the treatment was removed and replaced with a fresh suspension for the following cycle. The machine was maintained active throughout the entire series of treatments, continuously recording pressure, including during decompression phases when the pressure returned to ambient levels, resulting in the appearance of a sequential pressure profile in the figure, although each cycle was conducted separately.

Under these conditions, no infectious virus was detected for either lineage by endpoint titration, suggesting complete viral inactivation. To confirm the inactivation achieved, treated viral stocks were cultured on Vero E6 cells and replication was monitored using qRT-PCR. Change in viral load during incubation was calculated using the delta Ct method. 400 MPa treatment temporarily suppressed viral replication, but was insufficient to maintain long-term inhibition, allowing a significant rebound in viral replication for both lineages at 72 hours post-infection. At 500 and 600 MPa, viral replication was consistently suppressed, and viral load declined progressively from 0 to 72 hours post-infection (Figure 24).

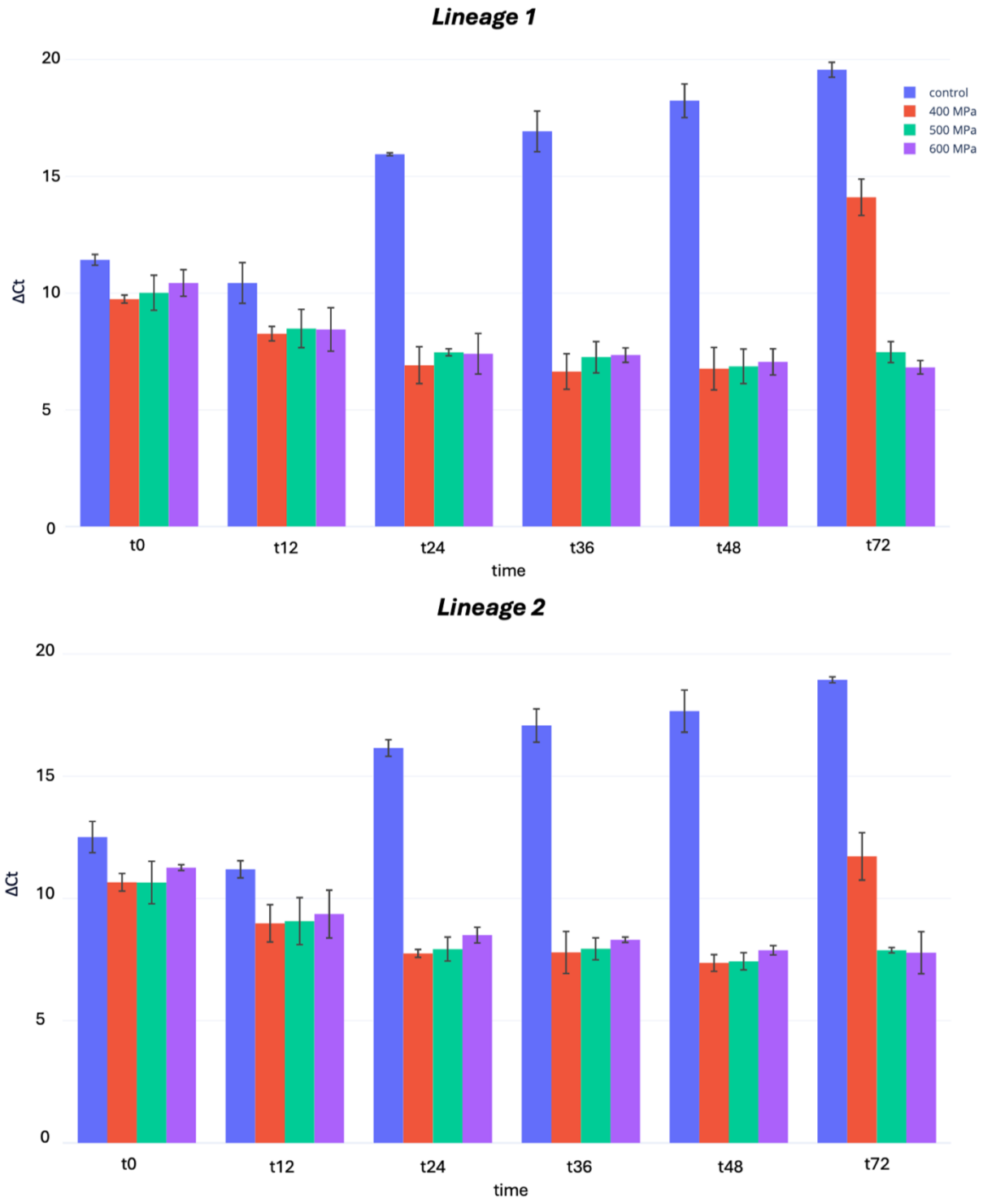

Figure 24. Viral replication dynamics, measured as ΔCt values of Real-Time PCR, for 10-minute-HHP-treated and non-HHP treated WNV lineage 1 and lineage 2 over time. Bar graph showing ΔCt values measured at six time points (t0, t12, t24, t36, t48, and t72 hours after infection) in samples treated with different HHP conditions (400 MPa, 500 MPa, 600 MPa) compared to an untreated control group. Error bars represent standard deviations.

The apparent discrepancy observed for the treatment at 400 MPa, where classical viral titration suggested a complete suppression of viral replication while qRT-PCR

performed on cultured HHP-treated viral isolates, can be explained by differences in the sensitivity of the detection methods employed. While titration assays indicated the absence of visible cytopathic effect, molecular analyses revealed the presence of residual replication potential. This outcome is consistent with the higher sensitivity of molecular techniques and highlights the importance of integrating both infectivity-based and molecular assays for a comprehensive evaluation of viral inactivation efficiency.

4.2.3 Structural and antigenicity analysis

4.2.3.1 Negative Staining Electron Microscopy (nsEM)

Negative-stain electron microscopy was employed to examine the ultrastructural characteristics of West Nile virus particles in virus stocks subjected to high hydrostatic pressure treatments at 400, 500, and 600 MPa for 10 minutes, and in untreated control preparations. The objective was to assess the morphological integrity of viral particles following exposure to the different pressure levels, in order to provide complementary structural evidence to the infectivity and molecular analyses described above.In untreated control preparations, numerous discrete particles consistent in morphology and size with mature WNV virions were observed. These particles appeared predominantly spherical to slightly ovoid in shape, with diameters in the range of approximately 40-45 nm. The particle surfaces were delineated by a continuous outer envelope, and careful inspection of the high-contrast periphery revealed the presence of fine, spike-like projections extending radially from the envelope surface. These projections, measuring only a few nanometers in length, are consistent with the arrangement of envelope glycoproteins. The overall morphology of these control particles corresponded closely with reference micrographs of WNV reported in the literature, supporting their identification as structurally intact virions.

In sharp contrast, nsEM analysis of the HHP-treated viral preparations, whether subjected to 400, 500, or 600 MPa, revealed a marked absence of particles with morphology typical of WNV. Across all pressure conditions, no well-defined spherical particles with the characteristic dimensions and surface features observed in controls could be reliably identified. Instead, the visual field was populated by irregular, poorly delineated structures, often appearing as collapsed or flattened remnants, lacking the smooth, continuous contour and radial projections of intact virions. These altered structures exhibited heterogeneous sizes and shapes, and in many cases, they presented as diffuse, low-contrast areas rather than discrete particles. Findings of

nsEM are summarized in Figure 25. Although the overall abundance of electron-dense material remained detectable in the treated samples, its organization no longer resembled that of native virions. Rather, the material appeared fragmented or amorphous, in some cases forming what could be interpreted as partially preserved shells or “skeletal” remains of the viral envelope. The absence of identifiable surface projections in all treated samples suggests a loss or severe alteration of the envelope glycoprotein organization.

Importantly, no significant differences were noted between the three pressure levels in terms of qualitative ultrastructural appearance. Whether treated at 400, 500, or 600 MPa, the virus-derived material in the preparations displayed the same lack of intact, spherical particles and the same predominance of morphologically degraded structures. This observation implies that the structural damage inflicted by HHP is already maximal at the lowest tested pressure, at least within the 10-minute treatment duration employed in the modified protocol.

In considering the possible nature of the residual structures observed in the treated samples, it is plausible that they correspond to envelope fragments or partially collapsed enveloped shells from which the internal nucleocapsid has been lost or extensively reorganized. Alternatively, some of the diffuse electron-dense regions could represent aggregates of denatured viral proteins, possibly interspersed with RNA fragments, adhering to remnants of the lipid bilayer. The inability to identify intact virions in these preparations supports the conclusion that HHP treatment applied for 10 minutes, even at the lowest pressure tested in the present study, can produce profound morphological disruption to the WNV particle architecture, exceeding the thresholds at which protein quaternary structure is known to be destabilized, making it plausible that both the lipid and protein components of the WNV envelope are extensively damaged under these conditions.

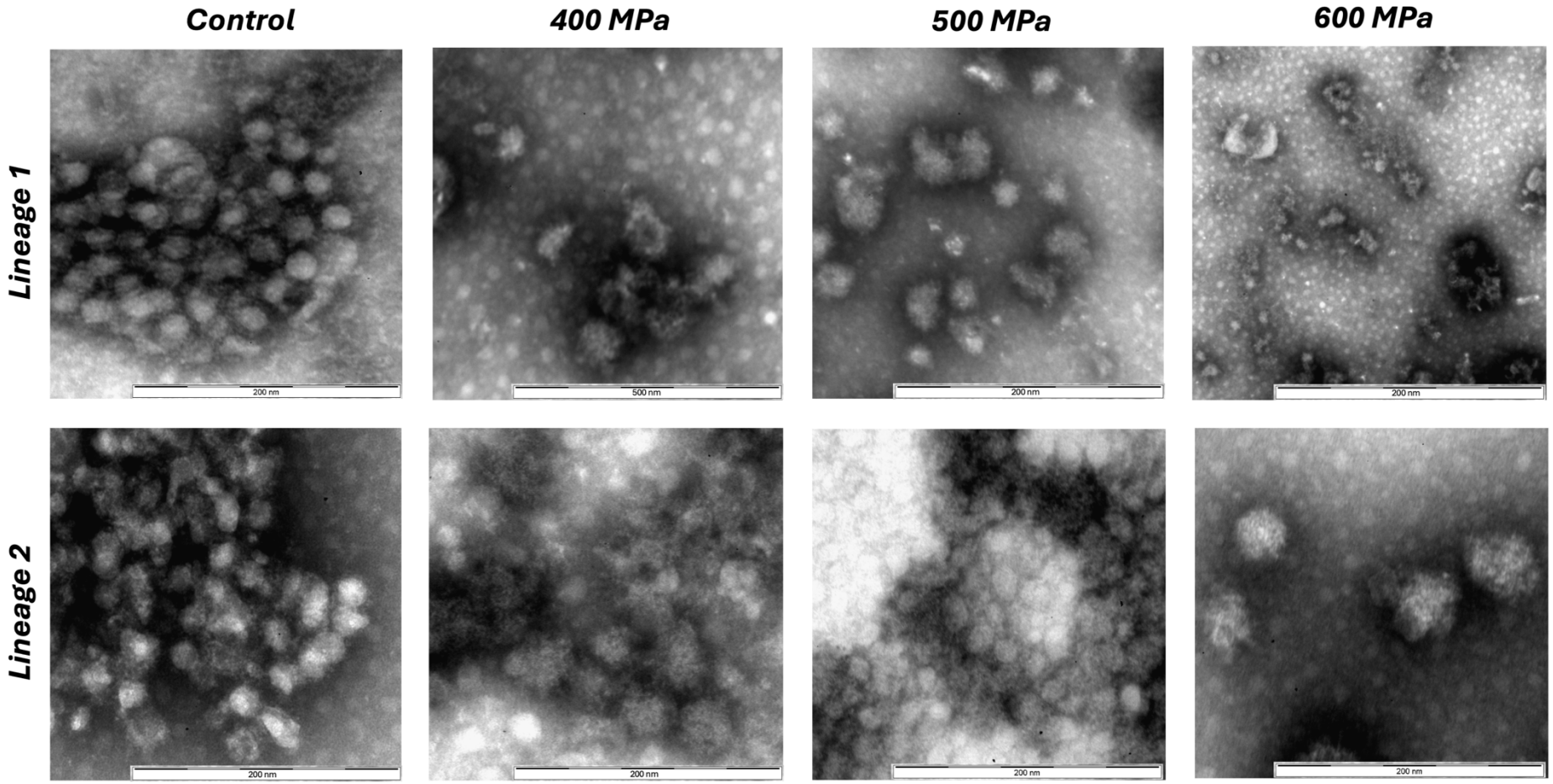

Figure 25. nsEM images of WNV lineage 1 and 2 viral particles subjected to different levels of high hydrostatic pressure: untreated control, 400 MPa, 500 MPa, and 600 MPa for 10 minutes. Increasing pressure levels induce progressive morphological alterations in viral structure, with a marked loss of envelope integrity observed at higher pressures. Scale bar: 200 nm.

4.2.3.2 Western blot

Western blot analysis was performed to assess the integrity and detectability of three major WNV proteins, NS1, Envelope, and Capsid, in untreated controls and in samples from both WNV lineage 1 and lineage 2 subjected to HHP at 400, 500, and 600 MPa. Heat-inactivated preparations of each lineage were also included for comparison.

For NS1, the western blot analysis consistently revealed a distinct and well-resolved immunoreactive band migrating at approximately 45 kDa, corresponding to the expected molecular weight of the West Nile virus nonstructural protein 1. This band was present in all tested samples, encompassing untreated controls, HHP–treated preparations for both lineage 1 and lineage 2 at 400, 500, and 600 MPa, as well as heat-inactivated controls for each lineage. Across the pressure-treated samples, no appreciable variation in either band intensity or sharpness was observed, suggesting that the NS1 protein retains its antigenic epitopes and remains fully detectable following exposure to HHP at all applied pressure levels. The persistence of the NS1 band even at the highest tested pressure (600 MPa) indicates that NS1 may possess a comparatively high resistance to the denaturing effects of hydrostatic compression, at least over the 10-minute exposure period employed here. This pattern was consistent for both viral lineages, indicating that the preservation of NS1 immunoreactivity is not lineage-specific and is likely attributable to intrinsic structural stability of this protein under the tested pressurization conditions. Similarly, the detection of NS1 in heat-treated samples, with only minimal if any loss in band intensity compared to untreated controls, suggests that this protein is also relatively resilient to thermal denaturation under the conditions used for heat inactivation. Taken together, these observations imply that NS1 is structurally robust and that neither HHP nor the applied thermal treatment substantially compromise its detectability in western blot assays. From an applied perspective, the stability of NS1 antigenicity under these inactivation conditions may have implications for the development of diagnostic assays or vaccines.

For the Envelope (E) protein, a major structural component of the West Nile virus virion, untreated control samples for both lineage 1 and lineage 2 displayed strong, sharp, and well-resolved immunoreactive bands. Following high hydrostatic pressure (HHP) treatment at 400, 500, and 600 MPa for 10 minutes, the Envelope protein remained clearly detectable in both viral lineages. Band profiles in these pressurized samples retained similar sharpness and electrophoretic migration patterns compared

to the untreated controls, and no substantial qualitative differences in intensity were observed across the three tested pressures. This suggests that, under the conditions employed, HHP does not cause significant loss of antigenic epitopes recognized by the anti-E antibody, nor does it induce protein fragmentation or aggregation detectable by western blot analysis. The preservation of E protein immunoreactivity across both lineages under pressure conditions may indicate that the core antigenic structure of the glycoprotein is relatively tolerant to the types of conformational stress induced by hydrostatic compression, at least over the 10-minute exposure period. In contrast, the heat-treated preparations for both lineages exhibited a marked reduction in band intensity relative to both untreated and HHP-treated samples. The weaker and slightly more diffuse bands observed in these thermally inactivated samples are consistent with partial denaturation or conformational alteration of the E protein, potentially accompanied by epitope masking or degradation. Given that the E glycoprotein is highly structured, with multiple domains stabilized by disulfide bonds and dependent on precise folding for epitope presentation, heat-induced disruption of tertiary and quaternary structure could impair epitope recognition and immune response activation. From an applied standpoint, the stability of the Envelope protein under HHP conditions could be advantageous for contexts in which preservation of native-like antigenic determinants is desired, such as in the preparation of inactivated vaccines or in antigen production for diagnostic assays. Conversely, its relative vulnerability to heat highlights the potential limitations of thermal inactivation when the preservation of surface glycoprotein antigenicity is a critical objective.

The Capsid protein was readily detected under all experimental conditions for both lineage 1 and lineage 2 viruses. In the untreated control samples, the Capsid band appeared as a sharp and well-defined signal of consistent intensity, corresponding to the expected molecular size reported for the WNV C protein. Following HHP treatment at 400, 500, and 600 MPa for 10 minutes, the Capsid protein remained clearly detectable, with no appreciable changes in electrophoretic mobility or obvious reduction in signal intensity compared to the respective lineage controls. This stability in the band profile suggests that the capsid protein remains intact after pressurization, indicating preservation of the protein's immunoreactive properties across the full range of tested pressures. Its resistance to detectable antigenic loss under HHP treatment could be explained by its compact, predominantly α-helical structure, which has been reported to confer a certain degree of resilience to both chemical and physical stresses. Moreover, since the C protein is located internally within the virion, it is

plausible that any structural alterations to the envelope and associated proteins during HHP exposure may not directly compromise the antigenic domains of the Capsid detectable by western blotting. Heat-treated preparations of both viral lineages also displayed clear Capsid bands; however, these exhibited a slight reduction in intensity relative to the untreated controls. This attenuation was reproducible across replicate blots and may reflect partial thermal denaturation, aggregation, or degradation of the protein, which could mask or destroy a proportion of the epitopes recognized by the primary antibody.

Results of Western blot analysis performed on HHP- and heat-inactivated propagates are reported in Figure 26.

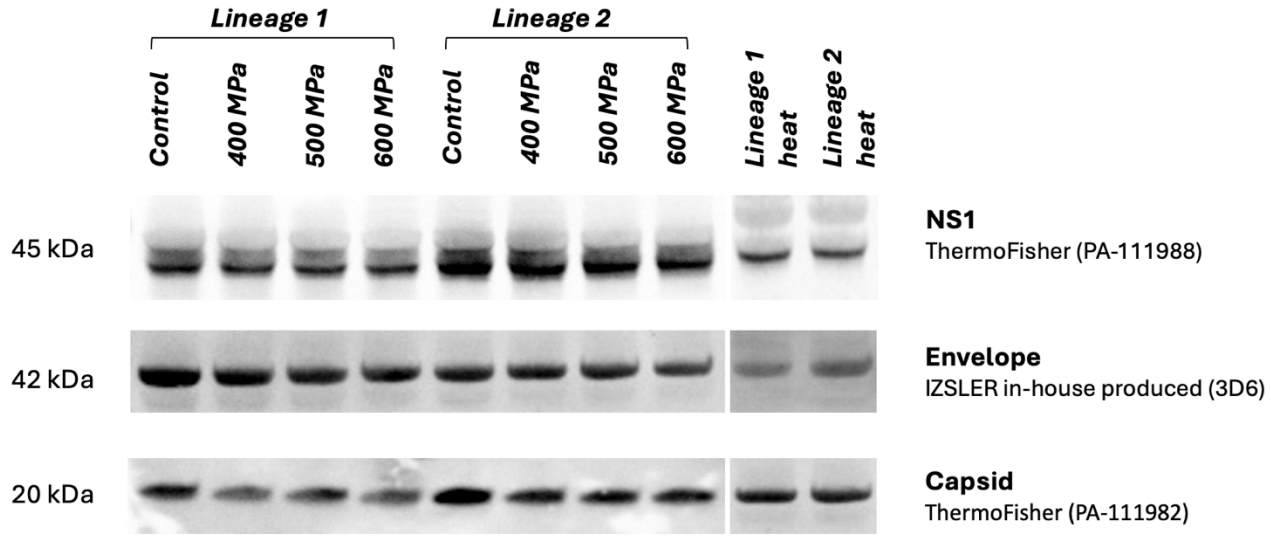

Figure 26. Western blot analysis of WNV structural proteins (Envelope and Capsid) and non-structural protein NS1 in viral particles from lineage 1 and 2 subjected to HHP treatments at 400, 500, and 600 MPa for 10 minutes, as well as heat inactivation. Untreated controls for both lineages are included for comparison. Protein detection was performed using specific primary monoclonal and polyclonal antibodies: NS1 (ThermoFisher PA-111988), Envelope (IZSLER in-house produced, 3D6), Capsid (ThermoFisher PA_111982). Protein band intensities indicate progressive loss or modification of Envelope protein structure under increasing HHP, with relative preservation of Capsid and NS1 proteins.

Overall, the western blot results demonstrate that all three tested viral proteins remain immunoreactive after HHP treatment at 400-600 MPa for both WNV lineages, with no significant qualitative differences observed between pressures. In contrast, heat treatment resulted in some loss of detectable Envelope signal, suggesting that HHP preserves viral protein antigenicity more effectively than thermal inactivation.

5. Discussion

The persistent disparity in vaccine access between high-income and low-income countries remains one of the most pressing and complex challenges confronting global health today. Despite remarkable scientific progress, high production costs and limited distribution capacity continue to hinder equitable access to vaccines worldwide. Vaccine manufacturing is a complex, resource-intensive process that is largely centralized in high-income countries, where advanced biotechnological infrastructure, technical expertise, and stable funding are more readily available. As a result, most low- and middle-income countries depend heavily on imports or international donations, which often result in delays, insufficient supply volumes, and limited autonomy in public health decision-making[284]. This inequitable distribution not only reignited global debates around intellectual property rights, vaccine nationalism, and ethical resource allocation[285], but also underscored the profound ethical obligation to ensure equitable access to vaccines but also the pragmatic reality that global health security is intrinsically interconnected: no nation can be fully protected from a pandemic until all nations are adequately safeguarded. The pandemic has thus served as a powerful stress test, exposing critical vulnerabilities in the existing global health architecture and reinforcing the need to build a more resilient, inclusive, and equitable system in which life-saving vaccines and essential health interventions are universally accessible, irrespective of geographic location, economic status or sociopolitical context[19].

While the glaring inequities witnessed during the COVID-19 crisis captured international attention, disparities in vaccine access are neither new nor limited to emergent infectious diseases. They extend to a range of long-standing, vaccine-preventable illnesses such as pneumococcal infections, rotavirus, and human papillomavirus[343], for which effective vaccines have been widely available in high-income countries for decades, yet remain inaccessible to significant proportions of the population in low- and middle-income countries. In these settings, preventable diseases continue to exact a heavy toll in terms of morbidity and mortality, perpetuating cycles of poor health and economic hardship.

Multiple interrelated factors contribute to this persistent inequity. Chief among them are the high costs associated with vaccine research, development, and production, which frequently place advanced vaccines out of reach for lower-income nations. Additional challenges include the stringent requirements for cold chain storage and transportation, as well as significant logistical complexities related to distribution to geographically isolated, underserved, or conflict-affected regions. These challenges are further exacerbated by the reliance on sophisticated, resource-intensive technologies, which, while highly effective, are often incompatible with the operational realities of low-resource settings. Consequently, structural, financial, and technological barriers continue to limit vaccine accessibility, undermining global efforts to achieve comprehensive immunization coverage and equitable health outcomes.

In response to this enduring and multifaceted crisis, there is an urgent need to rethink and transform current models of vaccine production, distribution and implementation. Innovation must be directed toward the development of scalable, cost-effective, and contextually adaptable solutions capable of overcoming existing barriers. Such strategies involve not only scientific and technological advances, such as alternative inactivation methods, simplified formulation approaches, and heat-stable vaccines, but also concerted efforts in capacity building and equitable international collaboration. Pursuing these goals is not merely a scientific or technical endeavor, but a moral and public health imperative. It demands an integrated approach that encompasses technological innovation with local empowerment, sustainable infrastructure development, and strategic partnerships across nations, sectors, and communities.

Developing low-cost vaccine production strategies is essential to meet growing global demand, especially in LMICs, and to work toward achieving health equity. Developing low-cost vaccine production is not only a moral imperative but also an economic and strategic necessity. Affordable and accessible vaccines can help mitigate the economic impacts of disease outbreaks by reducing healthcare costs and maintaining workforce productivity[286]. Moreover, increased vaccine accessibility promotes health security and stability by reducing the risk of disease spread, which benefits both LMICs and HICs by preventing outbreaks from escalating into global pandemics[287,288]. Ultimately, ensuring equitable access to vaccines represents both a cornerstone of global health justice and a fundamental investment in international stability, resilience, and the sustainability of future public health preparedness.

Among the innovative approaches potentially applicable to vaccine production, high hydrostatic pressure technology emerges as a particularly promising alternative to conventional vaccine inactivation methods. Traditional inactivation techniques, such as heat treatment or chemical exposure, often risk compromising the structural integrity of viral surface antigens, leading to a reduction in vaccine immunogenicity and efficacy. In contrast, HHP inactivation applies uniform isostatic pressure to viral particles, effectively disrupting their infectivity while preserving the conformational structure of key antigenic epitopes. This unique mechanism of action enables the production of vaccines that maintain critical immunological properties, thereby enhancing their capacity to elicit a robust and protective immune response. Importantly, HHP-based vaccine production does not rely on harsh chemicals or elevated temperatures, offering additional advantages in terms of biosafety, environmental impact, and potential manufacturing scalability.

By preserving antigenicity while ensuring complete viral inactivation, HHP technology addresses some of the fundamental limitations associated with existing vaccine production processes, such as those employing β-propiolactone or formaldehyde, which have long been considered gold standards for the production of inactivated vaccines. However, these methods present well-documented limitations in terms of processing time, residual toxicity, and alteration of antigenic structures. In contrast, HHP offers a reagent-free, rapid, and controllable process that ensures complete viral inactivation while minimizing structural damage to immunologically relevant proteins. Moreover, compared with chemical methods, HHP shortens inactivation times from several hours or days to minutes, eliminates the use of toxic

reagents requiring downstream removal, and avoids protein cross-linking that can impair antigen recognition. From an economic perspective, the simplification of purification steps and reduction of biosafety requirements can significantly decrease production costs, making the technology particularly suitable for decentralized manufacturing in LMICs.

Furthermore, its operational simplicity and adaptability to diverse production settings align closely with the need to develop vaccine manufacturing strategies that are not only scientifically robust but also accessible, scalable, and sustainable in a variety of public health contexts, particularly in resource-limited environments. The establishment of regional HHP-based manufacturing hubs could foster vaccine sovereignty and reduce geopolitical dependency, promoting a more equitable global distribution landscape.

Thus, the integration of HHP into vaccine development represents a strategic innovation with the potential to significantly enhance the global reach and effectiveness of immunization programs, contributing meaningfully to the advancement of global health equity.

Although the majority of HHP studies have concentrated on inactivating foodborne viruses, growing evidence supports its application in vaccine development, showcasing its capability to inactivate viruses while maintaining antigenic structures vital for immune recognition and thus immune response inactivation. This innovative approach has been explored across various pathogenic viruses, positioning HHP as a promising platform for vaccine production, providing pivotal contribution to expand the understanding of HHP's effectiveness across a diverse range of human and animal viruses[326–329]. Building on this body of work, our study further explores HHP potential, situating our research within the existing framework and advancing the application of HHP in vaccine development. By leveraging the groundwork laid by previous studies, we aimed to contribute to the evolving field of HHP-based vaccines, which holds significant promise for addressing existing barriers to vaccine access, with the ultimate aim of enhancing the utility of vaccination as a public health tool.

The present study focuses on the development and validation of a novel method for vaccine production using high hydrostatic pressure technology, an approach with significant potential to address some of the key barriers to equitable vaccine distribution. In this study, we investigated the effects of HHP on viral inactivation, with a focus on understanding the structural alterations induced by pressure and their

impact on immunogenicity. The research was conducted through a series of experiments including structural and antigenicity analysis of HHP-treated virus, followed by immune response assessment in an animal model. By leveraging the unique properties of HHP for viral inactivation while preserving antigenicity and immunogenicity, this methodology could help bridge the gap between the developed and developing world in vaccine accessibility, especially for resource-constrained settings. By focusing on technological innovation that aligns with the principles of equity, scalability, and sustainability, this work seeks to contribute to the development of more resilient vaccine supply chains and to the advancement of global health equity.

This study aimed to develop and validate an HHP-based methodology for producing inactivated vaccines against SARS-CoV-2 and WNV. SARS-CoV-2 (B.1 and BQ.1.1 lineages) and WNV (lineages 1 and 2) were selected as representative models of pandemic and endemic threats.

For what concerns SARS-CoV-2, the first step in this investigation involved examining the pressure-induced morphological changes of HHP-treated viral isolates. Our findings highlighted the pressure-dependent effects of HHP on viral replication and morphology. At 400 MPa, the virus exhibited a partial suppression of infectivity, with only minor alterations in its structural integrity. However, as the pressure increased to 500 MPa and 600 MPa, which led to a complete loss of infectivity, significant morphological damage was observed, especially at 600 MPa. Notably, at 600 MPa, the virus lost its spike proteins, a key structural component essential for infectivity. This loss of the spike protein provided evidence for a potential mechanism of viral inactivation.

In parallel, Western blot analysis was employed to explore the molecular changes induced by HHP treatment. The results highlighted pressure-induced alterations in the spike protein, including the reduction of both the monomeric and trimeric forms, alongside the formation of high molecular weight aggregates, more abundant at higher pressure and potentially indicative of macromolecular aggregation, a phenomenon that may be triggered by the HHP treatment and may contribute to viral inactivation. In contrast, the membrane and nucleocapsid proteins exhibited greater structural stability, with no significant degradation observed under the applied pressure conditions, suggesting these proteins are more resilient to HHP treatments. Moreover, when compared with heat inactivation, HHP treatment resulted in less overall protein degradation, particularly in the spike protein, suggesting that HHP

might offer a less disruptive method of inactivating the virus while maintaining a more stable overall protein structure. The differential effects of HHP and heat on the viral proteins observed in these analyses have important implications for their use in vaccine development and viral inactivation strategies. Heat inactivation led to significant degradation of the viral structure, especially of the exposed S protein, which could impact virus ability to induce an immune response. On the other hand, HHP treatment preserves more of the viral structure, including external S protein and critical internal proteins like the M and N proteins, while still reducing the infectivity of the virus by compromising the spike protein. These findings suggest that HHP may offer a more nuanced and potentially more effective approach to viral inactivation, especially in the context of developing vaccines or therapeutics that require the preservation of certain viral components for immune recognition.

The interpretation of these results nonetheless requires consideration of the intrinsic limitations of the technique. Western blotting is performed under strongly denaturing conditions, including exposure to sodium dodecyl sulfate, reducing agents, and heat, which irreversibly disrupt protein tertiary and quaternary structures. As a result, proteins are fully linearized, uniformly negatively charged, and separated based solely on molecular weight rather than native conformation. This methodological context directly affects the evaluation of antigenicity. Conformational epitopes, which depend on the three-dimensional folding of proteins and the spatial arrangement of discontinuous amino acid residues, are destroyed during SDS-PAGE and blotting. Consequently, Western blot analysis detects only linear epitopes corresponding to continuous amino acid sequences that remain accessible after denaturation. Therefore, antigenic reactivity observed in western blot does not reflect the preservation of native protein structure but rather the integrity of the primary amino acid sequence and linear antigenic determinants. In the context of HHP-treated viral antigens, this distinction is particularly relevant. High hydrostatic pressure primarily disrupts non-covalent interactions stabilizing higher-order protein structures, while generally preserving covalent bonds. Depending on pressure intensity and exposure time, HHP may induce partial unfolding or dissociation of multimeric complexes without extensive protein degradation. However, because Western blot analysis is conducted under fully denaturing conditions, any pressure-induced changes in native tertiary or quaternary structure are masked. Accordingly, Western blot results should be interpreted as a proxy for overall antigenic integrity rather than a direct assessment of native epitope preservation.

Despite these limitations, the retention of immunoreactivity in Western blot remains biologically meaningful. A positive signal following HHP treatment indicates preservation of viral protein integrity and of linear epitopes, suggesting that inactivation does not cause extensive proteolysis or irreversible chemical damage. From a vaccine development perspective, linear epitopes are relevant not only for antibody recognition but also for cellular immunity, as they can be efficiently processed and presented by antigen-presenting cells to activate virus-specific T cells.

Within a comprehensive antigenicity assessment, western blotting represents a robust quality control tool. Although insufficient on its own to evaluate native antigenicity, positive western blot results contribute important evidence in an integrated in vitro evaluation and support the advancement of HHP-inactivated preparations toward in vivo immunogenicity studies.

Following the structural and antigen analysis, we indeed evaluated the immunogenicity of the HHP-inactivated viruses in an animal model. Our findings demonstrated that the method of inactivation and the applied pressure significantly influenced the immune responses. The 500 MPa treatment induced a robust immune response, producing the highest and most sustained IgG antibody titers. In contrast, the heat-inactivated virus elicited lower peak antibody titers and a slower immune response, highlighting the efficacy of HHP in generating a more potent humoral immune response. Treatment at 600 MPa, while still effective, resulted in the weakest IgG response, with lower antibody titers across all time points.

When analyzing neutralizing antibody responses, both 500 MPa and 600 MPa treatments outperformed the heat-inactivated group. The neutralizing antibody titers in the 500 MPa group were consistently the highest, followed by the 600 MPa group, which demonstrated robust neutralizing capacity, despite exhibiting the lowest overall antibody responses. The heat-inactivated virus induced a much weaker and less sustained neutralizing antibody response, with minimal improvement beyond the 28-day time point. The observed difference in the magnitude and kinetic of the humoral response correlate with antigenic integrity. In fact, 500 MPa HHP treatment, preserved key antigens like the spike protein thus elicited the strongest and most sustained antibody titers. Heat inactivation, on the contrary, and as highlighted by Western blot analysis, caused antigen degradation, leading to weaker responses. Meanwhile, the 600 MPa HHP treatment, though preserving viral structure to some extent, induced a weaker immune response, possibly due to excessive pressure causing subtle structural

disruptions that impacted antigenicity. These findings further reinforced the superior efficacy of HHP in preserving viral antigenicity, which is critical for eliciting strong and sustained neutralizing antibody responses. Supporting the findings from the neutralization assays, Western blot analysis performed on sera from immunized mice revealed significant differences in the immune responses elicited by HHP-treated and heat-inactivated viruses. The HHP-treated viruses induced a more comprehensive antibody response, targeting both the spike and nucleocapsid proteins, while the heat-inactivated virus generated a response primarily against the nucleocapsid protein. While a strong anti-nucleocapsid response may still provide some level of immunity, the absence of an anti-spike response could reduce the overall efficacy of the immune response, particularly in terms of neutralization and prevention of viral entry. These findings suggest that HHP treatment may be a more effective method for generating broad immune responses that target multiple viral proteins, which could enhance the overall protective efficacy of vaccines developed using HHP-inactivated viruses. This observation is particularly significant given that the spike protein is the primary inducer of neutralizing antibody responses. The absence of a spike-specific response in the heat-inactivated group likely accounts for the weaker neutralizing antibody titers observed in this group, underscoring the importance of preserving the structural integrity of the spike protein during inactivation to ensure the generation of robust and protective immune responses. These findings highlight the superiority of HHP inactivation in maintaining the antigenic properties of key viral proteins critical for eliciting effective immunity.

In addition to antibody responses, we also assessed T-cell activation through ELISpot. The 500 MPa treatment consistently elicited the strongest and most reliable T-cell responses, particularly in spleen samples. The 600 MPa treatment also triggered T-cell activation, though with more variability. In stark contrast, the heat-inactivated group showed minimal T-cell activation, both in whole blood and spleen, which emphasized the limitations of heat inactivation in eliciting a strong cellular immune response. This broader immune response generated by HHP inactivation was seen as a significant advantage in the context of vaccine development, as it could provide a more comprehensive protective immune response.

The main limitation of this study is the lack of efficacy data derived from *in vivo* challenge studies. While such models can yield valuable insights into vaccine

performance, they are associated with several scientific, logistical, and ethical challenges that may compromise their generalizability and reliability.

Scientifically, the selection of an appropriate animal model is a significant constraint. Most standard laboratory animals are either not naturally susceptible to SARS-CoV-2 infection or do not recapitulate the full spectrum of human disease. Although transgenic mice expressing human ACE2 receptors, ferrets, and non-human primates have been employed, each model presents important physiological and immunological differences compared to humans. These interspecies discrepancies limit the translational relevance of efficacy data obtained in animal models. Protective responses observed in these systems may not accurately predict outcomes in human populations, and conversely, adverse effects may be under- or overrepresented.

In light of the above results, this study nonetheless provides strong evidence for the potential of HHP as an effective method for viral inactivation, demonstrating its ability to preserve viral antigenicity while inducing robust immune responses. The pressure-dependent effects observed on viral morphology and protein integrity suggest that HHP inactivation could offer a more efficient and less disruptive alternative to traditional heat inactivation methods. Importantly, HHP inactivation demonstrated higher immunogenicity in both humoral and cell-mediated immune responses, with the 500 MPa treatment showing the most promising results.

Another critical aspect of this study was the evaluation of the thermostability of the 500 MPa HHP-inactivated vaccine candidate. The ability to maintain antigenic integrity under various storage conditions is a crucial factor in the practicality of vaccine distribution, particularly in regions with limited access to ultra-cold storage facilities. Our findings demonstrated that HHP-inactivated viruses, when stored at refrigeration temperatures (4 °C), maintained their antigenic stability for at least 30 days. This is particularly important for vaccine distribution, as it suggests that HHP-inactivated vaccines could be stored under less stringent conditions than those requiring ultra-cold freezing, thereby reducing logistical challenges and costs associated with cold-chain maintenance, which poses significant challenges in low-resource settings, refrigeration provides a more flexible and accessible option for the storage of vaccines. The stability of the antigenic properties of HHP-inactivated viruses under refrigeration offers an innovative solution for improving vaccine accessibility in low-income and resource-limited areas, where strict dependencies of mRNA vaccines from ultra-cold chain storage represented a constrain to mass

vaccination. This also suggests that HHP inactivation could be a cost-effective and scalable method for the production of vaccines, making it a valuable tool for improving global vaccine distribution.

From this point of view, the introduction of mRNA-based vaccines against SARS-CoV-2 marked a pivotal advancement in immunization technology, offering rapid development timelines and high efficacy. However, the widespread distribution of these vaccines has been hindered by stringent storage requirements, particularly the need for ultra-cold chain logistics. Unlike conventional vaccines, which are typically stable at 2-8 °C, first-generation mRNA vaccines such as BNT162b2 (Pfizer-BioNTech) and mRNA-1273 (Moderna) initially required storage at -70 °C and -20 °C, respectively. These extreme temperature requirements posed significant logistical challenges, especially for LMICs, where cold chain infrastructure is often limited or entirely absent.

The introduction of mRNA vaccines required substantial adaptations in LMICs, where distribution systems are historically built to support traditional immunization programs relying on heat-stable or mildly refrigerated vaccines, including the procurement of ultra-low temperature freezers, stable electricity supplies, and temperature monitoring systems. In rural or underserved regions, where power outages are common and transportation infrastructure is weak, maintaining a consistent cold chain became a major obstacle. The lack of reliable cold storage not only delayed vaccine delivery but, in some cases, led to vaccine wastage due to thermal excursions outside of recommended storage ranges.

These challenges exacerbated existing inequities in vaccine access between high-income and low-income countries. While wealthier nations were able to rapidly deploy mRNA vaccines thanks to robust logistics and supply chains, LMICs often depended on international aid or donations, which were not always synchronized with local capacities to store and distribute the vaccines effectively. The situation highlighted a critical vulnerability in global health preparedness: the reliance on technologies that are not universally compatible with existing infrastructures. In this context, the initial rollout period was sufficient to reveal how technological innovations, while scientifically transformative, must also be matched by practical considerations related to deployment in diverse geographic and socioeconomic contexts. As the global community prepares for future pandemics, it is imperative that vaccine development strategies integrate delivery feasibility into early planning

stages, ensuring that life-saving interventions are accessible not only where they are developed, but also where they are most urgently needed.

In this context, vaccines produced through HHP technology offer a compelling alternative, particularly due to their favorable stability profiles under non-stringent storage conditions. Unlike mRNA vaccines that require ultra-cold storage conditions, HHP-inactivated vaccines have demonstrated medium-term stability at ambient temperature for up to 14 days, and long-term stability for at least 30 days under mild refrigeration at 4 °C. This thermal resilience represents a substantial logistical advantage in low- and middle-income countries (LMICs), where cold chain infrastructure is often limited to standard refrigeration, and ultra-cold storage is either unavailable or prohibitively expensive to implement and maintain. The reduced dependence on cold chain complexity facilitates broader geographic reach, enabling vaccine delivery to remote or underserved areas without compromising product integrity. Moreover, the extended stability at higher temperatures simplifies stockpiling, field deployment, and last-mile distribution, all of which are critical for rapid response in outbreak scenarios or routine immunization campaigns. The ability to maintain vaccine potency under less restrictive storage conditions positions HHP-based vaccines as a highly viable solution for equitable immunization in resource-limited settings, contributing to improved global health resilience.

The study has also demonstrated a key scientific and practical strength of the HHP process: its physical mechanism of action. This purely physical mechanism makes it highly improbable that genetic variations among viral strains would exert an influence on the efficacy of the inactivation process. This is evidenced by the findings of the present study, which yielded comparable results with early lineage B.1 and more genetically divergent BQ.1.1 lineages. In light of this, HHP technology is highly adaptable and would enables expeditious modification to newly emerging variants without necessitating extensive alterations of manufacturing protocols. This feature has significant implications for the development of vaccines, particularly in the context of rapidly mutating RNA viruses such as influenza and coronaviruses, which present significant challenges to traditional vaccine development methods.

The COVID-19 pandemic has highlighted the difficulties inherent in vaccine development against rapidly evolving RNA viruses. SARS-CoV-2 has in fact exhibited a high rate of mutation, leading to the emergence of numerous variants of concern (VOCs), such as Alpha, Delta, and multiple Omicron sub-lineages. These genetic shifts

have frequently affected the spike protein, the primary target of most first-generation vaccines, reducing their efficacy over time and necessitating repeated reformulation and booster campaigns. The need to update vaccines in response to each new variant has placed significant pressure on global manufacturing capabilities, regulatory pathways, and public health systems. Results obtained here, showing equivalent inactivation outcomes for two distinct SARS-CoV-2 lineages suggests that vaccine formulations based on HHP-treated virions could maintain broad efficacy without requiring constant adaptation to genetic drift. Similarly, HHP has the potential to overcome several longstanding challenges of seasonal influenza virus vaccine reformulation, necessary to match circulating strains, which presents a persistent challenge to global public health systems due to the rapid and unpredictable antigenic evolution of circulating influenza viruses, which can lead to substantial mismatches between vaccine strains and the dominant strains in circulation, often leading to suboptimal vaccine effectiveness. This process is not only scientifically complex, relying on predictive modeling of future dominant variants, but also industrially demanding.

In general, by maintaining efficacy independent of genetic variation, HHP represents a powerful tool for ensuring an agile and effective vaccine response to the ongoing evolution of viral threats, thereby reducing the time required to develop and deploy vaccines against emerging variants, thereby improving the timeliness of vaccine distribution during outbreaks and pandemics, where delays in vaccine deployment can have severe public health consequences.

Additionally, one of the most significant operational advantages of the HHP inactivation method herein described is the markedly brief processing time compared to other HHP inactivation protocols proposed in literature[326,327]. The high-pressure treatment protocol herein proposed lasts only a few minutes and enables the rapid inactivation of large volumes of viral suspension (up to 400-450 liters) within a single batch. The high throughput of the HHP process aligns with the demands of industrial-scale vaccine production and may be particularly advantageous in outbreak scenarios, where speed is crucial to responding to the demand for vaccines in a timely manner, thus mitigating bottlenecks in vaccine production.

Current HHP technologies, initially developed for the food industry, are already capable of processing large volumes of materials at a relatively high throughput. The scalability demonstrated in the food sector, where HHP is used for microbial

inactivation in packaged products, suggests that similar systems can be adapted for biopharmaceutical applications. At an industrial level, scalability also depends on the capacity to integrate HHP systems into existing vaccine production pipelines. This includes the seamless connection of the HHP treatment stage with upstream (such as cell culture or bioreactor harvesting) and downstream (such as purification, formulation, and packaging) processes. The modularity of HHP systems means that vaccine production by HHP can be easily accommodated without the need for extensive redesigns of the entire production line.

A further crucial benefit of the HHP process is its low operational cost. The mass production of viral suspensions using HHP is estimated to cost approximately 0.10-0.30 € per kilogram[297], which represents a significant reduction in cost compared to traditional production methods. For instance, the mRNA-based vaccine BNT162b2 (Pfizer-BioNTech) requires advanced lipid nanoparticle formulation, cold chain logistics (-70°C), and high-purity raw materials, driving per-dose production costs to approximately $10-$15[169]. In contrast, a hypothetical SARS-CoV-2 vaccine produced via HHP would involve pressurizing whole inactivated virions in a buffered medium, with minimal downstream purification and formulation with adjuvants. Such a platform could reduce production costs to as low as a few cents per dose. The affordability of HHP-based production could have a transformative impact on the development of cost-effective vaccines that are accessible to a broader population, particularly in LMICs. This could lead to a reduction in the financial burden on healthcare systems and international aid organizations tasked with vaccine distribution.

Despite the low operational cost, the initial capital investment required for HHP infrastructure can be high. Industrial-scale HHP systems are complex and require significant upfront investment in pressure vessels, associated control systems, and supporting infrastructure. These costs can be a barrier to entry for some manufacturers, particularly in LMICs. However, the modular nature of HHP systems means that manufacturers can begin with smaller units and scale up as production needs increase, which could help spread costs over time. In addition to the capital investment in equipment, operational costs such as maintenance, energy consumption, and labor must also be considered. HHP systems require high amounts of energy to generate the necessary pressures, and the energy costs associated with large-scale operations can be substantial. However, as HHP systems become more widely

adopted, the cost of energy and maintenance is likely to decrease due to technological advancements and economies of scale. Furthermore, HHP equipment, though initially capital intensive, can be reused across multiple production cycles and for different pathogens, enhancing long-term cost-effectiveness.

Lastly, on the social level, the use of the same inactivated virus as the basis for the vaccine could enhance public trust and acceptance, particularly among individuals who harbor concerns about vaccines developed using advanced molecular techniques, such as genetic engineering or mRNA-based platforms.

During the COVID-19 pandemic, a substantial segment of the global population expressed skepticism toward mRNA vaccines, citing fears related to their novelty, the perceived lack of long-term safety data, and misinformation linking mRNA technology to genetic manipulation or infertility[344,345]. For instance, in several European countries, surveys conducted in 2021 revealed that a notable proportion of respondents preferred "traditional" vaccines, such as those based on inactivated or protein subunit platforms, over mRNA-based alternatives, even when the latter had higher efficacy rates. Similar trends were observed in parts of the United States, where some vaccine-hesitant individuals explicitly stated they would be more willing to accept a vaccine based on a "dead virus" rather than one using "experimental genetic material"[346,347].

This hesitancy was often reinforced by the rapid rollout of mRNA vaccines under emergency use authorizations, which, while scientifically justified, fueled public concern that safety evaluations had been rushed. Moreover, social media amplified fears about the mechanism of action of mRNA vaccines, with widespread false claims that such vaccines could alter DNA or affect reproductive health, concerns not commonly associated with inactivated virus vaccines, which have a long-established history in public immunization programs for diseases such as polio, hepatitis A, and influenza[348–352].

In this context, vaccine candidates developed using HHP for viral inactivation could represent a strategic advantage. HHP preserves the structural integrity of viral antigens while eliminating infectivity through a physical, non-chemical process. This aligns with the expectations of vaccine-hesitant individuals who favor "minimally manipulated" or "natural" interventions. Moreover, the transparent communication of the HHP mechanism, emphasizing its physical, non-genetic nature, may help reduce perceived risks and increase vaccine acceptability. Consequently, HHP-based

vaccines may help overcome resistance rooted in fears of novel technologies, thereby facilitating higher uptake rates and contributing to more effective immunization campaigns, albeit the present corpus of scientific literature does not provide an unambiguous consensus on an overall preference for inactivated vaccines over mRNA vaccines, as vaccine acceptance may be influenced by cultural factors, the availability of the vaccines, public communication, and trust in local health authorities[353,354].

Despite its considerable promise, the implementation of HHP technology for vaccine production is accompanied by several significant challenges, foremost among which is the regulatory uncertainty surrounding its approval for both human and veterinary use. A fundamental obstacle lies in the current lack of a clearly defined regulatory framework that explicitly accommodates HHP as a recognized and validated method for pathogen inactivation. Regulatory agencies such as the European Medicines Agency (EMA), the U.S. Food and Drug Administration (FDA), and the World Organization for Animal Health (WOAH) have well-established guidelines for the assessment and approval of inactivated vaccines. However, these guidelines are predominantly oriented toward traditional inactivation methods, such as chemical agents (e.g., formaldehyde, β-propiolactone) or heat treatment, whose mechanisms of action, safety margins, and long-term performance have been thoroughly documented and standardized over decades of use.

In contrast, although HHP confers clear theoretical and practical advantages, such as improved epitope preservation, elimination of toxic residues, and potentially reduced production costs, the novelty of the approach means that it falls outside current regulatory precedents. As such, developers face considerable ambiguity regarding which validation criteria, preclinical studies, and manufacturing standards must be met to satisfy regulatory expectations, to assess the robustness and reproducibility of pressure-induced inactivation and demonstrate batch consistency.

The lack of specific regulatory guidelines or reference standards for HHP and the absence of any prior licensed vaccine products based on HHP technology, which means that regulatory bodies have no precedent on which to model their evaluations, may necessitate a case-by-case approach to define acceptable development pathways, introducing uncertainty, prolonging timelines, and increasing the complexity and cost of product development.

As a result, regulatory approval currently constitutes one of the most formidable barriers to the implementation and industrialization of this innovative platform. The

uncertainty surrounding the regulatory acceptance of HHP-based vaccines can act as a significant disincentive for both public and private investment, especially when compared to more conventional vaccine technologies with predictable development pathways and well-understood regulatory requirements. This perceived regulatory risk may ultimately delay or even prevent the translation of promising preclinical results into clinical applications or field use, despite growing evidence supporting the immunological efficacy and safety of HHP-inactivated pathogens.

In light of these challenges, the advancement of comprehensive research to further investigate the application of HHP technology in vaccine production, alongside the validation of standardized operating procedures for viral inactivation and the implementation of collaborative pilot programs to demonstrate preclinical robustness, may serve as critical enablers for the transition from preclinical investigation to clinical evaluation. Such efforts are essential for facilitating the broader adoption of this potentially transformative platform in both human and veterinary vaccine development, particularly as global health systems seek scalable, rapid-response solutions to infectious disease threats. Given that HHP equipment and processes are already standardized in the food biotechnology sector, regulatory translation to vaccine production could be accelerated through adapted GMP (Good manufacturing Practices) frameworks, reducing the technological gap between research and industrial application

Although the present study focused on SARS-CoV-2 and WNV as model viruses, the underlying principles of HHP-mediated inactivation can be broadly applicable to a wide range of viral pathogens of public health relevance, including both enveloped and non-enveloped viruses. One of the most pressing challenges in modern vaccinology is the ability to respond swiftly and effectively to emerging viral threats. HHP can be quickly adapted to new viral agents through modulation of pressure and exposure parameters, making the technology particularly attractive for emergency contexts, such as the early phases of a pandemic, where time is a critical factor. While SARS-CoV-2 and WNV served effectively as a proof of concept, it is anticipated that other viral agents may require tailored adjustments in pressure intensity, exposure duration, or temperature conditions to achieve complete inactivation while preserving critical antigenic epitopes. Nonetheless, the inherent adaptability of HHP technology renders it an especially attractive platform for the development of vaccines against both endemic and emerging infectious diseases.

The modular nature of HHP technology, composed of distinct yet interoperable units, represents a key advantage in its potential application to the production of inactivated vaccines, potentially facilitating rapid adaptation of the production workflow to different pathogens, minimizing the need for major process revalidation or facility redesign.

The concept of a "plug-and-play" HHP-based vaccine platform exemplifies this modularity. Within such a framework, the core manufacturing infrastructure and the downstream processing steps can remain largely constant, while pressure/time parameters are modified to suit the physicochemical and structural properties of the new target virus. This feature significantly reduces both the lead time and the resource investment required to transition from one vaccine candidate to another, providing a flexible, scalable solution for both routine immunization and outbreak scenarios, thereby increasing the responsiveness of vaccine production systems in the face of emerging infectious threats.

Moreover, once regulatory standards and inactivation protocols for HHP are standardized and approved, this framework could facilitate rapid regulatory clearance of new vaccines based on previously validated processes. This way, it may become feasible to rapidly generate immunogenic and safe vaccines against novel pathogens, thereby reducing the lead time and financial burden typically associated with conventional vaccine development. This technological flexibility and adaptability are particularly advantageous in the context of pandemic preparedness, where the ability to rapidly design and produce effective vaccines can play a pivotal role in mitigating disease transmission and impact, offering strategic advantages in responding to unforeseen public health emergencies, including zoonotic spillovers and vector-borne outbreaks.

The promising outcomes obtained through the application of HHP technology to SARS-CoV-2 vaccine prototypes have underscored the potential of this approach as a reliable and scalable platform for viral inactivation, providing a strong experimental foundation for considering HHP as a next-generation platform for the development of inactivated vaccines. However, to fully exploit its potential, it is essential to assess the translatability of this technology to other viral systems with distinct structural and biochemical characteristics.

In this respect, arboviruses may constitute an important and challenging test case. Arboviruses represent an increasingly pressing concern for both human and animal

health, with their capacity for rapid emergence and geographic spread posing continuous challenges to global health systems. In the context of accelerating climate change and widespread exploitation of natural habitats, the ecological balance of reservoir hosts and vectors is undergoing profound modifications, with important implications for arbovirus transmission dynamics. For Europe in particular, projections suggest that arboviruses are likely to become increasingly relevant in human pathology, not only through the introduction of exotic pathogens but also via the expansion and diversification of endemic ones. Evidence already indicates that environmental degradation and habitat loss have altered bird migration routes, thereby facilitating the spread of arboviruses to previously unaffected areas[355]. Simultaneously, unregulated urban expansion creates conditions that favor mosquito proliferation, amplifying the potential for local transmission of vector-borne diseases[356]. These anthropogenic drivers, acting in concert with climate variability, are therefore expected to provide arboviruses with unprecedented opportunities to expand, adapt, and evolve[357].

Looking ahead, several converging factors are predicted to intensify this trend. First, climate change is expected to reshape vector ecology by increasing average temperatures, altering rainfall patterns, and lengthening the warm seasons in which mosquitoes can breed and remain active[358]. Warmer winters and milder transitional seasons will facilitate the overwintering of mosquito populations and extend their geographical range into northern and central Europe[359]. Second, globalization and human mobility will continue to act as conduits for the introduction of arboviruses from endemic regions, with international travel and trade accelerating the risk of imported cases that may ignite local outbreaks if competent vectors are present[360]. Third, agricultural intensification and land-use changes are progressively disrupting natural ecosystems, reducing biodiversity, and creating ecological niches where vectors and reservoir hosts thrive in close contact with human populations[246]. Fourth, demographic growth and unplanned urbanization, particularly in peri-urban and rural-urban transition zones, will contribute to the expansion of environments with stagnant water, poor waste management, and limited vector-control measures, all of which support high densities of *Aedes* and *Culex* mosquitoes[361]. Fifth, socioeconomic disparities and weakened public health infrastructures in certain regions may undermine the capacity to implement surveillance, prevention, and rapid-response strategies, further facilitating silent transmission chains[362]. Finally, viral evolution itself, accelerated by the high mutation rates typical of RNA viruses,

will likely generate variants with enhanced fitness, including improved transmission efficiency, immune evasion, or adaptation to new vector species, thereby complicating control efforts[363].

Taken together, these factors underscore that the anticipated increase in arboviral burden across Europe is not the result of a single driver but the consequence of a complex interplay between environmental, ecological, demographic, and virological dynamics. Addressing this multifaceted challenge will require integrated strategies that combine climate adaptation policies, urban planning, vector-control interventions, and the development of effective vaccines capable of curbing both endemic and emerging arboviruses[364].

The current surge in Dengue cases in the Americas[189] exemplifies the potential trajectory of arbovirus epidemiology under changing environmental conditions. Similar scenarios are conceivable in Europe, where rising vector competence and expanding mosquito populations create the conditions for autochthonous outbreaks of pathogens previously considered exotic[365,366]. Within this evolving landscape, HHP-based vaccines may represent an innovative tool to strengthen preparedness, offering an alternative platform that combines safety, antigen preservation, and scalability. Their development and integration into vaccination programs could therefore play a decisive role in mitigating the burden of arboviral infections and shaping the trajectory of human pathology in the decades to come, with non-negligible translational relevance beyond the laboratory.

In regions experiencing ecological disruption, urbanization, and increasing vector densities, the rapid deployment of safe and effective vaccines could act as a critical barrier to arbovirus establishment. By reducing the pool of susceptible hosts, HHP-derived vaccines could limit viral amplification in humans and, indirectly, restrict the feedback loop to vector populations. In this way, such vaccines would not only protect individuals from disease but also contribute to population-level reductions in viral circulation, thereby attenuating the ecological and epidemiological impact of arboviruses.

Against this background of growing demand for effective vaccines against emerging and re-emerging arboviral diseases, such as but not limited to WNV, HHP has been tested for the inactivation of WNV. Preliminary investigations have demonstrated that WNV exhibits a comparatively higher resilience to HHP inactivation than other enveloped RNA viruses previously evaluated using this method, such as SARS-CoV-

2. This increased resistance is likely attributable to the structural stability of the viral envelope, lacking prominent surface projections represented by spike glycoproteins, whose presence in coronaviruses could render the virion envelope more vulnerable to pressure-induced structural disruption. For this reason, WNV necessitated a tailored optimization of the inactivation protocol. Specifically, experiments have shown that standard pressure levels (ranging from 400 to 600 MPa) applied over brief durations (5 minutes) have been insufficient to completely abolish WNV infectivity. Longer exposure times (10 minutes) were required to ensure complete inactivation. These findings underscore the need for virus-specific refining of HHP parameters when deploying this technology as a broad-spectrum vaccine platform.

Despite the challenges associated with optimizing the inactivation protocol, the initial characterization of HHP-treated WNV particles was encouraging, but also suggested further refinement of HHP processing protocol may be warranted depending on virus specific morphological characteristics.

Viral preparations treated at 400, 500, or 600 MPa for 10 minutes contained no identifiable intact particles; instead, they were dominated by irregular, amorphous, or collapsed structures lacking both the characteristic size and the surface projections of native virions. These findings demonstrate that HHP treatment, at all tested pressures, resulted in severe morphological damage to WNV particles, consistent with loss of infectivity and in agreement with the results from biological assays. Complementary western blot analyses targeting both structural proteins (e.g., envelope protein E and capsid protein C) and non-structural components (e.g., NS1) revealed strong immunoreactivity post-treatment, suggesting that epitopes critical for immune recognition and immune response activation remain intact following pressurization. These results are particularly significant as the maintenance of conformational epitopes is a key determinant for vaccine-induced protection.

The preservation of the envelope (E) protein integrity is of particular immunological relevance, as this glycoprotein constitutes the principal target of neutralizing antibodies in flavivirus infections, mediating critical functions such as receptor binding, viral entry, and membrane fusion. The conformational epitopes located within the E protein's domain III are especially important for eliciting high-affinity, virus-neutralizing antibody responses capable of preventing infection by blocking viral attachment or fusion. Therefore, maintaining the structural conformation of E following pressurization directly supports the antigenic fidelity required for effective

vaccine-induced protection. In this context, the observed immunoreactivity implies that HHP treatment does not compromise the tertiary or quaternary organization of E protein epitopes, which are indispensable for inducing a protective neutralizing antibody repertoire.

Equally noteworthy is the retention of immunoreactivity for the non-structural protein NS1, a multifunctional antigen that, despite not being a component of the viral particle, plays a key role in modulating the host immune response, with direct involvement in immune evasion, complement inhibition, and endothelial dysfunction during infection. Importantly, NS1-specific antibodies can confer protection through non-neutralizing mechanisms such as complement-mediated cytotoxicity and antibody-dependent cellular cytotoxicity, thereby contributing to viral clearance and disease mitigation. The preservation of NS1 antigenicity following HHP treatment therefore expands the potential immunogenic spectrum of inactivated preparations, suggesting that both neutralizing (E-mediated) and non-neutralizing (NS1-mediated) immune pathways could be effectively engaged.

Also in this case, as Western blot was performed under strongly denaturing conditions, it allowed detection exclusively of linear epitopes, while conformational epitopes, dependent on native protein folding, could not be evaluated. In this context, antigenic reactivity observed after HHP treatment should not be interpreted as direct evidence of native structural preservation, but rather as an indicator of overall protein integrity and conservation of primary sequence–dependent antigenic determinants. Although this approach cannot capture conformational antigenicity, the retention of Western blot reactivity remains biologically relevant. Preservation of linear epitopes indicates limited protein degradation and supports the maintenance of antigenic substrates relevant for antigen processing and T-cell activation. Therefore, positive western blot results provide meaningful supporting evidence within a comprehensive in vitro antigenicity assessment and contribute to the interpretation of subsequent in vivo immunogenicity outcomes.

All in all, this dual preservation of structural and non-structural epitopes provides a strong rationale for the further evaluation of HHP-based formulations as vaccine candidates, where the induction of both antibody- and T cell-mediated immunity is essential for achieving durable and cross-protective responses. The conservation of E and NS1 epitopes following pressurization thus represents a crucial step toward

developing safe, antigenically faithful vaccines capable of eliciting balanced, multi-faceted immune protection against West Nile virus and related flaviviruses.

In light of these results, adjustments to the exposure time could nonetheless be considered, with durations shorter than 10 minutes but exceeding the 5-minute interval found to be insufficient in preliminary trials. Such intermediate time points may allow for efficient viral inactivation while potentially reducing unnecessary structural degradation or other unwanted effects on sample properties. Alternatively, or in combination, refinement of the applied pressure levels could be explored to identify the minimal conditions that achieve complete inactivation. Systematic evaluation of these variables would provide a more precise understanding of the relationship between treatment intensity and virological outcomes, ultimately supporting the development of a protocol that balances efficacy with preservation of sample integrity.

Unlike the situation faced during the COVID-19 pandemic, where continuous viral evolution dictated the pace of vaccine adaptation, the major obstacle for West Nile virus prevention lies in its ecological expansion driven by climate change rather than in antigenic diversification.

The genetic stability of West Nile virus represents a defining feature of its evolutionary biology and a central element in understanding its epidemiology and public-health implications. Unlike many RNA viruses characterized by rapid mutation rates and high antigenic plasticity, WNV exhibits a relatively constrained pattern of genetic diversification. This reduced variability stems from the ecological and molecular constraints imposed by its enzootic transmission cycle, which alternates between avian reservoirs and mosquito vectors, primarily of the *Culex* genus. Each host type exerts distinct, and often opposing, selective pressures on the viral genome, alternating adaptive diversification and purifying selection, creating a dynamic evolutionary bottleneck that maintains viral stability across lineages. Transmission from vector to vertebrate host further accentuates this genetic constraint. During infection of the mosquito, viral populations undergo sequential bottlenecks, first during midgut infection, then dissemination to secondary tissues, and finally at salivary gland escape, each step reducing intra-host diversity. Although expansion within the mosquito's salivary glands can partially restore population size, the transmitted inoculum to the vertebrate host typically comprises a genetically narrow subset of the initial viral quasispecies. In vertebrates, additional bottlenecks occur during systemic

dissemination, ensuring that only a limited fraction of genotypes contributes to onward transmission. Collectively, these processes act as evolutionary filters, reinforcing genetic homogeneity and slowing the overall rate of molecular evolution. This stands in stark contrast to the dynamics observed in viruses that replicate exclusively within vertebrate hosts, where the absence of alternating host barriers allows for more rapid adaptation and lineage diversification.

The implications of this constrained variability are profound when compared to the evolutionary behavior of SARS-CoV-2. The coronavirus pandemic has exemplified how high mutation rates and adaptive evolution can continuously reshape viral epidemiology, pathogenesis, and the global public-health response. In SARS-CoV-2, selective pressures exerted by population-level immunity, whether induced by infection or vaccination, facilitated the emergence of variants of concern (VOCs) with enhanced transmissibility and immune evasion properties. Mutations in the spike glycoprotein, particularly within the receptor-binding domain, dramatically altered viral phenotype, driving waves of infection that rendered first-generation vaccines progressively less effective. This relentless antigenic evolution necessitated the periodic reformulation of vaccines, mirroring the iterative approach used for influenza viruses. The adaptive landscape of SARS-CoV-2 thus demonstrated the intimate link between viral genetic variability and the continuous need for vaccine updates to maintain herd immunity and reduce morbidity and mortality.

In contrast, WNV presents a fundamentally different challenge. The evolutionary bottlenecks inherent in its transmission cycle, coupled with its low substitution rate, result in limited antigenic drift. Despite the existence of multiple genetic lineages, the antigenic structure of key immunogenic proteins, particularly the envelope (E) glycoprotein, remains largely conserved. Neutralizing epitopes recognized by the host immune system exhibit minimal variation, and cross-protection among strains within the same lineage is generally robust. Consequently, vaccine development for WNV does not face the continuous arms race between viral evolution and host immunity that characterizes pathogens like SARS-CoV-2. The absence of frequent immune-escape variants implies that a single, lineage-specific, well-designed vaccine could confer long-term protection without recurrent reformulation.

Nevertheless, this apparent virological stability does not diminish the urgency of preventive measures. The growing epidemiological threat posed by WNV arises not from antigenic evolution but from ecological and climatic transformations that have

expanded the spatial and temporal boundaries of viral transmission. Warmer temperatures, milder winters, and altered precipitation patterns have extended the seasonal activity of *Culex* vectors, facilitated their northward spread, and promoted overwintering of infected mosquito populations. These processes have established endemic foci of transmission in previously unaffected regions of Europe, particularly in the Mediterranean Basin and Central and Eastern Europe. The increased interaction between competent vectors and susceptible avian species has reinforced local transmission cycles, transforming WNV from a sporadic zoonosis into a recurrent seasonal pathogen with significant public-health and veterinary impact.

In this context, the rationale for WNV vaccine development diverges sharply from that for SARS-CoV-2. While the urgency of coronavirus vaccine deployment during the pandemic was driven by the virus rapid antigenic evolution and global spread, requiring continuous adaptation of immunization strategies to emerging variants, for WNV the necessity of vaccination is dictated by ecological expansion and the establishment of stable endemic transmission zones rather than by the emergence of novel immune-escape strains. Thus, while the SARS-CoV-2 pandemic underscored the challenges of dynamic vaccine design in the face of fast-evolving viruses, the WNV situation highlights the importance of proactive preparedness for geographically expanding, yet genetically stable, arboviruses.

Although the immunogenicity of the HHP-inactivated WNV candidate vaccine remains to be demonstrated in appropriate animal models, the preliminary data suggest that the high-pressure inactivation process can effectively preserve the structural integrity of critical surface antigens while ensuring complete loss of infectivity. Building upon the promising results obtained with the application of HHP technology to WNV, although it presented a greater inactivation challenge under HHP compared to SARS-CoV-2, it is reasonable to consider the broader potential of this approach for vaccine development against other arboviruses of public health relevance, supporting the translatability of the technology to other members of the *Flaviviridae* family, such as but not limited to Dengue virus, paving the way for the development of safe, effective, and rapidly deployable inactivated vaccines against a wide spectrum of arboviruses, thereby reinforcing the role of HHP as an emerging and flexible platform for vaccine production against vector-borne diseases.

The case of WNV underscores a broader paradigm applicable to arboviruses in general. The increasing frequency of localized outbreaks of imported arboviruses in

temperate regions of Europe demonstrates how climatic and environmental changes can create new niches for transmission, even in the absence of significant viral evolution. These pathogens, like WNV, depend on competent vectors whose distribution and seasonal activity are highly sensitive to temperature and humidity shifts. The establishment of *Aedes albopictus* and *Aedes aegypti* populations in Southern and Central Europe has already enabled sporadic autochthonous transmission of arboviruses traditionally restricted to tropical regions. The lessons derived from the WNV experience therefore extend beyond a single pathogen, emphasizing that the epidemiological landscape of vector-borne diseases is being reshaped more by environmental and anthropogenic factors than by intrinsic viral mutability.

This broader perspective redefines how vaccine prioritization and deployment should be approached in the context of emerging and re-emerging arboviruses. While SARS-CoV-2 demanded a reactive, variant-driven strategy with continual antigenic updates, WNV and similar arboviruses call for a preventive and geographically targeted approach. Vaccine development for these pathogens should focus on ensuring cross-lineage efficacy, long-term stability, and logistical feasibility for rapid deployment in areas experiencing new or re-emerging transmission. The concept of a "standing vaccine readiness", a platform capable of being quickly adapted or deployed as vector distributions shift, could prove essential for mitigating the public-health impact of arboviruses in a warming world.

In summary, the evolutionary and epidemiological trajectories of WNV and SARS-CoV-2 exemplify two distinct models of viral emergence and control. SARS-CoV-2 represents a paradigm of rapid genetic adaptability demanding continuous immunological and technological innovation. WNV, conversely, epitomizes ecological resilience within genetic constraint, a virus whose stability simplifies antigenic targeting but whose spread is increasingly fueled by environmental change. Consequently, while the urgency of COVID-19 vaccination was driven by the need to counteract viral evolution and maintain protective immunity, the imperative for WNV vaccination arises from the geographical expansion and ecological entrenchment of the virus. Extending this reasoning to other arboviruses, it becomes evident that global health preparedness must integrate both molecular surveillance and environmental monitoring. Addressing the twin challenges of viral evolution and ecological transformation will require complementary strategies: adaptive vaccine redesign for

rapidly mutating pathogens and proactive vaccine deployment for ecologically expanding yet genetically stable viruses such as WNV.

The climate-driven expansion of West Nile virus exemplifies a broader trend affecting numerous arboviruses whose transmission dynamics are increasingly shaped by environmental and anthropogenic factors. Within this global context, Dengue virus represents the most striking example of how such forces can amplify disease burden and challenge current preventive measures, including vaccination efforts.

In the context of Arboviruses, Dengue virus represents one of the most significant global public health threats among arboviruses. The World Health Organization estimates that approximately 390 million Dengue infections occur annually, of which nearly 100 million manifest clinically, and around 500.000 progress to severe forms such as Dengue hemorrhagic fever or Dengue shock syndrome, particularly in children and immunologically primed individuals[367]. In recent decades, the geographic distribution and incidence of Dengue have expanded dramatically, driven by urbanization, international travel, vector proliferation, and climate change, with an estimated 3.9 billion people at risk of infection[190,368]. This epidemiological burden underscores the urgent need for safe, effective, and widely accessible vaccines.

Current alarming global epidemiological situation has positioned Dengue as a major priority in the field of vector-borne disease research.

Despite extensive efforts, the development of a universally effective and safe Dengue vaccine remains elusive. Dengvaxia® (CYD, Chimeric Yellow fever Dengue) produced by Sanofi Pasteur, the first Dengue licensed vaccine, a live attenuated tetravalent chimeric vaccine based on the yellow fever 17D backbone, incorporating structural genes (encoding envelope [E] and membrane protein precursor [prM] proteins) from the four Dengue virus serotypes, has demonstrated limited efficacy and its use is restricted to individuals with prior Dengue exposure due to safety concerns in seronegative recipients[369,370]. In contrast, currently employed Qdenga® TAK-003) by Takeda GmbH, is a live attenuated tetravalent vaccine derived from a DENV-2 backbone, expressing structural proteins of all four serotypes, and has demonstrated favorable safety and efficacy profiles in both seropositive and seronegative individuals[371–373]. Despite its promising profile, Qdenga® presents several limitations that warrant consideration. Its efficacy is not uniformly distributed across all dengue virus serotypes, with reduced protection observed against DENV-3 and DENV-4 compared to DENV-2, the vaccine's backbone. The duration of immunity

beyond the initial years following vaccination remains uncertain[374]. Achieving balanced immunogenicity across all four serotypes while maintaining long-term safety and efficacy remains a major challenge. This underscores the critical need for next-generation vaccines that provide long-lasting, cross-serotype protection without increasing the risk of severe disease.

In this context, HHP technology presents a promising alternative platform for the production of inactivated Dengue vaccines. The production of a tetravalent Dengue vaccine using HHP inactivation may offer several operational and manufacturing advantages, eliciting a broad and balanced immune response against all four Dengue serotypes.

A whole-inactivated virus vaccine could theoretically reduce the risk of ADE primarily due to its ability to induce a broad and more balanced immune response. A whole-inactivated virus vaccine presents all structural proteins of the virus to the immune system, including the pre-membrane (prM) and envelope (E) proteins, which are the primary targets of the antibody response. This broad antigenic exposure can generate a more diverse repertoire of neutralizing antibodies against different proteins of all four Dengue serotypes, thereby decreasing the likelihood that a secondary infection with a heterologous serotype would be facilitated by ADE. In contrast, a vaccine designed to elicit a response against a single epitope, such as a specific region of the E protein, may generate antibodies that are only partially neutralizing. Suboptimal neutralization has been associated with ADE, particularly when antibodies bind but fail to prevent viral entry effectively.

Furthermore, while whole-inactivated virus vaccines primarily induce humoral immunity and may not elicit strong CD8+ T-cell responses, they can still activate CD4+ T-cell responses and immunological memory against multiple viral antigens. The broader antigenic stimulation provided by whole-inactivated virus vaccines may confer a higher potential for reducing ADE compared to mRNA vaccines targeting a single epitope. However, the efficacy of HHP as a new vaccine platform for Dengue ultimately depends on its ability to induce a well-balanced and sufficiently neutralizing immune response against all four Dengue serotypes, thereby enhancing cross-serotype protection and preventing partial immunity that could facilitate ADE.

All in all, the application of HHP to DENV has the potential to yield an inactivated vaccine with a favorable safety profile and preserved immunogenicity, potentially reducing the risk of ADE by maintaining antigen presentation that mimics the native

virion. Moreover, the HHP platform lends itself to rapid adaptation and scalability, which are critical features for addressing both endemic and epidemic Dengue scenarios, particularly in resource-limited settings. Thermostability of vaccines produced through HHP may, for its part, facilitate vaccine distribution in low-resource settings and underserved region of the World, where Dengue represents a primary threat for resident populations.

Given the increasing global incidence of Dengue, the limitations of current vaccine platforms, and the unpredictable dynamics of serotype circulation, the development of an HHP-based inactivated tetravalent Dengue vaccine is the next step of this research and could represent a transformative advance in HHP technology validation for inactivated vaccine production. By enabling the production of an effective, safer, potentially more broadly acceptable vaccine, HHP technology may contribute significantly to the global strategy for Dengue prevention and control.

Given all the above argumentations, expanding the scope of HHP application could lead to the development of a versatile, cost-effective platform for vaccine production that contributing to the development of vaccines targeting emerging infectious threats, addressing global disparities in vaccine access, thereby improving public health outcomes worldwide. Albeit HHP technology addresses many barriers to vaccine production, access, and distribution, it is not a standalone solution. While its modularity and scalability may help overcome several logistical and technical barriers, such as those related to cold-chain dependency, production bottlenecks, and reliance on pathogen-specific manufacturing facilities, these improvements operate within broader systemic and socio-political constraints that continue to hinder vaccine equity. Broader systemic issues, such as inadequate healthcare infrastructure, vaccine hesitancy, and geopolitical factors, must also be addressed to ensure equitable access to vaccines. The successful integration of HHP-based vaccines into existing immunization programs and public health frameworks can thus be achieved only through the synergistic interaction between technological innovation and systemic reform and will require coordinated efforts and sustained investment from governments, non-governmental organizations, and international stakeholders, ultimately ensuring that technological advances translate into tangible health benefits for all populations, irrespective of geographic or economic status.

In conclusion, the integration of innovative technologies such as HHP within the broader framework of vaccine research and production represents not only a scientific

advancement in addressing the global challenges of vaccine access and distribution but also a strategic opportunity to strengthen global health resilience and equity. By offering scalable, safe, and antigen-preserving inactivation of diverse pathogens, HHP technology addresses critical limitations in traditional vaccine manufacturing, enabling more flexible, rapid, and cost-effective responses to both endemic and emerging infectious diseases.

Crucially, the potential of HHP extends beyond the boundaries of human health, aligning closely with the principles of the One Health framework, which recognizes the interconnectedness of human, animal, and environmental health within a shared and dynamic ecosystem. The increasing frequency of emerging and re-emerging infectious diseases, including those caused by arboviruses such as West Nile virus, Dengue virus, and others, has underscored the extent to which anthropogenic activities, ecological disturbances, and climate change can disrupt the balance among species, facilitating viral spillover and sustained transmission across ecological barriers. In this context, HHP represents a promising technological innovation capable of supporting preventive and control measures across multiple domains of the One Health continuum.

Beyond its demonstrated efficacy in inactivating viral pathogens such as West Nile virus while preserving antigenic integrity, HHP possesses a broad versatility that renders it suitable for diverse applications, spanning from the development of human vaccines to the preparation of veterinary immunogens. This dual potential is particularly relevant when considering zoonotic agents maintained in animal reservoirs, such as birds, equines, and livestock, which often serve as amplification hosts for viruses with spillover capacity. Implementing HHP-based strategies in veterinary vaccine development could therefore contribute to the reduction of viral circulation in animal populations, mitigating the likelihood of zoonotic transmission to humans and aligning with the One Health vision of proactive, upstream intervention in the infection chain. Moreover, the technology's scalability and adaptability also allow for integration into existing biomanufacturing frameworks, both in high-resource and resource-limited settings, potentially supporting local vaccine production capacity. This aspect is particularly valuable in the context of global health equity, as it promotes decentralized vaccine manufacturing and enhances preparedness against regionally emerging pathogens whose spread may be exacerbated by climatic shifts and ecosystem changes.

Ultimately, integrating HHP technology into a One Health strategy embodies the type of multidisciplinary innovation required to confront 21st-century infectious disease challenges. By bridging human and veterinary vaccinology, improving biosafety, and supporting environmentally sustainable production, HHP offers a tangible pathway toward resilient, cross-sectoral health systems. In doing so, it contributes not only to mitigating the threat posed by West Nile virus and other arboviruses but also to reinforcing global preparedness against future zoonotic outbreaks, exemplifying the operationalization of the One Health concept through technological and translational innovation.

At a systemic level, embedding HHP-based production within global vaccine preparedness strategies could contribute to the creation of more equitable, decentralized, and responsive vaccine manufacturing networks. The technology's modularity and adaptability may contribute to reducing dependency on centralized manufacturing hubs, facilitating rapid vaccine deployment in regions affected by localized outbreaks. Such decentralization not only strengthens local capacity-building but also enhances global system resilience, promoting timely access to vaccines where they are needed most. However, achieving such transformative impact requires more than technological innovation alone, demanding coordinated efforts that extend beyond technological innovation alone, encompassing policy harmonization, international cooperation, and the development of shared frameworks for biosafety, regulation, and data exchange.

Ultimately, the promise of HHP technology lies not only in its demonstrated capacity to improve vaccine safety and efficacy but also in its potential to narrow the persistent gap between high- and low-income countries, fostering equitable access and strengthening resilience across health systems and ensuring more equitable access to life-saving immunizations. As the world continues to grapple with disparities in healthcare infrastructure, vaccine availability, and disease surveillance, particularly between high- and low-income regions, the scalability, affordability, and versatility of HHP-based platforms represent a tangible opportunity to narrow the persistent divide in immunization capacity. By enabling decentralized and safer vaccine production, HHP could empower regional manufacturing hubs, reduce dependency on centralized supply chains, and support more timely and context-specific responses to emerging and re-emerging infectious threats.

While continued research, optimization, and regulatory validation are essential to fully unlock the translational potential of HHP, its incorporation into a One Health-oriented and globally coordinated framework offers a compelling and forward-looking strategy to anticipate, prevent, and mitigate infectious disease threats. Within such a framework, the interconnection between human, animal, and environmental health becomes a guiding principle for innovation, ensuring that preventive measures address not only the biological dimensions of disease but also the ecological and socioeconomic contexts that shape their emergence. The ability of HHP to inactivate a wide spectrum of pathogens without compromising antigenic fidelity positions it as an enabling technology for both human and veterinary vaccine development, thus directly supporting upstream interventions that can reduce zoonotic spillover risks and strengthen collective health security.

In an era increasingly defined by the dual challenges of emerging pathogens and inequitable access to healthcare, technological innovations such as HHP will play a pivotal role in redefining preparedness and response strategies. The recent global experiences with pandemics have underscored that scientific excellence alone is insufficient unless paired with equitable implementation and international solidarity. Hence, integrating accessible, low-cost, and environmentally sustainable biotechnologies into global health agendas represents not merely a technical advancement but a moral imperative. Such integration will be fundamental for the construction of an inclusive and resilient health ecosystem, one capable of anticipating and countering infectious threats through collaboration, scientific innovation, and shared responsibility across nations and sectors.

The democratization of vaccine production through accessible and low-cost technologies embodies a paradigm shift in the philosophy of global health. It reflects a profound commitment to equity, sustainability, and collective resilience, values that must underpin the scientific enterprise in the 21st century. Within this paradigm, innovation is no longer conceived as a privilege of technologically advanced nations but as a shared global resource that can empower local communities, strengthen public health autonomy, and foster sustainable development. HHP thus represents more than a promising biotechnological tool; it stands as a symbol of how science, social justice, and ethical responsibility can converge to shape a more just and collaborative model of pandemic preparedness and public health governance.

In this vision, the future of vaccine development, and indeed, of infectious disease prevention, rests on the capacity of the global community to integrate technological progress with principles of fairness, cooperation, and environmental stewardship, reflecting a profound commitment to equity and resilience, exemplifying how scientific progress, social justice, and moral responsibility can converge to shape a more sustainable and inclusive model of pandemic preparedness and public health governance, ultimately redefining innovation as a shared instrument of resilience and global solidarity. The challenges ahead will undoubtedly require sustained investment, interdisciplinary collaboration, and adaptive policy frameworks. Yet, as the lessons of recent years have demonstrated, innovation that is guided by inclusivity and shared purpose can serve not only as an instrument of scientific progress but also as a foundation for global solidarity.

6. References

[1] S. Riedel, Edward Jenner and the History of Smallpox and Vaccination, Baylor University Medical Center Proceedings 18 (2005) 21–25. https://doi.org/10.1080/08998280.2005.11928028.

[2] D. Porter, Health, civilization, and the state: A history of public health from ancient to modern times, 1999.

[3] S. Plotkin, History of vaccination, Proceedings of the National Academy of Sciences 111 (2014) 12283–12287. https://doi.org/10.1073/pnas.1400472111.

[4] P. Debrè, Louis Pasteur, 1998.

[5] A.R. Hinman, State of immunity: The politics of vaccination in twentieth-century America, Journal of Clinical Investigation 117 (2007) 1118–1118. https://doi.org/10.1172/JCI32088.

[6] P.A. Offit, The Cutter Incident: How America's first polio vaccine led to a growing vaccine crisis, 2005.

[7] M. Cueto, The ORIGINS of Primary Health Care and SELECTIVE Primary Health Care, Am J Public Health 94 (2004) 1864–1874. https://doi.org/10.2105/AJPH.94.11.1864.

[8] P.J. Hotez, Blue marble health: An innovative plan to fight diseases of the poor amid wealth, 2016.

[9] World Health Organization, Expanded Programme on Immunization (EPI), Https://Www.Who.Int/Teams/Immunization-Vaccines-and-Biologicals/Expanded-Programme-on-Immunization (2022).

[10] J.R. Paul, A history of poliomyelitis, 1971.

[11] D.A. Henderson, Smallpox: The death of a disease, 2009.

[12] F., H.D.A., A.I., J.Z., & L.I.D. Fenner, Smallpox and its eradication, 1988.

[13] D.P. Fidler, SARS, governance and the globalization of disease, 2004.

[14] K.E. Jones, N.G. Patel, M.A. Levy, A. Storeygard, D. Balk, J.L. Gittleman, P. Daszak, Global trends in emerging infectious diseases, Nature 451 (2008) 990–993. https://doi.org/10.1038/nature06536.
[15] O.S. Levine, K.L. O'Brien, M. Knoll, R.A. Adegbola, S. Black, T. Cherian, R. Dagan, D. Goldblatt, A. Grange, B. Greenwood, T. Hennessy, K.P. Klugman, S.A. Madhi, K. Mulholland, H. Nohynek, M. Santosham, S.K. Saha, J.A. Scott, S. Sow, C.G. Whitney, F. Cutts, Pneumococcal vaccination in developing countries, The Lancet 367 (2006) 1880–1882. https://doi.org/10.1016/S0140-6736(06)68703-5.
[16] GAVI, Gavi, the Vaccine Alliance, Https://Www.Gavi.Org/ (2022).
[17] Z. Wang, F. Schmidt, Y. Weisblum, F. Muecksch, C.O. Barnes, S. Finkin, D. Schaefer-Babajew, M. Cipolla, C. Gaebler, J.A. Lieberman, T.Y. Oliveira, Z. Yang, M.E. Abernathy, K.E. Huey-Tubman, A. Hurley, M. Turroja, K.A. West, K. Gordon, K.G. Millard, V. Ramos, J. Da Silva, J. Xu, R.A. Colbert, R. Patel, J. Dizon, C. Unson-O'Brien, I. Shimeliovich, A. Gazumyan, M. Caskey, P.J. Bjorkman, R. Casellas, T. Hatziioannou, P.D. Bieniasz, M.C. Nussenzweig, mRNA vaccine-elicited antibodies to SARS-CoV-2 and circulating variants, Nature 592 (2021) 616–622. https://doi.org/10.1038/s41586-021-03324-6.
[18] A.D. Usher, A beautiful idea: how COVAX has fallen short, The Lancet 397 (2021) 2322–2325. https://doi.org/10.1016/S0140-6736(21)01367-2.
[19] O. Dyer, Covid-19: Countries are learning what others paid for vaccines, BMJ (2021) n281. https://doi.org/10.1136/bmj.n281.
[20] S. Szreter, The Population Health Approach in Historical Perspective, Am J Public Health 93 (2003) 421–431. https://doi.org/10.2105/AJPH.93.3.421.
[21] P.D. Minor, Live attenuated vaccines: Historical successes and current challenges, Virology 479–480 (2015) 379–392. https://doi.org/10.1016/j.virol.2015.03.032.
[22] M.M.J. Cox, Y. Hashimoto, A fast track influenza virus vaccine produced in insect cells, J Invertebr Pathol 107 (2011) S31–S41. https://doi.org/10.1016/j.jip.2011.05.003.
[23] N. Pica, P. Palese, Toward a Universal Influenza Virus Vaccine: Prospects and Challenges, Annu Rev Med 64 (2013) 189–202. https://doi.org/10.1146/annurev-med-120611-145115.
[24] I.R. Humphreys, S. Sebastian, Novel viral vectors in infectious diseases, Immunology 153 (2018) 1–9. https://doi.org/10.1111/imm.12829.
[25] J. Sadoff, G. Gray, A. Vandebosch, V. Cárdenas, G. Shukarev, B. Grinsztejn, P.A. Goepfert, C. Truyers, H. Fennema, B. Spiessens, K. Offergeld, G. Scheper, K.L. Taylor, M.L. Robb, J. Treanor, D.H. Barouch, J. Stoddard, M.F. Ryser, M.A. Marovich, K.M. Neuzil, L. Corey, N. Cauwenberghs, T. Tanner, K. Hardt, J. Ruiz-Guiñazú, M. Le Gars, H. Schuitemaker, J. Van Hoof, F. Struyf, M. Douoguih, Safety and Efficacy of Single-Dose Ad26.COV2.S Vaccine against Covid-19, New England Journal of Medicine 384 (2021) 2187–2201. https://doi.org/10.1056/NEJMoa2101544.
[26] M.D. Knoll, C. Wonodi, Oxford–AstraZeneca COVID-19 vaccine efficacy, The Lancet 397 (2021) 72–74. https://doi.org/10.1016/S0140-6736(20)32623-4.
[27] H.C. Ertl, Viral vectors as vaccine carriers, Curr Opin Virol 21 (2016) 1–8. https://doi.org/10.1016/j.coviro.2016.06.001.

[28] M. Olbert, A. Römer-Oberdörfer, C. Herden, S. Malberg, S. Runge, P. Staeheli, D. Rubbenstroth, Viral vector vaccines expressing nucleoprotein and phosphoprotein genes of avian bornaviruses ameliorate homologous challenge infections in cockatiels and common canaries, Sci Rep 6 (2016) 36840. https://doi.org/10.1038/srep36840.

[29] T. Ura, K. Okuda, M. Shimada, Developments in Viral Vector-Based Vaccines, Vaccines (Basel) 2 (2014) 624–641. https://doi.org/10.3390/vaccines2030624.

[30] C. García-Montero, O. Fraile-Martínez, C. Bravo, D. Torres-Carranza, L. Sanchez-Trujillo, A.M. Gómez-Lahoz, L.G. Guijarro, N. García-Honduvilla, A. Asúnsolo, J. Bujan, J. Monserrat, E. Serrano, M. Álvarez-Mon, J.A. De León-Luis, M.A. Álvarez-Mon, M.A. Ortega, An Updated Review of SARS-CoV-2 Vaccines and the Importance of Effective Vaccination Programs in Pandemic Times, Vaccines (Basel) 9 (2021) 433. https://doi.org/10.3390/vaccines9050433.

[31] M. Voysey, S.A.C. Clemens, S.A. Madhi, L.Y. Weckx, P.M. Folegatti, P.K. Aley, B. Angus, V.L. Baillie, S.L. Barnabas, Q.E. Bhorat, S. Bibi, C. Briner, P. Cicconi, A.M. Collins, R. Colin-Jones, C.L. Cutland, T.C. Darton, K. Dheda, C.J.A. Duncan, K.R.W. Emary, K.J. Ewer, L. Fairlie, S.N. Faust, S. Feng, D.M. Ferreira, A. Finn, A.L. Goodman, C.M. Green, C.A. Green, P.T. Heath, C. Hill, H. Hill, I. Hirsch, S.H.C. Hodgson, A. Izu, S. Jackson, D. Jenkin, C.C.D. Joe, S. Kerridge, A. Koen, G. Kwatra, R. Lazarus, A.M. Lawrie, A. Lelliott, V. Libri, P.J. Lillie, R. Mallory, A.V.A. Mendes, E.P. Milan, A.M. Minassian, A. McGregor, H. Morrison, Y.F. Mujadidi, A. Nana, P.J. O'Reilly, S.D. Padayachee, A. Pittella, E. Plested, K.M. Pollock, M.N. Ramasamy, S. Rhead, A. V Schwarzbold, N. Singh, A. Smith, R. Song, M.D. Snape, E. Sprinz, R.K. Sutherland, R. Tarrant, E.C. Thomson, M.E. Török, M. Toshner, D.P.J. Turner, J. Vekemans, T.L. Villafana, M.E.E. Watson, C.J. Williams, A.D. Douglas, A.V.S. Hill, T. Lambe, S.C. Gilbert, A.J. Pollard, M. Aban, F. Abayomi, K. Abeyskera, J. Aboagye, M. Adam, K. Adams, J. Adamson, Y.A. Adelaja, G. Adewetan, S. Adlou, K. Ahmed, Y. Akhalwaya, S. Akhalwaya, A. Alcock, A. Ali, E.R. Allen, L. Allen, T.C.D.S.C. Almeida, M.P.S. Alves, F. Amorim, F. Andritsou, R. Anslow, M. Appleby, E.H. Arbe-Barnes, M.P. Ariaans, B. Arns, L. Arruda, P. Azi, L. Azi, G. Babbage, C. Bailey, K.F. Baker, M. Baker, N. Baker, P. Baker, L. Baldwin, I. Baleanu, D. Bandeira, A. Bara, M.A.S. Barbosa, D. Barker, G.D. Barlow, E. Barnes, A.S. Barr, J.R. Barrett, J. Barrett, L. Bates, A. Batten, K. Beadon, E. Beales, R. Beckley, S. Belij-Rammerstorfer, J. Bell, D. Bellamy, N. Bellei, S. Belton, A. Berg, L. Bermejo, E. Berrie, L. Berry, D. Berzenyi, A. Beveridge, K.R. Bewley, H. Bexhell, S. Bhikha, A.E. Bhorat, Z.E. Bhorat, E. Bijker, G. Birch, S. Birch, A. Bird, O. Bird, K. Bisnauthsing, M. Bittaye, K. Blackstone, L. Blackwell, H. Bletchly, C.L. Blundell, S.R. Blundell, P. Bodalia, B.C. Boettger, E. Bolam, E. Boland, D. Bormans, N. Borthwick, F. Bowring, A. Boyd, P. Bradley, T. Brenner, P. Brown, C. Brown, C. Brown-O'Sullivan, S. Bruce, E. Brunt, R. Buchan, W. Budd, Y.A. Bulbulia, M. Bull, J. Burbage, H. Burhan, A. Burn, K.R. Buttigieg, N. Byard, I. Cabera Puig, G. Calderon, A. Calvert, S. Camara, M. Cao, F. Cappuccini, J.R. Cardoso, M. Carr, M.W. Carroll, A. Carson-Stevens, Y. de M. Carvalho, J.A.M. Carvalho, H.R. Casey, P. Cashen, T. Castro, L.C. Castro, K. Cathie, A. Cavey, J. Cerbino-Neto, J. Chadwick, D. Chapman, S. Charlton, I. Chelysheva, O. Chester, S. Chita, J.-S.

Cho, L. Cifuentes, E. Clark, M. Clark, A. Clarke, E.A. Clutterbuck, S.L.K. Collins, C.P. Conlon, S. Connarty, N. Coombes, C. Cooper, R. Cooper, L. Cornelissen, T. Corrah, C. Cosgrove, T. Cox, W.E.M. Crocker, S. Crosbie, L. Cullen, D. Cullen, D.R.M.F. Cunha, C. Cunningham, F.C. Cuthbertson, S.N.F. Da Guarda, L.P. da Silva, B.E. Damratoski, Z. Danos, M.T.D.C. Dantas, P. Darroch, M.S. Datoo, C. Datta, M. Davids, S.L. Davies, H. Davies, E. Davis, J. Davis, J. Davis, M.M.D. De Nobrega, L.M. De Oliveira Kalid, D. Dearlove, T. Demissie, A. Desai, S. Di Marco, C. Di Maso, M.I.S. Dinelli, T. Dinesh, C. Docksey, C. Dold, T. Dong, F.R. Donnellan, T. Dos Santos, T.G. dos Santos, E.P. Dos Santos, N. Douglas, C. Downing, J. Drake, R. Drake-Brockman, K. Driver, R. Drury, S.J. Dunachie, B.S. Durham, L. Dutra, N.J.W. Easom, S. van Eck, M. Edwards, N.J. Edwards, O.M. El Muhanna, S.C. Elias, M. Elmore, M. English, A. Esmail, Y.M. Essack, E. Farmer, M. Farooq, M. Farrar, L. Farrugia, B. Faulkner, S. Fedosyuk, S. Felle, S. Feng, C. Ferreira Da Silva, S. Field, R. Fisher, A. Flaxman, J. Fletcher, H. Fofie, H. Fok, K.J. Ford, J. Fowler, P.H.A. Fraiman, E. Francis, M.M. Franco, J. Frater, M.S.M. Freire, S.H. Fry, S. Fudge, J. Furze, M. Fuskova, P. Galian-Rubio, E. Galiza, H. Garlant, M. Gavrila, A. Geddes, K.A. Gibbons, C. Gilbride, H. Gill, S. Glynn, K. Godwin, K. Gokani, U.C. Goldoni, M. Goncalves, I.G.S. Gonzalez, J. Goodwin, A. Goondiwala, K. Gordon-Quayle, G. Gorini, J. Grab, L. Gracie, M. Greenland, N. Greenwood, J. Greffrath, M.M. Groenewald, L. Grossi, G. Gupta, M. Hackett, B. Hallis, M. Hamaluba, E. Hamilton, J. Hamlyn, D. Hammersley, A.T. Hanrath, B. Hanumunthadu, S.A. Harris, C. Harris, T. Harris, T.D. Harrison, D. Harrison, T.C. Hart, B. Hartnell, S. Hassan, J. Haughney, S. Hawkins, J. Hay, I. Head, J. Henry, M. Hermosin Herrera, D.B. Hettle, J. Hill, G. Hodges, E. Horne, M.M. Hou, C. Houlihan, E. Howe, N. Howell, J. Humphreys, H.E. Humphries, K. Hurley, C. Huson, A. Hyder-Wright, C. Hyams, S. Ikram, A. Ishwarbhai, M. Ivan, P. Iveson, V. Iyer, F. Jackson, J. De Jager, S. Jaumdally, H. Jeffers, N. Jesudason, B. Jones, K. Jones, E. Jones, C. Jones, M.R. Jorge, A. Jose, A. Joshi, E.A.M.S. Júnior, J. Kadziola, R. Kailath, F. Kana, K. Karampatsas, M. Kasanyinga, J. Keen, E.J. Kelly, D.M. Kelly, D. Kelly, S. Kelly, D. Kerr, R. de Á. Kfouri, L. Khan, B. Khozoee, S. Kidd, A. Killen, J. Kinch, P. Kinch, L.D.W. King, T.B. King, L. Kingham, P. Klenerman, F. Knapper, J.C. Knight, D. Knott, S. Koleva, M. Lang, G. Lang, C.W. Larkworthy, J.P.J. Larwood, R. Law, E.M. Lazarus, A. Leach, E.A. Lees, N.-M. Lemm, A. Lessa, S. Leung, Y. Li, A.M. Lias, K. Liatsikos, A. Linder, S. Lipworth, S. Liu, X. Liu, A. Lloyd, S. Lloyd, L. Loew, R. Lopez Ramon, L. Lora, V. Lowthorpe, K. Luz, J.C. MacDonald, G. MacGregor, M. Madhavan, D.O. Mainwaring, E. Makambwa, R. Makinson, M. Malahleha, R. Malamatsho, G. Mallett, K. Mansatta, T. Maoko, K. Mapetla, N.G. Marchevsky, S. Marinou, E. Marlow, G.N. Marques, P. Marriott, R.P. Marshall, J.L. Marshall, F.J. Martins, M. Masenya, M. Masilela, S.K. Masters, M. Mathew, H. Matlebjane, K. Matshidiso, O. Mazur, A. Mazzella, H. McCaughan, J. McEwan, J. McGlashan, L. McInroy, Z. McIntyre, D. McLenaghan, N. McRobert, S. McSwiggan, C. Megson, S. Mehdipour, W. Meijs, R.N.Á. Mendonça, A.J. Mentzer, N. Mirtorabi, C. Mitton, S. Mnyakeni, F. Moghaddas, K. Molapo, M. Moloi, M. Moore, M.I. Moraes-Pinto, M. Moran, E. Morey, R. Morgans, S. Morris, S. Morris, H.C. Morris, F. Morselli, G. Morshead, R. Morter, L. Mottal, A. Moultrie, N. Moya, M.

Mpelembue, S. Msomi, Y. Mugodi, E. Mukhopadhyay, J. Muller, A. Munro, C. Munro, S. Murphy, P. Mweu, C.H. Myasaki, G. Naik, K. Naker, E. Nastouli, A. Nazir, B. Ndlovu, F. Neffa, C. Njenga, H. Noal, A. Noé, G. Novaes, F.L. Nugent, G. Nunes, K. O'Brien, D. O'Connor, M. Odam, S. Oelofse, B. Oguti, V. Olchawski, N.J. Oldfield, M.G. Oliveira, C. Oliveira, A. Oosthuizen, P. O'Reilly, P. Osborne, D.R.J. Owen, L. Owen, D. Owens, N. Owino, M. Pacurar, B.V.B. Paiva, E.M.F. Palhares, S. Palmer, S. Parkinson, H.M.R.T. Parracho, K. Parsons, D. Patel, B. Patel, F. Patel, K. Patel, M. Patrick-Smith, R.O. Payne, Y. Peng, E.J. Penn, A. Pennington, M.P. Peralta Alvarez, J. Perring, N. Perry, R. Perumal, S. Petkar, T. Philip, D.J. Phillips, J. Phillips, M.K. Phohu, L. Pickup, S. Pieterse, J. Piper, D. Pipini, M. Plank, J. Du Plessis, S. Pollard, J. Pooley, A. Pooran, I. Poulton, C. Powers, F.B. Presa, D.A. Price, V. Price, M. Primeira, P.C. Proud, S. Provstgaard-Morys, S. Pueschel, D. Pulido, S. Quaid, R. Rabara, A. Radford, K. Radia, D. Rajapaska, T. Rajeswaran, A.S.F. Ramos, F. Ramos Lopez, T. Rampling, J. Rand, H. Ratcliffe, T. Rawlinson, D. Rea, B. Rees, J. Reiné, M. Resuello-Dauti, E. Reyes Pabon, C.M. Ribiero, M. Ricamara, A. Richter, N. Ritchie, A.J. Ritchie, A.J. Robbins, H. Roberts, R.E. Robinson, H. Robinson, T.T. Rocchetti, B.P. Rocha, S. Roche, C. Rollier, L. Rose, A.L. Ross Russell, L. Rossouw, S. Royal, I. Rudiansyah, S. Ruiz, S. Saich, C. Sala, J. Sale, A.M. Salman, N. Salvador, S. Salvador, M. Sampaio, A.D. Samson, A. Sanchez-Gonzalez, H. Sanders, K. Sanders, E. Santos, M.F.S. Santos Guerra, I. Satti, J.E. Saunders, C. Saunders, A. Sayed, I. Schim van der Loeff, A.B. Schmid, E. Schofield, G. Screaton, S. Seddiqi, R.R. Segireddy, R. Senger, S. Serrano, R. Shah, I. Shaik, H.E. Sharpe, K. Sharrocks, R. Shaw, A. Shea, A. Shepherd, J.G. Shepherd, F. Shiham, E. Sidhom, S.E. Silk, A.C. da Silva Moraes, G. Silva-Junior, L. Silva-Reyes, A.D. Silveira, M.B.V. Silveira, J. Sinha, D.T. Skelly, D.C. Smith, N. Smith, H.E. Smith, D.J. Smith, C.C. Smith, A. Soares, T. Soares, C. Solórzano, G.L. Sorio, K. Sorley, T. Sosa-Rodriguez, C.M.C.D.L. Souza, B.S.D.F. Souza, A.R. Souza, A.J. Spencer, F. Spina, L. Spoors, L. Stafford, I. Stamford, I. Starinskij, R. Stein, J. Steven, L. Stockdale, L. V. Stockwell, L.H. Strickland, A.C. Stuart, A. Sturdy, N. Sutton, A. Szigeti, A. Tahiri-Alaoui, R. Tanner, C. Taoushanis, A.W. Tarr, K. Taylor, U. Taylor, I.J. Taylor, J. Taylor, R. te Water Naude, Y. Themistocleous, A. Themistocleous, M. Thomas, K. Thomas, T.M. Thomas, A. Thombrayil, F. Thompson, A. Thompson, K. Thompson, A. Thompson, J. Thomson, V. Thornton-Jones, P.J. Tighe, L.A. Tinoco, G. Tiongson, B. Tladinyane, M. Tomasicchio, A. Tomic, S. Tonks, J. Towner, N. Tran, J. Tree, G. Trillana, C. Trinham, R. Trivett, A. Truby, B.L. Tsheko, A. Turabi, R. Turner, C. Turner, M. Ulaszewska, B.R. Underwood, R. Varughese, D. Verbart, M. Verheul, I. Vichos, T. Vieira, C.S. Waddington, L. Walker, E. Wallis, M. Wand, D. Warbick, T. Wardell, G. Warimwe, S.C. Warren, B. Watkins, E. Watson, S. Webb, A. Webb-Bridges, A. Webster, J. Welch, J. Wells, A. West, C. White, R. White, P. Williams, R.L. Williams, R. Winslow, M. Woodyer, A.T. Worth, D. Wright, M. Wroblewska, A. Yao, R. Zimmer, D. Zizi, P. Zuidewind, Safety and efficacy of the ChAdOx1 nCoV-19 vaccine (AZD1222) against SARS-CoV-2: an interim analysis of four randomised controlled trials in Brazil, South Africa, and the UK, The Lancet 397 (2021) 99–111. https://doi.org/10.1016/S0140-6736(20)32661-1.

[32] P. Richmond, L. Hatchuel, M. Dong, B. Ma, B. Hu, I. Smolenov, P. Li, P. Liang, H.H. Han, J. Liang, R. Clemens, Safety and immunogenicity of S-Trimer (SCB-2019), a protein subunit vaccine candidate for COVID-19 in healthy adults: a phase 1, randomised, double-blind, placebo-controlled trial, The Lancet 397 (2021) 682–694. https://doi.org/10.1016/S0140-6736(21)00241-5.

[33] T.K. Tan, P. Rijal, R. Rahikainen, A.H. Keeble, L. Schimanski, S. Hussain, R. Harvey, J.W.P. Hayes, J.C. Edwards, R.K. McLean, V. Martini, M. Pedrera, N. Thakur, C. Conceicao, I. Dietrich, H. Shelton, A. Ludi, G. Wilsden, C. Browning, A.K. Zagrajek, D. Bialy, S. Bhat, P. Stevenson-Leggett, P. Hollinghurst, M. Tully, K. Moffat, C. Chiu, R. Waters, A. Gray, M. Azhar, V. Mioulet, J. Newman, A.S. Asfor, A. Burman, S. Crossley, J.A. Hammond, E. Tchilian, B. Charleston, D. Bailey, T.J. Tuthill, S.P. Graham, H.M.E. Duyvesteyn, T. Malinauskas, J. Huo, J.A. Tree, K.R. Buttigieg, R.J. Owens, M.W. Carroll, R.S. Daniels, J.W. McCauley, D.I. Stuart, K.-Y.A. Huang, M. Howarth, A.R. Townsend, A COVID-19 vaccine candidate using SpyCatcher multimerization of the SARS-CoV-2 spike protein receptor-binding domain induces potent neutralising antibody responses, Nat Commun 12 (2021) 542. https://doi.org/10.1038/s41467-020-20654-7.

[34] X. Ding, D. Liu, G. Booth, W. Gao, Y. Lu, Virus-Like Particle Engineering: From Rational Design to Versatile Applications, Biotechnol J 13 (2018). https://doi.org/10.1002/biot.201700324.

[35] L.H.L. Lua, N.K. Connors, F. Sainsbury, Y.P. Chuan, N. Wibowo, A.P.J. Middelberg, Bioengineering virus-like particles as vaccines, Biotechnol Bioeng 111 (2014) 425–440. https://doi.org/10.1002/bit.25159.

[36] A. Roldão, M.C.M. Mellado, L.R. Castilho, M.J. Carrondo, P.M. Alves, Virus-like particles in vaccine development, Expert Rev Vaccines 9 (2010) 1149–1176. https://doi.org/10.1586/erv.10.115.

[37] B. V. Syomin, Y. V. Ilyin, Virus-Like Particles as an Instrument of Vaccine Production, Mol Biol 53 (2019) 323–334. https://doi.org/10.1134/S0026893319030154.

[38] V. Cimica, J.M. Galarza, Adjuvant formulations for virus-like particle (VLP) based vaccines, Clinical Immunology 183 (2017) 99–108. https://doi.org/10.1016/j.clim.2017.08.004.

[39] M.O. Mohsen, L. Zha, G. Cabral-Miranda, M.F. Bachmann, Major findings and recent advances in virus–like particle (VLP)-based vaccines, Semin Immunol 34 (2017) 123–132. https://doi.org/10.1016/j.smim.2017.08.014.

[40] H. Swann, A. Sharma, B. Preece, A. Peterson, C. Eldredge, D.M. Belnap, M. Vershinin, S. Saffarian, Minimal system for assembly of SARS-CoV-2 virus like particles, Sci Rep 10 (2020) 21877. https://doi.org/10.1038/s41598-020-78656-w.

[41] R. Xu, M. Shi, J. Li, P. Song, N. Li, Construction of SARS-CoV-2 Virus-Like Particles by Mammalian Expression System, Front Bioeng Biotechnol 8 (2020). https://doi.org/10.3389/fbioe.2020.00862.

[42] H. Garg, T. Mehmetoglu-Gurbuz, A. Joshi, Virus Like Particles (VLP) as multivalent vaccine candidate against Chikungunya, Japanese Encephalitis, Yellow Fever and Zika Virus, Sci Rep 10 (2020) 4017. https://doi.org/10.1038/s41598-020-61103-1.

[43] R. Verbeke, I. Lentacker, S.C. De Smedt, H. Dewitte, Three decades of messenger RNA vaccine development, Nano Today 28 (2019) 100766. https://doi.org/10.1016/j.nantod.2019.100766.
[44] I. Tombácz, D. Weissman, N. Pardi, Vaccination with Messenger RNA: A Promising Alternative to DNA Vaccination, in: 2021: pp. 13–31. https://doi.org/10.1007/978-1-0716-0872-2_2.
[45] C. V. Gould, J.E. Staples, C.Y.-H. Huang, A.C. Brault, R.J. Nett, Combating West Nile Virus Disease — Time to Revisit Vaccination, New England Journal of Medicine 388 (2023) 1633–1636. https://doi.org/10.1056/NEJMp2301816.
[46] N. Principi, S. Esposito, Development of Vaccines against Emerging Mosquito-Vectored Arbovirus Infections, Vaccines (Basel) 12 (2024) 87. https://doi.org/10.3390/vaccines12010087.
[47] F.P. Polack, S.J. Thomas, N. Kitchin, J. Absalon, A. Gurtman, S. Lockhart, J.L. Perez, G. Pérez Marc, E.D. Moreira, C. Zerbini, R. Bailey, K.A. Swanson, S. Roychoudhury, K. Koury, P. Li, W. V. Kalina, D. Cooper, R.W. Frenck, L.L. Hammitt, Ö. Türeci, H. Nell, A. Schaefer, S. Ünal, D.B. Tresnan, S. Mather, P.R. Dormitzer, U. Şahin, K.U. Jansen, W.C. Gruber, Safety and Efficacy of the BNT162b2 mRNA Covid-19 Vaccine, New England Journal of Medicine 383 (2020) 2603–2615. https://doi.org/10.1056/NEJMoa2034577.
[48] L.A. Jackson, E.J. Anderson, N.G. Rouphael, P.C. Roberts, M. Makhene, R.N. Coler, M.P. McCullough, J.D. Chappell, M.R. Denison, L.J. Stevens, A.J. Pruijssers, A. McDermott, B. Flach, N.A. Doria-Rose, K.S. Corbett, K.M. Morabito, S. O'Dell, S.D. Schmidt, P.A. Swanson, M. Padilla, J.R. Mascola, K.M. Neuzil, H. Bennett, W. Sun, E. Peters, M. Makowski, J. Albert, K. Cross, W. Buchanan, R. Pikaart-Tautges, J.E. Ledgerwood, B.S. Graham, J.H. Beigel, An mRNA Vaccine against SARS-CoV-2 — Preliminary Report, New England Journal of Medicine 383 (2020) 1920–1931. https://doi.org/10.1056/NEJMoa2022483.
[49] N. Pardi, M.J. Hogan, F.W. Porter, D. Weissman, mRNA vaccines — a new era in vaccinology, Nat Rev Drug Discov 17 (2018) 261–279. https://doi.org/10.1038/nrd.2017.243.
[50] C. García-Montero, O. Fraile-Martínez, C. Bravo, D. Torres-Carranza, L. Sanchez-Trujillo, A.M. Gómez-Lahoz, L.G. Guijarro, N. García-Honduvilla, A. Asúnsolo, J. Bujan, J. Monserrat, E. Serrano, M. Álvarez-Mon, J.A. De León-Luis, M.A. Álvarez-Mon, M.A. Ortega, An Updated Review of SARS-CoV-2 Vaccines and the Importance of Effective Vaccination Programs in Pandemic Times, Vaccines (Basel) 9 (2021) 433. https://doi.org/10.3390/vaccines9050433.
[51] K. Goyal, H. Goel, P. Baranwal, A. Tewary, A. Dixit, A.K. Pandey, M. Benjamin, P. Tanwar, A. Dey, F. Khan, P. Pandey, P.K. Gupta, D. Kumar, S. Roychoudhury, N.K. Jha, T.K. Upadhyay, K.K. Kesari, Immunological Mechanisms of Vaccine-Induced Protection against SARS-CoV-2 in Humans, Immuno 1 (2021) 442–456. https://doi.org/10.3390/immuno1040032.
[52] E. Dolgin, The tangled history of mRNA vaccines, Nature 597 (2021) 318–324. https://doi.org/10.1038/d41586-021-02483-w.
[53] K. V. Kalnin, T. Plitnik, M. Kishko, J. Zhang, D. Zhang, A. Beauvais, N.G. Anosova, T. Tibbitts, J. DiNapoli, G. Ulinski, P. Piepenhagen, S.M. Cummings,

D.S. Bangari, S. Ryan, P.-W.D. Huang, J. Huleatt, D. Vincent, K. Fries, S. Karve, R. Goldman, H. Gopani, A. Dias, K. Tran, M. Zacharia, X. Gu, L. Boeglin, J. Abysalh, J. Vargas, A. Beaulieu, M. Shah, T. Jeannotte, K. Gillis, S. Chivukula, R. Swearingen, V. Landolfi, T.-M. Fu, F. DeRosa, D. Casimiro, Immunogenicity and efficacy of mRNA COVID-19 vaccine MRT5500 in preclinical animal models, NPJ Vaccines 6 (2021) 61. https://doi.org/10.1038/s41541-021-00324-5.

[54] L.R. Baden, H.M. El Sahly, B. Essink, K. Kotloff, S. Frey, R. Novak, D. Diemert, S.A. Spector, N. Rouphael, C.B. Creech, J. McGettigan, S. Khetan, N. Segall, J. Solis, A. Brosz, C. Fierro, H. Schwartz, K. Neuzil, L. Corey, P. Gilbert, H. Janes, D. Follmann, M. Marovich, J. Mascola, L. Polakowski, J. Ledgerwood, B.S. Graham, H. Bennett, R. Pajon, C. Knightly, B. Leav, W. Deng, H. Zhou, S. Han, M. Ivarsson, J. Miller, T. Zaks, Efficacy and Safety of the mRNA-1273 SARS-CoV-2 Vaccine, New England Journal of Medicine 384 (2021) 403–416. https://doi.org/10.1056/NEJMoa2035389.

[55] A.I. Francis, S. Ghany, T. Gilkes, S. Umakanthan, Review of COVID-19 vaccine subtypes, efficacy and geographical distributions, Postgrad Med J 98 (2022) 389–394. https://doi.org/10.1136/postgradmedj-2021-140654.

[56] Md.M. Rahman, Md.H.U. Masum, S. Wajed, A. Talukder, A comprehensive review on COVID-19 vaccines: development, effectiveness, adverse effects, distribution and challenges, Virusdisease 33 (2022) 1–22. https://doi.org/10.1007/s13337-022-00755-1.

[57] C.M. Trombetta, E. Montomoli, Influenza immunology evaluation and correlates of protection: a focus on vaccines, Expert Rev Vaccines 15 (2016) 967–976. https://doi.org/10.1586/14760584.2016.1164046.

[58] D.H. Barouch, Covid-19 Vaccines — Immunity, Variants, Boosters, New England Journal of Medicine 387 (2022) 1011–1020. https://doi.org/10.1056/NEJMra2206573.

[59] S. Moni, S. Abdelwahab, A. Jabeen, M. Elmobark, D. Aqaili, G. Gohal, B. Oraibi, A. Farasani, A. Jerah, M. Alnajai, A. Mohammad Alowayni, Advancements in Vaccine Adjuvants: The Journey from Alum to Nano Formulations, Vaccines (Basel) 11 (2023) 1704. https://doi.org/10.3390/vaccines11111704.

[60] S. Elveborg, V. Monteil, A. Mirazimi, Methods of Inactivation of Highly Pathogenic Viruses for Molecular, Serology or Vaccine Development Purposes, Pathogens 11 (2022) 271. https://doi.org/10.3390/pathogens11020271.

[61] J.M. Tracy, D.G. Glass, M.J. Nicholson, H. Pivnick, Preservatives for Poliomyelitis (Salk) Vaccine II, J Pharm Sci 53 (1964) 659–663. https://doi.org/10.1002/jps.2600530618.

[62] T. Wilton, G. Dunn, D. Eastwood, P.D. Minor, J. Martin, Effect of Formaldehyde Inactivation on Poliovirus, J Virol 88 (2014) 11955–11964. https://doi.org/10.1128/JVI.01809-14.

[63] C. Herzog, K. Van Herck, P. Van Damme, Hepatitis A vaccination and its immunological and epidemiological long-term effects – a review of the evidence, Hum Vaccin Immunother 17 (2021) 1496–1519. https://doi.org/10.1080/21645515.2020.1819742.

[64] E. Olayan, M. El-Khadragy, A.F. Mohamed, A.K. Mohamed, R.I. Shebl, H.M. Yehia, Evaluation of Different Stabilizers and Inactivating Compounds for the

Enhancement of Vero Cell Rabies Vaccine Stability and Immunogenicity: *In Vitro* Study, Biomed Res Int 2019 (2019) 1–9. https://doi.org/10.1155/2019/4518163.
[65] T.J. Wiktor, H.G. Aaslestad, M.M. Kaplan, Immunogenicity of Rabies Virus Inactivated by β-Propiolactone, Acetylethyleneimine, and Ionizing Irradiation, Appl Microbiol 23 (1972) 914–918. https://doi.org/10.1128/am.23.5.914-918.1972.
[66] L.A. Grohskopf, L.H. Blanton, J.M. Ferdinands, J.R. Chung, K.R. Broder, H.K. Talbot, R.L. Morgan, A.M. Fry, Prevention and Control of Seasonal Influenza with Vaccines: Recommendations of the Advisory Committee on Immunization Practices — United States, 2022–23 Influenza Season, MMWR. Recommendations and Reports 71 (2022) 1–28. https://doi.org/10.15585/mmwr.rr7101a1.
[67] G. Di Mario, B. Garulli, E. Sciaraffia, M. Facchini, I. Donatelli, M.R. Castrucci, A heat-inactivated H7N3 vaccine induces cross-reactive cellular immunity in HLA-A2.1 transgenic mice, Virol J 13 (2016) 56. https://doi.org/10.1186/s12985-016-0513-7.
[68] N. Yang, A. Garcia, C. Meyer, T. Tuschl, T. Merghoub, J.D. Wolchok, L. Deng, Heat-inactivated modified vaccinia virus Ankara boosts Th1 cellular and humoral immunity as a vaccine adjuvant, NPJ Vaccines 7 (2022) 120. https://doi.org/10.1038/s41541-022-00542-5.
[69] A. V. Gracheva, E.R. Korchevaya, Yu.I. Ammour, D.I. Smirnova, O.S. Sokolova, G.S. Glukhov, A. V. Moiseenko, I. V. Zubarev, R. V. Samoilikov, I.A. Leneva, O.A. Svitich, V. V. Zverev, E.B. Faizuloev, Immunogenic properties of SARS-CoV-2 inactivated by ultraviolet light, Arch Virol 167 (2022) 2181–2191. https://doi.org/10.1007/s00705-022-05530-7.
[70] A. Vrablikova, M. Fojtikova, R. Hezova, P. Simeckova, V. Brezani, N. Strakova, M. Fraiberk, J. Kotoucek, J. Masek, I. Psikal, UV-C irradiation as an effective tool for sterilization of porcine chimeric VP1-PCV2bCap recombinant vaccine, Sci Rep 13 (2023) 19337. https://doi.org/10.1038/s41598-023-46791-9.
[71] S.S. Bhatia, S.D. Pillai, Ionizing Radiation Technologies for Vaccine Development - A Mini Review, Front Immunol 13 (2022). https://doi.org/10.3389/fimmu.2022.845514.
[72] R.D. Turan, C. Tastan, D. Dilek Kancagi, B. Yurtsever, G. Sir Karakus, S. Ozer, S. Abanuz, D. Cakirsoy, G. Tumentemur, S. Demir, U. Seyis, R. Kuzay, M. Elek, M.E. Kocaoglu, G. Ertop, S. Arbak, M. Acikel Elmas, C. Hemsinlioglu, O. Hatirnaz Ng, S. Akyoney, I. Sahin, C.K. Kayhan, F. Tokat, G. Akpinar, M. Kasap, A.S. Kocagoz, U. Ozbek, D. Telci, F. Sahin, K. Yalcin, S. Ratip, U. Ince, E. Ovali, Gamma-irradiated SARS-CoV-2 vaccine candidate, OZG-38.61.3, confers protection from SARS-CoV-2 challenge in human ACEII-transgenic mice, Sci Rep 11 (2021) 15799. https://doi.org/10.1038/s41598-021-95086-4.
[73] R. Rappuoli, C.W. Mandl, S. Black, E. De Gregorio, Vaccines for the twenty-first century society, Nat Rev Immunol 11 (2011) 865–872. https://doi.org/10.1038/nri3085.
[74] I.J. Amanna, M.K. Slifka, Contributions of humoral and cellular immunity to vaccine-induced protection in humans, Virology 411 (2011) 206–215. https://doi.org/10.1016/j.virol.2010.12.016.

[75] C.A., T.P., W.M., et al. Janeway, Immunobiology: The Immune System in Health and Disease, 2020.
[76] S.A., O.W.A., O.P.A., & E.K.M. Plotkin, Plotkin's Vaccines , 2017.
[77] N. Le Bert, A.T. Tan, K. Kunasegaran, C.Y.L. Tham, M. Hafezi, A. Chia, M.H.Y. Chng, M. Lin, N. Tan, M. Linster, W.N. Chia, M.I.-C. Chen, L.-F. Wang, E.E. Ooi, S. Kalimuddin, P.A. Tambyah, J.G.-H. Low, Y.-J. Tan, A. Bertoletti, SARS-CoV-2-specific T cell immunity in cases of COVID-19 and SARS, and uninfected controls, Nature 584 (2020) 457–462. https://doi.org/10.1038/s41586-020-2550-z.
[78] F. Sallusto, J. Geginat, A. Lanzavecchia, Central Memory and Effector Memory T Cell Subsets: Function, Generation, and Maintenance, Annu Rev Immunol 22 (2004) 745–763. https://doi.org/10.1146/annurev.immunol.22.012703.104702.
[79] Y. Chen, C. Hu, Z. Wang, J. Su, S. Wang, B. Li, X. Liu, Z. Yuan, D. Li, H. Wang, B. Zhu, Y. Shao, Immunity Induced by Inactivated SARS-CoV-2 Vaccine: Breadth, Durability, Potency, and Specificity in a Healthcare Worker Cohort, Pathogens 12 (2023) 1254. https://doi.org/10.3390/pathogens12101254.
[80] S. Feng, D.J. Phillips, T. White, H. Sayal, P.K. Aley, S. Bibi, C. Dold, M. Fuskova, S.C. Gilbert, I. Hirsch, H.E. Humphries, B. Jepson, E.J. Kelly, E. Plested, K. Shoemaker, K.M. Thomas, J. Vekemans, T.L. Villafana, T. Lambe, A.J. Pollard, M. Voysey, S. Adlou, L. Allen, B. Angus, R. Anslow, M.-C. Asselin, N. Baker, P. Baker, T. Barlow, A. Beveridge, K.R. Bewley, P. Brown, E. Brunt, K.R. Buttigieg, S. Camara, S. Charlton, E. Chiplin, P. Cicconi, E.A. Clutterbuck, A.M. Collins, N.S. Coombes, S.A.C. Clemens, M. Davison, T. Demissie, T. Dinesh, A.D. Douglas, C.J.A. Duncan, K.R.W. Emary, K.J. Ewer, S. Felle, D.M. Ferreira, A. Finn, P.M. Folegatti, R. Fothergill, S. Fraser, H. Garlant, L. Gatcombe, K.J. Godwin, A.L. Goodman, C.A. Green, B. Hallis, T.C. Hart, P.T. Heath, H. Hill, A.V.S. Hill, D. Jenkin, M. Kasanyinga, S. Kerridge, C. Knight, S. Leung, V. Libri, P.J. Lillie, S. Marinou, J. McGlashan, A.C. McGregor, L. McInroy, A.M. Minassian, Y.F. Mujadidi, E.J. Penn, C.J. Petropoulos, K.M. Pollock, P.C. Proud, S. Provstgaard-Morys, D. Rajapaska, M.N. Ramasamy, K. Sanders, I. Shaik, N. Singh, A. Smith, M.D. Snape, R. Song, S. Shrestha, R.K. Sutherland, E.C. Thomson, D.P.J. Turner, A. Webb-Bridges, T. Wrin, C.J. Williams, Correlates of protection against symptomatic and asymptomatic SARS-CoV-2 infection, Nat Med 27 (2021) 2032–2040. https://doi.org/10.1038/s41591-021-01540-1.
[81] J.M.E. Lim, S.K. Hang, S. Hariharaputran, A. Chia, N. Tan, E.S. Lee, E. Chng, P.L. Lim, B.E. Young, D.C. Lye, N. Le Bert, A. Bertoletti, A.T. Tan, A comparative characterization of SARS-CoV-2-specific T cells induced by mRNA or inactive virus COVID-19 vaccines, Cell Rep Med 3 (2022) 100793. https://doi.org/10.1016/j.xcrm.2022.100793.
[82] W.E. Matchett, V. Joag, J.M. Stolley, F.K. Shepherd, C.F. Quarnstrom, C.K. Mickelson, S. Wijeyesinghe, A.G. Soerens, S. Becker, J.M. Thiede, E. Weyu, S.D. O'Flanagan, J.A. Walter, M.N. Vu, V.D. Menachery, T.D. Bold, V. Vezys, M.K. Jenkins, R.A. Langlois, D. Masopust, Cutting Edge: Nucleocapsid Vaccine Elicits Spike-Independent SARS-CoV-2 Protective Immunity, The Journal of Immunology 207 (2021) 376–379. https://doi.org/10.4049/jimmunol.2100421.

[83] J. Chen, Y. Deng, B. Huang, D. Han, W. Wang, M. Huang, C. Zhai, Z. Zhao, R. Yang, Y. Zhao, W. Wang, D. Zhai, W. Tan, DNA Vaccines Expressing the Envelope and Membrane Proteins Provide Partial Protection Against SARS-CoV-2 in Mice, Front Immunol 13 (2022). https://doi.org/10.3389/fimmu.2022.827605.

[84] R. Bastola, G. Noh, T. Keum, S. Bashyal, J.-E. Seo, J. Choi, Y. Oh, Y. Cho, S. Lee, Vaccine adjuvants: smart components to boost the immune system, Arch Pharm Res 40 (2017) 1238–1248. https://doi.org/10.1007/s12272-017-0969-z.

[85] S.M. Kaech, E.J. Wherry, R. Ahmed, Effector and memory T-cell differentiation: implications for vaccine development, Nat Rev Immunol 2 (2002) 251–262. https://doi.org/10.1038/nri778.

[86] E. Hammarlund, M.W. Lewis, S.G. Hansen, L.I. Strelow, J.A. Nelson, G.J. Sexton, J.M. Hanifin, M.K. Slifka, Duration of antiviral immunity after smallpox vaccination, Nat Med 9 (2003) 1131–1137. https://doi.org/10.1038/nm917.

[87] Y. Peng, A.J. Mentzer, G. Liu, X. Yao, Z. Yin, D. Dong, W. Dejnirattisai, T. Rostron, P. Supasa, C. Liu, C. López-Camacho, J. Slon-Campos, Y. Zhao, D.I. Stuart, G.C. Paesen, J.M. Grimes, A.A. Antson, O.W. Bayfield, D.E.D.P. Hawkins, D.-S. Ker, B. Wang, L. Turtle, K. Subramaniam, P. Thomson, P. Zhang, C. Dold, J. Ratcliff, P. Simmonds, T. de Silva, P. Sopp, D. Wellington, U. Rajapaksa, Y.-L. Chen, M. Salio, G. Napolitani, W. Paes, P. Borrow, B.M. Kessler, J.W. Fry, N.F. Schwabe, M.G. Semple, J.K. Baillie, S.C. Moore, P.J.M. Openshaw, M.A. Ansari, S. Dunachie, E. Barnes, J. Frater, G. Kerr, P. Goulder, T. Lockett, R. Levin, Y. Zhang, R. Jing, L.-P. Ho, E. Barnes, D. Dong, T. Dong, S. Dunachie, J. Frater, P. Goulder, G. Kerr, P. Klenerman, G. Liu, A. McMichael, G. Napolitani, G. Ogg, Y. Peng, M. Salio, X. Yao, Z. Yin, J. Kenneth Baillie, P. Klenerman, A.J. Mentzer, S.C. Moore, P.J.M. Openshaw, M.G. Semple, D.I. Stuart, L. Turtle, R.J. Cornall, C.P. Conlon, P. Klenerman, G.R. Screaton, J. Mongkolsapaya, A. McMichael, J.C. Knight, G. Ogg, T. Dong, Broad and strong memory CD4+ and CD8+ T cells induced by SARS-CoV-2 in UK convalescent individuals following COVID-19, Nat Immunol 21 (2020) 1336–1345. https://doi.org/10.1038/s41590-020-0782-6.

[88] O. Kew, V. Morris-Glasgow, M. Landaverde, C. Burns, J. Shaw, Z. Garib, J. Andreś, E. Blackman, C.J. Freeman, J. Jorba, R. Sutter, G. Tambini, L. Venczel, C. Pedreira, F. Laender, H. Shimizu, T. Yoneyama, T. Miyamura, H. van der Avoort, M.S. Oberste, D. Kilpatrick, S. Cochi, M. Pallansch, C. de Quadros, Outbreak of Poliomyelitis in Hispaniola Associated with Circulating Type 1 Vaccine-Derived Poliovirus, Science (1979) 296 (2002) 356–359. https://doi.org/10.1126/science.1068284.

[89] World Health Organization, Polio vaccines: WHO position paper, Https://Www.Who.Int/Teams/Immunization-Vaccines-and-Biologicals/Policies/Position-Papers/Polio (2022).

[90] P. Van Damme, K. Van Herck, A review of the long-term protection after hepatitis A and B vaccination, Travel Med Infect Dis 5 (2007) 79–84. https://doi.org/10.1016/j.tmaid.2006.04.004.

[91] K.L. Dubischar, V. Kadlecek, B. Sablan, C.F. Borja-Tabora, S. Gatchalian, S. Eder-Lingelbach, S. Kiermayr, M. Spruth, K. Westritschnig, Immunogenicity of the Inactivated Japanese Encephalitis Virus Vaccine IXIARO in Children From a

Japanese Encephalitis Virus-endemic Region, Pediatric Infectious Disease Journal 36 (2017) 898–904. https://doi.org/10.1097/INF.0000000000001615.
[92] N. Zhu, D. Zhang, W. Wang, X. Li, B. Yang, J. Song, X. Zhao, B. Huang, W. Shi, R. Lu, P. Niu, F. Zhan, X. Ma, D. Wang, W. Xu, G. Wu, G.F. Gao, W. Tan, A Novel Coronavirus from Patients with Pneumonia in China, 2019, New England Journal of Medicine 382 (2020) 727–733. https://doi.org/10.1056/nejmoa2001017.
[93] P. Zhou, X. Lou Yang, X.G. Wang, B. Hu, L. Zhang, W. Zhang, H.R. Si, Y. Zhu, B. Li, C.L. Huang, H.D. Chen, J. Chen, Y. Luo, H. Guo, R. Di Jiang, M.Q. Liu, Y. Chen, X.R. Shen, X. Wang, X.S. Zheng, K. Zhao, Q.J. Chen, F. Deng, L.L. Liu, B. Yan, F.X. Zhan, Y.Y. Wang, G.F. Xiao, Z.L. Shi, A pneumonia outbreak associated with a new coronavirus of probable bat origin, Nature 579 (2020) 270–273. https://doi.org/10.1038/s41586-020-2012-7.
[94] F. Wu, S. Zhao, B. Yu, Y.M. Chen, W. Wang, Z.G. Song, Y. Hu, Z.W. Tao, J.H. Tian, Y.Y. Pei, M.L. Yuan, Y.L. Zhang, F.H. Dai, Y. Liu, Q.M. Wang, J.J. Zheng, L. Xu, E.C. Holmes, Y.Z. Zhang, A new coronavirus associated with human respiratory disease in China, Nature 579 (2020) 265–269. https://doi.org/10.1038/s41586-020-2008-3.
[95] R. Lu, X. Zhao, J. Li, P. Niu, B. Yang, H. Wu, W. Wang, H. Song, B. Huang, N. Zhu, Y. Bi, X. Ma, F. Zhan, L. Wang, T. Hu, H. Zhou, Z. Hu, W. Zhou, L. Zhao, J. Chen, Y. Meng, J. Wang, Y. Lin, J. Yuan, Z. Xie, J. Ma, W.J. Liu, D. Wang, W. Xu, E.C. Holmes, G.F. Gao, G. Wu, W. Chen, W. Shi, W. Tan, Genomic characterisation and epidemiology of 2019 novel coronavirus: implications for virus origins and receptor binding, The Lancet 395 (2020) 565–574. https://doi.org/10.1016/S0140-6736(20)30251-8.
[96] E. De Wit, N. Van Doremalen, D. Falzarano, V.J. Munster, SARS and MERS: Recent insights into emerging coronaviruses, Nat Rev Microbiol 14 (2016) 523–534. https://doi.org/10.1038/nrmicro.2016.81.
[97] J. Cui, F. Li, Z.L. Shi, Origin and evolution of pathogenic coronaviruses, Nat Rev Microbiol 17 (2019) 181–192. https://doi.org/10.1038/s41579-018-0118-9.
[98] C. Huang, Y. Wang, X. Li, L. Ren, J. Zhao, Y. Hu, L. Zhang, G. Fan, J. Xu, X. Gu, Z. Cheng, T. Yu, J. Xia, Y. Wei, W. Wu, X. Xie, W. Yin, H. Li, M. Liu, Y. Xiao, H. Gao, L. Guo, J. Xie, G. Wang, R. Jiang, Z. Gao, Q. Jin, J. Wang, B. Cao, Clinical features of patients infected with 2019 novel coronavirus in Wuhan, China, The Lancet 395 (2020) 497–506. https://doi.org/10.1016/S0140-6736(20)30183-5.
[99] N. Chen, M. Zhou, X. Dong, J. Qu, F. Gong, Y. Han, Y. Qiu, J. Wang, Y. Liu, Y. Wei, J. Xia, T. Yu, X. Zhang, L. Zhang, Epidemiological and clinical characteristics of 99 cases of 2019 novel coronavirus pneumonia in Wuhan, China: a descriptive study, The Lancet 395 (2020) 507–513. https://doi.org/10.1016/S0140-6736(20)30211-7.
[100] Y. Guan, B.J. Zheng, Y.Q. He, X.L. Liu, Z.X. Zhuang, C.L. Cheung, S.W. Luo, P.H. Li, L.J. Zhang, Y.J. Guan, K.M. Butt, K.L. Wong, K.W. Chan, W. Lim, K.F. Shortridge, K.Y. Yuen, J.S.M. Peiris, L.L.M. Poon, Isolation and characterization of viruses related to the SARS coronavirus from animals in Southern China, Science (1979) 302 (2003) 276–278. https://doi.org/10.1126/science.1087139.

[101] W. Li, Z. Shi, M. Yu, W. Ren, C. Smith, J.H. Epstein, H. Wang, G. Crameri, Z. Hu, H. Zhang, J. Zhang, J. McEachern, H. Field, P. Daszak, B.T. Eaton, S. Zhang, L.F. Wang, Bats are natural reservoirs of SARS-like coronaviruses, Science (1979) 310 (2005) 676–679. https://doi.org/10.1126/science.1118391.
[102] W. Li, S.-K. Wong, F. Li, J.H. Kuhn, I.-C. Huang, H. Choe, M. Farzan, Animal Origins of the Severe Acute Respiratory Syndrome Coronavirus: Insight from ACE2-S-Protein Interactions, J Virol 80 (2006) 4211–4219. https://doi.org/10.1128/jvi.80.9.4211-4219.2006.
[103] M. Bolles, E. Donaldson, R. Baric, SARS-CoV and emergent coronaviruses: Viral determinants of interspecies transmission, Curr Opin Virol 1 (2011) 624–634. https://doi.org/10.1016/j.coviro.2011.10.012.
[104] J.F.W. Chan, K.K.W. To, H. Chen, K.Y. Yuen, Interspecies transmission and emergence of novel viruses: lessons from bats and birds, Trends Microbiol 21 (2013) 544–55. https://doi.org/10.1016/j.tim.2013.05.005.
[105] H.A. Rothan, S.N. Byrareddy, The epidemiology and pathogenesis of coronavirus disease (COVID-19) outbreak, J Autoimmun 109 (2020) 102433. https://doi.org/10.1016/j.jaut.2020.102433.
[106] Z. Zhu, X. Lian, X. Su, W. Wu, G. Marraro, Y. Zeng, From SARS and MERS to COVID-19: a brief summary and comparison of severe acute respiratory infections caused by three highly pathogenic human coronaviruses, Respir Res 21 (2020) 224. https://doi.org/10.1186/s12931-020-01479-w.
[107] 28th 2020]. https://covid19.who.int/. World Health Organization. Coronavirus disease (COVID-2019) dashboard [cited January, No Title, (n.d.).
[108] R. Sarker, A.S.M. Roknuzzaman, Nazmunnahar, M. Shahriar, Md.J. Hossain, Md.R. Islam, The WHO has declared the end of pandemic phase of COVID-19: Way to come back in the normal life, Health Sci Rep 6 (2023). https://doi.org/10.1002/hsr2.1544.
[109] X. Ou, Y. Liu, X. Lei, P. Li, D. Mi, L. Ren, L. Guo, R. Guo, T. Chen, J. Hu, Z. Xiang, Z. Mu, X. Chen, J. Chen, K. Hu, Q. Jin, J. Wang, Z. Qian, Characterization of spike glycoprotein of SARS-CoV-2 on virus entry and its immune cross-reactivity with SARS-CoV, Nat Commun 11 (2020). https://doi.org/10.1038/s41467-020-15562-9.
[110] L. Piccoli, Y.J. Park, M.A. Tortorici, N. Czudnochowski, A.C. Walls, M. Beltramello, C. Silacci-Fregni, D. Pinto, L.E. Rosen, J.E. Bowen, O.J. Acton, S. Jaconi, B. Guarino, A. Minola, F. Zatta, N. Sprugasci, J. Bassi, A. Peter, A. De Marco, J.C. Nix, F. Mele, S. Jovic, B.F. Rodriguez, S. V. Gupta, F. Jin, G. Piumatti, G. Lo Presti, A.F. Pellanda, M. Biggiogero, M. Tarkowski, M.S. Pizzuto, E. Cameroni, C. Havenar-Daughton, M. Smithey, D. Hong, V. Lepori, E. Albanese, A. Ceschi, E. Bernasconi, L. Elzi, P. Ferrari, C. Garzoni, A. Riva, G. Snell, F. Sallusto, K. Fink, H.W. Virgin, A. Lanzavecchia, D. Corti, D. Veesler, Mapping Neutralizing and Immunodominant Sites on the SARS-CoV-2 Spike Receptor-Binding Domain by Structure-Guided High-Resolution Serology, Cell 183 (2020) 1024-1042.e21. https://doi.org/10.1016/j.cell.2020.09.037.
[111] Coronaviridae study group of the International Commitee on Taxonomy, The species Severe acute respiratory syndrome-related coronavirus: classifying 2019-nCoV and naming it SARS- CoV-2, Nat. Microbiol 5 (2020) 536–44.

[112] V.M. Corman, D. Muth, D. Niemeyer, C. Drosten, Hosts and Sources of Endemic Human Coronaviruses, Adv Virus Res 100 (2018) 163–88. https://doi.org/10.1016/bs.aivir.2018.01.001.
[113] P. V'kovski, A. Kratzel, S. Steiner, H. Stalder, V. Thiel, Coronavirus biology and replication: implications for SARS-CoV-2, Nat Rev Microbiol 19 (2021) 155–170. https://doi.org/10.1038/s41579-020-00468-6.
[114] A. Fehr, S. Perlman, Coronaviruses: An Overview of Their Replication and Pathogenesis, Methods Mol Biol 1282 (2015) 1–23. https://doi.org/10.1007/978-1-4939-2438-7.
[115] A.E. Gorbalenya, L. Enjuanes, J. Ziebuhr, E.J. Snijder, Nidovirales: Evolving the largest RNA virus genome, Virus Res 117 (2006) 17–37. https://doi.org/10.1016/j.virusres.2006.01.017.
[116] P.S. Masters, The Molecular Biology of Coronaviruses, Adv Virus Res 65 (2006) 193–292. https://doi.org/10.1016/S0065-3527(06)66005-3.
[117] D. Liu, T. Fung, K. Chong, A. Shukla, R. Hilgenfeld, Accessory proteins of SARS-CoV and other coronaviruses, Antiviral Res 109 (2014) 97–109. https://doi.org/10.1016/j.antiviral.2014.06.013.
[118] A.C. Walls, Y.-J. Park, M.A. Tortorici, A. Wall, A.T. McGuire, D. Veesler, Structure, Function, and Antigenicity of the SARS-CoV-2 Spike Glycoprotein, Cell 181 (2020) 281-292.e6. https://doi.org/10.1016/j.cell.2020.02.058.
[119] F. Li, Structure, Function, and Evolution of Coronavirus Spike Proteins, Annu Rev Virol 3 (2016) 237–261. https://doi.org/10.1146/annurev-virology-110615-042301.Structure.
[120] M. Letko, A. Marzi, V. Munster, Functional assessment of cell entry and receptor usage for SARS-CoV-2 and other lineage B betacoronaviruses, Nat Microbiol 5 (2020) 562–69. https://doi.org/10.1038/s41564-020-0688-y.
[121] A.C. Walls, Y. Park, M.A. Tortorici, A. Wall, A.T. Mcguire, D. Veesler, A.C. Walls, Y. Park, M.A. Tortorici, A. Wall, A.T. Mcguire, Structure, function, and antigenicity of the SARS-CoV-2 Spike Glycoprotein, Cell 181 (2020) 281-292.e6. https://doi.org/10.1016/j.cell.2020.02.058.
[122] M.A. Tortorici, D. Veesler, Structural insights into coronavirus entry, Adv Virus Res 105 (2020) 93–116. https://doi.org/10.1016/bs.aivir.2019.08.002.
[123] E. Hartenian, D. Nandakumar, A. Lari, M. Ly, J.M. Tucker, B.A. Glaunsinger, The molecular virology of coronaviruses, Journal of Biological Chemistry 295 (2020) 12910–34. https://doi.org/10.1074/jbc.REV120.013930.
[124] D. Wrapp, N. Wang, K.S. Corbett, J.A. Goldsmith, C.L. Hsieh, O. Abiona, B.S. Graham, J.S. McLellan, Cryo-EM structure of the 2019-nCoV spike in the prefusion conformation, Science (1979) 367 (2020) 1260–1263. https://doi.org/10.1126/science.abb2507.
[125] J. Shang, G. Ye, K. Shi, Y. Wan, C. Luo, H. Aihara, Q. Geng, A. Auerbach, F. Li, Structural basis of receptor recognition by SARS-CoV-2, Nature 581 (2020) 221–4. https://doi.org/10.1038/s41586-020-2179-y.
[126] J. Shang, Y. Wan, C. Luo, G. Ye, Q. Geng, A. Auerbach, F. Li, Cell entry mechanisms of SARS-CoV-2, PNAS 117 (2020) 11727–34. https://doi.org/10.1073/pnas.2003138117.

[127] Y. Yuan, D. Cao, Y. Zhang, J. Ma, J. Qi, Q. Wang, G. Lu, Y. Wu, J. Yan, Y. Shi, X. Zhang, G.F. Gao, Cryo-EM structures of MERS-CoV and SARS-CoV spike glycoproteins reveal the dynamic receptor binding domains, Nat Commun 8 (2017) 15092. https://doi.org/10.1038/ncomms15092.
[128] M. Gui, W. Song, H. Zhou, J. Xu, S. Chen, Y. Xiang, X. Wang, Cryo-electron microscopy structures of the SARS-CoV spike glycoprotein reveal a prerequisite conformational state for receptor binding, Cell Res 27 (2017) 119–129. https://doi.org/10.1038/cr.2016.152.
[129] P. Kwong, M. Doyle, D. Casper, C. Cicala, S. Leavitt, S. Majeed, T. Steenbeke, M. Venturi, I. Chaiken, M. Fung, H. Katinger, P. Parren, J. Robinson, D. Van Ryk, L. Wang, D. Burton, E. Freire, R. Wyatt, J. Sodroski, W. Hendrickson, J. Arthos, HIV-1 evades antibody-mediated neutralization through conformational masking of receptor-binding sites, Nature 420 (2002) 678–82. https://doi.org/10.1038/nature01188.
[130] M. Grossman, The canyon hypothesis. Hiding the host cell receptor attachment site on a viral surface from immune surveillance, J Biol Chem 264 (1989) 14587–90.
[131] Y. Cao, B. Su, X. Guo, W. Sun, Y. Deng, L. Bao, Q. Zhu, X. Zhang, Y. Zheng, C. Geng, X. Chai, R. He, X. Li, Q. Lv, H. Zhu, W. Deng, Y. Xu, Y. Wang, L. Qiao, Y. Tan, L. Song, G. Wang, X. Du, N. Gao, J. Liu, J. Xiao, X. Su, Z. Du, Y. Feng, C. Qin, C. Qin, R. Jin, X. Xie, Potent neutralizing antibodies against SARS-CoV-2 identified by high-throughput single-cell sequencing of convalescent patients' B cells, Cell 182 (2020) 73–84. https://doi.org/10.1016/j.cell.2020.05.025.
[132] T. Rogers, F. Zhao, D. Huang, N. Beutler, A. Burns, W. He, O. Limbo, C. Smith, G. Song, J. Woehl, L. Yang, R.K. Abbott, S. Callaghan, E. Garcia, J. Hurtado, M. Parren, L. Peng, S. Ramirez, J. Ricketts, M.J. Ricciardi, S.A. Rawlings, N.C. Wu, M. Yuan, D.M. Smith, D. Nemazee, J.R. Teijaro, J.E. Voss, I.A. Wilson, R. Andrabi, B. Briney, E. Landais, D. Sok, Isolation of potent SARS-CoV-2 neutralizing antibodies and protection from disease in a small animal model, Science (1979) 963 (2020) 956–963. https://doi.org/10.1126/science.abc7520.
[133] Y. Watanabe, J.D. Allen, D. Wrapp, J.S. McLellan, M. Crispin, Site-specific glycan analysis of the SARS-CoV-2 spike, Science (1979) 369 (2020) 330–333. https://doi.org/10.1126/science.abb9983.
[134] L. Piccoli, Y.-J. Park, M.A. Tortorici, N. Czudnochowski, A.C. Walls, M. Beltramello, C. Silacci-Fregni, D. Pinto, L.E. Rosen, J.E. Bowen, O.J. Acton, S. Jaconi, B. Guarino, A. Minola, F. Zatta, N. Sprugasci, J. Bassi, A. Peter, A. De Marco, J.C. Nix, F. Mele, S. Jovic, B.F. Rodriguez, S. V. Gupta, F. Jin, G. Piumatti, G. Lo Presti, A.F. Pellanda, M. Biggiogero, M. Tarkowski, M.S. Pizzuto, E. Cameroni, C. Havenar-Daughton, M. Smithey, D. Hong, V. Lepori, E. Albanese, A. Ceschi, E. Bernasconi, L. Elzi, P. Ferrari, C. Garzoni, A. Riva, G. Snell, F. Sallusto, K. Fink, H.W. Virgin, A. Lanzavecchia, D. Corti, D. Veesler, Mapping Neutralizing and Immunodominant Sites on the SARS-CoV-2 Spike Receptor-Binding Domain by Structure-Guided High-Resolution Serology, Cell 183 (2020) 1024-1042.e21. https://doi.org/10.1016/j.cell.2020.09.037.
[135] A. Grifoni, D. Weiskopf, S.I. Ramirez, J. Mateus, J.M. Dan, C.R. Moderbacher, S.A. Rawlings, A. Sutherland, L. Premkumar, R.S. Jadi, D. Marrama, A.M. de

Silva, A. Frazier, A.F. Carlin, J.A. Greenbaum, B. Peters, F. Krammer, D.M. Smith, S. Crotty, A. Sette, Targets of T Cell Responses to SARS-CoV-2 Coronavirus in Humans with COVID-19 Disease and Unexposed Individuals, Cell 181 (2020) 1489-1501.e15. https://doi.org/10.1016/j.cell.2020.05.015.

[136] T. Sekine, A. Perez-Potti, O. Rivera-Ballesteros, K. Strålin, J.-B. Gorin, A. Olsson, S. Llewellyn-Lacey, H. Kamal, G. Bogdanovic, S. Muschiol, D.J. Wullimann, T. Kammann, J. Emgård, T. Parrot, E. Folkesson, O. Rooyackers, L.I. Eriksson, J.-I. Henter, A. Sönnerborg, T. Allander, J. Albert, M. Nielsen, J. Klingström, S. Gredmark-Russ, N.K. Björkström, J.K. Sandberg, D.A. Price, H.-G. Ljunggren, S. Aleman, M. Buggert, M. Akber, L. Berglin, H. Bergsten, S. Brighenti, D. Brownlie, M. Butrym, B. Chambers, P. Chen, M.C. Jeannin, J. Grip, A.C. Gomez, L. Dillner, I.D. Lozano, M. Dzidic, M.F. Tullberg, A. Färnert, H. Glans, A. Haroun-Izquierdo, E. Henriksson, L. Hertwig, S. Kalsum, E. Kokkinou, E. Kvedaraite, M. Loreti, M. Lourda, K. Maleki, K.-J. Malmberg, N. Marquardt, C. Maucourant, J. Michaelsson, J. Mjösberg, K. Moll, J. Muva, J. Mårtensson, P. Nauclér, A. Norrby-Teglund, L.P. Medina, B. Persson, L. Radler, E. Ringqvist, J.T. Sandberg, E. Sohlberg, T. Soini, M. Svensson, J. Tynell, R. Varnaite, A. Von Kries, C. Unge, Robust T Cell Immunity in Convalescent Individuals with Asymptomatic or Mild COVID-19, Cell 183 (2020) 158-168.e14. https://doi.org/10.1016/j.cell.2020.08.017.

[137] A.T. Tan, M. Linster, C.W. Tan, N. Le Bert, W.N. Chia, K. Kunasegaran, Y. Zhuang, C.Y.L. Tham, A. Chia, G.J.D. Smith, B. Young, S. Kalimuddin, J.G.H. Low, D. Lye, L.-F. Wang, A. Bertoletti, Early induction of functional SARS-CoV-2-specific T cells associates with rapid viral clearance and mild disease in COVID-19 patients, Cell Rep 34 (2021) 108728. https://doi.org/10.1016/j.celrep.2021.108728.

[138] A. Tarke, J. Sidney, C.K. Kidd, J.M. Dan, S.I. Ramirez, E.D. Yu, J. Mateus, R. da Silva Antunes, E. Moore, P. Rubiro, N. Methot, E. Phillips, S. Mallal, A. Frazier, S.A. Rawlings, J.A. Greenbaum, B. Peters, D.M. Smith, S. Crotty, D. Weiskopf, A. Grifoni, A. Sette, Comprehensive analysis of T cell immunodominance and immunoprevalence of SARS-CoV-2 epitopes in COVID-19 cases, Cell Rep Med 2 (2021) 100204. https://doi.org/10.1016/j.xcrm.2021.100204.

[139] K.W. Cohen, S.L. Linderman, Z. Moodie, J. Czartoski, L. Lai, G. Mantus, C. Norwood, L.E. Nyhoff, V.V. Edara, K. Floyd, S.C. De Rosa, H. Ahmed, R. Whaley, S.N. Patel, B. Prigmore, M.P. Lemos, C.W. Davis, S. Furth, J.B. O'Keefe, M.P. Gharpure, S. Gunisetty, K. Stephens, R. Antia, V.I. Zarnitsyna, D.S. Stephens, S. Edupuganti, N. Rouphael, E.J. Anderson, A.K. Mehta, J. Wrammert, M.S. Suthar, R. Ahmed, M.J. McElrath, Longitudinal analysis shows durable and broad immune memory after SARS-CoV-2 infection with persisting antibody responses and memory B and T cells, Cell Rep Med 2 (2021) 100354. https://doi.org/10.1016/j.xcrm.2021.100354.

[140] A. Tarke, C.H. Coelho, Z. Zhang, J.M. Dan, E.D. Yu, N. Methot, N.I. Bloom, B. Goodwin, E. Phillips, S. Mallal, J. Sidney, G. Filaci, D. Weiskopf, R. da Silva Antunes, S. Crotty, A. Grifoni, A. Sette, SARS-CoV-2 vaccination induces immunological T cell memory able to cross-recognize variants from Alpha to

Omicron, Cell 185 (2022) 847-859.e11. https://doi.org/10.1016/j.cell.2022.01.015.
[141] Y. Gao, C. Cai, A. Grifoni, T.R. Müller, J. Niessl, A. Olofsson, M. Humbert, L. Hansson, A. Österborg, P. Bergman, P. Chen, A. Olsson, J.K. Sandberg, D. Weiskopf, D.A. Price, H.-G. Ljunggren, A.C. Karlsson, A. Sette, S. Aleman, M. Buggert, Ancestral SARS-CoV-2-specific T cells cross-recognize the Omicron variant, Nat Med 28 (2022) 472–476. https://doi.org/10.1038/s41591-022-01700-x.
[142] R. Keeton, M.B. Tincho, A. Ngomti, R. Baguma, N. Benede, A. Suzuki, K. Khan, S. Cele, M. Bernstein, F. Karim, S. V. Madzorera, T. Moyo-Gwete, M. Mennen, S. Skelem, M. Adriaanse, D. Mutithu, O. Aremu, C. Stek, E. du Bruyn, M.A. Van Der Mescht, Z. de Beer, T.R. de Villiers, A. Bodenstein, G. van den Berg, A. Mendes, A. Strydom, M. Venter, J. Giandhari, Y. Naidoo, S. Pillay, H. Tegally, A. Grifoni, D. Weiskopf, A. Sette, R.J. Wilkinson, T. de Oliveira, L.-G. Bekker, G. Gray, V. Ueckermann, T. Rossouw, M.T. Boswell, J.N. Bhiman, P.L. Moore, A. Sigal, N.A.B. Ntusi, W.A. Burgers, C. Riou, T cell responses to SARS-CoV-2 spike cross-recognize Omicron, Nature 603 (2022) 488–492. https://doi.org/10.1038/s41586-022-04460-3.
[143] W. Dejnirattisai, D. Zhou, H.M. Ginn, H.M.E. Duyvesteyn, P. Supasa, J.B. Case, Y. Zhao, T.S. Walter, A.J. Mentzer, C. Liu, B. Wang, G.C. Paesen, J. Slon-Campos, C. López-Camacho, N.M. Kafai, A.L. Bailey, R.E. Chen, B. Ying, C. Thompson, J. Bolton, A. Fyfe, S. Gupta, T.K. Tan, J. Gilbert-Jaramillo, W. James, M. Knight, M.W. Carroll, D. Skelly, C. Dold, Y. Peng, R. Levin, T. Dong, A.J. Pollard, J.C. Knight, P. Klenerman, N. Temperton, D.R. Hall, M.A. Williams, N.G. Paterson, F.K.R. Bertram, C.A. Siebert, D.K. Clare, A. Howe, J. Radecke, Y. Song, A.R. Townsend, K.-Y.A. Huang, E.E. Fry, J. Mongkolsapaya, M.S. Diamond, J. Ren, D.I. Stuart, G.R. Screaton, The antigenic anatomy of SARS-CoV-2 receptor binding domain, Cell 184 (2021) 2183-2200.e22. https://doi.org/10.1016/j.cell.2021.02.032.
[144] H. Di, E.A. Pusch, J. Jones, N.A. Kovacs, N. Hassell, M. Sheth, K.S. Lynn, M.W. Keller, M.M. Wilson, L.M. Keong, D. Cui, S.H. Park, R. Chau, K.A. Lacek, J.D. Liddell, M.K. Kirby, G. Yang, M. Johnson, S. Thor, N. Zanders, C. Feng, D. Surie, J. DeCuir, S.N. Lester, L. Atherton, H. Hicks, A. Tamin, J.L. Harcourt, M.M. Coughlin, W.H. Self, J.P. Rhoads, K.W. Gibbs, D.N. Hager, N.I. Shapiro, M.C. Exline, A.S. Lauring, B. Rambo-Martin, C.R. Paden, R.J. Kondor, J.S. Lee, J.R. Barnes, N.J. Thornburg, B. Zhou, D.E. Wentworth, C.T. Davis, Antigenic Characterization of Circulating and Emerging SARS-CoV-2 Variants in the U.S. throughout the Delta to Omicron Waves, Vaccines (Basel) 12 (2024) 505. https://doi.org/10.3390/vaccines12050505.
[145] D. Goldblatt, G. Alter, S. Crotty, S.A. Plotkin, Correlates of protection against <scp>SARS</scp> - <scp>CoV</scp> -2 infection and COVID-19 disease, Immunol Rev 310 (2022) 6–26. https://doi.org/10.1111/imr.13091.
[146] R. Carrasco-Hernandez, R. Jácome, Y.L. Vidal, S.P. de León, Are RNA viruses candidate agents for the next global pandemic? A review, ILAR J 58 (2017) 343–358. https://doi.org/10.1093/ilar/ilx026.

[147] S.F. Elena, R. Miralles, J.M. Cuevas, P.E. Turner, A. Moya, The two faces of mutation: Extinction and adaptation in RNA viruses, IUBMB Life 49 (2000) 5–9. https://doi.org/10.1080/152165400306296.
[148] E.C. Holmes, Error thresholds and the constraints to RNA virus evolution, Trends Microbiol 11 (2003) 543–546. https://doi.org/10.1016/j.tim.2003.10.006.
[149] D. generale della prevenzione sanitaria Ministero Della Salute, Circolare aggiornamento variante Delta, 2021.
[150] T. Starr, A. Greaney, A. Addetia, W. Hannon, M. Choudhary, A. Dingens, J. Li, J. Bloom, Prospective mapping of viral mutations that escape antibodies used to treat COVID-19, Science (1979) 371 (2021) 850–4. https://doi.org/10.1126/science.abf9302.
[151] S. Iketani, L. Liu, Y. Guo, L. Liu, J.F.-W. Chan, Y. Huang, M. Wang, Y. Luo, J. Yu, H. Chu, K.K.-H. Chik, T.T.-T. Yuen, M.T. Yin, M.E. Sobieszczyk, Y. Huang, K.-Y. Yuen, H.H. Wang, Z. Sheng, D.D. Ho, Antibody evasion properties of SARS-CoV-2 Omicron sublineages, Nature 604 (2022) 553–556. https://doi.org/10.1038/s41586-022-04594-4.
[152] L. Liu, S. Iketani, Y. Guo, J.F.-W. Chan, M. Wang, L. Liu, Y. Luo, H. Chu, Y. Huang, M.S. Nair, J. Yu, K.K.-H. Chik, T.T.-T. Yuen, C. Yoon, K.K.-W. To, H. Chen, M.T. Yin, M.E. Sobieszczyk, Y. Huang, H.H. Wang, Z. Sheng, K.-Y. Yuen, D.D. Ho, Striking antibody evasion manifested by the Omicron variant of SARS-CoV-2, Nature 602 (2022) 676–681. https://doi.org/10.1038/s41586-021-04388-0.
[153] N.P. Hachmann, J. Miller, A.Y. Collier, J.D. Ventura, J. Yu, M. Rowe, E.A. Bondzie, O. Powers, N. Surve, K. Hall, D.H. Barouch, Neutralization Escape by SARS-CoV-2 Omicron Subvariants BA.2.12.1, BA.4, and BA.5, New England Journal of Medicine 387 (2022) 86–88. https://doi.org/10.1056/NEJMc2206576.
[154] W.F. Garcia-Beltran, E.C. Lam, K.S. Denis, A.J. Iafrate, V. Naranbhai, A.B. Balazs, W.F. Garcia-beltran, E.C. Lam, K.S. Denis, A.D. Nitido, Z.H. Garcia, B.M. Hauser, Multiple SARS-CoV-2 variants escape neutralization by vaccine-induced humoral immunity ll Multiple SARS-CoV-2 variants escape neutralization by vaccine-induced humoral immunity, Cell 184 (2021) 2372-2383.e9. https://doi.org/10.1016/j.cell.2021.03.013.
[155] R.E. Chen, X. Zhang, J.B. Case, E.S. Winkler, Y. Liu, L.A. Vanblargan, J. Liu, J.M. Errico, X. Xie, N. Suryadevara, P. Gilchuk, S.J. Zost, S. Tahan, L. Droit, J.S. Turner, W. Kim, A.J. Schmitz, M. Thapa, D. Wang, A.C.M. Boon, R.M. Presti, J.A.O. Halloran, A.H.J. Kim, P. Deepak, D. Pinto, D.H. Fremont, J.E.C. Jr, D. Corti, H.W. Virgin, A.H. Ellebedy, Resistance of SARS-CoV-2 variants to neutralization by monoclonal and serum-derived polyclonal antibodies, Nat Med 27 (2021) 717–26. https://doi.org/10.1038/s41591-021-01294-w.
[156] S. Jangra, C. Ye, R. Rathnasinghe, D. Stadlbauer, F. Krammer, V. Simon, L. Martinez-Sobrido, A. Garcia-Sastre, M. Schotsaert, The E484K mutation in the SARS-CoV-2 spike protein reduces but does not abolish neutralizing activity of human convalescent and post-vaccination sera, MedRxiv (2021). https://doi.org/10.1101/2021.01.26.21250543.

[157] E. European Centre for Disease Prevention and Control, Threat Assessment Brief: Reinfection with SARS-CoV-2: considerations for public health response, (2020).
[158] R.K. Gupta, Will SARS-CoV-2 variants of concern affect the promise of vaccines?, Nat Rev Immunol 21 (2021) 340–341. https://doi.org/10.1038/s41577-021-00556-5.
[159] World Health Organization, COVID-19 Vaccine Tracker and Landscape , Https://Www.Who.Int/Teams/Blueprint/Covid-19/Covid-19-Vaccine-Tracker-and-Landscape (2023).
[160] World Health Organization, COVID19 Vaccine Tracker , Https://Covid19.Trackvaccines.Org/Agency/Who/ (2022).
[161] F. Bayani, N.S. Hashkavaei, S. Arjmand, S. Rezaei, V. Uskoković, M. Alijanianzadeh, V.N. Uversky, S.O. Ranaei Siadat, S. Mozaffari-Jovin, Y. Sefidbakht, An overview of the vaccine platforms to combat COVID-19 with a focus on the subunit vaccines, Prog Biophys Mol Biol 178 (2023) 32–49. https://doi.org/10.1016/j.pbiomolbio.2023.02.004.
[162] D. Deplanque, O. Launay, Efficacy of COVID-19 vaccines: From clinical trials to real life, Therapies 76 (2021) 277–283. https://doi.org/10.1016/j.therap.2021.05.004.
[163] S. Goryaynov, O. Gurova, Effect of Platform Type on Clinical Efficacy of SARS-CoV-2 Vaccines in Prime Vaccination Settings: A Systematic Review and Meta-Regression of Randomized Controlled Trials, Vaccines (Basel) 12 (2024) 130. https://doi.org/10.3390/vaccines12020130.
[164] X. Wu, K. Xu, P. Zhan, H. Liu, F. Zhang, Y. Song, T. Lv, Comparative efficacy and safety of COVID-19 vaccines in phase III trials: a network meta-analysis, BMC Infect Dis 24 (2024) 234. https://doi.org/10.1186/s12879-023-08754-3.
[165] A. Asundi, C. O'Leary, N. Bhadelia, Global COVID-19 vaccine inequity: The scope, the impact, and the challenges, Cell Host Microbe 29 (2021) 1036–1039. https://doi.org/10.1016/j.chom.2021.06.007.
[166] M. Bayati, R. Noroozi, M. Ghanbari-Jahromi, F.S. Jalali, Inequality in the distribution of Covid-19 vaccine: a systematic review, Int J Equity Health 21 (2022) 122. https://doi.org/10.1186/s12939-022-01729-x.
[167] United Nations Development Programme, Inequality in Access to Essential Health and Medicine: COVID-19 Vaccines, 2021.
[168] L.N.H. Md Khairi, M.L. Fahrni, A.I. Lazzarino, The Race for Global Equitable Access to COVID-19 Vaccines, Vaccines (Basel) 10 (2022) 1306. https://doi.org/10.3390/vaccines10081306.
[169] M. Ferranna, Causes and costs of global COVID-19 vaccine inequity, Semin Immunopathol 45 (2024) 469–480. https://doi.org/10.1007/s00281-023-00998-0.
[170] D.M. Morens, G.K. Folkers, A.S. Fauci, The Concept of Classical Herd Immunity May Not Apply to COVID-19, J Infect Dis 226 (2022) 195–198. https://doi.org/10.1093/infdis/jiac109.
[171] World Health Organization, COVID-19 Data Explorer, Https://Ourworldindata.Org/Explorers/Covid?Tab=map&Metric=People+vaccinated&Interval=Cumulative&Relative+to+population=true (2024).

[172] UNICEF, COVID-19 Market Dashboard, Https://Www.Unicef.Org/Supply/Covid-19-Market-Dashboard (2025).
[173] International Monetary Found, World Economic Outlook, Https://Www.Imf.Org/En/Publications/WEO/Issues/2021/10/12/World-Economic-Outlook-October-2021 (2025).
[174] International Monetary Found, IMF-WHO COVID-19 VACCINE TRACKER, Https://Www.Imf.Org/En/Topics/Imf-and-Covid19/IMF-WHO-COVID-19-Vaccine-Tracker (2025).
[175] United Nations Development Program, Global Dashboard for Vaccine Equity, Https://Data.Undp.Org/Insights/Vaccine-Equity (n.d.).
[176] World Health Organization, COVAX. Working for global equitable access to COVID-19 vaccines, Https://Www.Who.Int/Initiatives/Act-Accelerator/Covax (n.d.).
[177] I.O. Ayenigbara, J.S. Adegboro, G.O. Ayenigbara, O.R. Adeleke, O.O. Olofintuyi, The challenges to a successful COVID-19 vaccination programme in Africa, Germs 11 (2021) 427–440. https://doi.org/10.18683/germs.2021.1280.
[178] V. Gamino, U. Höfle, Pathology and tissue tropism of natural West Nile virus infection in birds: A review, Vet Res 44 (2013). https://doi.org/10.1186/1297-9716-44-39.
[179] A. Tran, G. L'Ambert, G. Balança, S. Pradier, V. Grosbois, T. Balenghien, T. Baldet, S. Lecollinet, A. Leblond, N. Gaidet-Drapier, An Integrative Eco-Epidemiological Analysis of West Nile Virus Transmission, Ecohealth 14 (2017) 474–489. https://doi.org/10.1007/s10393-017-1249-6.
[180] J.A. Vaughan, R.A. Newman, M.J. Turell, Bird species define the relationship between West Nile viremia and infectiousness to Culex pipiens mosquitoes, PLoS Negl Trop Dis 16 (2022) 1–13. https://doi.org/10.1371/journal.pntd.0010835.
[181] J.M. García-Carrasco, A.R. Muñoz, J. Olivero, M. Segura, R. Real, Predicting the spatio-temporal spread of west nile virus in europe, PLoS Negl Trop Dis 15 (2021) 1–19. https://doi.org/10.1371/journal.pntd.0009022.
[182] M. Viglietta, R. Bellone, A.A. Blisnick, A.-B. Failloux, Vector Specificity of Arbovirus Transmission, Front Microbiol 12 (2021). https://doi.org/10.3389/fmicb.2021.773211.
[183] N. Ayhan, R.N. Charrel, An update on Toscana virus distribution, genetics, medical and diagnostic aspects, Clinical Microbiology and Infection 26 (2020) 1017–1023. https://doi.org/10.1016/j.cmi.2019.12.015.
[184] L. Lu, F. Zhang, B.B.O. Munnink, E. Munger, R.S. Sikkema, S. Pappa, K. Tsioka, A. Sinigaglia, E. Dal Molin, B.B. Shih, A. Günther, A. Pohlmann, U. Ziegler, M. Beer, R.A. Taylor, F. Bartumeus, M. Woolhouse, F.M. Aarestrup, L. Barzon, A. Papa, S. Lycett, M.P.G. Koopmans, West Nile virus spread in Europe: Phylogeographic pattern analysis and key drivers, PLoS Pathog 20 (2024) 1–25. https://doi.org/10.1371/journal.ppat.1011880.
[185] P. Dolman, W. Sutherland, The response of bird populations to habitat loss, Ibis 137 (1995) S38–S46. https://doi.org/10.1111/j.1474-919X.1995.tb08456.x.
[186] W.H.O. Pan Americal Health Organization, Epidemiological Alert Increase in Dengue Cases in the Region of the Americas (16 February 2024), 2024.

[187] I. Cassaniti, G. Ferrari, S. Senatore, E. Rossetti, F. Defilippo, M. Maffeo, L. Vezzosi, G. Campanini, A. Sarasini, S. Paolucci, A. Piralla, D. Lelli, A. Moreno, M. Bonini, M. Tirani, L. Cerutti, S. Paglia, A. Regazzetti, M. Farioli, A. Lavazza, M. Faccini, F. Rovida, D. Cereda, F. Baldanti, D. Lilleri, M. Furione, F. Zavaglio, M. Carrera, G. Scardina, M. Soresini, M. Barozzi, R. Brugnoli, N. Laini, F. Bonalda, S. Arfani, G. Zamboni, M. Piazza, F. Delfanti, P. Ferrari, A. Dafa, A. Negri, F. Parisi, M. Viscardi, F. Attanasi, G. Manarolla, M. Chiari, E. Tallarita, Preliminary results on an autochthonous dengue outbreak in Lombardy Region, Italy, August 2023, Eurosurveillance 28 (2023) 1–5. https://doi.org/10.2807/1560-7917.ES.2023.28.37.2300471.

[188] G. De Carli, F. Carletti, M. Spaziante, C.E.M. Gruber, M. Rueca, P.G. Spezia, V. Vantaggio, A. Barca, C. De Liberato, F. Romiti, M.T. Scicluna, S. Vaglio, M. Feccia, E. Di Rosa, F.P. Gianzi, C. Giambi, P. Scognamiglio, E. Nicastri, E. Girardi, F. Maggi, F. Vairo, Outbreaks of autochthonous Dengue in Lazio region, Italy, August to September 2023: preliminary investigation, Eurosurveillance 28 (2023) 1–5. https://doi.org/10.2807/1560-7917.ES.2023.28.44.2300552.

[189] World Health Organization, Disease Outbreak News. Dengue - Global situation, Https://Www.Who.Int/Emergencies/Disease-Outbreak-News/Item/2024-DON518 (2024).

[190] J.P. Messina, O.J. Brady, N. Golding, M.U.G. Kraemer, G.R.W. Wint, S.E. Ray, D.M. Pigott, F.M. Shearer, K. Johnson, L. Earl, L.B. Marczak, S. Shirude, N. Davis Weaver, M. Gilbert, R. Velayudhan, P. Jones, T. Jaenisch, T.W. Scott, R.C. Reiner, S.I. Hay, The current and future global distribution and population at risk of dengue, Nat Microbiol 4 (2019) 1508–1515. https://doi.org/10.1038/s41564-019-0476-8.

[191] T. Bakonyi, E. Ferenczi, K. Erdélyi, O. Kutasi, T. Csörgo, B. Seidel, H. Weissenböck, K. Brugger, E. Bán, N. Nowotny, Explosive spread of a neuroinvasive lineage 2 West Nile virus in Central Europe, 2008/2009, Vet Microbiol 165 (2013) 61–70. https://doi.org/10.1016/j.vetmic.2013.03.005.

[192] T. Bakonyi, É. Ivanics, K. Erdélyi, K. Ursu, E. Ferenczi, H. Weissenböck, N. Nowotny, Lineage 1 and 2 strains of encephalitic West Nile virus, Central Europe, Emerg Infect Dis 12 (2006) 618–623. https://doi.org/10.3201/eid1204.051379.

[193] J.-C. Saiz, M.A. Martín-Acebes, A.B. Blázquez, E. Escribano-Romero, T. Poderoso, N. Jiménez de Oya, Pathogenicity and virulence of West Nile virus revisited eight decades after its first isolation, Virulence 12 (2021) 1145–1173. https://doi.org/10.1080/21505594.2021.1908740.

[194] T.C. Pierson, M.S. Diamond, The continued threat of emerging flaviviruses, Nat Microbiol 5 (2020) 796–812. https://doi.org/10.1038/s41564-020-0714-0.

[195] A. Roy, Q. Liu, Y. Yang, A.K. Debnath, L. Du, Envelope Protein-Targeting Zika Virus Entry Inhibitors, Int J Mol Sci 25 (2024) 9424. https://doi.org/10.3390/ijms25179424.

[196] D.Z. Kocabiyik, L.F. Álvarez, E.L. Durigon, C. Wrenger, West Nile virus - a re-emerging global threat: recent advances in vaccines and drug discovery, Front Cell Infect Microbiol 15 (2025). https://doi.org/10.3389/fcimb.2025.1568031.

[197] S. Mukherjee, K.A. Dowd, C.J. Manhart, J.E. Ledgerwood, A.P. Durbin, S.S. Whitehead, T.C. Pierson, Mechanism and Significance of Cell Type-Dependent Neutralization of Flaviviruses, J Virol 88 (2014) 7210–7220. https://doi.org/10.1128/JVI.03690-13.
[198] J.K. Marzinek, R. Lakshminarayanan, E. Goh, R.G. Huber, S. Panzade, C. Verma, P.J. Bond, Characterizing the Conformational Landscape of Flavivirus Fusion Peptides via Simulation and Experiment, Sci Rep 6 (2016) 19160. https://doi.org/10.1038/srep19160.
[199] J.H. Chávez, J.R. Silva, A.A. Amarilla, L.T. Moraes Figueiredo, Domain III peptides from flavivirus envelope protein are useful antigens for serologic diagnosis and targets for immunization, Biologicals 38 (2010) 613–618. https://doi.org/10.1016/j.biologicals.2010.07.004.
[200] M. Mossenta, S. Marchese, M. Poggianella, J.L. Slon Campos, O.R. Burrone, Role of N-glycosylation on Zika virus E protein secretion, viral assembly and infectivity, Biochem Biophys Res Commun 492 (2017) 579–586. https://doi.org/10.1016/j.bbrc.2017.01.022.
[201] C.-T. Tang, M.-Y. Liao, C.-Y. Chiu, W.-F. Shen, C.-Y. Chiu, P.-C. Cheng, G.-J.J. Chang, H.-C. Wu, Generation of Monoclonal Antibodies against Dengue Virus Type 4 and Identification of Enhancing Epitopes on Envelope Protein, PLoS One 10 (2015) e0136328. https://doi.org/10.1371/journal.pone.0136328.
[202] M.A. White, D. Liu, M.R. Holbrook, R.E. Shope, A.D.T. Barrett, R.O. Fox, Crystallization and preliminary X-ray diffraction analysis of Langat virus envelope protein domain III, Acta Crystallogr D Biol Crystallogr 59 (2003) 1049–1051. https://doi.org/10.1107/S0907444903004475.
[203] M. V Cherrier, B. Kaufmann, G.E. Nybakken, S.-M. Lok, J.T. Warren, B.R. Chen, C.A. Nelson, V.A. Kostyuchenko, H.A. Holdaway, P.R. Chipman, R.J. Kuhn, M.S. Diamond, M.G. Rossmann, D.H. Fremont, Structural basis for the preferential recognition of immature flaviviruses by a fusion-loop antibody, EMBO J 28 (2009) 3269–3276. https://doi.org/10.1038/emboj.2009.245.
[204] D.E. Volk, F.J. May, S.H.A. Gandham, A. Anderson, J.J. Von Lindern, D.W.C. Beasley, A.D.T. Barrett, D.G. Gorenstein, Structure of yellow fever virus envelope protein domain III, Virology 394 (2009) 12–18. https://doi.org/10.1016/j.virol.2009.09.001.
[205] Y. Modis, S. Ogata, D. Clements, S.C. Harrison, Structure of the dengue virus envelope protein after membrane fusion, Nature 427 (2004) 313–319. https://doi.org/10.1038/nature02165.
[206] L. Goo, L.A. VanBlargan, K.A. Dowd, M.S. Diamond, T.C. Pierson, A single mutation in the envelope protein modulates flavivirus antigenicity, stability, and pathogenesis, PLoS Pathog 13 (2017) e1006178. https://doi.org/10.1371/journal.ppat.1006178.
[207] W.D. Crill, G.-J.J. Chang, Localization and Characterization of Flavivirus Envelope Glycoprotein Cross-Reactive Epitopes, J Virol 78 (2004) 13975–13986. https://doi.org/10.1128/JVI.78.24.13975-13986.2004.
[208] S.-S. Chiou, Y.-C. Fan, W.D. Crill, R.-Y. Chang, G.-J.J. Chang, Mutation analysis of the cross-reactive epitopes of Japanese encephalitis virus envelope

glycoprotein, Journal of General Virology 93 (2012) 1185–1192. https://doi.org/10.1099/vir.0.040238-0.
[209] S.L. Hanna, T.C. Pierson, M.D. Sanchez, A.A. Ahmed, M.M. Murtadha, R.W. Doms, N-Linked Glycosylation of West Nile Virus Envelope Proteins Influences Particle Assembly and Infectivity, J Virol 79 (2005) 13262–13274. https://doi.org/10.1128/JVI.79.21.13262-13274.2005.
[210] R. Fritz, J. Blazevic, C. Taucher, K. Pangerl, F.X. Heinz, K. Stiasny, The Unique Transmembrane Hairpin of Flavivirus Fusion Protein E Is Essential for Membrane Fusion, J Virol 85 (2011) 4377–4385. https://doi.org/10.1128/JVI.02458-10.
[211] F.X. Heinz, K. Stiasny, Flaviviruses and their antigenic structure, Journal of Clinical Virology 55 (2012) 289–295. https://doi.org/10.1016/j.jcv.2012.08.024.
[212] J.A. Roby, R.A. Hall, Y.X. Setoh, A.A. Khromykh, Post-translational regulation and modifications of flavivirus structural proteins, Journal of General Virology 96 (2015) 1551–1569. https://doi.org/10.1099/vir.0.000097.
[213] A.J. McAuley, M. Torres, J.A. Plante, C.Y.-H. Huang, D.A. Bente, D.W.C. Beasley, Recovery of West Nile Virus Envelope Protein Domain III Chimeras with Altered Antigenicity and Mouse Virulence, J Virol 90 (2016) 4757–4770. https://doi.org/10.1128/JVI.02861-15.
[214] S. Chakraborty, Computational analysis of perturbations in the post-fusion Dengue virus envelope protein highlights known epitopes and conserved residues in the Zika virus, F1000Res 5 (2016) 1150. https://doi.org/10.12688/f1000research.8853.2.
[215] J. Blazevic, H. Rouha, V. Bradt, F.X. Heinz, K. Stiasny, Membrane Anchors of the Structural Flavivirus Proteins and Their Role in Virus Assembly, J Virol 90 (2016) 6365–6378. https://doi.org/10.1128/JVI.00447-16.
[216] D. Langosch, M. Hofmann, C. Ungermann, The role of transmembrane domains in membrane fusion, Cellular and Molecular Life Sciences 64 (2007) 850–864. https://doi.org/10.1007/s00018-007-6439-x.
[217] V.C. Luca, J. AbiMansour, C.A. Nelson, D.H. Fremont, Crystal Structure of the Japanese Encephalitis Virus Envelope Protein, J Virol 86 (2012) 2337–2346. https://doi.org/10.1128/JVI.06072-11.
[218] S. Mukhopadhyay, B.-S. Kim, P.R. Chipman, M.G. Rossmann, R.J. Kuhn, Structure of West Nile Virus, Science (1979) 302 (2003) 248–248. https://doi.org/10.1126/science.1089316.
[219] D.W.C. Beasley, L. Li, M.T. Suderman, A.D.T. Barrett, Mouse Neuroinvasive Phenotype of West Nile Virus Strains Varies Depending upon Virus Genotype, Virology 296 (2002) 17–23. https://doi.org/10.1006/viro.2002.1372.
[220] G.E. Nybakken, T. Oliphant, S. Johnson, S. Burke, M.S. Diamond, D.H. Fremont, Structural basis of West Nile virus neutralization by a therapeutic antibody, Nature 437 (2005) 764–769. https://doi.org/10.1038/nature03956.
[221] T. Oliphant, M.S. Diamond, The molecular basis of antibody-mediated neutralization of West Nile virus, Expert Opin Biol Ther 7 (2007) 885–892. https://doi.org/10.1517/14712598.7.6.885.
[222] R.J. Kuhn, W. Zhang, M.G. Rossmann, S. V. Pletnev, J. Corver, E. Lenches, C.T. Jones, S. Mukhopadhyay, P.R. Chipman, E.G. Strauss, T.S. Baker, J.H. Strauss,

Structure of Dengue Virus, Cell 108 (2002) 717–725. https://doi.org/10.1016/S0092-8674(02)00660-8.
[223] L. Goo, K. Debbink, N. Kose, G. Sapparapu, M.P. Doyle, A.W. Wessel, J.M. Richner, K.E. Burgomaster, B.C. Larman, K.A. Dowd, M.S. Diamond, J.E. Crowe, T.C. Pierson, A protective human monoclonal antibody targeting the West Nile virus E protein preferentially recognizes mature virions, Nat Microbiol 4 (2018) 71–77. https://doi.org/10.1038/s41564-018-0283-7.
[224] B. Kaufmann, M.G. Rossmann, Molecular mechanisms involved in the early steps of flavivirus cell entry, Microbes Infect 13 (2011) 1–9. https://doi.org/10.1016/j.micinf.2010.09.005.
[225] W.M.P.B. Wahala, A.M. De Silva, The Human Antibody Response to Dengue Virus Infection, Viruses 3 (2011) 2374–2395. https://doi.org/10.3390/v3122374.
[226] T.C. Pierson, M.S. Diamond, Degrees of maturity: the complex structure and biology of flaviviruses, Curr Opin Virol 2 (2012) 168–175. https://doi.org/10.1016/j.coviro.2012.02.011.
[227] S. Brandler, F. Tangy, Vaccines in Development against West Nile Virus, Viruses 5 (2013) 2384–2409. https://doi.org/10.3390/v5102384.
[228] K. Shirato, H. Miyoshi, A. Goto, Y. Ako, T. Ueki, H. Kariwa, I. Takashima, Viral envelope protein glycosylation is a molecular determinant of the neuroinvasiveness of the New York strain of West Nile virus, Journal of General Virology 85 (2004) 3637–3645. https://doi.org/10.1099/vir.0.80247-0.
[229] T.P. Monath, P.F.C. Vasconcelos, Yellow fever, Journal of Clinical Virology 64 (2015) 160–173. https://doi.org/10.1016/j.jcv.2014.08.030.
[230] M.S. Diamond, B. Shrestha, E. Mehlhop, E. Sitati, M. Engle, Innate and Adaptive Immune Responses Determine Protection against Disseminated Infection by West Nile Encephalitis Virus, Viral Immunol 16 (2003) 259–278. https://doi.org/10.1089/088282403322396082.
[231] B. Shrestha, M.A. Samuel, M.S. Diamond, CD8 T Cells Require Perforin To Clear West Nile Virus from Infected Neurons, J Virol 80 (2006) 119–129. https://doi.org/10.1128/JVI.80.1.119-129.2006.
[232] E.M. Sitati, M.S. Diamond, CD4 T-Cell Responses Are Required for Clearance of West Nile Virus from the Central Nervous System, J Virol 80 (2006) 12060–12069. https://doi.org/10.1128/JVI.01650-06.
[233] M.A. Samuel, M.S. Diamond, Pathogenesis of West Nile Virus Infection: a Balance between Virulence, Innate and Adaptive Immunity, and Viral Evasion, J Virol 80 (2006) 9349–9360. https://doi.org/10.1128/JVI.01122-06.
[234] R.B. Tesh, J. Arroyo, A.P.A. Travassos da Rosa, H. Guzman, S.-Y. Xiao, T.P. Monath, Efficacy of Killed Virus Vaccine, Live Attenuated Chimeric Virus Vaccine, and Passive Immunization for Prevention of West Nile virus Encephalitis in Hamster Model, Emerg Infect Dis 8 (2002) 1392–1397. https://doi.org/10.3201/eid0812.020229.
[235] A.E. Calvert, G.F. Kalantarov, G.-J.J. Chang, I. Trakht, C.D. Blair, J.T. Roehrig, Human monoclonal antibodies to West Nile virus identify epitopes on the prM protein, Virology 410 (2011) 30–37. https://doi.org/10.1016/j.virol.2010.10.033.
[236] K.M. Chung, B.S. Thompson, D.H. Fremont, M.S. Diamond, Antibody Recognition of Cell Surface-Associated NS1 Triggers Fc-γ Receptor-Mediated

Phagocytosis and Clearance of West Nile Virus-Infected Cells, J Virol 81 (2007) 9551–9555. https://doi.org/10.1128/JVI.00879-07.
[237] S.J. Wong, R.H. Boyle, V.L. Demarest, A.N. Woodmansee, L.D. Kramer, H. Li, M. Drebot, R.A. Koski, E. Fikrig, D.A. Martin, P.-Y. Shi, Immunoassay Targeting Nonstructural Protein 5 To Differentiate West Nile Virus Infection from Dengue and St. Louis Encephalitis Virus Infections and from Flavivirus Vaccination, J Clin Microbiol 41 (2003) 4217–4223. https://doi.org/10.1128/JCM.41.9.4217-4223.2003.
[238] J.M. Richner, G.B. Gmyrek, J. Govero, Y. Tu, G.J.W. van der Windt, T.U. Metcalf, E.K. Haddad, J. Textor, M.J. Miller, M.S. Diamond, Age-Dependent Cell Trafficking Defects in Draining Lymph Nodes Impair Adaptive Immunity and Control of West Nile Virus Infection, PLoS Pathog 11 (2015) e1005027. https://doi.org/10.1371/journal.ppat.1005027.
[239] J.D. Brien, J.L. Uhrlaub, A. Hirsch, C.A. Wiley, J. Nikolich-Žugich, Key role of T cell defects in age-related vulnerability to West Nile virus, Journal of Experimental Medicine 206 (2009) 2735–2745. https://doi.org/10.1084/jem.20090222.
[240] E.A. James, T.J. Gates, R.E. LaFond, S. Yamamoto, C. Ni, D. Mai, V.H. Gersuk, K. O'Brien, Q.-A. Nguyen, B. Zeitner, M.C. Lanteri, P.J. Norris, D. Chaussabel, U. Malhotra, W.W. Kwok, Neuroinvasive West Nile Infection Elicits Elevated and Atypically Polarized T Cell Responses That Promote a Pathogenic Outcome, PLoS Pathog 12 (2016) e1005375. https://doi.org/10.1371/journal.ppat.1005375.
[241] M.C. Lanteri, K.M. O'Brien, W.E. Purtha, M.J. Cameron, J.M. Lund, R.E. Owen, J.W. Heitman, B. Custer, D.F. Hirschkorn, L.H. Tobler, N. Kiely, H.E. Prince, L.C. Ndhlovu, D.F. Nixon, H.T. Kamel, D.J. Kelvin, M.P. Busch, A.Y. Rudensky, M.S. Diamond, P.J. Norris, Tregs control the development of symptomatic West Nile virus infection in humans and mice, Journal of Clinical Investigation (2009). https://doi.org/10.1172/JCI39387.
[242] A.T. Ciota, West Nile virus and its vectors, Curr Opin Insect Sci 22 (2017) 28–36. https://doi.org/10.1016/j.cois.2017.05.002.
[243] O. Engler, G. Savini, A. Papa, J. Figuerola, M. Groschup, H. Kampen, J. Medlock, A. Vaux, A. Wilson, D. Werner, H. Jöst, M. Goffredo, G. Capelli, V. Federici, M. Tonolla, N. Patocchi, E. Flacio, J. Portmann, A. Rossi-Pedruzzi, S. Mourelatos, S. Ruiz, A. Vázquez, M. Calzolari, P. Bonilauri, M. Dottori, F. Schaffner, A. Mathis, N. Johnson, European Surveillance for West Nile Virus in Mosquito Populations, Int J Environ Res Public Health 10 (2013) 4869–4895. https://doi.org/10.3390/ijerph10104869.
[244] D.M. Fonseca, J.L. Smith, R.C. Wilkerson, R.C. Fleischer, Pathways of expansion and multiple introductions illustrated by large genetic differentiation among worldwide populations of the southern house mosquito., Am J Trop Med Hyg 74 (2006) 284–9.
[245] B. Gomes, C.A. Sousa, J.L. Vicente, L. Pinho, I. Calderón, E. Arez, A.P. Almeida, M.J. Donnelly, J. Pinto, Feeding patterns of molestus and pipiens forms of Culex pipiens (Diptera: Culicidae) in a region of high hybridization, Parasit Vectors 6 (2013) 93. https://doi.org/10.1186/1756-3305-6-93.

[246] L. Lu, F. Zhang, B.B.O. Munnink, E. Munger, R.S. Sikkema, S. Pappa, K. Tsioka, A. Sinigaglia, E. Dal Molin, B.B. Shih, A. Günther, A. Pohlmann, U. Ziegler, M. Beer, R.A. Taylor, F. Bartumeus, M. Woolhouse, F.M. Aarestrup, L. Barzon, A. Papa, S. Lycett, M.P.G. Koopmans, West Nile virus spread in Europe: Phylogeographic pattern analysis and key drivers, PLoS Pathog 20 (2024). https://doi.org/10.1371/journal.ppat.1011880.

[247] G. Mencattelli, M.H.D. Ndione, A. Silverj, M.M. Diagne, V. Curini, L. Teodori, M. Di Domenico, R. Mbaye, A. Leone, M. Marcacci, A. Gaye, E. Ndiaye, D. Diallo, M. Ancora, B. Secondini, V. Di Lollo, I. Mangone, A. Bucciacchio, A. Polci, G. Marini, R. Rosà, N. Segata, G. Fall, C. Cammà, F. Monaco, M. Diallo, O. Rota-Stabelli, O. Faye, A. Rizzoli, G. Savini, Spatial and temporal dynamics of West Nile virus between Africa and Europe, Nat Commun 14 (2023) 6440. https://doi.org/10.1038/s41467-023-42185-7.

[248] J. Sejvar, Clinical Manifestations and Outcomes of West Nile Virus Infection, Viruses 6 (2014) 606–623. https://doi.org/10.3390/v6020606.

[249] D. Erazo, L. Grant, G. Ghisbain, G. Marini, F.J. Colón-González, W. Wint, A. Rizzoli, W. Van Bortel, C.B.F. Vogels, N.D. Grubaugh, M. Mengel, K. Frieler, W. Thiery, S. Dellicour, Contribution of climate change to the spatial expansion of West Nile virus in Europe, Nat Commun 15 (2024) 1196. https://doi.org/10.1038/s41467-024-45290-3.

[250] E.B. Hayes, N. Komar, R.S. Nasci, S.P. Montgomery, D.R. O'Leary, G.L. Campbell, Epidemiology and transmission dynamics of West Nile virus disease, Emerg Infect Dis 11 (2005) 1167–1173. https://doi.org/10.3201/eid1108.050289a.

[251] J.J. Sejvar, Clinical Manifestations and Outcomes of West Nile Virus Infection, Viruses (2014) 606–623. https://doi.org/10.3390/v6020606.

[252] L. Petersen, Clinical manifestations and diagnosis of West Nile virus infection, Published Online on UpToDate (2024). https://www.uptodate.com/contents/clinical-manifestations-and-diagnosis-of-west-nile-virus-infection (accessed February 24, 2024).

[253] E.C. for D.P. and C. ECDC, Epidemiological update: West Nile virus transmission season in Europe, 2018, (2018). https://www.ecdc.europa.eu/en/news-events/epidemiological-update-west-nile-virus-transmission-season-europe-2018 (accessed February 24, 2024).

[254] E.C. for D.P. and C. ECDC, Epidemiological update: West Nile virus transmission season in Europe, 2019, (2019). https://www.ecdc.europa.eu/en/news-events/epidemiological-update-west-nile-virus-transmission-season-europe-2019 (accessed February 24, 2024).

[255] E.C. for D.P. and C. ECDC, Epidemiological update: West Nile virus transmission season in Europe, 2020, (2020). https://www.ecdc.europa.eu/en/news-events/epidemiological-update-west-nile-virus-transmission-season-europe-2020 (accessed February 24, 2024).

[256] E.C. for D.P. and C. ECDC, Epidemiological update: West Nile virus transmission season in Europe, 2021, (2021). https://www.ecdc.europa.eu/en/news-events/epidemiological-update-west-nile-virus-transmission-season-europe-2021 (accessed February 24, 2024).

[257] E.C. for D.P. and C. ECDC, Epidemiological update: West Nile virus transmission season in Europe, 2022, (2022). https://www.ecdc.europa.eu/en/news-events/epidemiological-update-west-nile-virus-transmission-season-europe-2022 (accessed February 24, 2024).
[258] E.C. for D.P. and C. ECDC, Weekly updates: 2023 West Nile virus transmission season, (2023). https://www.ecdc.europa.eu/en/west-nile-fever/surveillance-and-disease-data/disease-data-ecdc (accessed February 24, 2024).
[259] E.R. Schwarz, M.T. Long, Comparison of West Nile Virus Disease in Humans and Horses: Exploiting Similarities for Enhancing Syndromic Surveillance, Viruses 15 (2023) 1230. https://doi.org/10.3390/v15061230.
[260] T. Bakonyi, É. Ivanics, K. Erdélyi, K. Ursu, E. Ferenczi, H. Weissenböck, N. Nowotny, Lineage 1 and 2 Strains of Encephalitic West Nile Virus, Central Europe, Emerg Infect Dis 12 (2006) 618–623. https://doi.org/10.3201/eid1204.051379.
[261] G. Jerzak, K.A. Bernard, L.D. Kramer, G.D. Ebel, Genetic variation in West Nile virus from naturally infected mosquitoes and birds suggests quasispecies structure and strong purifying selection, Journal of General Virology 86 (2005) 2175–2183. https://doi.org/10.1099/vir.0.81015-0.
[262] R.M. Moudy, B. Zhang, P.-Y. Shi, L.D. Kramer, West Nile virus envelope protein glycosylation is required for efficient viral transmission by Culex vectors, Virology 387 (2009) 222–228. https://doi.org/10.1016/j.virol.2009.01.038.
[263] R.M. Moudy, M.A. Meola, L.-L.L. Morin, G.D. Ebel, L.D. Kramer, A newly emergent genotype of West Nile virus is transmitted earlier and more efficiently by Culex mosquitoes., Am J Trop Med Hyg 77 (2007) 365–70.
[264] G. Worwa, A.A. Hutton, M. Frey, N.K. Duggal, A.C. Brault, W.K. Reisen, Increases in the competitive fitness of West Nile virus isolates after introduction into California, Virology 514 (2018) 170–181. https://doi.org/10.1016/j.virol.2017.11.017.
[265] N.K. Duggal, W.K. Reisen, Y. Fang, R.M. Newman, X. Yang, G.D. Ebel, A.C. Brault, Genotype-specific variation in West Nile virus dispersal in California, Virology 485 (2015) 79–85. https://doi.org/10.1016/j.virol.2015.07.004.
[266] S.M. Bialosuknia, A.P. Dupuis II, S.D. Zink, C.A. Koetzner, J.G. Maffei, J.C. Owen, H. Landwerlen, L.D. Kramer, A.T. Ciota, Adaptive evolution of West Nile virus facilitated increased transmissibility and prevalence in New York State, Emerg Microbes Infect 11 (2022) 988–999. https://doi.org/10.1080/22221751.2022.2056521.
[267] K.A. Fitzpatrick, E.R. Deardorff, K. Pesko, D.E. Brackney, B. Zhang, E. Bedrick, P.-Y. Shi, G.D. Ebel, Population variation of West Nile virus confers a host-specific fitness benefit in mosquitoes, Virology 404 (2010) 89–95. https://doi.org/10.1016/j.virol.2010.04.029.
[268] D.E. Brackney, J.E. Beane, G.D. Ebel, RNAi Targeting of West Nile Virus in Mosquito Midguts Promotes Virus Diversification, PLoS Pathog 5 (2009) e1000502. https://doi.org/10.1371/journal.ppat.1000502.
[269] N.D. Grubaugh, J.R. Fauver, C. Rückert, J. Weger-Lucarelli, S. Garcia-Luna, R.A. Murrieta, A. Gendernalik, D.R. Smith, D.E. Brackney, G.D. Ebel, Mosquitoes

Transmit Unique West Nile Virus Populations during Each Feeding Episode, Cell Rep 19 (2017) 709–718. https://doi.org/10.1016/j.celrep.2017.03.076.
[270] A.T. Ciota, D.J. Ehrbar, G.A. Van Slyke, A.F. Payne, G.G. Willsey, R.E. Viscio, L.D. Kramer, Quantification of intrahost bottlenecks of West Nile virus in Culex pipiens mosquitoes using an artificial mutant swarm, Infection, Genetics and Evolution 12 (2012) 557–564. https://doi.org/10.1016/j.meegid.2012.01.022.
[271] D.E. Brackney, K.N. Pesko, I.K. Brown, E.R. Deardorff, J. Kawatachi, G.D. Ebel, West Nile Virus Genetic Diversity is Maintained during Transmission by Culex pipiens quinquefasciatus Mosquitoes, PLoS One 6 (2011) e24466. https://doi.org/10.1371/journal.pone.0024466.
[272] N.D. Grubaugh, J. Weger-Lucarelli, R.A. Murrieta, J.R. Fauver, S.M. Garcia-Luna, A.N. Prasad, W.C. Black, G.D. Ebel, Genetic Drift during Systemic Arbovirus Infection of Mosquito Vectors Leads to Decreased Relative Fitness during Host Switching, Cell Host Microbe 19 (2016) 481–492. https://doi.org/10.1016/j.chom.2016.03.002.
[273] A.M. Bosco-Lauth, R.A. Bowen, West Nile Virus: Veterinary Health and Vaccine Development, J Med Entomol 56 (2019) 1463–1466. https://doi.org/10.1093/jme/tjz125.
[274] Merial Ltd. (2023). RECOMBITEK® Equine west nile virus (MERIAL LTD.). Available online at: https://datasheets.scbt.com/sc-359390_mfr.pdf , n.d.
[275] Zoetis (2024). WEST NILE-INNOVATOR® - safety data sheet. Available online at: https://www.zoetisus.com/products/equine/west-nile-equine-vaccine-for-horses:~:text=WEST%20NILE%2DINNOVATOR%C2%AE%20vaccines%20contain%20the%20adjuvant%20MetaStim%C2%AE,immunity%20to%20West%20Nile%20virus, n.d.
[276] T. Ng, D. Hathaway, N. Jennings, D. Champ, Y.W. Chiang, H.J. Chu, Equine vaccine for West Nile virus., Dev Biol (Basel) 114 (2003) 221–7.
[277] H. El Garch, J.M. Minke, J. Rehder, S. Richard, C. Edlund Toulemonde, S. Dinic, C. Andreoni, J.C. Audonnet, R. Nordgren, V. Juillard, A West Nile virus (WNV) recombinant canarypox virus vaccine elicits WNV-specific neutralizing antibodies and cell-mediated immune responses in the horse, Vet Immunol Immunopathol 123 (2008) 230–239. https://doi.org/10.1016/j.vetimm.2008.02.002.
[278] M. De Filette, S. Ulbert, M. Diamond, N.N. Sanders, Recent progress in West Nile virus diagnosis and vaccination, Vet Res 43 (2012) 16. https://doi.org/10.1186/1297-9716-43-16.
[279] A.K. Pinto, J.M. Richner, E.A. Poore, P.P. Patil, I.J. Amanna, M.K. Slifka, M.S. Diamond, A Hydrogen Peroxide-Inactivated Virus Vaccine Elicits Humoral and Cellular Immunity and Protects against Lethal West Nile Virus Infection in Aged Mice, J Virol 87 (2013) 1926–1936. https://doi.org/10.1128/JVI.02903-12.
[280] Merck Animal Health. (2024). PRESTIGE® WNV. Available online at: https://www.merck-animal-health-usa.com/species/equine/products/prestige-wnv, n.d.

[281] G. Dayan, K. Pugachev, J. Bevilacqua, J. Lang, T. Monath, Preclinical and Clinical Development of a YFV 17 D-Based Chimeric Vaccine against West Nile Virus, Viruses 5 (2013) 3048–3070. https://doi.org/10.3390/v5123048.
[282] A.P. Durbin, P.F. Wright, A. Cox, W. Kagucia, D. Elwood, S. Henderson, K. Wanionek, J. Speicher, S.S. Whitehead, A.G. Pletnev, The live attenuated chimeric vaccine rWN/DEN4Δ30 is well-tolerated and immunogenic in healthy flavivirus-naïve adult volunteers, Vaccine 31 (2013) 5772–5777. https://doi.org/10.1016/j.vaccine.2013.07.064.
[283] Y. Du, Y. Deng, Y. Zhan, R. Yang, J. Ren, W. Wang, B. Huang, W. Tan, The recombinant truncated envelope protein of West Nile virus adjuvanted with Alum/CpG induces potent humoral and T cell immunity in mice, Biosaf Health 5 (2023) 300–307. https://doi.org/10.1016/j.bsheal.2023.06.003.
[284] H.A. Ali, A.-M. Hartner, S. Echeverria-Londono, J. Roth, X. Li, K. Abbas, A. Portnoy, E. Vynnycky, K. Woodruff, N.M. Ferguson, J. Toor, K.A. Gaythorpe, Vaccine equity in low and middle income countries: a systematic review and meta-analysis, Int J Equity Health 21 (2022) 82. https://doi.org/10.1186/s12939-022-01678-5.
[285] A.M. Ekström, C. Berggren, G. Tomson, L.O. Gostin, P. Friberg, O.P. Ottersen, The battle for COVID-19 vaccines highlights the need for a new global governance mechanism, Nat Med 27 (2021) 739–740. https://doi.org/10.1038/s41591-021-01288-8.
[286] C. Mesa-Vieira, F. Botero-Rodríguez, A. Padilla-Muñoz, O.H. Franco, C. Gómez-Restrepo, Reprint of: The Dark Side of the Moon: Global challenges in the distribution of vaccines and implementation of vaccination plans against COVID-19, Maturitas 150 (2021) 61–63. https://doi.org/10.1016/j.maturitas.2021.05.012.
[287] L. Forman, C. Jackson, K. Fajber, Can we move beyond vaccine apartheid? Examining the determinants of the COVID-19 vaccine gap, Glob Public Health 18 (2023). https://doi.org/10.1080/17441692.2023.2256822.
[288] E. Boro, B. Stoll, Barriers to COVID-19 Health Products in Low-and Middle-Income Countries During the COVID-19 Pandemic: A Rapid Systematic Review and Evidence Synthesis, Front Public Health 10 (2022). https://doi.org/10.3389/fpubh.2022.928065.
[289] D. Farr, High pressure technology in the food industry, Trends Food Sci Technol 1 (1990) 14–16. https://doi.org/10.1016/0924-2244(90)90004-I.
[290] European Food Safety Authority, High-pressure processing: food safety without compromising quality, Https://Www.Efsa.Europa.Eu/En/News/High-Pressure-Processing-Food-Safety-without-Compromising-Quality#:~:Text=HPP%20is%20a%20non%2Dthermal,%2C%20appearance%2C%20or%20nutritional%20values. (2022).
[291] A. Iqbal, A. Murtaza, C.A. Pinto, J.A. Saraiva, X. Liu, Z. Zhu, J.M. Lorenzo, K. Marszałek, High-pressure processing for food preservation, in: Innovative and Emerging Technologies in the Bio-Marine Food Sector, Elsevier, 2022: pp. 495–518. https://doi.org/10.1016/B978-0-12-820096-4.00006-7.

[292] D.G. Yordanov, G.V. Angelova, High Pressure Processing for Foods Preserving, Biotechnology & Biotechnological Equipment 24 (2010) 1940–1945. https://doi.org/10.2478/V10133-010-0057-8.
[293] C.-Y. Wang, H.-W. Huang, C.-P. Hsu, B.B. Yang, Recent Advances in Food Processing Using High Hydrostatic Pressure Technology, Crit Rev Food Sci Nutr 56 (2016) 527–540. https://doi.org/10.1080/10408398.2012.745479.
[294] K. Yamamoto, High hydrostatic pressure in food industry applications, in: Nontraditional Activation Methods in Green and Sustainable Applications, Elsevier, 2021: pp. 559–574. https://doi.org/10.1016/B978-0-12-819009-8.00010-4.
[295] V.M. (Bala) Balasubramaniam, S.I. Martínez-Monteagudo, R. Gupta, Principles and Application of High Pressure–Based Technologies in the Food Industry, Annu Rev Food Sci Technol 6 (2015) 435–462. https://doi.org/10.1146/annurev-food-022814-015539.
[296] M.F. San Martín, G. V. Barbosa-Cánovas, B.G. Swanson, Food Processing by High Hydrostatic Pressure, Crit Rev Food Sci Nutr 42 (2002) 627–645. https://doi.org/10.1080/20024091054274.
[297] K. Aganovic, C. Hertel, Rudi.F. Vogel, R. Johne, O. Schlüter, U. Schwarzenbolz, H. Jäger, T. Holzhauser, J. Bergmair, A. Roth, R. Sevenich, N. Bandick, S.E. Kulling, D. Knorr, K. Engel, V. Heinz, Aspects of high hydrostatic pressure food processing: Perspectives on technology and food safety, Compr Rev Food Sci Food Saf 20 (2021) 3225–3266. https://doi.org/10.1111/1541-4337.12763.
[298] X. Felipe, M. Capellas, A.J.R. Law, Comparison of the Effects of High-Pressure Treatments and Heat Pasteurization on the Whey Proteins in Goat's Milk, J Agric Food Chem 45 (1997) 627–631. https://doi.org/10.1021/jf960406o.
[299] E. Rendueles, M.K. Omer, O. Alvseike, C. Alonso-Calleja, R. Capita, M. Prieto, Microbiological food safety assessment of high hydrostatic pressure processing: A review, LWT - Food Science and Technology 44 (2011) 1251–1260. https://doi.org/10.1016/j.lwt.2010.11.001.
[300] R. Winter, C. Jeworrek, Effect of pressure on membranes, Soft Matter 5 (2009) 3157. https://doi.org/10.1039/b901690b.
[301] K. Yamamoto, X. Zhang, T. Inaoka, K. Morimatsu, K. Kimura, Y. Nakaura, Bacterial Injury Induced by High Hydrostatic Pressure, Food Engineering Reviews 13 (2021) 442–453. https://doi.org/10.1007/s12393-020-09271-8.
[302] Q.-A. Syed, M. Buffa, B. Guamis, J. Saldo, Factors Affecting Bacterial Inactivation during High Hydrostatic Pressure Processing of Foods: A Review, Crit Rev Food Sci Nutr 56 (2016) 474–483. https://doi.org/10.1080/10408398.2013.779570.
[303] Y. Wang, C. Ma, Y. Yang, B. Wang, X. Liu, Y. Wang, X. Bian, G. Zhang, N. Zhang, Effect of high hydrostatic pressure treatment on food composition and applications in food industry: A review, Food Research International 195 (2024) 114991. https://doi.org/10.1016/j.foodres.2024.114991.
[304] D. Knorr, A. Froehling, H. Jaeger, K. Reineke, O. Schlueter, K. Schoessler, Emerging Technologies in Food Processing, Annu Rev Food Sci Technol 2 (2011) 203–235. https://doi.org/10.1146/annurev.food.102308.124129.

[305] R.K. Simpson, A. Gilmour, The resistance ofListeria monocytogenesto high hydrostatic pressure in foods, Food Microbiol 14 (1997) 567–573. https://doi.org/10.1006/fmic.1997.0117.
[306] S. Bulut, Inactivation of *Escherichia coli* in milk by high pressure processing at low and subzero temperatures, High Press Res 34 (2014) 439–446. https://doi.org/10.1080/08957959.2014.981262.
[307] E.P. Black, P. Setlow, A.D. Hocking, C.M. Stewart, A.L. Kelly, D.G. Hoover, Response of Spores to High-Pressure Processing, Compr Rev Food Sci Food Saf 6 (2007) 103–119. https://doi.org/10.1111/j.1541-4337.2007.00021.x.
[308] M. Sanz-Puig, P. Moreno, M.C. Pina-Pérez, D. Rodrigo, A. Martínez, Combined effect of high hydrostatic pressure (HHP) and antimicrobial from agro-industrial by-products against S. Typhimurium, LWT 77 (2017) 126–133. https://doi.org/10.1016/j.lwt.2016.11.031.
[309] A. Jofré, T. Aymerich, N. Grèbol, M. Garriga, Efficiency of high hydrostatic pressure at 600 MPa against food-borne microorganisms by challenge tests on convenience meat products, LWT - Food Science and Technology 42 (2009) 924–928. https://doi.org/10.1016/j.lwt.2008.12.001.
[310] P. Giannini, M. Jermini, L. Leggeri, M. Nüesch-Inderbinen, R. Stephan, Detection of Hepatitis E Virus RNA in Raw Cured Sausages and Raw Cured Sausages Containing Pig Liver at Retail Stores in Switzerland, J Food Prot 81 (2018) 43–45. https://doi.org/10.4315/0362-028X.JFP-17-270.
[311] K. Szabo, E. Trojnar, H. Anheyer-Behmenburg, A. Binder, U. Schotte, L. Ellerbroek, G. Klein, R. Johne, Detection of hepatitis E virus RNA in raw sausages and liver sausages from retail in Germany using an optimized method, Int J Food Microbiol 215 (2015) 149–156. https://doi.org/10.1016/j.ijfoodmicro.2015.09.013.
[312] E. Pavoni, G. Arcangeli, E. Dalzini, B. Bertasi, C. Terregino, F. Montesi, A. Manfrin, E. Bertoli, A. Brutti, G. Varisco, M.N. Losio, Synergistic Effect of High Hydrostatic Pressure (HHP) and Marination Treatment on the Inactivation of Hepatitis A Virus in Mussels (Mytilus galloprovincialis), Food Environ Virol 7 (2015) 76–85. https://doi.org/10.1007/s12560-014-9167-z.
[313] X. Li, H. Chen, D.H. Kingsley, The influence of temperature, pH, and water immersion on the high hydrostatic pressure inactivation of GI.1 and GII.4 human noroviruses, Int J Food Microbiol 167 (2013) 138–143. https://doi.org/10.1016/j.ijfoodmicro.2013.08.020.
[314] S. Isbarn, R. Buckow, A. Himmelreich, A. Lehmacher, V. Heinz, Inactivation of Avian Influenza Virus by Heat and High Hydrostatic Pressure, J Food Prot 70 (2007) 667–673. https://doi.org/10.4315/0362-028X-70.3.667.
[315] E. Araud, E. DiCaprio, Z. Yang, X. Li, F. Lou, J.H. Hughes, H. Chen, J. Li, High-Pressure Inactivation of Rotaviruses: Role of Treatment Temperature and Strain Diversity in Virus Inactivation, Appl Environ Microbiol 81 (2015) 6669–6678. https://doi.org/10.1128/AEM.01853-15.
[316] K. Kovač, M. Bouwknegt, M. Diez-Valcarce, P. Raspor, M. Hernández, D. Rodríguez-Lázaro, Evaluation of high hydrostatic pressure effect on human adenovirus using molecular methods and cell culture, Int J Food Microbiol 157 (2012) 368–374. https://doi.org/10.1016/j.ijfoodmicro.2012.06.006.

[317] D.H. Kingsley, H. Chen, D.G. Hoover, Inactivation of selected picornaviruses by high hydrostatic pressure, Virus Res 102 (2004) 221–224. https://doi.org/10.1016/j.virusres.2004.01.030.
[318] D.H. Kingsley, D.G. Hoover, E. Papafragkou, G.P. Richards, Inactivation of Hepatitis A Virus and a Calicivirus by High Hydrostatic Pressure, J Food Prot 65 (2002) 1605–1609. https://doi.org/10.4315/0362-028X-65.10.1605.
[319] G. Demazeau, N. Rivalain, The development of high hydrostatic pressure processes as an alternative to other pathogen reduction methods, J Appl Microbiol 110 (2011) 1359–1369. https://doi.org/10.1111/j.1365-2672.2011.05000.x.
[320] N. Rivalain, J. Roquain, G. Demazeau, Development of high hydrostatic pressure in biosciences: Pressure effect on biological structures and potential applications in Biotechnologies, Biotechnol Adv 28 (2010) 659–672. https://doi.org/10.1016/j.biotechadv.2010.04.001.
[321] K. Koutsoumanis, A. Alvarez-Ordóñez, D. Bolton, S. Bover-Cid, M. Chemaly, R. Davies, A. De Cesare, L. Herman, F. Hilbert, R. Lindqvist, M. Nauta, L. Peixe, G. Ru, M. Simmons, P. Skandamis, E. Suffredini, L. Castle, M. Crotta, K. Grob, M.R. Milana, A. Petersen, A.X. Roig Sagués, F. Vinagre Silva, E. Barthélémy, A. Christodoulidou, W. Messens, A. Allende, The efficacy and safety of high-pressure processing of food, EFSA Journal 20 (2022). https://doi.org/10.2903/j.efsa.2022.7128.
[322] N.K. Rastogi, K.S.M.S. Raghavarao, V.M. Balasubramaniam, K. Niranjan, D. Knorr, Opportunities and Challenges in High Pressure Processing of Foods, Crit Rev Food Sci Nutr 47 (2007) 69–112. https://doi.org/10.1080/10408390600626420.
[323] F. Lou, H. Neetoo, H. Chen, J. Li, High Hydrostatic Pressure Processing: A Promising Nonthermal Technology to Inactivate Viruses in High-Risk Foods, Annu Rev Food Sci Technol 6 (2015) 389–409. https://doi.org/10.1146/annurev-food-072514-104609.
[324] S.P.C. Barroso, A.C. Vicente dos Santos, P. Souza dos Santos, J.N. dos Santos Silva Couceiro, D. Fernandes Ferreira, D. Nico, A. Morrot, J. Lima Silva, A. Cheble de Oliveira, Inactivation of avian influenza viruses by hydrostatic pressure as a potential vaccine development approach, Access Microbiol 3 (2021). https://doi.org/10.1099/acmi.0.000220.
[325] P. Bouquet, V. Alexandre, M. De Lamballerie, D. Ley, J. Lesage, A. Goffard, L. Cocquerel, Effect of High Hydrostatic Pressure Processing and Holder Pasteurization of Human Milk on Inactivation of Human Coronavirus 229E and Hepatitis E Virus, Viruses 15 (2023) 1571. https://doi.org/10.3390/v15071571.
[326] S.P.C. Barroso, A.C. Vicente Dos Santos, P. Souza Dos Santos, J.N. Dos Santos Silva Couceiro, D. Fernandes Ferreira, D. Nico, A. Morrot, J. Lima Silva, A. Cheble de Oliveira, Inactivation of avian influenza viruses by hydrostatic pressure as a potential vaccine development approach., Access Microbiol 3 (2021) 000220. https://doi.org/10.1099/acmi.0.000220.
[327] A.R. de Souza, M. Yamin, D. Gava, J.R.C. Zanella, M.S.V. Gatti, C.F.S. Bonafe, D.F. de Lima Neto, Porcine parvovirus VP1/VP2 on a time series epitope mapping: exploring the effects of high hydrostatic pressure on the immune

recognition of antigens, Virol J 16 (2019) 75. https://doi.org/10.1186/s12985-019-1165-1.
[328] A.E.H. Shearer, K.E. Kniel, High Hydrostatic Pressure for Development of Vaccines, J Food Prot 72 (2009) 1500–1508. https://doi.org/10.4315/0362-028X-72.7.1500.
[329] J.L. Silva, S.P.C. Barroso, Y.S. Mendes, C.H. Dumard, P.S. Santos, A.M.O. Gomes, A.C. Oliveira, Pressure-Inactivated Virus: A Promising Alternative for Vaccine Production, in: 2015: pp. 301–318. https://doi.org/10.1007/978-94-017-9918-8_15.
[330] N.C. Ammerman, M. Beier-Sexton, A.F. Azad, Growth and Maintenance of Vero Cell Lines, Curr Protoc Microbiol 11 (2008). https://doi.org/10.1002/9780471729259.mca04es11.
[331] M. Brandolini, G. Dirani, F. Taddei, S. Zannoli, A. Denicolò, V. Arfilli, A. Battisti, M. Manera, A. Mancini, L. Grumiro, M.M. Marino, G. Gatti, M. Fantini, S. Semprini, V. Sambri, Mutational induction in SARS-CoV-2 major lineages by experimental exposure to neutralising sera, Sci Rep 12 (2022) 12479. https://doi.org/10.1038/s41598-022-16533-4.
[332] A. Zhu, P. Wei, M. Man, X. Liu, T. Ji, J. Chen, C. Chen, J. Huo, Y. Wang, J. Zhao, Antigenic characterization of SARS-CoV-2 Omicron subvariants XBB.1.5, BQ.1, BQ.1.1, BF.7 and BA.2.75.2, Signal Transduct Target Ther 8 (2023) 125. https://doi.org/10.1038/s41392-023-01391-x.
[333] K. Gangavarapu, A.A. Latif, J.L. Mullen, M. Alkuzweny, E. Hufbauer, G. Tsueng, E. Haag, M. Zeller, C.M. Aceves, K. Zaiets, M. Cano, X. Zhou, Z. Qian, R. Sattler, N.L. Matteson, J.I. Levy, R.T.C. Lee, L. Freitas, S. Maurer-Stroh, M.A. Suchard, C. Wu, A.I. Su, K.G. Andersen, L.D. Hughes, Outbreak.info genomic reports: scalable and dynamic surveillance of SARS-CoV-2 variants and mutations, Nat Methods 20 (2023) 512–522. https://doi.org/10.1038/s41592-023-01769-3.
[334] GISAID, Lineage Mutation Tracker - BQ.1.1 Lineage Report, Https://Outbreak.Info/Situation-Reports?Xmin=2024-09-03&xmax=2025-03-03&pango=BQ.1.1 (n.d.).
[335] M. Brandolini, A.M. De Pascali, I. Zaghi, G. Dirani, S. Zannoli, L. Ingletto, A. Lavazza, D. Lelli, M. Dottori, M. Calzolari, M. Guerra, C. Biagetti, F. Cristini, P. Bassi, R. Biguzzi, M. Cricca, A. Scagliarini, V. Sambri, Advancing West Nile virus monitoring through whole genome sequencing: Insights from a One Health genomic surveillance study in Romagna (Italy), One Health 19 (2024) 100937. https://doi.org/10.1016/j.onehlt.2024.100937.
[336] L. Burnett, M.J. McQueen, J.J. Jonsson, F. Torricelli, IFCC Position Paper: Report of the IFCC Taskforce on Ethics: Introduction and framework, Clinical Chemical Laboratory Medicine 45 (2007). https://doi.org/10.1515/CCLM.2007.199.
[337] C. Lei, J. Yang, J. Hu, X. Sun, On the Calculation of TCID50 for Quantitation of Virus Infectivity, Virol Sin 12250 (2020). https://doi.org/10.1007/s12250-020-00230-5.
[338] L. Reed, H. Muench, A simple method of estimating fifty per cent endpoints, Am J Epidemiol 27 (1938) 493–497. https://doi.org/10.1093/oxfordjournals.aje.a118408.

[339] Seegene Inc., Allplex SARS-CoV-2 Assay - Instructions for use. Available at: http://www.seegene.com/upload/images/sars_cov_2/allplex_sars_cov_2_assay_200917.pdf., n.d.
[340] Y. Tang, C. Anne Hapip, B. Liu, C.T. Fang, Highly sensitive TaqMan RT-PCR assay for detection and quantification of both lineages of West Nile virus RNA, Journal of Clinical Virology 36 (2006) 177–182. https://doi.org/10.1016/j.jcv.2006.02.008.
[341] A. Lavazza, S. Pascucci, D. Gelmetti, Rod-shaped virus-like particles in intestinal contents of three avian species., Vet Rec 126 (1990) 581.
[342] A. Lavazza, C. Tittarelli, M. Cerioli, The Use of Convalescent Sera in Immune-Electron Microscopy to Detect Non-Suspected/New Viral Agents, Viruses 7 (2015) 2683–2703. https://doi.org/10.3390/v7052683.
[343] World Health Organization, Global vaccine market report 2024, 2024.
[344] M. Schwarzinger, V. Watson, P. Arwidson, F. Alla, S. Luchini, COVID-19 vaccine hesitancy in a representative working-age population in France: a survey experiment based on vaccine characteristics, Lancet Public Health 6 (2021) e210–e221. https://doi.org/10.1016/S2468-2667(21)00012-8.
[345] S. Neumann-Böhme, N.E. Varghese, I. Sabat, P.P. Barros, W. Brouwer, J. van Exel, J. Schreyögg, T. Stargardt, Once we have it, will we use it? A European survey on willingness to be vaccinated against COVID-19, The European Journal of Health Economics 21 (2020) 977–982. https://doi.org/10.1007/s10198-020-01208-6.
[346] S. Kreps, S. Prasad, J.S. Brownstein, Y. Hswen, B.T. Garibaldi, B. Zhang, D.L. Kriner, Factors Associated With US Adults' Likelihood of Accepting COVID-19 Vaccination, JAMA Netw Open 3 (2020) e2025594. https://doi.org/10.1001/jamanetworkopen.2020.25594.
[347] J. V. Lazarus, S.C. Ratzan, A. Palayew, L.O. Gostin, H.J. Larson, K. Rabin, S. Kimball, A. El-Mohandes, A global survey of potential acceptance of a COVID-19 vaccine, Nat Med 27 (2021) 225–228. https://doi.org/10.1038/s41591-020-1124-9.
[348] S. Loomba, A. de Figueiredo, S.J. Piatek, K. de Graaf, H.J. Larson, Measuring the impact of COVID-19 vaccine misinformation on vaccination intent in the UK and USA, Nat Hum Behav 5 (2021) 337–348. https://doi.org/10.1038/s41562-021-01056-1.
[349] S.L. Wilson, C. Wiysonge, Social media and vaccine hesitancy, BMJ Glob Health 5 (2020) e004206. https://doi.org/10.1136/bmjgh-2020-004206.
[350] H.J. Larson, C. Jarrett, E. Eckersberger, D.M.D. Smith, P. Paterson, Understanding vaccine hesitancy around vaccines and vaccination from a global perspective: A systematic review of published literature, 2007–2012, Vaccine 32 (2014) 2150–2159. https://doi.org/10.1016/j.vaccine.2014.01.081.
[351] A. de Figueiredo, C. Simas, E. Karafillakis, P. Paterson, H.J. Larson, Mapping global trends in vaccine confidence and investigating barriers to vaccine uptake: a large-scale retrospective temporal modelling study, The Lancet 396 (2020) 898–908. https://doi.org/10.1016/S0140-6736(20)31558-0.

[352] E. Dubé, C. Laberge, M. Guay, P. Bramadat, R. Roy, J.A. Bettinger, Vaccine hesitancy, Hum Vaccin Immunother 9 (2013) 1763–1773. https://doi.org/10.4161/hv.24657.
[353] G. Troiano, A. Nardi, Vaccine hesitancy in the era of COVID-19, Public Health 194 (2021) 245–251. https://doi.org/10.1016/j.puhe.2021.02.025.
[354] E. Dubé, C. Laberge, M. Guay, P. Bramadat, R. Roy, J. Bettinger, Vaccine hesitancy: an overview., Hum Vaccin Immunother 9 (2013) 1763–73. https://doi.org/10.4161/hv.24657.
[355] A.M. Kilpatrick, S.E. Randolph, Drivers, dynamics, and control of emerging vector-borne zoonotic diseases., Lancet 380 (2012) 1946–55. https://doi.org/10.1016/S0140-6736(12)61151-9.
[356] J. Rocklöv, R. Dubrow, Climate change: an enduring challenge for vector-borne disease prevention and control, Nat Immunol 21 (2020) 479–483. https://doi.org/10.1038/s41590-020-0648-y.
[357] S. Paz, Climate change impacts on West Nile virus transmission in a global context., Philos Trans R Soc Lond B Biol Sci 370 (2015). https://doi.org/10.1098/rstb.2013.0561.
[358] S.J. Ryan, C.J. Carlson, E.A. Mordecai, L.R. Johnson, Global expansion and redistribution of Aedes-borne virus transmission risk with climate change, PLoS Negl Trop Dis 13 (2019) e0007213. https://doi.org/10.1371/journal.pntd.0007213.
[359] J.C. Semenza, J.E. Suk, Vector-borne diseases and climate change: a European perspective, FEMS Microbiol Lett 365 (2018). https://doi.org/10.1093/femsle/fnx244.
[360] A.J. Tatem, D.J. Rogers, S.I. Hay, Global Transport Networks and Infectious Disease Spread, in: 2006: pp. 293–343. https://doi.org/10.1016/S0065-308X(05)62009-X.
[361] J.M. Medlock, S.A. Leach, Effect of climate change on vector-borne disease risk in the UK, Lancet Infect Dis 15 (2015) 721–730. https://doi.org/10.1016/S1473-3099(15)70091-5.
[362] A. Wilder-Smith, D.J. Gubler, S.C. Weaver, T.P. Monath, D.L. Heymann, T.W. Scott, Epidemic arboviral diseases: priorities for research and public health, Lancet Infect Dis 17 (2017) e101–e106. https://doi.org/10.1016/S1473-3099(16)30518-7.
[363] S.C. Weaver, N. Vasilakis, Molecular evolution of dengue viruses: Contributions of phylogenetics to understanding the history and epidemiology of the preeminent arboviral disease, Infection, Genetics and Evolution 9 (2009) 523–540. https://doi.org/10.1016/j.meegid.2009.02.003.
[364] World Health Organization, Global vector control response 2017–2030 (GVCR), 2017.
[365] L. Lazzarini, L. Barzon, F. Foglia, V. Manfrin, M. Pacenti, G. Pavan, M. Rassu, G. Capelli, F. Montarsi, S. Martini, F. Zanella, M.T. Padovan, F. Russo, F. Gobbi, First autochthonous dengue outbreak in Italy, August 2020, Eurosurveillance 25 (2020). https://doi.org/10.2807/1560-7917.ES.2020.25.36.2001606.
[366] C. Sacco, A. Liverani, G. Venturi, S. Gavaudan, F. Riccardo, G. Salvoni, C. Fortuna, K. Marinelli, G. Marsili, A. Pesaresi, C.M. Grané, I. Mercuri, M. Manica,

S. Caucci, D. Morelli, L. Sebastianelli, M. Marcacci, F. Ferraro, M. Di Luca, I. Pascucci, C. Merakou, A. Duranti, I. Pati, L. Lombardini, D. Fiacchini, G. Filipponi, F. Maraglino, A.T. Palamara, P. Poletti, P. Pezzotti, F. Filippetti, S. Merler, M. Del Manso, S. Menzo, Autochthonous dengue outbreak in Marche Region, Central Italy, August to October 2024, Eurosurveillance 29 (2024). https://doi.org/10.2807/1560-7917.ES.2024.29.47.2400713.

[367] S. Bhatt, P.W. Gething, O.J. Brady, J.P. Messina, A.W. Farlow, C.L. Moyes, J.M. Drake, J.S. Brownstein, A.G. Hoen, O. Sankoh, M.F. Myers, D.B. George, T. Jaenisch, G.R.W. Wint, C.P. Simmons, T.W. Scott, J.J. Farrar, S.I. Hay, The global distribution and burden of dengue, Nature 496 (2013) 504–507. https://doi.org/10.1038/nature12060.

[368] O.J. Brady, P.W. Gething, S. Bhatt, J.P. Messina, J.S. Brownstein, A.G. Hoen, C.L. Moyes, A.W. Farlow, T.W. Scott, S.I. Hay, Refining the Global Spatial Limits of Dengue Virus Transmission by Evidence-Based Consensus, PLoS Negl Trop Dis 6 (2012) e1760. https://doi.org/10.1371/journal.pntd.0001760.

[369] D. Tully, C.L. Griffiths, Dengvaxia: the world's first vaccine for prevention of secondary dengue, Ther Adv Vaccines Immunother 9 (2021). https://doi.org/10.1177/25151355211015839.

[370] S. Sridhar, A. Luedtke, E. Langevin, M. Zhu, M. Bonaparte, T. Machabert, S. Savarino, B. Zambrano, A. Moureau, A. Khromava, Z. Moodie, T. Westling, C. Mascareñas, C. Frago, M. Cortés, D. Chansinghakul, F. Noriega, A. Bouckenooghe, J. Chen, S.-P. Ng, P.B. Gilbert, S. Gurunathan, C.A. DiazGranados, Effect of Dengue Serostatus on Dengue Vaccine Safety and Efficacy, New England Journal of Medicine 379 (2018) 327–340. https://doi.org/10.1056/NEJMoa1800820.

[371] M. Angelin, J. Sjölin, F. Kahn, A. Ljunghill Hedberg, A. Rosdahl, P. Skorup, S. Werner, S. Woxenius, H.H. Askling, Qdenga® - A promising dengue fever vaccine; can it be recommended to non-immune travelers?, Travel Med Infect Dis 54 (2023) 102598. https://doi.org/10.1016/j.tmaid.2023.102598.

[372] A. Wilder-Smith, TAK-003 dengue vaccine as a new tool to mitigate dengue in countries with a high disease burden, Lancet Glob Health 12 (2024) e179–e180. https://doi.org/10.1016/S2214-109X(23)00590-9.

[373] S. Biswal, H. Reynales, X. Saez-Llorens, P. Lopez, C. Borja-Tabora, P. Kosalaraksa, C. Sirivichayakul, V. Watanaveeradej, L. Rivera, F. Espinoza, L. Fernando, R. Dietze, K. Luz, R. Venâncio da Cunha, J. Jimeno, E. López-Medina, A. Borkowski, M. Brose, M. Rauscher, I. LeFevre, S. Bizjajeva, L. Bravo, D. Wallace, Efficacy of a Tetravalent Dengue Vaccine in Healthy Children and Adolescents, New England Journal of Medicine 381 (2019) 2009–2019. https://doi.org/10.1056/NEJMoa1903869.

[374] S. Sridhar, A. Luedtke, E. Langevin, M. Zhu, M. Bonaparte, T. Machabert, S. Savarino, B. Zambrano, A. Moureau, A. Khromava, Z. Moodie, T. Westling, C. Mascareñas, C. Frago, M. Cortés, D. Chansinghakul, F. Noriega, A. Bouckenooghe, J. Chen, S.-P. Ng, P.B. Gilbert, S. Gurunathan, C.A. DiazGranados, Effect of Dengue Serostatus on Dengue Vaccine Safety and Efficacy, New England Journal of Medicine 379 (2018) 327–340. https://doi.org/10.1056/NEJMoa1800820.

Funded by the European Union - Next Generation EU, Mission 4, Component 2, Investment 3.3 (Ministerial Decree 117/2023) CUP J33C22001900002.